ergy

SOLAR

DIRECT FLUX SOLAR CHEMICAL REACTORS

Final Report for the Period September 27, 1983—January 31, 1984

By
B. D. Yudow
J. D. Schreiber
R. H. Carty
R. J. Remick

September 1984
Date Published

Institute of Gas Technology
IIT Center
Chicago, Illinois

Technical Information Center
Office of Scientific and Technical Information
United States Department of Energy

DISCLAIMER

DIRECT FLUX SOLAR CHEMICAL REACTORS

Project 61065 Final Report
For the Period September 27, 1983 Through January 31, 1984

Prepared by
B. D. Yudow
J. D. Schreiber
R. H. Carty
R. J. Remick

Institute of Gas Technology
IIT Center, 3424 S. State Street
Chicago, Illinois 60616

Date Published — September 1984

Prepared for the

UNITED STATES DEPARTMENT OF ENERGY

TABLE OF CONTENTS

TABLE OF CONTENTS, Cont.

TABLE OF CONTENTS, Cont.

LIST OF FIGURES

LIST OF TABLES

xi

LIST OF TABLES, Cont.

INTRODUCTION

This report was prepared by the Institute of Gas Technology (IGT) of Chicago, Illinois to present the results of the Direct Flux Solar Chemical Reactors conceptual design study. The project was sponsored by the United States Department of Energy. The major effort was the conceptual design of two direct flux solar chemical reactors. The reactor developed for the reaction of limestone to lime (that is, limestone calcination) was a windowless conveyor kiln. The reactor developed for the catalytic, gas phase steam reforming of methane to product synthesis gas for hydrogen production was a tubular, packed bed reactor.

IGT was the prime contractor for this project. Sanders Associates, Inc. of Nashua, New Hampshire was a subcontractor responsible for assessment of the status of materials of construction for direct flux reactors, design considerations in the construction of windowed or tubular reactors, radiation heat transfer modeling, and mechanical engineering of limestone kiln components. Badger Engineers, Inc. of Cambridge, Massachusetts was a subcontractor assisting in the development of the conceptual design of the solar fired steam reformer. Badger assisted the project team in identification of principle design issues requiring resolution before direct flux steam reformers can economically compete with metallic solar steam reformer designs.

Solar thermal technology that was originally aimed at power generation has now been broadened to include the use of solar energy for the production of fuels and chemicals. One important group of industrial fuels and chemicals processes that is of interest for this application consists of those processes that involve high-temperature endothermic chemical reactions. For many commercial processes of this type, the use of concentrated solar energy instead of electricity or fossil fuels could be a significant factor in the conservation of our nonrenewable fuels. In addition, concentrated solar energy has the potential for improving process efficiency and product quality because of its unique characteristics of direct, high-temperature, high flux heating in a noncontaminating atmosphere.

Several important questions are: 1) Why the interest in direct flux reactors and 2) What defines a direct flux reactor? Given the multimegawatt scale of commercial chemical processes and the desirability of centralized handling of feedstocks and reaction products, central receivers are the only heat source considered appropriate for large scale chemical processing.

There are three basic methods for using concentrated solar energy to power chemical reactions:

1. Energy transfer to the reactor via an intermediate fluid (process heat)

2. Energy transfer to reactants directly through the opaque reactor wall

3. Energy transfer to the reactants by direct exposure to the solar flux.

In the first two of these methods, reaction temperature is limited by the temperature capability of the intermediate fluid or containment vessel wall, and the rate of energy input is limited by the heat transfer characteristics of the reactor vessel. By avoiding such limitations, a direct flux solar chemical reactor offers the potential of higher reaction temperatures and much higher heat transfer rates.

The design and construction of direct flux solar chemical reactors has thus far been limited to bench-scale devices. One of the ultimate aims of DOE's Solar Fuels and Chemicals Program is to determine if the use of direct flux solar reactors can be proven economically and technically feasible, and, if it can, to determine what difficulties in design, construction, materials, and cost must be resolved.

The objective of the direct flux reactor project was to determine the technical feasibility, utility, and practicality of using direct flux solar chemical reactors to operate thermochemical processes on a commercial scale. In essence, the issues are whether it is possible to utilize direct flux reactors for chemical processing, and if so, are the benefits compelling enough to justify their development and commercialization. The study focused on two promising solar reactor configurations that possess widespread applicability to industrial processes utilizing high-temperature reactions.

The tower mounted reactor must not have any opaque heat transfer surfaces to qualify as a direct flux reactor. Reaction heat can be supplied by any single or combination of direct solar radiation, reflected solar radiation, and reradiant solar energy from hot surfaces within the reactor. The interest in direct flux reactors is, of course, because of potential economic benefits. A potential benefit may come in the form of more compact reactors because direct flux heating may permit high heat transfer rates through reduction in heat transfer resistances and thus reduce required heat transfer areas. Reduction in heat transfer resistance effectively lowers the reactor

temperature required to deliver heat to the reaction. This may increase receiver thermal efficiency resulting in reduced heliostat field size and cost.

The use of direct flux heat transfer is also of interest in reactions that may benefit from the high-temperature, high flux reaction environment in terms of product specificity. Direct flux irradiation of reactants is also of interest in applications where photon chemistry is important. However, the thrust of the effort was to focus on representative, commercial scale, industrial processes for direct flux reactor conceptual design. This orientation tends to emphasize the benefits of potential efficiency gains and possible economic benefits at the expense of assessing possible unique direct flux chemistry.

The project effort was accomplished in five sections.

Section I.   Review and Evaluation of High-Temperature Receiver/Reactor Concepts and Experiments

Section II.   Selection of Reactants

Section III. Selection of Reactor Configurations and Conceptual Designs

Section IV.   Evaluation of Reactor Concepts

Section V.   Research and Development Plans

The objective of Section I was to review and characterize the existing data base of conceptual and experimental solar reactors and receivers, considering designs that use either direct or indirect methods for heating reactants or process fluids. This assessment included evaluations of technical status, compatibility with central receiver or dish solar collectors, versatility of application, mechanical design characteristics, and thermal performance. The review effort of this section was accomplished through a literature search and telephone contacts with developers of concepts, experimenters, and hardware developers. The results of the review effort are presented in the form of schematic diagrams showing the layout of receiver/ reactor components and as tables and/or text describing technical aspects of receiver/reactors. A primary goal of the literature review was to establish the relevancy of previous work to the design of the solid and gas phase reactors to be developed as part of this work. The review was useful to gain background on the thoughts of other solar reactor developers but shed very

3

little light on the problems of commercial scale direct flux reactor design. Essentially, the problem was that experiments and conceptual designs were confined to small scales of 2 to 100 kW (6.8×10^3 to 341×10^3 Btu/h). It was found that no direct flux work had been done in gas phase reactions except in laboratory scale, radiant heated experiments. Furthermore, most investigations have been for chemical heat pipe or thermochemical hydrogen applications, not for endothermic reactions of commercial significance. Direct flux work had been done for solid reactions, however. With the exception of work done in France on the decomposition (calcination) of calcium carbonate in small windowed rotary kiln and fluid bed reactors, no work had been done on chemical reactions of commercial significance.

A key finding was that designs of conventional high-temperature reactors are relevant to direct flux reactor design because the primary heat transfer mechanism is radiation. It was from conventional high-temperature commercial reactor designs that conceptual designs for direct flux solar reactors were developed.

The objective of Section II was the selection of an appropriate reaction from each reactant type (that is, one each of solids and gases) to be used in the reactor design study in Section III. These were endothermic reactions operating at temperatures up to 1100°C (2012°F) that are applicable to commercially significant processes. This section utilized previous surveys of proposed solar fuels and chemicals processes as a basis for compilation of the candidate reactions. To justify the selection of reactants, candidate fuels and chemicals processes were evaluated on the basis of factors such as process data availability, commercial significance, operating temperature, operating pressure, and interface issues with direct flux reactor components (such as corrosive and erosive attacks on windows, optical vessels, or kinetics). The review of candidate processes lead to a rational selection of reactants that could be evaluated for application to reactor concepts developed in Section III.

The solid phase reaction selected was the calcination of calcium carbonate:

$$CaCO_3 \text{ (Limestone)} \xrightarrow[\substack{870°C \text{ to } 1200°C \\ (1598°F \text{ to } 2192°F)}]{\text{Heat}} CaO \text{ Lime} + CO_2$$

4
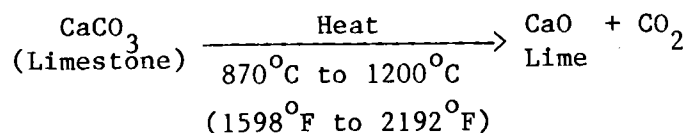
Calcination is an industrially significant reaction with broad application in the chemical industry, steel making, agriculture, and construction. Using premium fuels such as gas and fuel oil, lime production uses 2000 Btu/lb (4.66×10^3 Joule/gram) of lime with an annual energy requirement in 1976 of 9.2×10^{13} Btu (19.7×10^{16} Joule). Compared to most futuristic solar fuels and chemicals processes requiring substantial development of the entire chemical process rather than reactor development, calcination is a well established process. This allows R&D dollars to be concentrated on solar reactor development. This reaction is generic and design work can be applied to design of reactors for such processes as Portland cement manufacturing, ore roasting, or gypsum calcination.

The gas phase reaction selected was the steam reforming of methane:

$$CH_4 + H_2O \xrightarrow[\text{790}^\circ\text{C (1454}^\circ\text{F)}]{\text{Nickel Catalyst}} CO + 3H_2$$
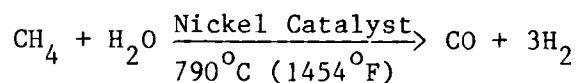
Steam reforming is of major industrial significance providing hydrogen for ammonia production, hydrogenation processes for vegetable oils and upgrading of petroleum products, and combined with carbon monoxide, providing a feedstock for methanol production. In essence, hydrogen and carbon monoxide are the building blocks of the chemical industry. At 238 Btu/SCF (8.87×10^6 Joule/nm^3) of hydrogen, steam reforming is an enormously energy intensive industry consuming 6×10^{14} Btu/yr (6.3×10^{17} Joule/yr).

Since steam reforming is a well established process, research priorities for reactor design can be emphasized, rather than overall process development. The feedstock to this process is natural gas which is widely available. This reaction is generic and design work can be applied to design of reactors for catalytic reforming of propane and naphtha, the thermal cracking of ethane, and the catalytic decomposition of sulfuric acid.

The object of Section III was the development of two conceptual designs for direct flux solar chemical reactors. In this section, a) designs were identified based on sound engineering principles, b) designs were characterized in sufficient detail to establish their feasibility for being manufactured, and c) thermal performance, chemical reaction yield and throughput, and reactor dimensions were determined. Inputs to Section III were results established in Section I, and the two industrial fuels and

chemicals processes identified in Section II. Technical characterization of conceptual designs included such factors as the thermal scale of operation (as a function of reactant); product throughput; thermal performance versus temperature considering primary thermal loss mechanisms; sizing of the reactor based on modeling of combined heat transfer/chemical kinetics; concept layout, including schematic drawings, component description and justification (especially optical components); heliostat field interface; and methods of transport of reactants/products into and out of the reactor.

A number of candidate reactor types were reviewed as candidates for direct flux reactors. The approach taken for reactor selection was conservative with reactor designs derived from reactors used currently for the conduct of calcination and steam reforming reactions. Although innovative approaches to reactor design were considered, several major factors influenced this approach. DOE has outlined a 10-year program for demonstration of solar fuels and chemicals reactors. The risk involved in the development of reactors departing significantly from reactors in commercial use was judged too high. Because industry is the ultimate consumer of this technology, recognition of the conservatism of industry to new approaches was judged a significant barrier to novel designs. This strongly suggested that adaptation of conventional reactor designs would provide the element of relevancy to industry needed to attract their interest. Because this study is one of the earliest efforts to develop concepts for commercial scale solar reactors, the design approach may be viewed as a baseline to which the potential benefits of other reactor designs may be compared.

The choices for reactor concepts were a windowless conveyor kiln for the calcination of calcium carbonate and a multitube packed bed cavity receiver/ reactor for the steam reforming of methane. The steam reformer is essentially the reactor type used industrially for this reaction. The conveyor kiln was derived from rotary kilns conventionally used in industry for limestone calcination. In the conveyor kiln the cavity walls do not rotate. The design is mechanically simple. The cavity shape may be tailored to enhance irradiation of the reactants. An Incoloy 800H screw conveyor immersed in the bed of reactants uses intermeshing screws to convey the solids and provides good mixing with little dusting. The burden may be easily tilted to intercept more direct flux.

The objective of Section IV was an assessment of the conceptual reactor designs through an evaluation of the advantages and disadvantages of the reactor concepts, based on such design attributes as performance, versatility of application, and relative cost. An essential output of this evaluation was the identification of major problems/limitations of the concepts, which aided in suggesting areas for research and development that may lead to the successful demonstration and commercialization of direct flux solar chemical reactor technology.

The major finding was that the conveyor kiln is a technically feasible concept for a direct flux reactor for limestone calcination. The transparent, direct flux steam reformer is not technically feasible because of significant uncertainties in material performance, size availability of transparent tubes, and transparent material durability. Existing materials are far too costly to compete against a solar steam reformer design based on use of metallic materials.

The objective of Section V was the identification of research and development areas and the preparation of a development plan, including schedule, that will lead to the establishment of a technical design data base for the use of direct flux solar chemical reactors for industrial process applications. The primary input for meeting the objective of Section V was the evaluation of the two reactor design concepts developed in Section IV. Primary areas in which research and development are likely to be necessary are chemical engineering, systems integration, and systems analysis. Chemical engineering includes such areas as materials selection and evaluation; reactor performance modeling, construction, testing, scale-up, and demonstration; and reactor cost analysis. Systems integration addresses issues that may be required to demonstrate and commercialize solar reactor technology as an integrated part of chemical process plant operations. Systems analysis is oriented to the larger view of solar reactors for chemical process applications. Issues to be addressed include the need for or appropriateness of direct flux reactors and the development of target costs for reactors and processes that would make them competitive with conventional process methods.

An ambitious schedule leading to demonstration in 1995 of 30 MW (1.02×10^8 Btu/h) calcination and metallic steam reformer plants has been developed.

7

TECHNICAL DISCUSSION

I. Review and Evaluation of High-Temperature Receiver/Reactor Concepts and Experiments

Objective

The objective of the effort reported on in this section was to review and evaluate high-temperature receiver/chemical reactor concepts and experiments which use concentrated solar radiation to drive endothermic chemical reactions. This review forms the basis for characterizing and evaluating solar receiver/reactor designs which may be suitable as direct flux solar chemical reactors. Reaction heat in a direct flux reactor can be supplied by any single or combination of sources including direct solar radiation, reflected solar radiation, or reradiant solar energy from hot surfaces within the reactor. Potential benefits of developing a direct flux reactor include smaller reactor sizes, higher heat transfer rates, and higher thermal efficiencies. The literature was reviewed and personal contacts made taking into consideration the numerous facets of direct flux solar reactor design.

Fundamentals of Receiver/Reactor Design

A direct flux solar reactor represents the integration of a solar receiver and a chemical reactor. Although the temperature levels of concentrated solar energy from parabolic dish collectors and central receiver heliostat fields represents a good match to many chemical reactions, control and distribution of this heat makes reactor design difficult. This is because reactor design is greatly influenced by the specific chemical reactions which are desired. The general goal of the receiver design is to maximize the utilization of solar radiation (that is, attain high thermal efficiency — maximize delivery of solar energy to the process) while providing the desired heat flux profile to the chemical reaction as consistently as possible. Frequently, the ideal receiver design does not coincide with the ideal reactor design.

For the receiver design, an externally heated or cavity configuration can be used. The cavity configuration offers potentially greater thermal performance by minimizing reradiative energy losses through the receiver aperture. Transparent vessels or a window can also be incorporated into the receiver design. Windows may be necessary to reduce heat losses by convection

and/or radiation or to prevent reactants from escaping. Important criteria used to evaluate transparent materials include, whether used in a vessel or window, high spectral transmissivity to solar radiation. Windows should have low infrared (IR) transmissivity but tubes should have high IR transmissivity. This must be coupled with a relative inertness to the reactants and products as well as the thermal conditions prevailing. Depending on the type of design, window sealing, and cleaning methods may also be critical.

The reactor design should take advantage of the solar radiation and efficiently process the reactants. The reactor design must also consider the scale of application, flux capabilities, operating temperatures and pressure, materials handling, transient performance and diurnal cycling capability. The reactor design is further complicated by the desirability of mounting the reactor on a tower at or near the focal point of the heliostat field and orientating the reactor at such an angle as to accept the solar radiation. In order to minimize reactor costs the design should ideally be easy to fabricate, and relatively easy to control and operate.

Chemical reactors used in industry form the basis for any direct flux solar reactor design. These chemical reactors are broadly classified by the type of operation or the design features of the reactor. Reactors classified by the type of reaction can be described as batch, continuous, and semi-continuous types. Batch type reactors are typically in the shape of a tank and are principally used for small-scale production. Commonly used for homogeneous reactions, the batch reactor is defined as a reactor where no reactant or products leave during the reaction process. Continuous reactions simultaneously introduce reactants and withdraw products from the reaction vessel. These reactors are frequently used in large-scale applications. Semicontinuous reactors cover the remaining reactor types where some reactants or products are continuously or intermittently introduced or removed.

A more refined reactor classification technique is by the reactor features. These features commonly describe the operation or physical properties of the reactor. Reactor feature classification include tank, tubular, and tower reactors, as well as fixed, moving, entrained, and fluidized bed reactors. Rotary kilns are a type of moving bed reactor. Tank, tubular, and tower reactors are commonly used for liquid, gaseous, and liquid-gas phase reactions. Tank reactors are tank shaped, as their name implies,

and frequently incorporate some means of agitation such as a stirrer and heat exchange surface. These reactors find use in both continuous and batch type operations where backmixing (near perfect mixing) is desirable. Tubular reactors utilize a single continuous or several parallel tubes in which the reactions occur. Reactants are introduced at one end and products are withdrawn from the other end with a continuously variable mixture of reactants and products occurring in-between. This type of reactor which minimizes back mixing can be equipped with heat exchange surfaces, packed with catalytic or inert materials, or baffles to promote a small degree of agitation.

Tower reactors form a third and broad range of reactors. Typically, they have a vertical cylindrical shape with a large height-to-diameter ratio. Commonly employed in large scale continuous heterogeneous reactions, these reactors may be configured as an empty tower, packed bed with catalysts, reactants or inert solids or trays as in the case of distillation operations. Tower reactors are used for numerous types of reactions ranging from gas phase to solids.

Fixed, moving, entrained, and fluidized bed reactors are frequently used for reactions involving gas-solids phases. Fixed bed reactors are typically loaded with solids or packed with catalysts and are used in gas-solid decomposition reactions. This type of reactor usually requires relatively large and uniformly sized solids and is generally unsuitable for continuous types of operations involving solids decomposition. They are more appropriate for gas phase reactions. For large scale operations the large bed cross-sectional area may inhibit temperature control resulting in large temperature gradients. When proper temperature control can be maintained, the plug flow of gaseous reactants through the bed can result in nearly complete conversion. Additionally, due to the requirements for large particle sizes, pressure drop across the fixed bed reactor can be low. In high-temperature operations that are anticipated with direct flux solar radiation, material fusion properties should be controlled to avoid particle agglomeration.

Moving bed reactors are similar to fixed-bed reactors except that continuous operation is possible and both solids and gas movement within the reactor are more pronounced. Temperature control within the bed is somewhat more controllable in the moving bed reactor relative to the fixed bed reactor due to potential for higher gas flows and some solids circulation within the

bed. Fairly uniform solids loading is still required for this type of reactor. Increased operating flexibility in this design allows for near perfect cocurrent or countercurrent contacting which makes almost complete conversion possible.

A subset of the moving bed reactor is the rotary kiln reactor. This reactor consists of a slightly inclined horizontally oriented tube with a large length-to-diameter ratio. It is primarily used in industrial applications for high-temperature solid decomposition reactions. The tube or shell of the reactor is of welded construction with diameters exceeding 3.05 meters (10 feet) and length longer than 91.4 meters (300 feet) not uncommon. Due to the typically high temperature of operation the kiln is lined with refractory and possibly a second course of insulating brick to protect the metal walls. Feed is introduced at the upper end of the kiln and tumbles down the length of the reactor which is slowly rotating. Because the solid material is retained in the lower part of the cylinder, gas-solids contacting is less efficient than in other reactor designs. For industrial applications hot combustion gases flowing through the reactor provide reaction heat. Heat transfer to the exposed bed material is through radiation and convection from the hot gases and radiation from the kiln brickwork.

A third type of gas-solid or gas-liquid reactor is the entrained bed reactor. In this design solids or liquid are entrained with the gas stream. This type of reactor is only suitable for rapidly occurring reactions since the residence time of the reactants in the reactor is short. With sufficient circulation within the reactor temperature gradients in the direction of the gas flow can be minimized. Due to the rapid reaction rate requirements and near gas and solid cocurrent plug flow in the reactor, high conversion rates are possible. When fine particles are involved in the reaction, the pressure drop in the entrained flow reactor can be low.

The last type of reactor discussed here utilizes the fluidized bed principle. A fluidized bed is made up of small granular or nonfriable powdery solids or catalyst which are suspended in a stream of gas. The gas velocity is maintained at a sufficient level to suspend the particles yet keep them from being entrained in the exit stream. Due to the high degree of circulation within the bed, temperature distribution within the bed can be very uniform. Thus, the fluid bed acts as a well-mixed reactor for solids

12

reactions (as opposed to plug-flow). A wide range of solids can be introduced into the bed for reaction. Both continuous and batch operations are practical in this reactor. The pressure drop characteristics of fluidized bed reactors are usually higher than other types of reactors. Depending on the bed depth, pressure drops can be very high. Another drawback of the fluidized bed reactor is the backmixing flow of solids and poor contacting patterns which can reduce the conversion rate of gaseous reactants.

Review of Previous Solar Receiver/Reactor Designs

Research on high-temperature receiver/reactor concepts and experiments was reviewed and categorized. Categorization is based on the reactor types as presented above. This review indicated that much of the past high-temperature receiver/reactor work does not shed new light on the problems of commercial scale direct flux reactor design. Although the primary heat transfer mechanism for both types of reactors is radiation, most of the conceptual designs or experiments were confined to small-scale reactors in the 2 to 100 kW (6.83×10^3 to 3.41×10^5 Btu/h) range. In addition, very little work has been done on commercial scale high-temperature solar receiver/reactor design for commercially significant chemical reactions. Much of the past work has focused on thermochemical hydrogen applications and not commercially significant reactions. Exceptions to this include a steam-methane reforming reactor design by PFR Engineering Systems and calcination experiments in small-windowed rotary kiln and fluidized bed reactors have been done in France. The remaining discussion presents a review and evaluation of past high-temperature receiver/reactor research based on reactor types. Further discussion and figures are contained in the Appendix.

Packed Bed Reactor Summary for Gas Phase Reactions

A number of packed bed receiver/reactor configurations were found in the literature. All of the designs reviewed in this reactor category were for gas phase applications with the majority designed to operate at the focal point of a parabolic dish collector. The gas phase reactions included in these designs are:

$$SO_3 \rightarrow SO_2 + O_2$$
$$CO_2 + CH_4 \rightarrow 2CO + 2H_2$$
$$2NH_3 \rightarrow N_2 + 3H_2$$
$$CH_4 + H_2O \rightarrow CO + 3H_2$$

13

The advantage of all the packed bed reactors analyzed is that they have continuous processing capabilities. They are particularly appropriate for gas or liquid phase catalytic reactions. A problem encountered in the design of these reactors is that the direct flux illumination and/or radiation of solids nearest to the outside of the reactor can lead to nonuniform temperature within the packed beds due to the absorption of flux on the exposed surface of solids. This results in temperature differentials and hence a variable reaction rate over the cross-section of the bed. Through the uniform control of flux within or around the packed bed and the proper selection of bed width, this problem can be minimized. For packed bed reactors using parabolic dish collectors, reactor design is less complicated due to the independence of the flux profile from time dependent effects within the reactor cavity. On the other hand, packed bed reactors designed for central receiver applications are more complex in design due to the time-dependent and directionally dependent flux variations on the multiple tubes comprising the reactor. In the much larger central receiver/reactor design larger mass flows, multiple flow paths, and potentially different reactant temperatures further complicate the reactor design.

The distribution and utilization of the flux is critical in all the designs reviewed. All conceptual designs appear capable of accepting up to 2000 kW/m^2 (6.342 X 10^5 Btu/h-ft^2) flux rates at the aperture of the reactor. However, proper cavity design was of utmost importance to provide large heat transfer areas that reduced local flux levels in order to match conductive and convective heat transfer rates to the incident radiant heat flux. For instance, typical steam reformer flux levels average 60 kW/m^2 (1.9 X 10^4 Btu/h-ft^2).

Control of flux rates is not only important from the standpoint of controlling reaction rates, but also from the standpoint of material compatibility. Materials used in the designs evaluated include transparent quartz, high strength steel alloys, and ceramic materials. In radiant heat laboratory experiments, New Mexico State University and the Naval Research Laboratory tested a transparent quartz laboratory reactor for sulfur trioxide decomposition. The reactor has successfully operated at temperatures up to 1173°C (2144°F). However, at higher temperatures in the range of 1000°C (1832°F) to 1200°C (2192°F) serious fused quartz devitrification has occurred.

Remedies to this problem have been suggested. This includes operation only in reducing atmospheres and the avoidance of contact with water vapor. This may limit the use of quartz as either a tube or window material should reactor applications involve window or tube temperature conditions above 1000°C (1832°F). Another limitation of quartz relative to metallic construction materials is its lack of strength. For high pressure operations quartz reactor or window wall thickness may be prohibitively large. On the other hand, quartz is a moderate cost material with excellent solar spectral transmissivity and good high-temperature performance in terms of hardness and chemical resistance. However, quartz does have poor IR transmissivity compared to such materials as sapphire or polycrystalline alumina. If transparent materials such as sapphire are required for direct flux reactors because of resistance to corrosion or high IR transmissivity, cost factors may make metallic or ceramic materials more attractive. Based on our review, little information is available on transparent materials that is appropriate to construction of commercial scale solar chemical reactors. Although a small-scale quartz reactor has been successfully fabricated, techniques to fabricate long, large diameter transparent reactor tubes, glass to metal, and glass to ceramic joints that will survive severe chemical and thermal environments still require research. Windowed reactors require large, transparent apertures. Transparent windows larger than one foot diameter have not been demonstrated. Solar experiments with windowed reactors have frequently encountered quartz devitrification and corrosion.

As mentioned earlier, nearly all studies of packed bed reactors were directed at small-scale concepts or experimental reactors for parabolic dish applications. Although information on transparent materials and materials of construction are somewhat applicable to direct flux reactor design, these designs have been conceived for under 100 kW (3.41×10^5 Btu/h) inputs and as a result are generally not applicable for scale up to large commercial scale central receiver facilities. An exception to this is the central receiver/reactor conceptual design work on methane-steam reforming that PFR Engineering Systems[1] performed, under DOE sponsorship. The objective of the PFR conceptual design was to study the feasibility of retrofitting a 34.5 MW (1.81×10^8 Btu/h) (at aperture plane) receiver/reactor in parallel to a conventional methane-steam reformer at an existing ammonia plant. The study included a detailed look at the reformer design and involved extensive cavity,

15

heat transfer and kinetic modeling of the reactor. The design considered trade-offs in such areas as aperture sizing, insulation thickness and weight, tube materials and wall thicknesses as well as control methods.

The design developed was for a cavity receiver with a single elliptical aperture. The receiver/reactor is an octagonal shape with metallic reaction tubes located in the middle. A shock wall constructed of refractory material is positioned in the longitudinal axis of the receiver/reactor and recessed from the aperture plane. The ceramic shock wall protects the tubes from direct solar radiation. The tubes are heated by solar and thermal radiation reflected and reradiated from the cavity interior surfaces. The shape and size of the walls and aperture provide uniform heat flux to all the tubes and minimal variations in circumferential flux distribution around the tubes. Reaction tubes are arranged in eight panels placed in two rows along the longitudinal axis of the receiver. Flow to each panel is controlled by a valve upstream of the preheat coils. The two row design was selected to limit receiver depth. The pitch ratio was a compromise between the desire for uniform circumferential heat flux distribution around each tube and receiver depth. The PFR design closely resembles fossil fired, radiant heated steam reformer designs.

Tube and manifold material selections for this design were based on conventional methane-steam reformer materials. The design basis included a maximum wall temperature of 871°C (1600°F) and a working pressure of 2.76 MPa (400 psig). Material selection criteria included cost, weldability, fabrication, good stress, creep, and rupture characteristics. In view of the thermal cycling inherent in solar operations, particular emphasis was paid to stress, creep, and rupture characteristics. The material also had to have a high chrome and nickel composition which has proven to be resistant to oxidation, carbonization, and embrittlement which have posed problems in conventional steam reformers in the past. The results indicated that Manaurite 36X and Manaurite 900 were acceptable materials for the tube and manifolds, respectively. Tube life was estimated to be about 5 years which is typical for conventional methane-steam reforming reactors.

Another important issue addressed in the PFR conceptual design study was reactor performance during transients. To maintain reactor performance, a thermal storage technique was desirable. A compromise of the thermal storage

16

weight on the reactor tower and the amount of storage was made. Although a lightweight insulating refractory material such as Kaowool (product of Babcock and Wilcox) had excellent properties in respect to solar exposure conditions, thermal storage capabilities to maintain process flow were less than one minute when the material was used to line the cavity walls. Thermal storage time was increased to allow approximately 11 minutes of process flow before shutdown by using a combination of heavy refractory brick and castable Purotab N (product of Kaiser Refractories) on the cavity walls. This increased not only the reactor performance, but also increased the cost of the reactor and support tower by increasing reactor weight.

The issue of thermal storage as a management technique to maintain reactor performance during transients will require more detailed study as reactor designs evolve to the point of hardware construction. Weight limitations on tower mounted reactors may limit the use of thermal storage. Trade-off studies of the sensitivity of different reaction types to transient operation are still required. Reactions with temperature dependent reaction paths such as steam reforming of methane may have problems such as carbon deposition when operated outside the desired temperature range. It is expected that a combination of close control of mass flow, flow distribution and use of thermal storage will be necessary to accommodate daily flux variations and transients.

Tables 1 through 3 present a summary of the eight packed bed receiver/ reactor experiments and conceptual designs which were reviewed. A more detailed description of each of these reviews is presented in the Appendix. Figure numbers in the tables refer to figures in the Appendix. Table 1 presents a summary of the four gas-phase sulfur trioxide decomposition reviews. For this reaction only small scale, parabolic dish mounted, cavity receiver/reactors were proposed. Design scales ranged from 6 to 25 kWth $(2.05 \times 10^4$ to 53×10^4 Btu/h). Materials of construction included ceramics, high-performance steels, and a transparent quartz reactor. For the sulfur trioxide reaction operating temperatures were 900°C (1652°F) and pressures ranges from 152 kPa to 304 kPa (22 psi to 44.1 psi).

Tables 2 and 3 present the summary of findings for two ammonia dissociation studies and two methane reforming studies; one using carbon dioxide and the other using steam. Both ammonia dissociation conceptual

Table 1. REACTOR TYPE: PACKED BED/GAS PHASE CATALYTIC
(Sulfur Trioxide Decomposition)

Reaction	SO$_3$ Decomposition	SO$_3$ Decomposition	SO$_3$ Decomposition	SO$_3$ Decomposition
Researcher	Chubb/Naval Research Laboratory	Westinghouse	New Mexico State University/NRL/JPL	NMSU/NRL
Reference Number	1	3	4	4
Scope of Effort	Conceptual Design	Conceptual	Experimental	Experimental
Objective	Outline of Technical Features of Concept	Proof of Principle	Proof of Principle	Proof of Principle
Design Scale	25 kWth (85,300 Btu/h)	12.5 kWth (42,700 Btu/h)	6 kWth (20,500 Btu/h) (Elec. Resistance Heat)	6 kWth (20,500 Btu/h)
Scale of Intended Application	Parabolic Dish Heat Source	Parabolic Dish Heat Source	Parabolic Dish Heat Source	Parabolic Dish Heat Source
Flux Coupling Method	Indirect/Opaque Heat Transfer Surfaces	Indirect/Opaque Heat Transfer Surfaces	Indirect/Opaque Heat Transfer Surfaces	Transparent Heat Transfer Surfaces
Material of Construction	Ceramic	Alonized 316 Stainless Steel	Kanthal A-1/316 Stainless Steel	Quartz
Configuration	Cavity	Cavity	Cavity	Cavity
Windowed Aperture	No	No	No	No
Schematic Figure Number	1	3	Similar to 1	Similar to 1
Principal Dimensions:				
Aperture Diameter	0.20 m (0.66 ft)		Not Applicable	Not Applicable
Cavity Diameter	30.45 cm (11.99 in.)	25.4 cm (10 in.)	30.5 cm (12.0 in.)	30.5 cm (12.0 in.)
Cavity Length	45.7 cm (18.0 in.)	31.8 cm (12.5 in.)	102 cm (3.35 ft)	152.4 cm (5.0 ft)
Thermal Efficiency	93% (Calculated)	64% (Assumed)	Not Applicable to Laboratory Model	Not Applicable to Laboratory Model
Flux Capability:				
Basis	Not Available	Assumed	Not Applicable	Not Applicable
At Aperture		Not Available	Not Applicable	Not Applicable
In Reactor		Uniform Flux Assumed	Not Applicable	Not Applicable
Temperature of Operation	900°C (1652°F)	900°C (1652°F)	900°C (1652°F)	900°C (1652°F)
Process Fluid Temperature Profile	Not Available	Figure No. 4	Not Available	Not Available
Refractory Temperature	Not Applicable	Not Applicable	Not Applicable	Not Applicable
Window Temperature	Not Applicable	Not Applicable	Not Applicable	Not Applicable
Operating Pressure	304 kPa (44.1 psi)	304 kPa (44.1 psi)	304 kPa (44.1 psi)	152 kPa (22 psi)
Pressure Drop ($\Delta P/P$, %)	1.6 (Calculated)	7 (Calculated)	13 (Measured)	36 (Measured)
Evaluation	Conceptual Design Only.	Single tube lab experiment successful. No test of conceptual design.	Adequate conversion. Stainless Steel corrosion problems.	Concept proved. Technical feasibility not established.

18

Table 2. REACTOR TYPE: PACKED BED/GAS PHASE CATALYTIC
(Ammonia Dissociation)

Reaction	Ammonia Dissociation	Ammonia Dissociation
Researcher	Lenz/CSU	Williams
Reference Number	6	7
Scope of Effort	Proof of Concept	Proof of Concept
Objective	Conceptual Design	Conceptual Design
Design Scale	10 kWth (34,100 Btu/h)	12.5 kWth (42,700 Btu/h)
Scale of Intended Application	Parabolic Dish Heat Source	Parabolic Dish Heat Source
Flux Coupling Method	Indirect/Opaque Heat Transfer Surfaces	Indirect/Opaque Heat Transfer Surfaces
Material of Construction	Inconel 617	Inconel 617
Configuration	Cavity	Cavity
Windowed Aperture	No	No
Schematic Figure Number	6	7
Principal Dimensions:		
Aperture Diameter	12.5 cm (4.92 in.)	8 cm (3.15 in.)
Cavity Diameter	30.5 cm (12 in.)	16 cm Maximum (6.30 in.)
Cavity Length	20.3 cm (8 in.)	30 cm (11.81 in.)
Thermal Efficiency	Not Available	90% Calculated
Flux Capability:		
Basis		
At Aperture	Not Available	Not Available
In Reactor	Not Available	8.0 w/cm^2 Average (25,400 Btu/h-ft^2)
Temperature of Operation	650°C (1202°F) Product Exit Temperature	Wall Temperature 750°C (1382°F)
Process Fluid Temperature Profile	Not Available	Figure No. 7
Refractory Temperature	Not Available	Not Applicable
Window Temperature	Not Applicable	Not Applicable
Operating Pressure	29.99 MPa (4350 psi)	19.99 MPa (2900 psi)
Pressure Drop (ΔP/P, %)	0.2	10
Evaluation	Conceptual Design Only. Explored a number of tube configurations.	Conceptual Design Only

Table 3. REACTOR TYPE: PACKED BED/GAS PHASE CATALYTIC
(Methane Reforming)

Reaction	Carbon Dioxide/Methane Reforming	Steam Reforming of Methane
Researcher	NRL	PFR
Reference Number	5	1
Scope of Effort	Experimental	Conceptual
Objective	Proof of Principle	Technical Feasibility Study
Design Scale	15 kWth (51,200 Btu/h)	34.5 MWth (1.18 X 10^8 Btu/h) at Aperture
Scale of Intended Application	Parabolic Dish Heat Source	Same as Design Scale
Flux Coupling Method	Indirect/Opaque Heat Transfer Surfaces	Indirect/Opaque Heat Transfer Surfaces
Material of Construction	316 Stainless Steel	Manaurite 36X Nickel Alloy
Configuration	Cavity	Cavity
Windowed Aperture	No	No
Schematic Figure Number	5	5
Principal Dimensions:		
Aperture Diameter	20.3 cm (7.99 in.)	33 m^2 (355 ft^2) (Elliptical)
Cavity Diameter	30 cm (11.8 in.)	Octagonal Shape
Cavity Length	Approximately 50 cm (19.7 in.)	Tubes are 12 m (39.4 ft) Heated Lengths; 10.16 cm (4.0 in.) ID; 11.8 cm (4.65 in.) OD
Thermal Efficiency	62%	78.2%
Flux Capability:		
Basis		Calculated
At Aperture	Not Available	1.23 MW/m^2 (3.90 X 10^5 Btu/h-ft^2) Average
In Reactor	Not Available	Pk Tube Flux 99.66 kW/m^2 (3.16 X 10^4 Btu/h-ft^2) Pk Wall Flux 113 kW/m^2 (3.58 X 10^4 Btu/h-ft^2) 80 kW/m^2 Avg. Tube Flux (2.54 X 10^4 Btu/h-ft^2) (ID Basis) – Figure 9
Temperature of Operation	900°C (1652°F) (Range 625°C to 1025°C, 1157°F to 1877°F)	538°C (1000°F) Inlet/790°C (1454°F) Outlet
Process Fluid Temperature Profile	Not Available	Figure 9
Refractory Temperature	Not Available	Figure 10
Window Temperature	Not Applicable	Not Applicable
Operating Pressure	405 kPa (58.8 psi)	2.61 MPa (379 psi) (Inlet)
Pressure Drop ($\Delta P/P$, %)	Not Available	8.31
Evaluation	Concept proved. Technical feasibility not established.	Technical feasibility of of conceptual design established.

design studies were for cavity type receiver/reactors for parabolic dish applications operating at 650° to 700°C (1202° to 1292°F) at pressure levels of 20 MPa to 30 MPa (2900 psi to 4350 psi). Design scales were in the range of 10 to 12.5 kWth (3.4×10^3 to 4.27×10^4 Btu/h). Both designs used Inconel 617 as the reactor material of construction. For the methane reforming reactions presented in Table 3 one study involved the construction of a small scale 15 kWth (5.12×10^4 Btu/h) experimental proof of principle reactor for the carbon dioxide/methane reforming reaction. This experimental receiver/ reactor was designed for parabolic dish applications and uses a cavity design configuration. The reactor was constructed of 316 stainless steel and operated at 625° to 1025°C (1160° to 1877°F) and at 405 kPa (58.8 psi). The second methane-steam reforming design reviewed was of a conceptual technical feasibility nature. The design scale was 34.5 MWth (1.18×10^8 Btu/h) for use with a central receiver/heliostat field. Materials of construction were envisioned to be Manaurite 36X nickel alloy operating at up to 790°C (1454°F) and 2.61 MPa (379 psi) pressures.

Fixed and Moving Bed Reactors Summary for Solid Phase Reactions

Several small scale experiments involving fixed and moving bed reactors using direct flux irradiation of reactants have been operated. Reactions carried out in these types of reactors include:

- Steam or carbon dioxide gasification of coal, coke, activated carbon, and biomass

- Dissociation of cadmium oxide

- Elemental phosphorus production.

Fixed and moving bed reactors can be used for continuous, semicontinuous, and batch type of operations where solids decomposition occurs. Moving bed reactors are applied to continuous processes. Generally, fixed bed reactors are applied to batch and semicontinuous processes. Although total decomposition of the solids is desirable, ash or slag can be removed from the reactor if necessary. These types of reactors are also acceptable for reactions producing solid and gaseous products, such as zinc sulfate decomposition. Although there is limited experience with fixed or moving bed solar reactors, considerable experience exists in industry. Techniques for materials handling such as lockhoppers or screw feeders are available. Bed stirring devices and techniques have also been developed by industry which may

21

be applicable to solar reactor design. Reactor fabrication methods are straightforward except where transparent materials are concerned.

For application to large scale processing of solids, fixed or moving bed reactors may be conceived of as a large number of vertical, transparent tubes arrayed in a generally circular pattern around the receiver periphery to intercept the concentrated flux from a heliostat field. The material is fed from the top of the tubes. The radiation impinges upon the reactant and the reaction occurs as heat is transferred to the material by direct absorption, by conduction through the bed of solids, and by convection from product gases. In direct flux applications, it is the surface of the bed where direct irradiation of reactants occurs, and where potentially high heat transfer rates are possible. Because conductive and convective heat transfer rates are relatively slow compared to radiative heat transfer, significant temperature gradients and variable reaction rates across the cross section of the bed are likely to occur. In may be speculated that a thin bed of extensive surface area is desired to expose the bulk of the reactant to direct flux rather than heat conducted or convected through the bed. Conceptually, this may be accomplished by such approaches as small diameter tubes, confining the reactant to a narrow annular space, or actively stirring the solids to augment the exposure of solids to direct flux. Design of the reactor includes consideration of proper dilution of flux over a sufficiently large surface area as in a cavity design to match flux absorption to reaction rate while attempting to avoid severe temperature gradients across the bed. Use of a cavity to provide proper dilution of flux impinging on reactants should allow high thermal efficiencies.

To make best use of direct flux heating of reactants, thin beds of solids are necessary. It is expected that the low thermal inertia of a thin bed of solids will make fixed and moving bed reactors responsive to transient variations in incident flux. For reactions without temperature-dependent side reactions, transients may be accommodated by control of reactant flow. More temperature-sensitive reactions that may produce unwanted products may require the use of additional thermal mass in addition to flow control to help maintain reaction temperature at the desired level. Thick beds provide additional thermal mass but will have the problem of variable reaction rates with depth and poor control over undesired reactions across the reactor cross

section. The low thermal inertia of the thin beds will result in relatively short startup and shutdown times. Detailed analytical calculations must be carried out to investigate these qualitative speculations.

The temperature capability of a direct flux packed bed reactor is limited by corrosion of the transparent container. With a quartz container, operating temperature is limited to about 900°C (1652°F) with 1000°C (1832°F) possible in a dry, reducing atmosphere. Sulfates and carbonates may react with quartz at high temperatures. A tubular reactor may require moderately thick walls to operate under pressure since quartz is not a strong material. Based on room temperature strength a 4-inch ID tube requires a wall thickness of 8.4 mm (0.33 in.) at 1.03 MPa (150 psi), and 5.08 cm (2.0 in.) at 4.31 MPa (625 psi).

A packed bed reactor for solids will be of moderately complex design and will probably be more applicable for central receiver/heliostat applications due to the materials handling problem associated with small scale, distributed parabolic dish applications. Because of the daily and seasonal flux variations on reactor components within the cavity, feeding and collection of reactants and products may be a major problem due to the need for proper distribution and control of flow to the multiple tubes comprising the reactor.

A summary of the fixed and moving bed reactors reviewed in this study is presented in Table 4. All designs were for a cavity type configuration with a windowed aperture. Three of the four studies reviewed were of an experimental proof of concept nature performed on a 30 kWth (1.02 X 10^5 Btu/h) scale. The fourth represents a patented conceptual design which requires a down focusing heat source. The three experimental studies used a refractory lined stainless steel reactor. Operating temperatures ranged from 900° to 1500°C (1652° to 2732°F) with pressures from atmospheric to 34.5 kPa (5 psig). A more detailed review of each study is presented in the Appendix.

Entrained Flow Reactors Summary for Solid Phase Reactions

Entrained flow reactors are used in industry where reaction rates are high and material residence times are short (<5 sec). This continuous operation reactor is capable of fast response times due to the low inventory of material in the reaction zone. The reaction zone is contained within the reactor walls where reactants are either dropped in or injected. For solid reactions the material must be finely ground both to increase its surface area

Table 4. FIXED AND MOVING BED REACTORS FOR SOLID PHASE REACTIONS

Reaction	Steam Gasification of Coal	Cadmium Oxide Dissociation	Elemental Phosphorus Production	Coal Gasification
Researcher	Gregg	Yudow	Yudow	Gregg
Reference Number	8	9	10	11
Scope of Effort	Experimental	Experimental	Experimental	Conceptual (Patent)
Objective	Proof of Principle	Proof of Principle	Proof of Principle	
Design Scale	30 kW (1.02 X 10^5 Btu/h)	30 kW (1.02 X 10^5 Btu/h)	30 kW (1.02 X 10^5 Btu/h)	
Scale of Intended Application	Not Applicable	Not Applicable	Not Applicable	Central Receiver Heat Source
Flux Coupling Method	Direct	Direct	Indirect	Direct
Material of Construction	Stainless Steel/ Refractory Lined	Stainless Steel/ Refractory Lined	Stainless Steel/ Refractory Lined	Metal Shell/Refractory Liner
Configuration	Cavity	Cavity	Cavity	Cavity
Windowed Aperture	Yes (Quartz)	Yes (Quartz)	Yes (Quartz)	Yes (Unspecified, Could be Quartz)
Schematic Figure Number	18	19 and 20	19	21
Principal Dimensions:				
Aperture Diameter	20 cm (7.87 in.)	15.2 cm (6 in.)	15.2 cm (6 in.)	Not Available
Cavity Diameter	30 cm (11.81 in.)	15.2 cm (6 in.)	15.2 cm (6 in.)	Not Available
Cavity Length	1 m (3.28 ft)	10.2 cm (4 in.)	10.2 cm (4 in.)	Not Available
Thermal Efficiency	19 to 48%	Not Available	Not Available	Not Available
Flux Capability:				
Basis				
At Aperture	Not Available	Not Available	Not Available	Not Available
In Reactor	Not Available	Not Available	Not Available	Not Available
Temperature of Operation	902° to 1152°C (1655° to 2105°F)	1500°C (2732°F)	1500°C (2732°F)	827°C (1520°F)
Process Fluid Temperature Profile	Not Available	Not Available	Not Available	Figure 4
Refractory Temperature	Not Available	Not Available	Not Available	Not Available
Window Temperature	502° to 702°C (935° to 1295°F) (802°C/1475°F Max.)	Not Available	Not Available	Not Available
Operating Pressure	101 kPa (14.7 psi)	27.6 kPa (4 psig)	27.6 kPa (4 psig)	Not Available
Pressure Drop (ΔP/P, %)	Not Available	Not Available		Not Available
Evaluation	Proof of principle. Window remained rather clear. No thermal shock problems.	Proof of principle. Considerable problems with window devitrification and corrosion.	Proof of principle. Problems with window corrosion and devitrification.	Conceptual only. Requires a downward focusing heat source.

24

for the reaction, for rapid dispersement throughout the reaction zone, and to permit entrainment. Reactants may also be injected with catalytic material which becomes entrained in the flow and promotes the reaction.

Two types of entrained flow configuration reactions were found in the literature. Both external configuration designs involved carbonaceous material gasification in quartz tubes. In one approach, solids were entrained in an upward flow of steam. In the second method, solids were introduced into the top of the reactor where they fell downward countercurrently through an upward flow of steam. In both designs the reactants are directly irradiated by solar flux. These single tube reactors may be considered prototypes of commercial designs involving a cavity lined with such tubes.

From the literature it is not clear if the transparent tubes will be subject to deposition of reactants or products or to corrosive attack. Reports of yellowish films, carbon deposits, as well as solid and liquid adhesion have been cited in the literature. Therefore, "fogging" of the material may be a problem. Suggestions to cure this "fogging" include the hydrodynamic management of flow. However, this method is still unproven. Only limited materials evaluations have been done in terms of the corrosive attack on the quartz material. For instance, the quartz literature suggests that the presence of carbon will reduce fused quartz at temperatures above 1200°C (2192°F). This indicates that carbonaceous material gasification may be restricted to this upper temperature limit.

Erosion of the tube also seems to be a possibility. Although quartz is relatively hard, char particles may scratch the quartz. Scratches will reduce transmissivity and can lead to structural failure. Short-term experiments have not experienced this problem to a great degree but it may be a problem for commercial designs. Another problem not clearly resolved in the literature is the devitrification of quartz due to daily thermal cycling below the phase change temperature of ~250°C (482°F). Quartz tubes or windows may have to be maintained at high temperatures to avoid devitrification.

In the proof of principle experiments reviewed involving entrained bed reactors, flux levels up to 1600 kW/m^2 (5.07 X 10^5 Btu/h-ft^2) were tested in reactor sizes of less than 100 kWth (3.4 X 10^5 Btu/h). Operating conditions in the quartz reactors were maintained at temperatures up to 1000°C (1832°F) and pressures in one of the experiments of up to 517 MPa (75 psig).

An interesting phenomenon observed in the quartz entrained reactor experiments is the dual temperature condition. This occurs when the concentrated radiant energy rapidly heats up the opaque solid particles in the reactors to temperatures over 2273°C (4120°F). The transparent gaseous material in the reactor remains relatively cold depending on the solids loading and solid to gas heat transfer rate. Particles less than 1 μm have been shown to heat rapidly and transfer heat effectively to their surroundings. Thus, they are very close in temperature to the surrounding gas and in fact may be used to heat gases to high temperatures. Larger particles, on the other hand, may heat faster than the rate of heat transfer to the surrounding gas and may therefore achieve higher temperatures than the surrounding media. This would indicate that material size is an important criteria in reactor design. Unfortunately, grinding costs to very small size particles or even material characteristics may exclude certain reactions from consideration. The possibility also exists that through material sizing product characteristics can be changed. Volatile matter flashed from the solids may be quenched before being cracked to lighter hydrocarbons. This would facilitate the production of liquid products.

A more detailed discussion of the two entrained flow reactor experiments reviewed is presented in the Appendix. Table 5 presents a summary of the entrained flow reactor designs.

Fluidized Bed Reactor Summary

When a gas is passed upward through a bed of solid particles at a sufficient rate that the drag force matches the weight of the particles, a suspension, or fluidized bed, of particles results. The fluidized bed is characterized by large local instabilities in flow fields that result in bubbles similar in appearance to those that occur when bubbling a gas through a liquid. These bubbles rise through the bed causing the surrounding suspended particles to circulate around them, making the solids in the bed well-mixed. Mixing increases with increased gas flow.

Reasons for the use of fluidized bed technology for chemical processes are:

●   The high solids-gas interfacial area results in excellent heat and mass transfer between these two phases

Table 5.   REACTOR TYPE: ENTRAINED FLOW

	Carbon/Steam Gasification	Biomass Pyrolysis
Reaction	Carbon/Steam Gasification	Biomass Pyrolysis
Researcher	Georgia Institute of Technology	Antal
Reference Number	Personal Communication with R. Cassanova	15 and 16
Scope of Effort	Experimental	Experimental
Objective	Proof of Principle	Proof of Principle
Design Scale	Less than 100 kW (3.41 X 10^5 Btu/h)	Less than 100 kW (3.41 X 10^5 Btu/h)
Scale of Intended Application	Not Applicable	Not Applicable
Flux Coupling Method	Direct	Direct
Material of Construction	Quartz	Quartz
Configuration	External	External
Windowed Aperture	Yes: Transparent Tube	Yes: Transparent Tube
Schematic Figure Number	32	32
Principal Dimensions:		
Aperture Diameter		
Cavity Diameter	Tube Diameter = 12.7 cm (5 in.)	Tube Diameter (Laboratory) = 25 mm (0.98 in.) OD; Tube Diameter (Odeillo) = 50 mm (1.97 in.) OD
Cavity Length	Tube Length = 1.02 m (40 in.)	Not Available
Thermal Efficiency	Not Available	Not Available
Flux Capability:		
Basis	Measured	Measured
At Aperture	Not Applicable	Not Applicable
In Reactor	Approx. 50 to 100 kW/m^2 (1.6 X 10^4 to 3.2 X 10^4 Btu/h)	20 to 1600 kW/m^2 (6.3 X 10^3 to 5.1 X 10^5 Btu/h) at Odeillo
Temperature of Operation	1000°C (1832°F)	700° to 1000°C (1292° to 1832°F)
Process Fluid Temperature Profile	Not Available	Not Available
Refractory Temperature	Not Available	Not Applicable
Window Temperature	Not Available	Not Applicable
Operating Pressure	51.7 kPa (75 psig)	Not Available
Pressure Drop (ΔP/P, %)	Not Available	Not Available
Evaluation	Low conversion experiments. Walls of tube are covered with carbon reducing transmissivity. Quartz devitrifies.	Qualitative demonstration successful. Product mix different from expected. Considerable deposition of materials on quartz reactor wall.

- The excellent mixing results in a bed of very uniform temperature for good control of reaction yields and selectivity

- The solids movement acts to disturb boundary layers on containing walls and immersed heat transfer surfaces, reducing film heat transfer resistance, and causing rapid heat transfer between these surfaces and the bed

- The fluidized solids behave like a liquid and can be easily transported into or out of the bed during continuous processing.

As shown in Figure 1 for a gas phase reaction, a commercial scale fluidized bed reactor may be conceived of as a large number of vertical, transparent tubes arrayed in a generally circular pattern to intercept the concentrated flux from a heliostat field. The radiation impinges upon the fluidized solids and the reaction occurs as heat is transferred to the bed by direct absorption, by the mixing action of the bed, and by convective heat transfer between solids and the fluidizing gas. The fluidized bed reactor may be configured as a cavity for good thermal performance at high temperatures or externally heated for lower temperature applications.

Experiments reviewed, Table 6, demonstrated the heating of gases in the fluidized bed reactor and the calcination of limestone. All designs used a transparent quartz reactor vessel in an externally heated configuration. These experiments in small 1.75 to 79 kW (5.97×10^3 to 2.70×10^5 Btu/h) reactors indicate that bed material selection is important both from the perspective of solar absorption and chemical reaction with the quartz container. Discoloration of the reactor walls were observed with silicon carbide and copper shot bed materials. However, reactor performance was not dramatically affected by the discoloration possibly because of the thinness of the layer or its heat transfer qualities. Another interesting result observed in the experiments was a pronounced vertical temperature gradient which is not normally associated with fluidized bed reactors. This condition was attributed to the low gas fluidization velocity used in the experiments and the flux intensity which was directed primarily at the bottom of the fluidized bed. Increased fluidization gas velocity can minimize these temperature gradients. The possibility also exists through gas velocity control and bed material density variances to establish different temperature zones within the reactor.

Fluidized bed reactors have demonstrated capability to absorb high flux levels in direct flux component configurations because of excellent bed

Figure 1. FLUID BED REACTOR CONCEPT FOR A GAS PHASE REACTION

B83020237

Table 6.   FLUID BED REACTORS

Reaction	Air Heating	Air Heating	Limestone Calcination
Researcher	Westinghouse/Georgia Inst. of Tech.	Odeillo Solar Facility	Odeillo Solar Facility
Reference Number	19	12	12
Scope of Effort	Experimental (Series of Experiments)	Experimental	Experimental
Objective	Proof of Principle	Proof of Principle	Proof of Principle
Design Scale	28 to 79 kW (9.6×10^4 to 2.7×10^5 Btu/h)	1.75 kW (6000 Btu/h)	1.75 kW (6000 Btu/h)
Scale of Intended Application	Central Receiver Heat Source	Central Receiver Heat Source	Central Receiver Heat Source
Flux Coupling Method	Direct	Direct	Direct
Material of Construction	Quartz	Quartz	Quartz
Configuration	External	External	External
Windowed Aperture	No	No	No
Schematic Figure Number	12 and 13	16	16
Principal Dimensions:			
Aperture Diameter	45.7 cm (18 in.) Bed Depth Unexpanded	10^{-3} m^2 (1.55 in.^{2}) Cross Section	10^{-3} m^2 (1.55 in.^{2}) Cross Section
Cavity Diameter	30.5 cm (1 ft) OD Tube	10^{-3} m^2 (1.55 in.^{2}) Cross Section	10^{-3} m^2 (1.55 in.^{2}) Cross Section
Cavity Length	41.22 m (4 ft) Length/ 2.5 mm (0.10 in.) Wall	0.3 m (11.8 in.) Length	0.3 m (11.8 in.) Length
Thermal Efficiency	Range 19 to 53%; Dependent on Bed Temperature	40%	20%
Flux Capability:			
Basis	Measured		
At Aperture	Not Applicable	Not Available	Not Available
In Reactor	5 to 10 W/cm^2 (1.59×10^4 to 3.17×10^4 Btu/h-ft^2)	Not Available	Not Available
Temperature of Operation	677° to 1109°C (1251° to 2028°F)	600°C (1112°F)	850° to 950°C (1562° to 1742°F)
Process Fluid Temperature Profile	Figure 14	Figure 17	Not Available
Refractory Temperature	Not Available	Not Available	Not Available
Window Temperature	Not Applicable	Not Available	Not Available
Operating Pressure	101 kPa (14.7 psi)	101 kPa (14.7 psi)	101 kPa (14.7 psi)
Pressure Drop ($\Delta P/P$, %)	Not Available	Not Available	
Evaluation	Proof of principle. Quartz suffered erosion/corrosion. No chemical reactions studied.	Proof of principle. No erosion/corrosion observed.	Proof of principle. Batch process only. No corrosion/erosion observed.

mixing, continuous exposure of fresh material to direct flux heating, and very high heat transfer rates within the bed. The temperature capability of a direct flux fluidized bed reactor is limited by corrosion of the transparent container. Operating temperature of a quartz container is limited to about 900°C (1652°F), with 1000°C (1832°F) possible in a dry, reducing atmosphere. Although quartz is quite hard, it may also be subject to erosion.

When operated in a cavity configuration, fluidized bed reactors are capable of high thermal efficiencies. However, operated as an externally heated reactor, reflection losses may be excessive because of the angle at which flux impinges on the wall. Externally heated designs are simpler and more compact than cavities, but have lower thermal efficiency. Compared to packed bed and rotary kiln reactors, fluidized beds may have significant parasitic power requirements. The fluidizing gas is heated as it passes through the bed. This is acceptable and desirable if the gas participates in the reaction. If the gas does not react, then it is taking energy away from the process. In any case, heat recovery from process gases is essential to maintain efficiency.

In one of the experiments reviewed, which is summarized in Table 6, the receiver absorbed power levels ranging from 28 to 80 kW (9.6×10^4 to 2.7×10^5 Btu/h). Bed temperatures ranged from 706° to 1109°C (1303° to 2028°F). A considerable range of efficiencies were observed consistent with variations in bed materials, particle sizes, air flow rate, and bed temperature. The range was roughly 20% to 40% thermal efficiency. In the other two experiments, Table 6, the reactor was scaled to a downward focusing solar furnace producing an input of power of 1.75 kW (5.97×10^3 Btu/h). At 600°C (1112°F) an efficiency of 40% was observed when operating as a gas heater. Operating at temperatures ranging from about 850° to 950°C (1562° to 1742°F), the reactor efficiency in reacting calcium carbonate was 20%. Efficiency varies as the reaction proceeds because the radiative properties of the system are continuously modified due to the chemical reaction. The radiative properties of the bed are determined by the bed porosity and bubbling behavior as affected by fluidization velocity; particle type, and particle diameter. A more detailed presentation of the fluidized bed receiver/reactor designs reviewed is presented in the Appendix.

Fluidized beds have high thermal inertia and should not be subject to wide temperature swings during transients. Feed rate and gas flow rate may be used to control temperature. Because of inertia, start-up and shutdown times may be long. However, use of smaller tubes with less solids holdup may be considered to speed start-up, if appropriate. Because fluidized beds require a vertical orientation and also need considerable support equipment for feed and discharge, they are strictly applicable only to central receiver applications.

Rotary Kiln Reactor Summary

Many kinds of industrial processes can be performed in a rotary kiln. Some of the more common metallurgical and chemical processes that use the rotary kilns are:

a. Direct Reduction of Iron Ores. Crushed iron ore or iron ore pellets are mixed with excess coal/coke and heated to 1100°C (2012°F) to reduce the ore to metallic iron. The metallurgical product is further processed in electric furnaces to produce steel.

b. Calcination of Limestone. Limestone ($CaCO_3$) is calcined at 1100°C (2012°F) to produce lime (CaO). Dolomite ($CaCO_3 \cdot MgCO_3$) is calcined at 900°C (1652°F) to produce dolomitic lime.

c. Oil Shale and Tar Sands. Retorting by solar heating is possible using pebbles as a heat exchange media; this is much like the TOSCO process, which uses hot pebbles to retort crushed oil shale.

d. Roasting. Ores of gold, silver, iron, etc., containing sulfur and arsenic are roasted at 530° to 1370°C (986° to 2500°F) in air to convert them into oxides. Mercury is recovered by retorting ores in rotary kilns.

e. Calcining. Alumina (Al_2O_3) is produced by calcining aluminum hydroxide from bauxite at temperatures of 1000° to 1400°C (1832° to 2552°F) in rotary kilns. Magnesite ($MgCO_3$), brucite ($Mg(OH)_2$), etc., are calcined at 780° to 1760°C (1436° to 3200°F) to produce magnesia for ceramic applications.

f. Titaniferous Ore. Ilmenite is mixed with carbon and heated in rotary kilns to produce sponge iron and titania (TiO_2).

g. Production of Portland Cement. Limestone, clay, and shale (wet slurry or dry powder) are calcined at 830°C (1526°F) and agglomerated at 1400°C (2552°F) in rotary kilns to produce cement clinker.

Many of these processes operate in the range of 700° to 1200°C (1292° to 2192°F) and the amount of process heat required is significant. The heating

is usually accomplished industrially by a central burner using either natural gas or oil. Use of solar energy to provide the heat requirements for these processes can save substantial amounts of energy.

In contrast to a conventional kiln, a solar rotary kiln need not be extremely long in order to process solids. Kilns are ordinarily heated by combustion gases and the long length is required because convective heat transfer rates from the gas to the solid are slow. In the solar kiln the radiative heat transfer processes are very effective in transporting heat to the reactants so an extremely long kiln is not required.

Kilns are primarily used for solids. It is conceivable that a bed of inerts or catalyst coated inerts might be used for gas phase reactions, but solid-gas contact will not be as good as in a packed bed or fluidized bed unit. With proper selection of materials and material handling devices corrosives and abrasives may be handled. It is also possible that the kiln may be able to handle liquid products such as slag.

Rotary kilns are not suited for distributed collector systems. The flow of materials through the reactor would be negatively affected by the traveling focus. Solids handling for a distributed collector field would be extremely difficult and almost certainly uneconomic.

Rotary kilns are expected to have the capability of accepting flux of 2 MW/m^2 (6.34 X 10^5 Btu/h-ft^2). The cavity effect reduces flux impinging on solids by exposing them to reflected and reradiated flux (for the case of a tower mounted kiln) allowing the matching of heat transfer rate to reaction rate. Retention time may be adjusted by varying the tilt angle of the kiln, kiln length, using flights or chains to hold up material, and adjusting rotational speed to allow sufficient time at reaction temperature so that desired conversions may be achieved. There is no question that commercial kilns are capable of extremely high-temperature operation. The main constraints on solar kiln operation are expected to be materials limitations that result from the need to achieve very high temperatures at the refractory surface that is directly exposed to the flux so that it may reradiate to the cooler reactants. Because the kiln rotates, the hot refractory will continuously rotate in and out of the flux thus exposing it to cyclic temperature variations greater than 500°C (932°F) causing potential thermal shock and fatigue problems.

As expected, the key design issue for scale-up is the design of the transparent aperture. Of course a windowed aperture is not always necessary in cases where gaseous products are nonexistent or innocuous and they need not be collected for further processing. However, products frequently are toxic (that is, carbon monoxide) or they must be processed further (that is, sulfur dioxide from zinc sulfate decomposition). This requires a sealed system and hence a windowed aperture. A window may be necessary to prevent solids from drifting out the aperture and blocking the flux. It may be possible to operate a slight negative pressure to sweep air through the open aperture and collect gases at the feed end if this will not impede downstream processing or significantly reduce collection efficiency. A potential advantage of the kiln is that the window may be positioned away from the reaction zone where it may avoid contact with gases or solids or at least be exposed only to relatively cool solids and gases with the reduced likelihood of chemical or physical interaction that would impede continuous operation.

Based on the literature reviewed, it appears that standard materials handling methods for rotary kilns will be appropriate to solar kilns. However, since the kiln may be windowed, a modified design may be appropriate to isolate products from the window and allowing gaseous products to be safely contained. A possible approach is the use of a "can" or containment vessel around the kiln through which feed and discharge (gas and solid) ports are passed. The containment vessel may have the windowed aperture as part of its structure.

Designs reviewed do not use the flights or chains commonly used in conventional kilns. These devices may throw up a cloud of solids which will "see" the aperture and reduce the cavity effect while also possibly permitting solids to contact the window. Experiments with zinc sulfate decomposition also experienced considerable problems with agglomeration. It may be possible through judicious use of flights and chains within the region of the reactor where this occurs to avoid agglomeration and yet limit the formation of a cloud of particles.

Rotary kilns have fairly high thermal inertia due to holdup of materials within the kiln. They should have reasonable transient performance in that kiln rotational speed and feed rates may be adjusted to compensate for reduced flux while maintaining the reaction. Due to the significant thermal inertia,

start-up times may be long. However, start-up time can be manipulated by adjusting feed rates and rotational speed. Some fossil fuel use may be required to maintain hot standby conditions for rapid start-up. Downstream process equipment must accommodate a varying mix of products and unconverted reactants. Uneven circumferential incident solar flux can lead to failure of the refractory liner due to thermal shock. An insulated aperture shutter may be desirable to reduce heat loss and lower cooling rates during standby.

Table 7 presents a summary of the three rotary kiln research efforts which were reviewed. Experimental reactors ranged in size from 2 to 4 KWth $(6.8 \times 10^3$ to 1.4×10^4 Btu/h). The largest reactor dimensions were 0.30 meters (1 ft) in diameter by 0.91 meters (3 ft) long. Operating temperatures ranged from 800° to 1000°C (1472° to 1832°F) with operating pressures near atmospheric conditions. A conceptual design of a 2 to 3 MW $(6.8 \times 10^6$ to 10^7 Btu/h) rotary kiln reactor for use at the CRTF was also reviewed. The conceptual design reactor is 1.8 meters (6 ft) in diameter and 3.7 meters (12 ft) long with a 1.2 meter (4 foot) aperture diameter. Flux at the aperture is expected to be 1593 kW/m^2 $(5.05 \times 10^5$ Btu/h-ft^2) and the operating temperature 700° to 1200°C (1292° to 2192°F). A more detailed review of these research efforts is presented in the Appendix.

Many uncertainties still exist in solar kiln design. Long term window performance is unknown. It is unknown at this time if large windows can be constructed. Thermal performance of kilns, especially as tied to reaction kinetics is poorly defined. Versatility of reaction capability is apparent from industrial use but not established for the solar environment. Considerable development in regards to windows, transient effects, materials and thermal shock, and performance modeling and scale-up will be required.

Summary of Review

This review of high-temperature solar receiver/reactor research has highlighted the various reactor and reaction types that may be applicable to direct flux reactor design. However, due to the fact that most of the designs reviewed were for small scale applications, especially with parabolic dish receiver, little direct knowledge can be gained from these designs which is relevant to large scale central receiver direct flux reactor design. The primary criteria that can be used to judge applicability of each design reviewed includes:

35

Table 7. REACTOR TYPE: ROTARY KILNS FOR SOLID PHASE REACTIONS

Reaction	Limestone Calcination	Zinc Sulfate Decomposition	Test Facility
Researcher	Odeillo	Shell	SRI International
Reference Number	12	14	18
Scope of Effort	Experimental	Experimental	Conceptual
Objective	Proof of Principle	Proof of Principle	Proof of Principle
Design Scale	2 kW (6800 Btu/h)	9 kW to 14 kW (30,700 to 47,800 Btu/h)	2 MW to 3 MW (6.83 X 10^6 to 1.02 X 10^7 Btu/h)
Scale of Intended Application	Not Available	Not Available	CRTF at Sandia, Albuquerque
Flux Coupling Method	Direct	Direct	Direct
Material of Construction	Metal Shell/Refractory Lined	Metal Shell/Refractory Lined	Metal Shell/Refractory Lined
Configuration	Cavity	Cavity	Cavity
Windowed Aperture	No	Yes (Quartz)	No
Schematic Figure Number	2	1	3
Principal Dimensions:			
Aperture Diameter	0.02 m (0.79 in.)	Not Available	1.22 m (4 ft)
Cavity Diameter	0.02 m (0.79 in.)	30.5 cm (1 ft)	1.83 m (6 ft)
Cavity Length	0.09 m (3.54 in.)	0.91 m (3 ft)	3.66 (12 ft)
Thermal Efficiency	15% (Overall)	Not Available	70% at 1200°C (2192 °F); 80% at 1100°C (2012°F) (Calculated)
Flux Capability:			
Basis	Not Available	Not Available	Average (Çalculated)
At Aperture	Not Available	Not Available	1593 kW/m^2 (5.05 X 10^5 Btu/h-ft^2)
In Reactor	Not Available	Not Available	Not Available
Temperature of Operation	800° to 1400°C (1472° to 2552°F)	1000°C (1832°F)	700° to 1200°C (1292° to 2192°F)
Process Fluid Temperature Profile	Not Available	Not Available	Not Applicable
Refractory Temperature	Not Available	Not Available	Not Available
Window Temperature	Not Applicable	Not Available	Not Available
Operating Pressure	101 kPa (14.7 psi)	101 kPa (14.7 psi)	101 kPa (14.7 psi)
Pressure Drop ($\Delta P/P$, %)	Not Available	Not Available	Not Available
Evaluation	Proof of principle. Batch operation only.	Proof of principle. No serious problems with window. Serious materials handling problems with agglomerating reactant.	Appears technically feasible based on conceptual design.

• The closeness to a commercial scale design

• The use of radiant energy

• The use of direct flux coupling.

Although most of the designs reviewed utilized radiant solar energy, few employed direct flux. Of the experimental reactors that have undergone testing only the rotary kiln reactor concept developed for the CRTF design reviewed could be considered as having a commercially scalable basis. Even this experimental reactor conceptual design was several orders of magnitude away in size from rotary kilns commonly used in industrial applications. The closeness of all reactor designs reviewed to industrial reactor designs is important in order to minimize the risk of scale-up and take advantage of the know-how and technical experience gained in industry through the design and operation of industrially used reactor configurations.

Two of the conceptual designs reviewed; the PFR Engineering Systems steam-methane reforming reactor; and the direct flux rotary kiln developed for the CRTF show promise as the basis for large scale direct flux reactor designs. Extensive industrial experience in high-temperature radiantly heated solids reactors — rotary kilns, and in radiantly heated gas phase reactors — reformers, form the basis for selecting these two designs. Derivations of these conceptual and commercial designs can form the baselines for conceptual direct flux reactor design.

The most seriously limiting factor for direct flux reactor development is the limited availability of, and experience with, transparent material designs. More development and experience is required to demonstrate materials compatibility, erosion, and corrosion of these transparent materials. This indicates a high level of technical uncertainty in the design of commercial scale direct flux receiver/reactors.

37

II. Selection of Reactants

Objective

The objective of this section was to evaluate major issues related to reactant type and to select appropriate reactions for use in assessing engineering and design implications of each reaction on the reactor configuration to be developed in the conceptual design effort in Section III.

Constraints on Reactant Selection

The following important constraints were placed upon reaction selection by the contract work statement.

1. Reaction must be high temperature and endothermic

2. Reaction must be scalable to commercial sizes

3. Reaction must be representative of or applicable to a class of industrial processes.

Since the reactant of choice was to be used as an evaluative tool for purposes of determining technical feasibility, utility, and practicality, the following additional restraints were placed upon reactant selection.

4. The reaction must be well characterized with all pertinent reaction parameters known (for example, heat of reaction, heat capacity, etc.)

5. Products must be of commercial significance either as a fuel or chemical

6. Preference is to be given to simple reactions uncomplicated by side reactions or undesirable by-products.

Processes that depend on solar derived electricity (photovoltaics), photochemistry, or solar produced steam were specifically excluded from consideration in the contract as not falling within the definition of direct flux thermochemical reactions. Also eliminated are processes that require temperatures in excess of 1100°C (2012°F).

A lower temperature has also been used in evaluating reactions for direct solar flux application. It is expected that reactions which proceed rapidly at temperatures below 650°C (1202°F) will be most efficiently performed using indirect solar heating with a secondary heat transfer fluid.[2]

A summary of practical and contractual constraints placed upon the reactant selection activity is as follows:

- 1100°C (2012°F) maximum temperature and 650°C (1202°F) minimum temperature

- Process is endothermic

- Product is of commercial significance

- Reaction is well characterized including kinetics and operating parameters

- Products of reaction are known and predictable

- Thermal requirements (heat of reaction, heat capacity) are known

- Corrosion properties of reactants and products are known

- Transport properties are known.

Preliminary Reactant Evaluation

During the past several years, a large number of processes have been proposed as candidate reactions for solar energy applications. Many of these reactions were reviewed in the course of selecting reactants. Table 8 is a list of the more relevant reactions which were reviewed and eliminated as not fitting the selection criteria. Table 9 lists those reactions which did survive the initial screening procedure. A more detailed discussion of these five reactions follows.

Steam Gasification of Coal or Char

The gasification of coal or char to produce hydrogen and carbon monoxide dates back to 1850.[5] Coal was charged inside an airtight vessel or retort and heated. This distillation or pyrolysis of coal produced methane, and other light hydrocarbons with a heat content of 2.05×10^7 to 2.42×10^7 Joules/m^3 (550 to 650 Btu/cu ft) and coke. Air or oxygen was then blown through the heated coke to raise the temperature to above 1000°C (1832°F). Steam was passed over the hot coke to accomplish the endothermic water-gas reaction.

$$C + H_2O \rightarrow CO + H_2$$
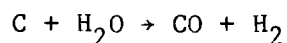
The gas produced was called "blue gas" or "water gas" and had a heat content of 1.12×10^7 Joules/m^3 (300 Btu/cu ft). Today this combination of hydrogen and carbon monoxide is known as synthesis gas. Although gas manufactured from coal made a significant contribution to the U.S. economy in the first part of this century, reaching a peak of 2.83×10^{18} Joules (2.68×10^{15} Btu) in 1949,

Table 8. SOLAR PROCESSES REVIEWED AND REJECTED

Process	Reason for Rejection
1. Ethanol by fermentation	Distillation process only – uses steam as an intermediate heat-transfer fluid.
2. Flash pyrolysis of biomass to produce methanol, char, and hydrocarbons	Good solar match but reactions are insufficiently characterized to use as an evaluative tool for direct flux reactor conceptual design.
3. Gasification of biomass to produce synthesis gas and hydrocarbons	Good direct flux match but reactions are insufficiently characterized to use as an evaluative tool.
4. Furfural production from biomass, sulfuric acid, and steam	Uses steam as a secondary heat-transfer fluid.
5. Flash pyrolysis of coal to produce gas, liquids, tar and coke	Good solar match but reaction is complicated, having many uncharacterized products and high reactant variability.
6. Calcium carbide production from lime and coke[3]	Requires temperatures in excess of 2000°C (3632°F).
7. Shale oil retorting	Requires that temperatures remain below 550°C (1022°F) to avoid carbonate decomposition.
8. Ethylene from catalytic dehydration of ethanol[3]	Temperature range 330°C (626°F) to 360°C (680°F). Best performed using intermediate heat-transfer fluid.
9. Carbothermic reduction of metal ores, including iron ore, alumina and magnesia	Temperature range in excess of 1500°C (2732°F).
10. Elemental phosphorus production from fluorapatite, coke and silica	Temperature range in excess of 1300°C (2372°F).
11. Roasting of sulfide ores to produce metal oxides and sulfur dioxide	Exothermic reactions.
12. Roasting of metals to produce metal oxide pigments	Exothermic reactions.

Table 8, Cont.   SOLAR PROCESSES REVIEWED AND REJECTED

13. Hydrogen sulfide decomposition to produce hydrogen and sulfur[4]

Process is still in bench-scale experimental stages. Conditions are not well characterized.

14. Decomposition of metal oxides to metal vapor and oxygen as one step in a thermochemical water splitting cycle (zinc oxide and cadmium oxide)

Requires temperatures in excess of 1500°C (2732°F). Conditions are not well characterized.

15. Decomposition of sulfuric acid vapor as one step in a thermochemical water splitting cycle

All present day embodiments of this process use either air or steam as an intermediate heat transfer fluid.

Table 9.   REACTIONS IDENTIFIED AS POTENTIAL CANDIDATES
FOR DIRECT SOLAR FLUX APPLICATIONS

Reaction	Product
1. Coal or char gasification with steam	Carbon monoxide and hydrogen
2. Steam reforming of natural gas[3]	Hydrogen and carbon monoxide
3. Thermal cracking of naphtha or higher hydrocarbons[3]	Ethylene, propylene
4. Calcination of limestone	Calcium oxide
5. Metal sulfate decomposition as one step in a thermochemical water splitting cycle.	Oxygen, sulfur dioxide, metal oxide

its use has declined significantly since then in large part as the result of the low price and high heat content, 3.73×10^7 Joules/m^3 (1000 Btu/cu ft), of natural gas. However, with recent increasing demand for natural gas as a clean fuel has come renewed interest in gasification of coal for the production of synthesis gas.

Significant progress has been made in coal gasification in recent years and the cyclic process of air followed by steam followed by air which was used in the past to produce synthesis gas has been surplanted by continuous processes. However, one of the major disadvantages of the coal gasification schemes which use continuous air-blown gasifiers is the low heating value of the fuel produced, 4.10×10^6 to 6.71×10^6 Joules/m^3 (110 to 180 Btu/cu ft). Of course, oxygen and steam can be used to produce a medium-Btu fuel but in both cases as with the earlier cyclic process, a portion of the coal must be consumed to produce the heat for the endothermic reaction, about 1.12×10^4 Joules/gram (4800 Btu/lb). The use of direct solar flux to provide this energy can serve a dual purpose; first, to conserve natural resources, and second, to convert solar energy to a useful chemical form.

Gregg et al.[6] have successfully demonstrated the steam gasification of coal and coke at the White Sands test facility using a direct flux packed bed reactor. Reported results indicate that 1) as much as 48% of the solar energy at the focus of the reactor was converted to chemical energy, 2) about 20% of the heating value of the product gases was due to stored solar energy, and 3) rate of gas production was directly related to flux intensity while product gas composition was independent of flux intensity.

Taylor et al.[7] have investigated the steam gasification of carbonaceous materials in both a packed bed and a fluidized bed reactor using a 2 meter (6.6 ft) diameter parabolic mirror. Reported results indicated that the packed bed was more efficient in converting solar energy to chemical energy than was the fluidized bed (40% versus 10% solar conversion).

Steam Reforming of Natural Gas

Synthesis gas (hydrogen and carbon monoxide) is usually produced by the catalytic steam reforming of natural gas. This synthesis gas is then processed to yield ammonia, hydrogen, or methanol. Approximately 5.7×10^{10} m^3/yr (2×10^{12} SCF/yr) of this synthesis gas are produced in the United

States using 2.85×10^{17} Joules/yr (2.7×10^{14} Btu/yr). In the usual fossil fueled plants, steam and methane are passed through parallel reactor tubes that are filled with nickel catalyst. The inlet of the reactor is maintained at 480°C (896°F) and the outlet at 816°C (1500°F).

$$CH_4 + H_2O \rightarrow CO + 3H_2$$
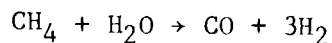
Because the reaction is highly endothermic and the moles of product exceed the moles of reactant, the reaction is favored at high temperature and low pressure (less than 2.76 MPa [400 psi]). An excess of steam is usually used to drive the reaction to completion and help prevent carbon formation.

Temperature control is critical to prevent tube damage and ensure the desired degree of conversion. There may be side reactions including carbon deposition if the gas temperature drops out of the desired temperature range.

Synthesis gas or syngas, is used to produce ammonia, hydrogen, methanol, and oxo-alcohols. These, in turn, are basic building blocks of the fertilizer, petroleum refining, synfuels, and petrochemical industries. Production of ammonia, both in the USA and the world, exceeds that of any other single chemical.

Approximately one-third of this country's feed and fiber production can be attributed to nitrogenous fertilizers nearly all of which are made from ammonia. Hydrogen is used extensively in the petroleum, petrochemical, and food processing industries. It is of particular importance in coal liquefaction, in the production of synfuels and in upgrading of heavy crude oil. Methanol may become an important motor fuel and/or motor fuel additive. A process exists to produce gasoline from methanol and the first commercial application of this process will shortly start-up. Methanol is currently used in the production of many chemicals, including MTBE, an antiknock additive for unleaded gasoline, and formaldehyde, a basic ingredient for urea formaldehyde foam insulation and other polymers. Steam reforming is an economically important process both now and in the foreseeable future.

Steam reforming is also an excellent candidate for investigation as a solar energy user. Roughly half of the hydrocarbons entering a syngas production unit must be burned to provide heat for the endothermic steam reforming reaction. The cost of energy is, therefore, a significant portion of the cost of production of synthesis gas. Alternatively, and for the same

reasons, the steam hydrocarbon reforming reaction is a prime candidate for a means to transform solar energy into a transportable, versatile medium with high energy availability. Steam reforming of hydrocarbons using solar energy would probably be an important segment of a hydrogen economy.

Hydrogen production is the process of choice for direct solar applications for the following reasons. Hydrogen plants are commercial in a variety of sizes from small skid-mounted units to large refinery-scale, whereas commercial ammonia and methanol plants almost invariably require very large reformers. It is desirable that early installations of new technology be both commercially viable and relatively small in scale. Reformers for hydrogen production operate at a temperature between that for ammonia and methanol production. Oxo-alcohol production is not as important economically as ammonia, hydrogen, and methanol; operating temperatures are quite high [over 900°C (1652°F)] and the carbon dioxide recycle would add an unnecessary complication to the study. Hydrogen is the only major application where purge gas is not used extensively as fuel in the reformer. This means that solar energy can potentially have a larger economic impact on hydrogen production than on the other processes.

Thermal Cracking of Naphtha

At the present time, much of the U.S. demand for ethylene and propylene is being met by the thermal cracking of ethane and propane and other light hydrocarbons found in natural gas liquids. It is expected, however, that as the price of natural gas and the associated gas liquids increases, ethylene feedstocks will move toward heavier feeds.[8] Ethylene and propylene can be produced by cracking of hydrocarbon feeds ranging from ethane to vacuum gas oil (boiling range 350°C [662°F] to 600°C [1112°F]). The 1979 U.S. production of ethylene was 13 million metric tons (mmt) having a worth of $4 billion. Principal uses for ethylene are in the production of polyethylene, 5.6 mmt; ethylene oxide and ethylene glycol, 2.5 mmt; and ethylene dichloride, 2 mmt.

In a typical cracking process, feedstock is vaporized and mixed with super-heated steam in a preheater which is supplied with energy from the exhaust gases of the cracking furnace.[9] To bias the product yields in favor of olefins and away from methane and coke formation, low pressures (300 kPa [3 atm]), low hydrocarbon to steam ratios (1:3), are combined with high pyrolysis temperatures (750°C [1382°F] to 900°C [1652°F]) and short residence

times (0.1 to 0.6 sec). The pyrolysis reactor consists of an externally
heated tube of high nickel content steel (ASTM-HP40). The reaction is
catalyzed by the tube walls; no other catalyst is needed. Typical pyrolysis
heater characteristics are listed in Table 10.

Table 10. PYROLYSIS HEATER CHARACTERISTICS

Characteristics	Value
Number of tubes	2 to 20
Length of tube	50 m (164 ft) to 80 m (262 ft)
Gas outlet temperature	750°C (1382°F) to 900°C (1652°F)
Tube wall temperatures	950°C (1742°F) to 1050°C (1922°F)
Maximum wall temperature	1040°C (1904°F) to 1100°C (2012°F)
Average heat absorption	50 to 80 kW/m^2 (1.6 X 10^4 to 2.5 X 10^4 Btu/h-ft^2)
Residence time in reactor	0.15 to 0.6 sec.
Inside coil diameter	50 mm (2 in.) to 200 mm (7.9 in.)
Yearly production of ethylene	8.8 X 10^7 kg (20 X 10^3 tons) to 3.1 X 10^8 kg (70 X 10^3 tons)

Calcination of Limestone

Calcium oxide (CaO) is the second most important bulk chemical, after
sulfuric acid, required by industry. The steel industry consumes over 40%,
water treatment about 14%, and ceramics 8% of U.S. production. Calcium oxide
is produced by decarbonation of calcium carbonate at temperatures between
815°C (1500°F) and 1340°C (2444°F).

$$CaCO_3 \rightarrow CaO + CO_2$$
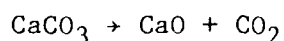
This process is highly endothermic and under operating conditions requires a
heat input of about 8.2 X 10^3 Joules/gram (7.4 X 10^6 Btu/ton). The
calcination is normally carried out in a rotary kiln or vertical stationary
kiln using either natural gas, oil, or coal for the heating.

Although the reaction looks simple and straightforward, in practice, lime
burning is quite complex. The reaction is limited by the heat transfer
through the calcined layer as the reaction proceeds gradually from the outer
surface of the stone particle inward. In general, the larger the particle
size, the higher the temperature required for complete calcination.

If dissociation of the particle is incomplete, there is an unreacted core of $CaCO_3$ and the material is referred to as underburnt. On the other hand, if the stone is calcined for long periods of time at high temperature the lime may be hard-burned or dead-burned. This condition is caused by shrinkage of the lime causing a loss in porosity and reactivity. The objective of the calcination process is to produce soft-burned lime with a core of unreacted $CaCO_3$ of 1% to 2% as this material is more porous and chemically reactive.

Besides the temperature and retention time the size distribution and sulfur content are the most important factors in determining the quality of the product. Relatively narrow size distribution is preferred and the oxidation potential of the gas in the reactor must be carefully controlled to reduce the sulfur content.

In the United States, most lime is calcined in rotary kilns. Although these kilns require higher temperatures, are more expensive, and higher energy consumption than vertical kilns, they also produce the best quality lime at higher output. Rotary kilns also require a more elaborate dust removal system as the dust loading averages 10% of the kiln feed.

One type of vertical kiln that operates at 950° to 1050°C (1742° to 1922°F) consists of two or more shafts within one large refractory-lined shell. The waste heat gases from the shaft that is calcining are used to preheat the feed in an adjacent shaft. Thus, the charging, preheating, calcining, and discharging are performed cyclically at intervals of 10 to 15 minutes.

One factor that may affect the adaptation of calcination to direct solar heating is the ability of the particle to absorb and conduct the energy in a controlled manner to prevent burning of the lime and still produce an almost completely reacted particle. The absorptivity of the limestone can be increased by the addition of about 1% carbon to the feed. This has already been demonstrated in one solar experiment.

Lime, in its various forms, quicklime and hydrated lime, is the principal, lowest cost alkali. In 1981, over 15.4×10^{10} kg (17 million tons) of lime were consumed by the chemical-metallurgical process industries, irrespective of its old established uses in construction, agriculture, and as a refractory material.

Lime is the greatest tonnage chemical consumed in potable and industrial water treatment and probably also in sewage and industrial waste treatment, where its use is growing rapidly as a result of more stringent water and air abatement regulations. In recent years, lime has become a major chemical for scrubbing SO_2 from stack gases at power plants and industrial boilers.

Chemical lime is a term designating a type of quick or hydrated lime low in impurities and possessing a high degree of reactivity making it suitable for use in chemical processes. Commercially, chemical lime is obtained through the controlled calcination of high quality limestone.

Papermaking is one of the major uses of chemical lime where it is used to recover waste sodium carbonate for re-use in the Kraft process. About 90% to 98% of the lime can be recovered by dewatering the waste calcium carbonate and then calcining it in rotary kilns. The waste calcium carbonate is approximately 60% solids, 40% H_2O. The dewatering process requires a large amount of energy due to the vaporization of H_2O. Whereas preheating and calcining of dry carbonate requires approximately 4.8×10^3 Joules/gram (4.2×10^6 Btu/ton), processing of wet slurry requires approximately 8.2×10^3 to 9.3×10^3 Joules/gram (7 to 8×10^6 Btu/ton). Furthermore, the pulp and paper industry cannot use coal to drive the kiln due to fly ash contamination. Consequently, oil or gas, which is two to three times higher in cost per Joule, is used as the energy source. Given the energy intensive nature of this recovery process and the interest of paper manufacturers for alternate energy sources, this specific application is an excellent candidate for solar energy.

Zinc Sulfate Decomposition

An alternative to the decomposition of sulfuric acid used in the General Atomic and Westinghouse thermochemical water splitting cycles is the formation and decomposition of zinc sulfate.

The addition of the ZnO to sulfuric acid forms a solution of zinc sulfate that precipitates as the monohydrate on heating due to its retrograde solubility. The solubility of $ZnSO_4 \cdot H_2O$ approaches zero at about 252°C (485°F). The monohydrate is then dehydrated at temperatures above 202°C (395°F). The zinc sulfate decomposes at temperatures above 902°C (1655°F) and has a total equilibrium pressure of 101 kPa (1 atm) at about 1027°C (1880°F).

At this temperature, the SO_3/SO_2 equilibrium is also shifted toward the production of SO_2, thus reducing the amount of separation and recycle.

Krikorian and Shell have investigated the decomposition of zinc sulfate using both tungsten image lamps and solar energy as heat sources.[10,11] The decomposition occurs in two steps, first to the oxysulfate (ZnO·2 ZnSO$_4$) and then to the zinc oxide.

There is evidence that this reaction is kinetically controlled and that the formation of the zinc oxide has an autocatalytic effect on the decomposition. It also seems that rapid heating speeds the reaction either by "exploding" the particles of zinc sulfate as it passes from the alpha to beta phase or by causing the decomposition to bypass the formation of oxysulfate.

Krikorian and Shell's work using a solar rotary kiln pointed up some severe problems in conducting this reaction. The zinc sulfate agglomerated near the feed point at the back of the kiln when the temperature approached 702°C (1295°F). They used a mechanical scrapper and chains suspended at the inlet to break up these agglomerates and also found that the addition of 50% aluminum oxide prevented the agglomeration. They also reported that there was evidence of decomposition at temperatures as low as 702°C (1295°F) but only on the side of the particle exposed to the flux. This leads to the suspicion that the surface temperature of the particle is much higher than the measured temperatures. The rotary kiln window seemed to be self-cleaning when the flux was directed into the furnace except when dusting was so severe that the window became opaque. They concluded that much laboratory work remains to be done to solve the problems of agglomeration and decomposition kinetics.

Additional Selection Criteria

The following additional criteria was applied to the selection process to allow discrimination between the five candidate reactions.

1. The process selected must be site compatible with insolation and require a minimum number of changes in the chemical process to which it is applied.

2. The process should be tied to a chemical which is not rapidly declining in production and/or shifting to import.

3. The process must have substantial energy requirements not provided elsewhere such as through the burning of by-product gases.

4. The process must represent the potential to be a financially attractive investment.

5. Reactions should be consistent with efficient operation of a central (power tower) receiver/reactor.

6. Reactions should benefit from "solar unique" features of the application.

7. Both the overall process and the solar receiver/reactor must meet environmental protection and environmental impact criteria consistent with societal requirements.

8. The application should fit within federal funding guidelines to development of core technology with high-risk/high-payoff potentials.

Choice of the Gas Phase Reactant

Naphtha cracking fails to meet several of these final selection criteria. The production of ethylene is expected to move toward imports over the next decade as large quantities of gas liquids become available in northern Canada and the Middle East.[12] Naphtha vapor is essentially transparent to solar radiation and requires a solid material to intercept the solar flux and convert it to heat. However, since no catalyst bed is required for the reaction, the most likely candidate for a solid heat transfer material is a nickel-steel tubular reactor heated externally by direct flux. As a consequence, there would be no "solar unique" aspects to this design above and beyond those which are already in place at Barstow. Optimum pressure for naphtha cracking is between 101 and 304 kPa (1 and 3 atm) and, as a consequence, few demands would be placed on the materials. In other words, solar-powered naphtha cracking is not viewed as a high risk technology.

Steam reforming of natural gas, on the other hand, requires a supported catalyst, which could be mounted inside a transparent vessel, has an optimum operating pressure in the range of 1.01 and 3.04 MPa (10 to 30 atm), and produces an important product, hydrogen, which has no import competition. In general, the development of a direct flux reactor for this process represents a high technological risk whose payoff cannot be compromised by imports. Because of the perceived technical difficulties in adapting steam reforming to direct solar flux receiver/reactors, this process also represents a good driver for solar technology development.

Choice of the Solid Phase Reactant

The zinc sulfate decomposition reaction is a challenging process which fits well with the definition of high risk. The thermal decomposition aspects of the reaction can be viewed as generic and indeed a solar technology developed for zinc sulfate would have wide applicability in other areas such as the roasting of metal sulfide ores. However, when the zinc sulfate reaction is tied to a much larger and more complicated chemical process such as General Atomic's sulfur-iodine thermochemical water-splitting cycle, the mid-term financial incentives required to make this reaction the process of choice are lacking.

Ultimately, in the absence of government incentives, all schemes for converting solar energy to transportable fuels must compete in the market place with oil and natural gas on a dollars per 10^9 Joule basis. Current prices for natural gas delivered to the industrial consumer range from \$3.79 to \$6.62/10^9 Joule (\$4 to \$7/million Btu). Although these prices can be expected to rise as the use of expensive deep-well gas increases, the cost of solar-derived hydrogen will not be competitive with natural gas on a dollars per 10^9 Joule basis in the foreseeable future. Likewise, since the primary source of hydrogen for chemical use is the steam reforming of natural gas, the price of chemical hydrogen is tied to the price of natural gas as a feedstock.

Although thermochemical water-splitting is an excellent high-risk/high-payoff research pursuit, the time frame for its adoption as a commercial process must be placed sometime in the second decade of the 21st century: well beyond the mid-term time frame which this program addresses.

The steam gasification of coal or char to produce synthesis gas is also a good match for direct flux in every category of criteria except financial viability. In the near-term and mid-term, solar energy must be viewed as a source of high quality process heat for the production of chemicals. It is only in the long-term that dwindling supplies of fossil fuels make solar fuels a financially viable proposition. Thus, for the mid-term, the financial viability of solar energy is tied to the cost of the fuel which it replaces. For example, in the steam reforming of natural gas, the solar energy is used to replace that portion of the natural gas used for fuel, as opposed to that portion used for feedstock. Thus, a one-to-one correspondence exists between a Joule of collected solar energy and the Joule of natural gas it replaces.

In a thermochemical water splitting cycle, hydrogen is produced at a thermal efficiency of from 30% to 50%, but many of the inefficiencies are related to nonsolar processes. Therefore, it requires from 2 to 3 Joules of collected solar energy to produce 1 Joule of hydrogen energy. As a consequence, a Joule of solar energy used to displace natural gas in the steam reforming reaction is two to three times more valuable than a Joule of solar energy used in a thermochemical water splitting cycle even through hydrogen is the final product in both cases.

In the case of steam gasification of coal, the fuel being replaced is coal. Coal represents a far more abundant and less expensive fossil fuel than either natural gas or oil. Furthermore, one of the most important "solar unique" aspects of solar energy, environmental acceptability, would have little impact in this application since sulfur removal and particulate collection equipment would still be required to handle contaminants coming from the feedstock. Clearly, this application lacks both the environmental and financial incentives required.

Of the three solid phase reactants, the one which best fits all of our criteria is the calcination of limestone. In this application, solar energy would be used to displace oil or natural gas. The products of the reaction are environmentally benign. Storage of either reactants or products in off-hours does not present a problem. A minimum of process development leading up to and away from the solar receiver/reactor would be required for any future demonstration project thus freeing the maximum amount of available funds for solar technology development. On the other hand, the technological obstacles which must be overcome especially in the interfacing of the solar flux with the reactant and in process control place this choice in the high-risk/high-payoff category and makes it a good driver for solar technology development.

III. Selection of Reactor Configurations and Conceptual Designs

Objective

The objective of this section (selection of reactor configurations and conceptual designs) was to develop two conceptual designs (one solid phase reactor, one gas phase reactor) for direct flux chemical reactors. Selected designs are to be capable of operating at a scale typical of industrial fuels and chemicals operations. The goals are a) to identify the reactor designs based on sound engineering design principles, b) to evaluate construction and fabrication aspects of reactor designs in sufficient detail to establish the technical feasibility of the design concepts (that is, can they be made), and c) to estimate the technical performance specifications of the concepts (that is, thermal efficiency, product throughput, reactor dimensions).

Methodology

The development of conceptual designs of direct flux reactors consisted of the following activities:

- Review transparent material types, availability, physical characteristics, thermal and chemical performance, cost, and fabrication issues to determine influence on reactor selection and configuration

- Develop and apply a reactor screening methodology

- Identify calciner and steam reformer technical requirements and constraints

- Develop calciner and steam reformer initial design concepts

- Select operating scale

- Develop and implement reactor models

- Develop technical specifications and drawings.

Assessment of Transparent Materials

The Statement of Work calls for identification and analytical evaluation of direct flux solar chemical reactors. The term "Direct Flux" is understood to mean the reactants are heated by direct, reflected or reradiated solar flux without intervening opaque walls.

This definition constrains the direct flux reactor to have means for admitting the solar energy through an aperture into the reactor chamber

53

(cavity). The aperture may be windowless (open to the atmosphere), windowed (to contain noxious by-products or pressurized reactions), or may consist of transparent reaction chambers within a radiation cavity. External reactors, wherein the transparent reaction tubes are exposed to the concentrated solar flux without benefit of a radiation cavity, may also be considered. External reactors, however, characteristically exhibit low thermal efficiencies due to reradiation and convective losses and are too inefficient to be cost effective when operated at elevated temperatures.

Since most industrial chemical or thermochemical fuel reactions do involve noxious reactants, identification and assessment of chemically and mechanically compatible window materials is essential to the extension of direct solar chemical technology to other economically viable reactant/reactor couples.

The practicability of sealed direct flux chemical reactors, which require transparent materials (windows or tubes), obviously hinges on the availability of suitable materials in appropriate sizes for the application. Assessment of light transmitting materials and identification of research and development needs is thus given priority in this program.

Generic Window Issues

Solar Coupling

A radiation cavity with a large internal area to aperture area ratio (cavity ratio) radiates to a hemisphere as if the aperture were a diffuse flat plate radiating at the effective cavity temperature. Internal geometry of the cavity is relatively unimportant unless hot spots are physically near the aperture or have a large view factor to the outside.

At the high temperatures (700° to 1100°C [1292° to 2012°F]) of interest in this study, thermal reradiation from the receiver varies from 50 to 150 kW/m^2 (1.6 X 10^4 to 4.8 X 10^4 Btu/h-ft^2). This represents a power loss ranging from 3-1/2% to as much as 60%, depending on mirror field performance and receiver configuration. A well designed cavity receiver with optimum aperture sizing coupled with a high performance heliostat field would experience 3.5% to 10% reradiation losses depending on the operating temperature. External receivers with no cavity and large receiving area would experience the largest losses.

Receivers with open apertures are additionally subject to significant convection losses which can vary from 1% to 2% for downward facing apertures to as much as 15% to 20% for horizontal facing apertures. Cylindrical shapes, such as typical kilns with near horizontal orientations, would experience losses on the order of 15% unless fitted with downward facing aperture shrouds, convection suppression curtains (also known as air curtains or air windows), or windows.

Windows suppress convectively driven mass transfer loss through the aperture. Obviously, downward facing cavities (acting like a hot air balloon) are relatively insensitive to this effect, but side facing and upward facing cavities can suffer large losses (20% to 30% and more) through an open aperture.

Even radiant tube receivers with open apertures suffer substantial heat loss to the environment as the radiantly heated tubes are quenched by the relatively cool convection currents.

Reactors processing noxious material require a positive containment seal between the reaction and the ambient. In the case of a bulk cavity reactor processing noxious solids in a fluidized bed, entrained flow configuration, or kiln, a window at or near the aperture provides the containment.

Placement of a window at a cavity aperture affects receiver efficiency by counteracting factors. Reflection from the window surfaces and absorption within the window reduce the total solar energy delivered to the receiver cavity. Counteracting these effects, suppression of IR reradiation losses and elimination of convective and mass transport losses have the effect of increasing net power available within the receiver to drive endothermic reactions. Figures 2, 3, and 4 show these effects. The radiation loss values shown on the figures were calculated for a concentration ratio of 1500 suns as a function of temperature. Convection loss data in the figures are derived from measured and reported results of Sanders Associates 1/4 MWth receiver tested at Georgia Institute of Technology, their open aperture receivers tested at the Parabolic Dish Test Site at Edwards, California and the performance of the Solar One Receiver at Barstow, California. The top figure in Figure 2 has a side facing aperture (shown schematically at the top of the graph) like the Solar One Receiver. In general, thermal performance values are representative of receivers with a cavity ratio of five or greater. The

APERTURE LOSSES FROM A VERTICAL CAVITY

○ RADIATION
△ CONVECTION

HOT AIR CARRIES AWAY HEAT

RADIATION OUT

SOLAR IN

TUBES

CONVECTION: FLOW OF COOL AIR WIPES TUBES

APERTURE LOSSES FROM A CAVITY RECEIVER WITHOUT WINDOW

CONVECTION LOSSES ARE RELATIVELY SMALL

RADIATION OUT

SOLAR IN
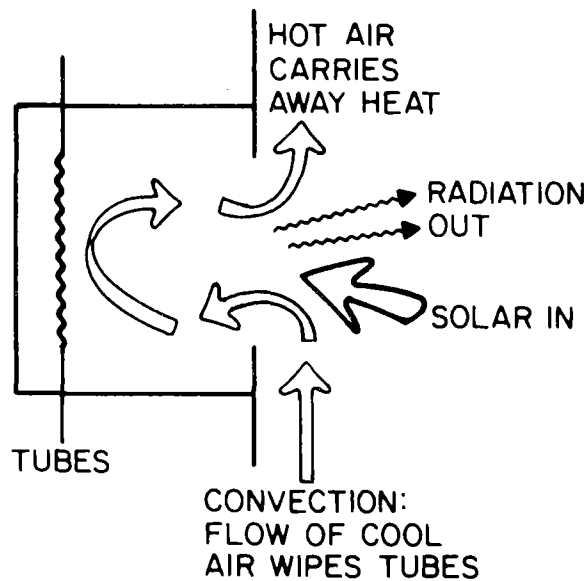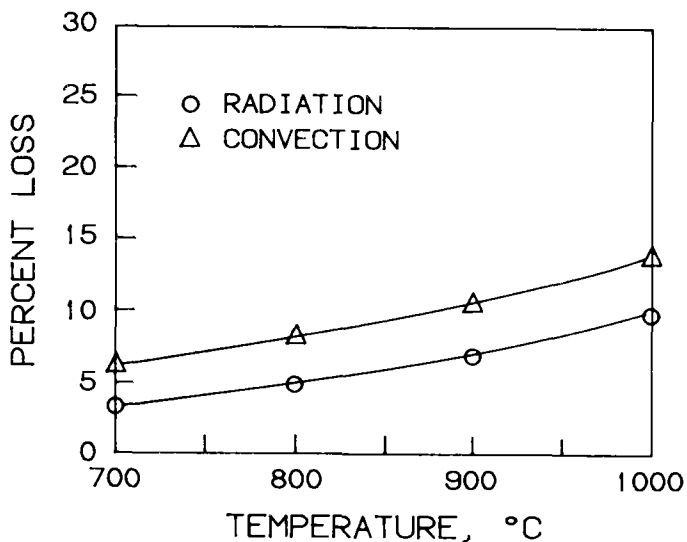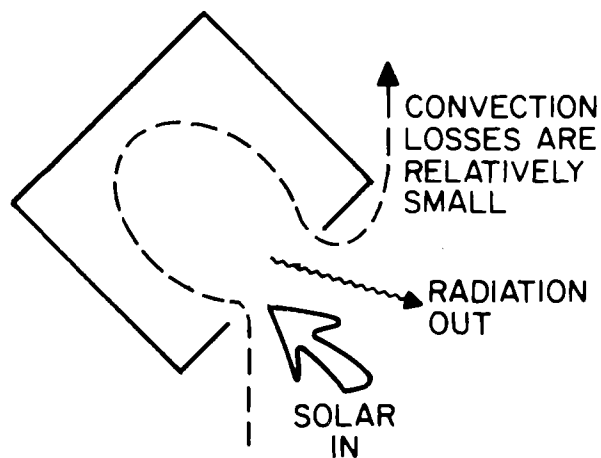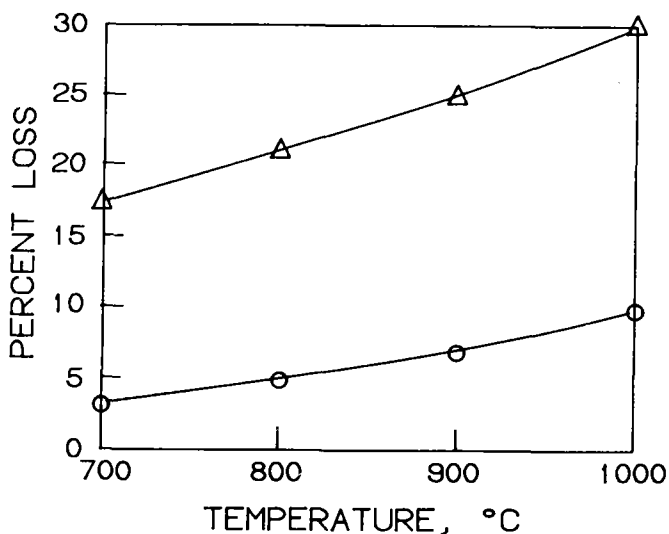
A84070641

A84060586H

Figure 2.   APERTURE LOSSES FROM A CAVITY RECEIVER WITHOUT WINDOW
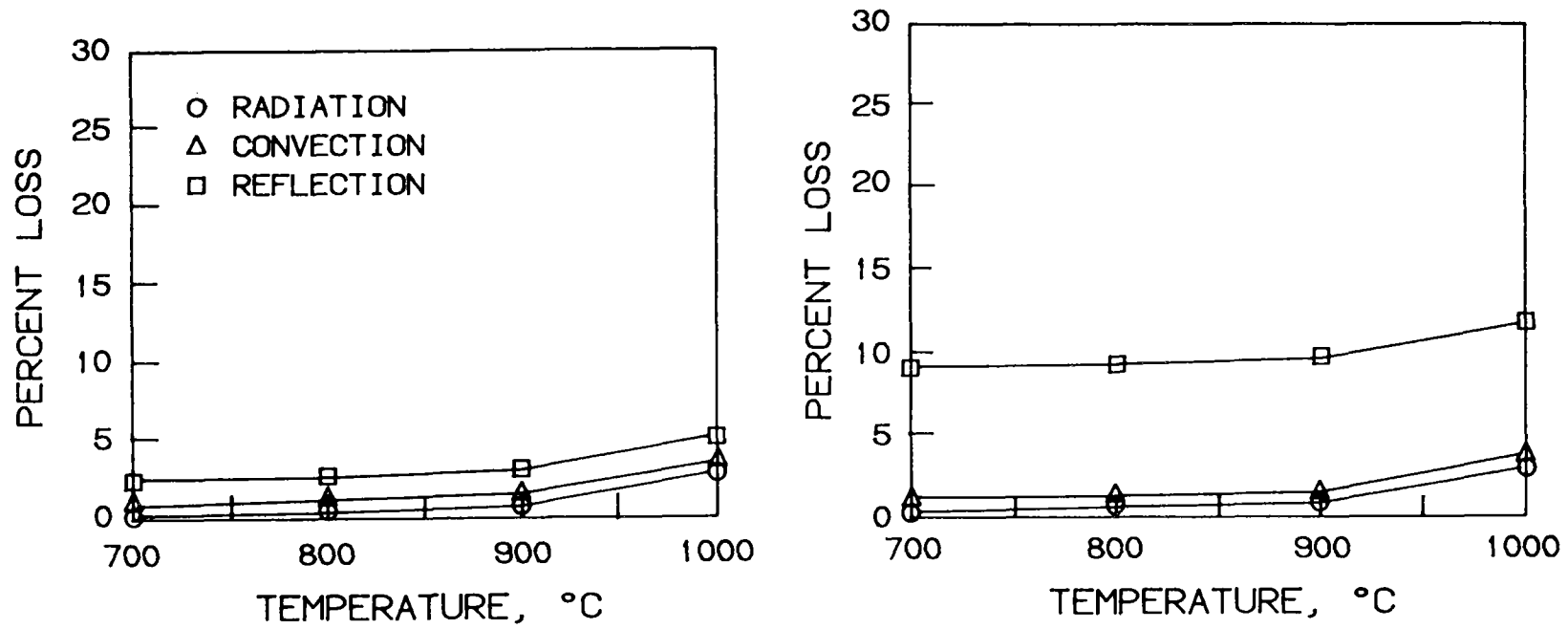
A84060587H

Figure 3. APERTURE LOSSES FROM A CAVITY RECEIVER WITH WINDOW
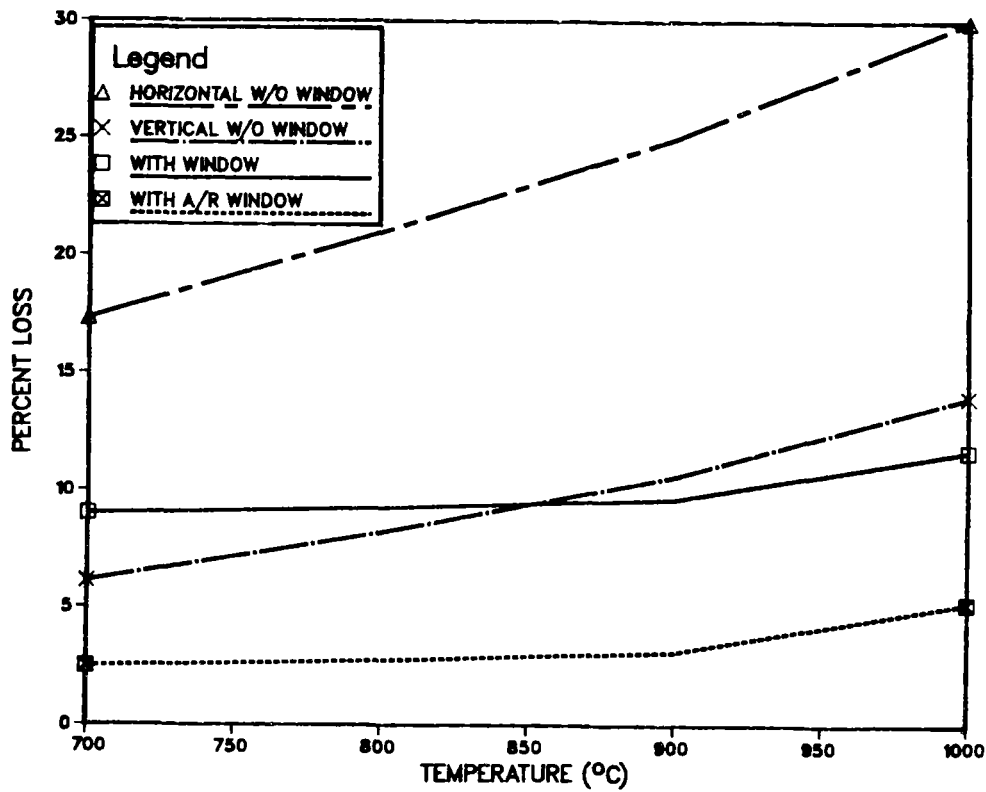
Figure 4.   COMPARISON OF APERTURE LOSS WITH AND WITHOUT WINDOWS

graph at the bottom of Figure 2 represents receivers with apertures oriented from zero to 20° of the vertical. The schematics in Figure 2 illustrate how the convective losses are influenced by receiver orientation. As shown in Figure 4, total convection and radiation losses from windowed receivers are generally less than from nonwindowed receivers. Losses from windowed receivers are not significantly sensitive to receiver orientation. The use of anti-reflective (AR) coatings on windows, if the technology can successfully be developed for high flux, high-temperature applications, will dramatically improve receiver performance.

As shown in Figures 3 and 4, from a net energy standpoint, a receiver coupled to a typical heliostat field with 1500:1 concentration enjoys efficiency improvements at most operating conditions when an aperture window is installed. If AR coatings (as are currently being pursued in support of the high energy laser programs) are successful, then the windowed receivers will enjoy even greater performance advantages over open (nonwindowed) receivers. A window coated with anti-reflective materials has a very low reflection loss. Losses are about 8% in windows without anti-reflection coatings.

Window Materials

Candidate window materials considered in this study were synthetic quartz, synthetic sapphire, spinel, and Vistal. Synthetic quartz is produced by melting of high purity silicon dioxide. Synthetic sapphire is a crystalline material with the chemical formula Al_2O_3. Spinel is a high purity material with the composition $MgAl_2O_4$. Vistal is a polycrystalline form of Al_2O_3.

Those key technical parameters selected for comparative assessment of candidate window materials are outlined in Tables 11 and 12. Table 11 highlights those parameters which are readily quantified, such as physical properties while Table 12 highlights those which are more qualitative. The relevance of each of these parameters as applied to a direct flux chemical reactor is discussed in the following subsections and summarized in Tables 13 and 14.

Table 11. PHYSICAL PROPERTIES OF MATERIALS

Property	Synthetic Quartz	Sapphire	Spinel	Vistal
Transmission, %				
Visible	90–95	86	86	80
IR	90–95 to 2μ	80–82 to 4μ	80 to 4.5μ	80 to 2.5μ
Index of Refraction @ 20°C–25°C (68°F–77°F) @ Sodium D. Line	1.46	1.76	1.719	Not Available
Max Op Temp, °C (°F)	952 (1746)	2000 (3632)	(melt pt) 2127 (3861)	1900 (3452)
Thermal Conductivity, W/m-°C, (Btu/h-ft^2-°F)	(@ 20°C/68°F) 1.38 (0.80) (@950°C/1742°F) 2.68 (1.55)	(@ 20°C/68°F) 36.0 (20.8) (@ 950°C/1742°F) 6.27 (3.62)	(@ 100°C/212°F) 14.93 (8.63) (@ 1200°C/2192°F) 0.0130 (7.51x10^{-3})	(@33°C/91.4°F) 39.7 (22.9) (@ 500°C/932°F) 7.78 (4.50)
Thermal Expansion, (per °C, per °F)	(0–100°C, 32–212°F) 5x10^{-7}, 2.8x10^{-7} (0–900°C, 32–1652°F) 4.8x10^{-7}, 2.7x10^{-7}	(25°C, 77°F) 4.9x10^{-7}, 2.7x10^{-7} (900°C, 1652°F) 8.5x10^{-6}, 4.7x10^{-6}	(10–200°C, 32–392°F) 5.6x10^{-6}, 3.11x10^{-6} (0–1000°C, 32–1832°F) 7.9x10^{-6}, 4.4x10^{-6}	(20–200°C, 68–392°F) 6.5x10^{-6}, 3.61x10^{-6} (25–1000°C, 77–1832°F) 8x10^{-6}, 4.4x10^{-6}
Tensile Strength N/m^2, psi	(20°C, 68°F) 5x10^7, 7.3x10^3 (1000°C, 1832°F) 5.1x10^7, 7.4x10^3	4.8x10^7, 7x10^3	1.2x10^8, 1.7x10^4	(25°C, 77°F) 2.07x10^8, 3.0x10^4 (1000°C, 1832°F) 1.03x10^8, 1.49x10^4
Specific Heat, (25°C, 77°F) cal/gm-°C (Btu/lb-°F)	0.18 (0.18)	0.18 (0.18)	0.20 (0.20)	0.21 (0.21)
Density, gm/cc (lb/ft^3)	2.20 (137)	3.97 (248)	3.58 (223)	3.95 (245)
Thermal Diffusivity	8.33x10^{-3}	0.120	4.98x10^{-2}	0.114

Table 12. WORKING PROPERTIES OF MATERIALS

Property	Synthetic Quartz	Sapphire	Spinel	Vistal
Chemical Resistance				
Acids	Fair	Good	Good	Good
Bases	Fair	Good	Good	Fair
Gases	Fair	Good	Good	Good
Sealing	Mechanical Only	Can be metallized	Can be metallized	Can be metallized
Addition of Reflective Coatings	Yes	Yes	Yes	Yes
Weather Resistance				
Surface Hardness	5.5 - 6.5 (Moh's)	9 (Moh's) 1525-2000 (Knoop)	1300 (Knoop)	1700 (Knoop)
Shapes Available				
Flat Plates	152 cm (60 in.) diameter	20.3 cm (8 in.) diameter	17.8 cm (7 in.) diameter	17.8 cm (7 in.) diameter
Cylinders	50.8 cm (20 in.) diameter	17.8 cm (7 in.) tube	Processing equipment currently not built	17.8 cm (7 in.) diameter by 17.8 cm (7 in.) height
Reference:	Heraceus Amersil	Saphikon/ Crystal Systems	Coors	Coors

61

Table 13. PHYSICAL PROPERTIES CRITERIA

Physical Parameters for Window Evaluation

Quantitative Parameters	Comments
Transmission, %	
Visible	Should be high
IR	High for tubes, low for windows
UV Resistance	Should be good, or reversible
Index of Refraction	Affects reflection losses: index of refraction should be low near that of air
Max Op Temp, °C (°F)	Windows 1027 (1881), Tubes 1327 (2421)
Thermal Conductivity	Low for window efficiency, high for tubes
Thermal Expansion	Low desired
Tensile Strength	High for pressure and thermal shock
Specific Heat	Low for thermal shock resistance
Density	Low for thermal shock resistance
Thermal Diffusivity	High for thermal shock resistance
Young's Modulus	Low for thermal shock resistance

Table 14. WORKING PROPERTIES CRITERIA

Parameters for Window Evaluation

Qualitative Parameters	Comments
Chemical Resistance	
Acids	Requires research of empirical data
Bases	specific to application for definitive assessment.
Gases	
Sealing	Expansion coefficients a key concern
Addition of Reflective Coatings	Heat resistance important, will improve receiver efficiency.
Weather Resistance	Important for windows and heliostats
Surface Hardness (Moh's or Knoop)	Indicates abrasion resistance
Shapes Available	A function of material and processes
Flat Plates	For windows
Cylinders	For tubes and vessels
Curved Plates	For pressurized windows

Optical

The first criteria for window selection is optical transmission of solar radiation. Percent optical transmission is critical not only for energy transfer efficiency but also for minimizing radiative absorption which would overheat the material. Figure 5 shows the spectral distribution of solar energy at the earth's surface (that is, including the effects of atmospheric attenuation). As most of the available solar radiation falls within 0.9 to 2.5 microns, materials were reviewed for transmission in this region.

As can be seen in Figure 5, less than 1% of the solar terrestrial spectrum falls within the UV region, therefore, transmission of UV was not heavily considered. However, prolonged UV absorption can discolor and degrade some window materials.

Optical transmission as a function of temperature was also considered, as the window will operate at elevated temperatures. Limited data was available for transmission at 1000°C (1832°F) temperatures.

The index of refraction is presented as this chiefly determines the reflection losses of the material. Those substrates (uncoated window materials) with lower indices of refraction allow higher entrance optical transmission over wide incident angles. The transmission values reported include these reflection losses.

Thermal

The temperature operating regime has previously been specified as 700° to 1100°C (1292° to 2012°F). To allow a margin of safety for possible process upsets, the window material should maintain its integrity at temperatures to 1400°C (2552°F). Materials exhibiting melting points less than 1100°C (2012°F) were considered unacceptable. For purposes of this review, a minimum non-operating temperature of 0°C (32°F) was arbitrarily chosen to evaluate behavior within the thermal cycling limits. The following discusses the thermal properties reviewed.

A low thermal conductivity value, k, is desired to minimize heat losses from within the reactor through the aperture to the environment. A low k value will, however, cause larger thermal gradients across the window face and induce higher stresses on the window. Note that thermal conductivity values vary with temperature, k(t), further complicating the evaluation.

64
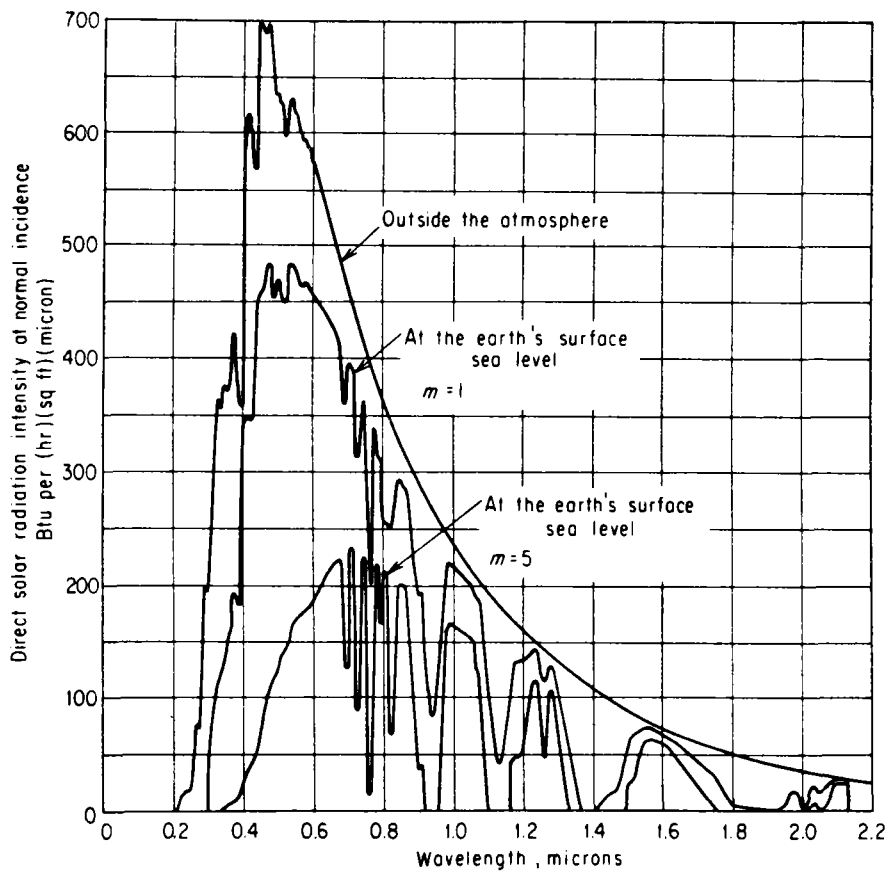
Figure 5. SPECTRAL DISTRIBUTION OF DIRECT SOLAR RADIATION INTENSITY
AT NORMAL INCIDENCE FOR THE UPPER LIMIT OF THE ATMOSPHERE
AND AT THE EARTH'S SURFACE DURING CLEAR DAYS

Similarly a low thermal expansion value is desired to enhance thermal shock resistance to reactor start-up and shutdown. Furthermore, a low thermal expansion value is desirable to maintain sealing integrity. Diurnal cycling, unless mitigated by standby heating at night and by the use of low expansion materials, will accelerate reactor aging and favor premature failure.

Density (ρ) and specific heat (c_p), were reviewed to determine the thermal diffusivity $\alpha = (k/\rho * c_p)$ of the materials. A higher α value indicates faster diffusion of heat through the material. Materials with a high thermal diffusivity and a low thermal expansion coefficient will exhibit good thermal shock resistance because localized thermally induced stresses are avoided.

Thermal Stresses

Thermal stresses are an important design concern in high-temperature solar receivers. A high thermal diffusivity and low thermal coefficient of expansion are helpful in reducing thermal stresses and so forestall material failures due to thermal cycle fatigue. The window aperture shape (flat plate or cylinder) will influence the stresses seen by the window.

Quartz was used as the flat plate window of the successful high-temperature solar receiver built and tested by Sanders Associates in 1980. However, at maximum receiver operating temperatures (1500°C [2732°F]) the window was stressed to approximately 18.6 MPa (2700 psi) due to the temperature gradient through the thickness of the window.

The relatively lower temperature of interest in this study will result in sharply reduced infrared heating of an aperture window; window thermal stresses will be well below 6.9 MPa (1000 psi).

A major problem experienced in opaque (tube) heat exchangers in several of the solar receivers developed since 1978 was the severe hoop (circumferential) stresses created in tube walls by radial temperature gradients. The problems are well known to boiler designers. Generous tube area is required to reduce the energy flux (power/unit area) in the tube walls.

Transparent tubes have an advantage here, because the visible solar energy is transmitted (radiated) and only the far IR portion of the energy must be conducted inward through the tube walls.

The greenhouse effect that is beneficial at a receiver aperture, however, is not necessarily beneficial at a transparent tube within a cavity receiver.

Unless the tubes have significantly more area than the cavity walls, much of the incoming solar radiation will impinge on the walls and, in effect, be converted to a flood of infrared radiation within the cavity. Quartz tubes are opaque to infrared beyond 2.65 microns, so they are subject to the same kind of stresses experienced by boiler tubes.

To address the possibly adverse effects of the greenhouse effect on transparent tubes in a cavity and to demonstrate transparent tube advantages over radiantly heated opaque tubes, a simple analysis was performed on five representative high-temperature materials that are (or could be) available in tube form. Spinel and sapphire are included, because their transmission in the IR extends further than quartz. (See Table 16.)

Representative stresses and factors of safety (defined as the ratio of tensile strength to thermal stress) are given for silicon carbide, Inconel, quartz, and spinel and sapphire tubes exposed to solar energy and IR from an adiabatic cavity wall. Assumptions are listed below in Table 15. Temperature gradients are based on a flux at the tube surface of 300 kW/m^2 (9.52 X 10^4 Btu/h-ft^2), which is the maximum flux a directly irradiated tube would see.

Table 15. BASELINE RECEIVER ASSUMPTIONS

Solar Concentration at Aperture	1500:1
Cavity Ratio (internal area ÷ aperture area)	10:1
View Factor, Aperture to Tube	.5
View Factor, Aperture to Cavity Wall	.5
View Factor, Cavity to Aperture	.2
Reaction Temperature	900°C (1652°F)
Cavity Wall is Perfectly Insulated	
Tube Wall Thickness	6.35 mm (.25 in.)

Review of the analysis results show both quartz and sapphire achieve high safety factors. A safety factor less than unity suggests the possibility of failure/rupture. Quartz by virtue of its very low coefficient of thermal expansion has low stresses. Sapphire, by combination of high IR transmissibility, high thermal conductivity, and low Young's modulus experience very low absolute stress levels. Note the significant temperature gradient in the quartz tube. Spinel and sapphire achieve low temperature gradients. This low temperature gradient reduces cavity temperature and hence

67

Table 16. THERMAL STRESS COMPARISON OF RADIANTLY HEATED TUBES

Material	SiC	Inconel	Quartz	Spinel	Sapphire
Conductivity, W/M°K (Btu/h-ft-°F)	7.7 (4.5)	7.7 (4.5)	2.2 (1.3)	8.0 (4.6)	13 (7.5)
Thermal Expansion Coefficient, per °C (per °F)	4E-6 (2.2E-6)	16.4E-6 (9.1E-6)	.48E-6 (2.7E-6)	7.9E-6 (4.4E-6)	8.5E-6 (4.7E-6)
Young's Modulus of Elasticity, MPa (psi)	4.1E05 (59.E6)	2.1E6 (30.E6)	8.0E04 (11.6E6)	2.7E5 (39E6)	3.2E4 (4.7E6)
Transmitted Flux, kW/m^2 (Btu/h-ft^2)	0	0	150 (47600)	250 (79300)	225 (71300)
Conducted Flux, kW/m^2 (Btu/h-ft^2)	300 (95100)	300 (95100)	150 (47600)	50 (15900)	75 (23800)
Temperature Gradient, °C (°F)	248 (446)	248 (446)	434 (981)	39.8 (71.6)	36.7 (66.1)
Stress, MPa (kpsi)	202 (29.3)	0.42 (61.0)	8.34E-03 (1.21)	4.3E-02 (6.23)	5.0E-03 (.73)
Factor of Safety	1.1	.67	8.56	1.57	8.0

radiation loss. Cavity temperature might be reduced by 210°C (378°F) by the use of spinel or sapphire instead of Inconel. This is the chief potential advantage of direct flux utilization. However, quartz does not offer significant advantages over metals when used in a cavity receiver configuration.

Mechanical

Differential pressures between the receiver and the ambient will impose bending stresses on windows and hoop stresses on tubes. The hoop stress in a thin walled tube due to an internal pressure is simply:

$$\sigma = \frac{pr}{t}$$

where:

σ = stress

p = pressure

r = inside radius of tube

t = tube wall thickness.

Longitudinal stress is half the hoop stress.

The maximum stress in a unclamped circular window uniformly loaded and supported around the edge is (from Mark's):

$$\sigma \text{ max} = \frac{1.125 \ r^2 p}{t^2}$$

where:

σ = stress

p = pressure

r = window radius

t = window thickness.

Depending on the materials selected, it is straightforward to determine maximum allowable pressures as a function of size and thickness.

The real issue is the avoidance of stress concentrations. Since ceramics and glasses are prone to fracture (they usually fail catastrophically in tension) from crack tip propagation or stress concentration, these materials

69

should be designed to operate with large factors of safety. Care should be taken to isolate the windows or tubes from point loads. Supports and sealing interfaces need to be detailed carefully.

Surface hardness gives some indication of the materials resistance to dust and other environmental factors. High durability will reduce maintenance requirements and operating costs. Ultimately, the resistance of the AR coatings, rather than that of window materials will assume greater relevance, if coatings are to be used with confidence and reliability. Provisions to protect window coatings from abrasion need to be given special attention in the materials handling and thermal compliance aspects of the receiver design.

Chemical

The materials were reviewed for their resistance against acids, bases and gases. Unfortunately, no quantitative unit of measure is available and/or comparable for the various materials. Therefore, the materials are simply rated as good or poor to indicate their general suitability to varied chemical exposures. There is limited information regarding chemical resistance at the elevated temperatures anticipated within the direct flux chemical reactor. As candidate reactions are selected, specific compatibility data will be required, and may be the object of relevant R&D programs. Mechanical resistance to abrasion/erosion was not fully evaluated, but surface hardness data does give an indication of erosion/abrasion resistance.

Shapes/Sizes

The materials were reviewed for availability of plates, tubes, and curved plates. The largest sizes manufactured to date are noted. All of the manufacturers indicated that size scalability is limited only by processing equipment size and not be of inherent limitations of the materials or manufacturing technology. At the same time though, the manufacturers indicated that, as they seldom receive requests for large sized pieces, they do not foresee investing in the required capital equipment. The one exception is that of spinel, a new material, for which Coors is currently adding new equipment to process larger (up to 17.8 cm [7 in.] diameter) pieces.

For the case of a large flat aperture, a multi-faceted window matrix may be more appropriate for maintenance and modular construction.

In this view, we have researched available materials. Our investigation indicates that the largest quartz lens built to date is approximately 3 meters (9.8 feet) diameter — as used in a Russian telescope.

It is obvious that single piece windows for large (100 MWth [3.4×10^8 Btu/h]) plants at approximately 10 meter (33 feet) diameter are currently beyond the state of the art. Large windows must be multifaceted, thus for a feasibility or pilot model, window designs should also be multifaceted to demonstrate scalability to commercial sizes.

Corning Glass is currently investigating an AR surface treatment for their 7940 fused silica windows. The process, if it works, is expected to survive to 1250°C (2200°F). Corning engineers anticipate per surface reflectivity of less than .5%, though the bandwidth of such AR performance was not specified. Test results of the process experiments have not been encouraging, but the obvious benefits of a successful process to the laser fusion program suggest work will continue.

The current and near term unavailability of large windows leads to the consideration of alternate approaches such as the use of transparent tubes within a windowless cavity. Fused silica (FS) tubes are available in sizes[*] compatible with packed bed reactors. Larger sizes of FS tubes might serve as fluidized bed or entrained flow reactors on a bench model scale, but pilot or production scale reactors would incur many of the same problems as a large single pane windowed receiver, unless scaling were accomplished by use of multiple bench scale modules. In any case, the poor performance of quartz tubes in a cavity receiver configuration will require the use of Vistal, spinel, or sapphire to realize the potential thermal efficiency benefits of direct flux reactor designs.

Sealing

Depending on the reactant properties and process temperatures and pressures, the complexity of window seal designs varies significantly. Similarly, the seals and window supports differ greatly according to window size, shape, and material.

---

[*] Diameters acceptable, but length is limited to maximum of six feet.

Given that within this report windows may be flat panes, cylindrical tubes, or formed vessels, a multiplicity of seal configurations must be considered.

The key requirements in sealing interfaces between dissimilar materials over large temperature ranges are: (1) to provide controlled compliance to avoid stress induced failures; (2) to protect gaskets, compounds, and parent materials from over (under) temperatures (3) and to maintain adequate interface pressure.

Flat plates (panes) normally use face sealing methods. The face seal tolerates relative motion parallel to the surfaces of the two pieces. Motion perpendicular to the surfaces as occurs when pieces warp or twist, quickly diminishes seal effectiveness. Many face sealing compounds or gaskets require high contact pressure. This requirement jeopardizes (ceramic, spinel, quartz) pane survival even when thermally induced strains are quite small. The requirement to maintain high seal contact pressures, however, incurs the need for locally rigid window frames. Isolation of the frames from structurally imposed strains requires that (high-temperature) mechanical compliance be provided between window frames. The solution is complex and costly, but not impossible.

Circumferential seals can be applied to round windows, but again the requirement to accommodate large temperature excursions significantly complicates the task. Sealing methods may include O-rings, metal (piston) rings, housekeeper seals and graded seals.

O-ring materials are generally short lived above 300°C (572°F) and would form unreliable gland seals in the reactor unless well isolated from the heat. Such isolation is probably not achievable in aperture windows but could be employed around tubes.

In-line (coaxial) ducts can be telescoped to compensate for lengthwise thermal expansion, and piston rings can be used to seal the sliding joint. While piston rings can be built to survive the temperature environment, the gap normally provided to accommodate circumferential expansion causes some unavoidable leakage.

Housekeeper seals, wherein thin walled (0.127 to 0.254 mm [.005 to .010 in.] thick) metal tubing is shrunk over the circumference of the pane or

72

tubes, are fragile and require delicate handling. Repair is difficult because of the shrink fit. Due to the unlike thermal coefficients of the metal tubing and window materials, stretching in the metal may exceed or approach limiting tensile stress limits and cause plastic failure or short fatigue life.

Graded seals use materials of intermediate thermal expansion coefficient between the two unlike materials to be joined. The philosophy is to share the stresses between two (or more) interfaces. In some instances, such as joining ceramics, a graded change in thermal coefficients can be achieved by varying parent material properties in the joint area.

Graded seals have a stress equilibrium temperature and, therefore, have (residual) thermal stresses at all other temperatures. Joints under these internal stresses are more prone to breakage during handling — though their temperature cycling life is better than that of housekeeper seals.

One viable sealing approach is metalizing of the window material such that the window can be brazed. Feasibility of metalizing materials is important in the assessment of applicable window materials. However, the metal joints, while providing good mechanical seals, may impose lower temperature limits on the reactor as well as impose problems due to dissimilar coefficients of thermal expansion.

Brazed joint seals can be made to metallized ceramics, but operation in the 700° to 1100°C (1292° to 2012°F) range may aggravate chemical attack or oxidation of the seal.

Sealing of the window material to metal and/or sealing of one window to another window is of major concern for gas and/or fluid reactors. The sealing techniques which are presented may not be all inclusive.

Further review of sealing techniques is necessary, and should be included in subsequent R&D efforts. In particular, temperature cycling of low leak seals represents a major technical challenge.

Additional design issues with the apertures include cleanliness and maintenance.

Preservation of window cleanliness is important; because, if the processes deposit char on the window or tube walls, two effects may degrade the system. First, the diminished transmissivity may cool the reaction and

overheat the window (tube). Second, the char deposit may react with the window material or initiate devitrification. Devitrification, the changing of glass from a vitreous to a crystalline condition, can occur in fused quartz at temperatures above 1500°C (2732°F) or at lower temperatures if surface contaminants are present. The practicability of using air curtains or electrostatic repulsion methods to keep the window free from process fines must be researched.

Maintainability

Any receiver/reactor will require periodic (annual) maintenance and testing during its lifetime. Catalyst beds, separate from the receiver materials, may need frequent replacement or cleaning. The design must accommodate routine maintenance and repair of failed tubes, seals or windows to avoid excessive reactor downtime and related plant inactivity and feedstock/product waste.

Durability

Window (tubes) must be sufficiently compatible with the reactants and high temperatures to allow economic and safe operation. Reactors handling solids must, additionally, be resistant to abrasion and erosion.

High durability, consequently, would reduce the maintenance requirements and operating cost.

Results

This study concludes that reactors using quartz tubes for containment of packed bed reactors can be built without excessive R&D requirements. However, the poor IR transmissivity of quartz tubes results in insignificant thermal efficiency improvements for solar reactors configured as cavity receivers. This forces the use of 200 to 600 times more expensive materials such as Vistal or spinel for reactors using tubes in cavity receiver configurations. In contrast, reactors using quartz in a window or containment vessel application will require significant development of large piece fabrication and handling techniques, cooled facet support systems, and large scale sealing systems that must remain effective over repeated wide temperature cycles. Other concerns like window abrasion, erosion, and dusting caused by contact with solid reactant particles pose as yet undetermined problems. Means to

prevent or minimize window contact by reactant particles through the use of an air window or electrostatic repulsion should be evaluated.

The problems associated with windowed cavity or clear tube reactors are significant, but it is essential these issues be addressed unless direct solar flux chemical reactors are to be restricted to only the narrowest range of applications.

A matrix of window material candidates versus aforementioned parameters is presented in the attached Tables 11 and 12 above. Other materials which were reviewed included plastics, such as Lexan, Pyrex, and calcium fluoride. All of these materials softened at temperatures below 800°C (1472°F). Other polycrystalline materials were reviewed but rejected due to their poor visible transmittance in visible wavelengths.

Naval Weapons Research at China Lake is currently experimentally reviewing the thermal and mechanical properties of both spinel and sapphire. This data base which will include thermal and mechanical properties at elevated temperatures up to 1650°C (3002°F), will be available shortly.

Quartz, sapphire, and spinel offer the highest solar spectrum optical transmission as well as the highest operating temperatures. Quartz technology is more mature and larger sizes are currently available. Sapphire and spinel can act as substrates for metalized coatings to allow for brazing, while quartz requires mechanical seals. Sapphire and spinel are stronger than quartz.

With regards to cost, at present quartz is lowest in cost for small standard sized pieces. However in all cases, speciality large sized windows will be expensive; current cost data on standard sizes may not be relevant to future cost data.

These alternate transparent materials are currently very expensive, but the spinel cost at least is projected to drop significantly with production. Sapphire, being a grown crystal, is likely to remain very expensive. Vistal, being in limited volume production, has some cost reduction potential, but the price will not drop as much as spinel prices could drop. Table 17 compared relative costs of the materials in current prices for tube forms.

Table 17. RELATIVE MATERIAL COST

Material	Cost/kg	(Cost/lb)	Cost Ratio
Inconel	$ 3.76	($ 8.3)	1.0
SiC	45.3	(100.)	12
Quartz	49.9	(110.)	13
Vistal	739.	(1630.)	196
Sapphire	1910.	(4210.)	507
Spinel	2240.	(4930.)	594

Reactor Screening Methodology

A methodology was developed for screening various reactor concepts to be used in the conceptual design of the direct flux reactor for limestone calcination and of the direct flux reactor for the catalytic steam reforming of methane. The approach to reactor selection may be summarized as follows:

- Describe assumptions used in screening reactor candidates

- Apply pertinent inputs from materials assessment

- Identify principal industrial reactor types

- Identify calciner and steam reformer technical requirements and constraints

- Review characteristics of principal reactor types

- Finalize selection by assessment of reactor types in view of characteristics, technical requirements, and constraints.

The methodology was a qualitative assessment of the applicability of the reactor concepts based on engineering judgement. Engineering judgement was used with the objective of defining promising reactor concepts that may establish the technical feasibility and practicality of direct flux reactors while identifying R&D issues in reactor development. The methodology produces a relative evaluation of reactor concepts. It is inappropriate that an optimum reactor selection can be made at this early stage of development of direct flux reactors. Optimum reactor selection requires comparative analytical, experimental, and economic analyses of several reactor designs emphasizing performance and cost trade-offs between opaque and direct flux designs.

The approach taken for reactor selection was conservative with reactor designs derived from reactors used currently for the conduct of calcination and steam reforming reactions. Although innovative approaches to reactor design were considered, several major factors influenced this approach. DOE has outlined a 10-year program for demonstration of solar fuels and chemical reactors with a target date of 1995 for a pilot scale demonstration of a solar fuels and chemicals plant. The risk involved in the development of reactors departing significantly from reactors in commercial use was judged too high for these reactors to be seriously considered in this conceptual design study. Since industry is the ultimate consumer of this technology, recognition of the conservatism of industry to new approaches was judged a significant barrier to novel designs. In particular, a reactor concept is viewed favorably if heat transfer is by radiant means so that similar design considerations such as mass flow rates, tube diameters and length, and radiant heat fluxes may be operative when direct flux heating of the reaction is used. Since this study is one of the earliest efforts to develop concepts for commercial scale solar reactors, the design approach may be viewed as a baseline to which the potential benefits of other reactor designs may be compared.

Assumptions Used in Screening Reactor Candidates

The following assumptions have been made in applying the reactor screening methodology.

1. The reactor is assumed to be tower mounted at the focus of a central receiver heliostat field. The use of solar central receivers as a heat source for chemical reactions is consistent with the large scale centralized processing of reactants that is commonplace in the chemical process industries.

2. Continuous processing during sunshine hours rather than batch processing is preferred to make greatest use of the available solar flux. This assumption does not preclude the use of supplemental fossil firing within the reactor for low insolation or nighttime operation, nor does it preclude the integration of energy or material storage to assure 'round-the-clock' operation of the balance of plant. However;

3. The means by which the reactor would be integrated into the process is not explicitly considered for purposes of this evaluation.

4. Quartz is the assumed standard material of construction for optical reactor vessels and/or windows because of its high transmissivity of

optical wavelengths, resistance to thermal shock, moderate hardness, good chemical stability at high temperatures, and widespread availability.

Implications of Materials Assessment to Reactor Selection

The pertinent results of the materials assessment to the development of a windowed reactor are:

● Windowed apertures are of complex design of uncertain serviceability at high fluxes and temperatures

● Windowed reactors are only capable of low-pressure operation

● It is unlikely that windowed reactors may be developed for a 1995 pilot scale demonstration

● Quartz is subject to high-temperature corrosion from calcium oxide

● Quartz is a costly material of construction.

The implications of these results to calciner reactor design are:

● Windowed reactors are of high risk

● Relatively innocuous reactants and products indicate that a reactor design may be developed without a window. This avoids the use of more corrosion resistant, more costly transparent materials than quartz for window fabrication while possibly permitting direct flux irradiation of reactants.

The implications of these results to steam reformer design are:

● While steam reforming may be done at low pressures, the poor economics of handling large volumes of products in downstream plant components or compressing products to typical downstream requirements (there are twice as many moles of product as reactant) indicate that windowed reactors are a poor candidate concept of steam reforming.

The pertinent results of the materials assessment to the development of a tubular reactor[*] are:

● Quartz is a costly material of construction, although Vistal, spinel, and sapphire are yet more costly

● Alternatives to quartz are very costly

● Quartz is substantially opaque to IR when used in a cavity reactor configuration

---

[*] Tubular reactors are: fixed (packed) beds, moving beds, fluidized beds, and entrained flow reactors.

78

- Transparent tubes are available in limited diameters and lengths

- Sealing details and reliability of seals is uncertain

- Tubes are capable of elevated pressure operation, but ceramic tubes used in Brayton cycle solar receivers are constrained to only 405 kPa (4 atm) operating pressure

- In the case of limestone calcination, quartz is subject to corrosion from lime

- Quartz is subject to corrosion from carbon deposition as a side reaction in steam reforming

- Quartz is subject to erosion from alumina catalyst supports used in packed bed steam reforming reactors.

The implications of these results to reactor design are:

- Materials such as Vistal, spinel, or sapphire are required to produce tubular reactors when cavity receivers are used[*]

- High cost of alternative materials implies that tubular direct flux reactors should only be designed if other alternative configurations are inappropriate

- Since direct flux must be at least competitive with opaque designs, use an opaque tubular reactor design to assess target costs for tubular direct flux reactors.

Principal Reactor Types

The principal reactor types were identified based on the Task 1 review of solar reactor concepts and experiments and review of reactors used in industrial practice for steam reforming and calcination. The principal reactor types for calcination are:

1. Rotary kiln

2. Moving bed

3. Fluidized bed

4. Entrained flow.

---

[*] Steam reforming of methane and limestone calcination reactions are carried out at temperatures greater than 700°C (1292°F). Above 700°C (1292°F) cavity receiver/reactor designs are required to reduce the magnitude of convective and radiative heat losses to maintain high thermal efficiencies for utilization of energy collected by the heliostat field.

The principal reactor types for steam reforming are:

1. Fixed bed (also known as packed bed reactors)

2. Moving bed

3. Fluidized bed

4. Entrained flow.

Calciner Technical Requirements and Constraints

The minimum technical requirements and constraints that a reactor for limestone calcination must meet were identified as:

o   Provide solar energy to the reactant stream undergoing calcination

   —   Heat process feed to reaction temperature

   —   Provide the endothermic heat of reaction

o   Provide adequate residence time for conversion of limestone to lime

o   Provide adequate heat transfer to reactants

o   Operate at high thermal efficiency (no excessive radiant or convective losses)

o   Minimum technology development for 1995 pilot plant demonstration

   —   Should be similar to industrial reactor designs currently in use

o   Provide adequate corrosion resistance. Reactor configurations that allow reactants and/or products to contact vessel walls are not favored since quartz may not be used thus requiring the use of more expensive transparent materials

o   Provide adequate erosion resistance. Fluidized particles or moving bed reactor configurations which allow solid reactants and/or products to contact vessel walls are not favored if the Mohs or Knoop hardness of the reactants or products exceeds the hardness of the transparent vessel material. All materials of construction, including quartz, are resistant to erosion by lime and limestone. However, alumina is present as an impurity in the calcination of limestone. Thus quartz is not an appropriate material of construction for the walls of a calciner reactor vessel.

Steam Reformer Technical Requirements and Constraints

The minimum technical requirements and constraints that a reactor for steam reforming of methane must meet were identified as:

80

o   Provide solar energy to the process stream (methane plus steam) undergoing steam reforming

—   Heat process feed to reaction temperature

—   Provide the endothermic heat of reaction

o   Provide adequate residence time to produce high quality product-reactor effluent of comparable composition to conventional fossil-fired reformer

o   Minimum technology development for 1995 pilot plant demonstration

—   Requires maximum use of existing fossil fired steam reformer technology which utilizes packed bed reactors heated by IR radiation

—   Reactor should be capable of achieving an axial flux distribution equivalent to current fossil fired reformer practice

—   Tube wall temperatures must remain constant throughout the operating diurnal cycle. Furthermore, tube temperature conditions should be identical for all the tubes in the cavity. This will require a uniform heat flux distribution for all the tubes with minimal circumferential variation.

o   Provide adequate corrosion resistance. Reactor configurations that allow corrosive materials such as carbon to contact vessel walls are not favored since quartz may not be used thus requiring the use of more expensive transparent materials. Carbon formation is the result of reactions occurring when the steam reforming process equilibrium is upset.

o   Provide adequate erosion resistance. Fluidized bed reactors, moving bed reactors, or entrained flow configurations which allow catalysts or catalyst supports to impact reactor walls are not favored if the Mohs or Knoop hardness of the catalysts or catalyst supports exceeds the hardness of the transparent vessel material. Alumina and silicon carbide are used as catalyst supports. These are harder than quartz. Thus more expensive materials must be used (for example, sapphire or spinel) as the material of construction if fluidized bed, moving bed, or entrained flow reactors are used.

Characteristics of Principal Reactor Types

The applicability of various reactor configurations for solid catalyzed gas phase reactions and gas-solid reactions is given in Table 18. The reactor configurations are also compared, in qualitative terms, as to the temperature distribution in the bed, particle size, pressure drop, heat transfer, and conversion that may be obtained in each type of reactor.

The residence time capability of fluid bed, entrained flow, and rotary kiln reactors for gas-solid reactions as a function of particle size and

81

Table 18.   COMPARISON OF TYPES OF CONTACTING FOR REACTING GAS-SOLID SYSTEMS[13]

	Solid Catalyzed Gas Phase Reaction	Gas Solid Reaction	Temperature Distribution in the Bed
Fixed Bed	Only for very slow or non-deactivating catalyst. Serious temperature control problems limit the size of units.	Unsuited for continuous operations, while batch operations yield non-uniform product.	Where much heat is involved large temperature gradients occur.
Moving Bed	For large granular easily de-activated catalyst. Fairly large-scale operations possible.	For fairly uniform sized feed with little or no fines. Large-scale operations possible.	Temperature gradients can be controlled by proper gas flow or can be minimized with sufficiently large solid circulation.
Rotary Kiln	Not applicable.	For fairly uniform sized feed with little or no fines. Large-scale operations are possible. Suited to batch scale operations.	Where much heat is involved large axial temperature gradients may occur. Temperature gradients can be controlled by proper flow of combustion products and by proper location of burners.
Fluidized Bed	For small granular powdery nonfriable rapidly deactivated catalyst. Excellent temperature control allows large-scale operations.	Can use wide size range of solids with much fines. Large-scale operations at uniform temperature possible. Excellent for batch operations, yielding a uniform product.	Temperature is almost constant throughout. This is controlled by heat exchange or by proper continuous feed feed and removal of solids.
Entrained Flow	Suitable only for rapid reactions.	Suitable only for rapid reactions.	Temperature gradients in direction of solids flow can be minimized by sufficient circulation of solid.

Table 18, Cont. COMPARISON OF TYPES OF CONTACTING FOR REACTING GAS-SOLID SYSTEMS

	Particles	Pressure Drop	Heat Exchange and Transport of Heat	Conversion
Fixed Bed	Fairly large and uniform. With poor temperature control these may sinter and clog the reactor.	Because of low gas velocity and large particle size, pressure drop is not a serious problem, except in low pressure systems.	Inefficient exchange, hence large exchanger surface needed. This is often the limiting factor in scale up.	With plug flow of gas and proper temperature control (which is difficult) close to 100% of the theoretical conversion is possible.
Moving Bed	Fairly large and uniform; upper limit governed by convenient application of gas lift in circulation system, lower limit by minimum fluidizing velocity in reactor.	Intermediate between fixed and fluidized bed.	Inefficient exchange but because of high heat capacity of solids, the heat transported by circulating solids can be fairly large.	Flexible and close to ideal countercurrent and cocurrent contacting allows close to 100% of the theoretical conversion.
Rotary Kiln	Fairly large and uniform.	Because of large cross section for gas flow, gas velocities may be low so that pressure drop is low.	Heat transport is somewhat inefficient. This leads to large heat transfer areas.	Flow of gas and solid close to plug flow. Allows close to 100% of the theoretical conversion.
Fluidized Bed	Wide size distribution and much fines possible. Erosion of vessel and pipelines, attrition of particles and their entrainment can be serious.	For deep beds pressure drop is high, resulting in large power consumption.	Efficient heat exchange and large heat transport by circulating solids that heat problems are seldom limiting in scale up.	For continuous operations, backmix flow of solids and poor contacting pattern for gas result in poorer performance than other reactor types. For high conversion, staging is necessary.
Entrained Flow	Same as fluidized bed. Upper size limit governed by minimum transport velocity.	Low for fine particles, but can be considerable for large particles.	Intermediate between fluidized and moving bed.	Flow of gas and solid is close to cocurrent plug flow, hence high conversion possible.

residence time is shown in Figure 6.[14] Moving bed reactors are capable of a similar range of residence time to rotary kilns, with a particle size range limited from about 0.8 mm to 10 mm (0.03 in. to 0.39 in.). As an example, calcining a 25.4 mm (1 in.) limestone particle requires one to four hours. Figure 6 indicates that rotary kilns and fluid beds are appropriate reactors for this application. Indeed, these are the type of reactors used industrially for the calcination reaction.

Application of Screening Methodology

Limestone Calcination

The principal reactor types are reviewed and assessed for applicability to the limestone calcination reaction in Table 19.

Steam Reforming of Methane

The principal reactor types are reviewed and assessed for applicability to the steam reforming of methane reaction in Table 20.

Reactor Selections

Limestone Calcination

The rotary kiln was selected as the reactor concept for limestone calcination. The rotary kiln meets the technical requirements and constraints. In particular, by avoiding the use of a window, the technical risk of development is substantially reduced since the uncertainties of window fabricability, sealing, surviveability and maintainability/cleanliness are avoided. In addition, the rotary kiln qualifies as a true direct flux reactor design since there are no opaque heat transfer surfaces through which heat must be transferred.

The fluidized bed reactor is also an attractive candidate. Mitigating against its selection are the problems of erosion and corrosion and the need for multiple fluid bed reactors to achieve complete conversion of limestone to lime. The moving bed reactor is well developed for calcination in particular and for solids reactions in general. However, the chief difference between conventional reactors and solar firing is critical: gas flowing axially through the bed delivers heat to all parts of a conventional packed bed; and provides nearly uniform temperatures at each cross section; heating around the circumference of a solar heated reactor requires small diameter beds for
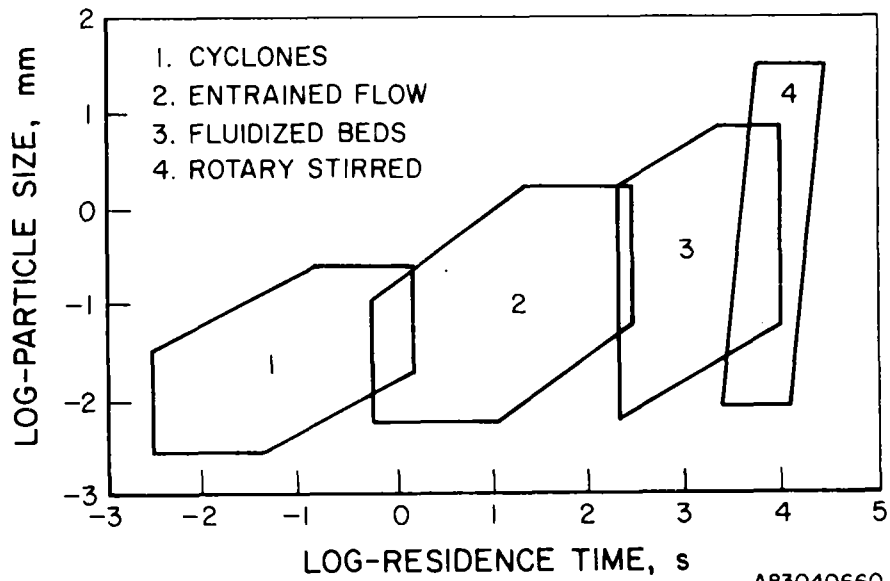
Figure 6. RANGE OF APPLICATION OF INDUSTRIAL GAS/SOLID REACTORS
IN RELATION TO PARTICLE SIZE AND SOLID RESIDENCE TIME

Table 19.   APPLICATION OF REACTOR SCREENING METHODOLOGY TO
CANDIDATE REACTOR CONCEPTS — LIMESTONE CALCINATION

Reactor	Comments
Moving Bed	• Adequate residence time possible[1]
	• Adequate conversion possible
	• Quartz subject to corrosion/erosion by reactants/products/ impurities
	• Expensive alternatives to quartz are required
	• Inefficient heat transfer requires the use of many small diameter tubes with associated solids handling difficulties in feeding and discharging reactants and products
	• While in industrial use as a calciner, packed beds are not in as wide use as rotary kilns
Fluid Bed	• Adequate residence time is possible
	• Excellent heat transfer implies large diameter (i.e., say 0.5 to one meter) reactor vessels are possible. This simplifies solids handling in feeding and discharging reactants and products
	• Quartz subject to erosion/corrosion by reactants and products and impurities
	• Expensive alternatives to quartz are required
	• Used by industry for calcination
	• Demonstrated by French in a small-scale, batch mode reactor
	• Difficult to obtain high conversion without complexity of multiple fluid bed reactor design
Entrained Flow	• Adequate residence time not possible
	• Quartz subject to erosion/corrosion
	• Not used in industry for calcination
Rotary Kiln	• Popular in industry/use well established for calcination
	• Used commonly for radiative heating of high temperature reactions
	• No window needed because of low toxicity of reactants and products
	• No erosion/corrosion problems
	• Adequate residence time is possible
	• Adequate conversion is possible
	• The most well developed solids reactor concept based on the French one megawatt kiln, and the SRI conceptual study of a rotary kiln for the CRTF
	• Holds promise as a generic solids reactor

---

[1]One-inch particle (typical size used in industrial operations) typically requires 1 to 4 hours residence time.

Table 20. APPLICATION OF REACTOR SCREENING METHODOLOGY TO CANDIDATE REACTOR CONCEPTS — STEAM REFORMING OF METHANE

Reactor	Comments
Fixed Bed**	o Adequate residence time possible
	o Adequate conversion possible
	o Widespread industry use, especially for radiative heating of high temperature reactions such as steam reforming of methane or naphtha, and thermal cracking of ethane
	o Conceptual design of commercial-scale solar steam reformer established by PFR
	o PFR study established:
	— Capability of achieving axial flux distribution equivalent to current fossil fired reformer practice
	o Small-scale solar packed bed reactors have been conceived and demonstrated for sulfur trioxide decomposition (metallic and quartz), ammonia decomposition, and sulfuric acid decomposition
	o Heat transfer is inefficient. Accommodated by well developed designs using multiple tubes of 15.2 cm (6 in.) or less diameter (10.2 cm [4 in.] typical). Flux levels limited by in-bed heat transfer.
	o Carbon deposition through side reactions may corrode quartz or lead to poor optical coupling of solar and IR radiation to catalyst bed
	o Expensive alternatives to quartz are required.
Fluidized Bed	o Adequate residence time is possible
	o Adequate conversion is possible
	o Excellent heat transfer
	o Not used by industry for steam reforming
	o In widespread industry use for other catalytic and non-catalytic gas phase reactions
	o Catalyst supports will erode quartz
	o Carbon deposition through side reactions may corrode quartz
	o Expensive alternatives to quartz are required
Entrained Flow	o Not used in industry for steam reforming
	o Insufficient residence time
	o Erosion of quartz
	o Good heat transfer
	o Used in industry for gas phase reactions

** Also known as "packed bed" and generally referred to as such in the remainder of this report.

87

cross-sectional temperature uniformity since conduction of heat is poor. This results in a design with many small diameter tubes — really many moving bed reactors — in which each must be controlled with each tube requiring means for reactant feed and product removal.

Steam Reforming of Methane

The packed or fixed bed reactor was selected as the reactor concept for steam reforming of methane. The packed bed reactor meets the technical requirements and constraints. The packed bed reactor is the design currently in widespread use for this reaction. The PFR conceptual study strongly suggests that a solar reactor may be derived from current industrial practice. Small scale experiments have established the packed bed reactor as technically feasible. The problem of chemical attack on quartz leads to the requirement of alternative transparent materials for a direct flux steam reformer. Furthermore, the substantial opacity of quartz to IR radiation when used in a cavity receiver configuration also demands that the more expensive alternative materials to quartz that have much higher IR transmissivity be specified for reactor construction.

Identification of Calciner Technical Requirements and Constraints

The next step in the design methodology is the identification of calciner and steam reformer technical requirements and constraints. This activity leads to the development of an initial design concept from which, through modeling and mechanical design, the final design concept, drawings, and specifications emerge. In this conceptual design effort, the "system" consists of the receiver/reactor, and heat recovery components that recover heat from hot solid products and hot gaseous products to preheat a diluent or sweep gas (air), and to preheat the limestone feed.

Overall System Technical Requirements and Constraints

● Produce high quality product

● Target for 1995 pilot plant demo

    — Requires maximum use of near term available solar technology

    — Requires maximum use of existing calcination technology (conventional and solar) consistent with constraints of solar operation such as thermal shock of refractory

- Operate as a stand-alone system[*]

- Responsive to diurnal variation of solar insolation.

Calciner Functional Requirements and Constraints

The calciner functional requirements and constraints were identified as follows:

- Provide solar energy to the process stream undergoing calcination

  — Heat process feed to reaction temperature

  — Provide the endothermic heat of reaction

- Responsive to diurnal variation of solar insolation

  — Maintain process conditions (process flow and temperature) to maintain stable process kinetics

  — Maintain high utilization of capital intensive process equipment

  — Responsive to variations in receiver flux distributions

  — Maintain high standby nighttime temperature to simplify daily start up procedures (if design foregoes use of fossil firing to maintain continuous operation at night or low insolation conditions)

- Provide interface to heat recovery apparatus

- Convey solids through reactor with good cross-sectional mixing to maintain uniform cross-sectional temperature

- Low weight to minimize tower cost

- Operate at high thermal efficiencies

---

[*] A key issue in the development of solar fuels and chemicals technology is the plant interface. The interface problem is generally one of creating circumstances in which the plant operations are disturbed as little as possible by the substitution of the solar heat source for the typical fossil heat source. The essence of the problem is twofold: 1) economic amortization of plant components generally requires operation of plant components on a 24 h/d basis and 2) plant operations are run at steady-state and process disruptions are costly. The expected requirement that solar reactor systems shall ultimately be required to operate without substantial fossil fuel use suggests that the system be required to operate in a stand-alone fashion, if possible. At the very least, if fossil fuel is burned so that the system operates at night (that is, that the system is responsive to the diurnal variation of solar insolation) then the costly duplication of components, such as the use of a ground based, fossil-fired calciner is to be avoided.

- Minimize dust carryover through aperture

- Reactor construction should be simple and low cost

- Minimize technology development for 1995 pilot plant demonstration

    - Reactor should be similar to industrial designs

    - Reactor design should make maximum use of existing reactor design know-how.

Heat Recovery Functional Requirements and Constraints

- Minimum component development. Utilize available technology

- Recover substantial energy from hot solids products and hot gaseous products. Cool hot solids to near ambient temperature. Cool hot gases to near ambient temperature. Preheat solids feed and preheat sweep gas

- Interface with receiver to utilize preheated solid feed and sweep gas.

Identification of Steam Reformer Technical Requirements and Constraints

In the conceptual design effort, the "system" consists of the receiver/ reactor, and heat recovery components that recover heat from reaction products and flue gases (if fossil firing is used) to preheat feed and to raise steam.

Overall System Technical Requirements and Constraints

- Produce high quality product — reactor effluent of comparable composition to conventional fossil reformer

- Target for 1995 pilot plant demo

    - Requires maximum use of near-term available solar technology such as existing packed bed reactor design studies (that is, PFR study)

    - Requires maximum use of existing fossil fired steam reformer technology

- Should operate as a stand-alone system

- Minimum effect on plant process conditions

- Minimum changes on plant hardware

- Responsive to diurnal variation of solar insolation

- Plant product should be required at small scales.

Steam Reformer Receiver/Reactor Technical Requirements and Constraints

- Provide solar energy to the process stream undergoing steam reforming

- Heat process feed to reaction temperature

- Provide the endothermic heat of reaction

⊙ Accommodate catalytic reaction taking place in receiver tubes

⊙ Achieve axial flux distribution equivalent to current fossil fired reformer practice. Axial flux distribution characteristic of current fossil fired reformer practice is shown in Figure 7

⊙ Tube wall temperatures must remain constant throughout the operating diurnal cycle. Furthermore, tube temperature conditions should be identical for all the tubes in the cavity. This will require a uniform heat flux distribution for all the tubes with minimal circumferential variation

⊙ Operating severity (that is process temperatures) should be moderate

⊙ Responsive to diurnal variation of solar insolation

- Maintain high utilization of capital intensive process equipment upstream and downstream of reactor

- Maintain continuous operation

- Maintain process conditions (mass flow, temperatures, and pressures) essentially constant

- Maintain stable reaction kinetics

- Minimize cycling

- Responsive to variations in receiver flux variations

⊙ Provide interface with heat recovery apparatus

⊙ Operate at high thermal efficiencies

⊙ Low weight to minimize tower cost

⊙ Reactor construction should be simple

⊙ Minimum technology development for 1995 pilot plant demonstration

- Reactor should be similar to industrial designs

- Reactor design should make maximum use of existing reactor design know how.

Heat Recovery Functional Requirements and Constraints

⊙ Minimum component development

BASED ON INSIDE DIAMETER
OF REFORMER TUBES
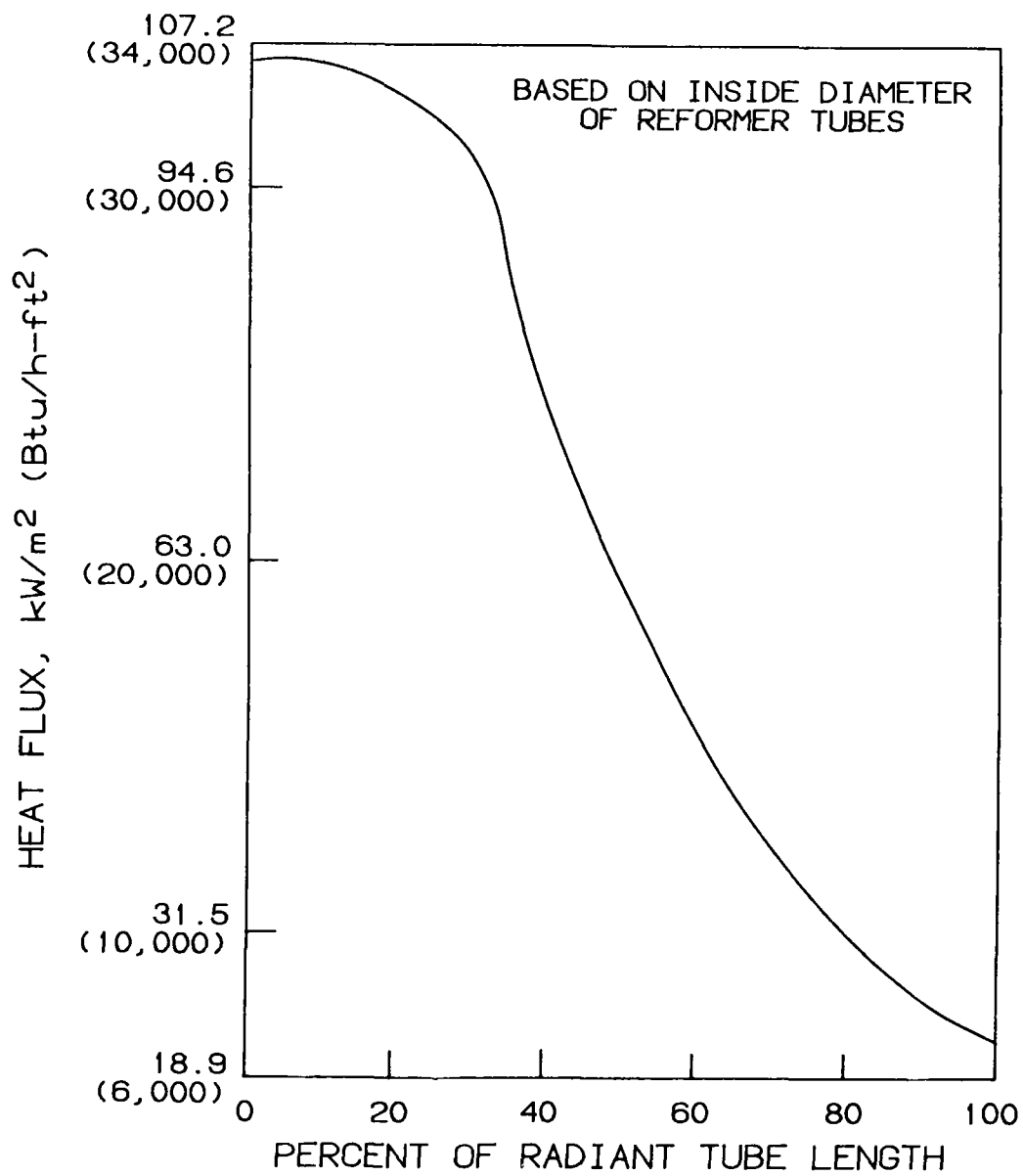
Figure 7. CONVENTIONAL STEAM REFORMER FLUX PROFILE

A84060589H

● Recover substantial energy from hot gaseous products. Cool hot flue and process gases. Preheat feed and raise steam

● Interface with receiver to utilize hot process and flue gases.

Calciner Initial Design Concept

An initial design concept of a solar calciner that meets the technical requirements and constraints was developed. The initial design concept consists of:[*]

● Reactor/receiver

● Heat recovery.

The calciner will be operated in a batch mode. Batch operation of the calciner is defined as follows: The solar calciner is shut down at night and receives no process flow. As the sun rises, flow commences into the solar calciner. It will be expected that process flow follows time dependent solar power profile at reactor aperture. Sufficient storage of limestone feed and lime products is assumed to be provided to allow balance of plant to operate as conventional plant.

As discussed earlier, a key issue in the development of solar fuels and chemicals technology is the plant interface. The interface problem is generally one of creating circumstances in which the plant operations are disturbed as little as possible by the substitution of the solar heat source for supplying the heat of reaction for the typical fossil heat source. In the case of a solids reaction such as limestone calcination a logical plant interface is to run the calciner only during sunny hours. Plant operations are maintained on their usual, steady-state, 'round-the-clock schedule by provision of storage of limestone feed and lime product. Batch operation results in a simplified reactor design responsive to the diurnal variation of solar insolation, without the complexity of integrating fossil heating components within the reactor for 24 hour operation. The simplicity and expected economy of solids storage recommends that this approach be taken for the plant interface. The expected requirement that solar systems shall ultimately be required to operate without substantial fossil fuel use also

---

[*] Tower and heliostat field design are outside the scope of this conceptual design study.

suggests that solids storage and batch operation be developed for solids reactions such as calcination.

The target for 1995 pilot plant demonstration of solar reactor technology requires the use of reactors similar to industrial practice to benefit from design know-how. This leads to use of kiln technology.

The requirements 1) that the reactor is responsive to receiver flux variations, 2) that the receiver be capable of high thermal efficiencies, and 3) that the reactor maintain high nighttime standby temperatures indicate that the cavity configuration inherent in the rotary kiln is appropriate and useful. A cavity tends to "level out" receiver incident flux variations. With an aperture door and supplemental fossil firing, high standby temperatures will readily be maintained.

Air is used as a sweep gas to ensure that the partial pressure of carbon dioxide is low, to entrain fines and prevent their escape through the aperture, and air is used as a heat transport medium to recover heat from hot solids products. In the initial design concept, the hot sweep gas is injected around the aperture. The relatively innocuous reactants and products lead to the use of an open aperture and allow solids reactor development without requiring a window. The relatively innocuous chemicals permit utilization of direct flux heating of reactants through combined direct, reflected, and reradiant heat transfer mechanisms.

The initial design concept may be summarized as follows:

Subsystem	Functional Requirement	Design Condition
Receiver/Reactor	Provide sensible and heat of reaction. Convey solid and gases.	Chemical reaction in direct flux bed of reactants by direct reflected and reradiant solar flux at 843° to 1204°C (1550° to 2200°F) in cavity receiver. Single cavity, single aperture rotary kiln.
		Aperture door and supplemental fossil firing to maintain hot standby condition.
Heat Recovery	Recover heat from hot solids and gas to preheat solids feed and sweep gas. Gas cleanup, sweep gas utilization.	Standard units mounted at tower top. Gas cleanup by conventional methods. Sweep gas injection at aperture.

Steam Reformer Initial Design Concept

An initial design concept that meets the technical requirements and constraints was developed. The initial design concept consists of:

● Receiver/reactor

● Heat recovery.

The timetable for 1995 demonstration requires the use of reactors similar to industrial practice to benefit from know-how. This leads to the use of packed bed reactor technology. The initial design concept is derived from the PFR conceptual design study for a solar steam reformer.

The initial design concept is configured as a fossil fired hybrid system for a number of reasons:

○ Plant hardware and process conditions are minimally affected

○ Tower mounted reactor is amortized over 24 h/d operation

○ Cycling is minimized

○ Reaction kinetics are maintained in a stable condition and constant process conditions may be maintained

● Fossil fired hybridization offers a means to achieve axial flux distribution equivalent to current fossil fired reformer practice

● Tube wall temperatures can remain constant throughout the operating diurnal cycle and will facilitate the establishment of identical catalyst tube temperature conditions

● The fossil fired hybrid 1) has retrofit potential, 2) has "fuel saver" potential to displace fossil fuel use by solar energy, and 3) is required because of the unavailability of high-temperature thermal energy storage technologies that could be integrated with the tower mounted reactor to allow 24 h/d operation.

The initial design concept employs a cavity receiver configuration to 1) operate at high thermal efficiencies and 2) to permit integration of the fossil burner.

The need to allow simultaneous fossil fired and solar operation leads to a "pressure balanced" cavity design employing a forced draft/induced draft flue gas handling system with 1) a near zero pressure difference across the aperture to minimize convection losses and 2) a downward flow of combustion products to minimize stack losses. An aperture door is provided to minimize

nighttime thermal losses and to permit reformer operation in the manner of a fossil fired unit.

The application of the reformer is to a hydrogen plant because of moderate reaction conditions (temperature and pressure), and the relatively small scale of operation.

One of the principal findings from the assessment of transparent materials was that the materials available to construct a steam reformer are very expensive, even in comparison to the nickel alloys used to construct conventional reformers. As a result, the large cost differential between transparent materials of uncertain performance leads to selection of a metallic reactor design using established nickel alloy materials of construction as a baseline to assess target costs of direct flux reformers.

The steam reformer initial design concept may be summarized as follows:

Subsystem	Functional Requirement	Design Condition
Receiver/Reactor	Provide sensible and heat of reaction. Transport feed and products. Provide a portion of daytime energy requirements and nighttime and low insolation operation through fossil firing.	Chemical reaction in catalyst filled metallic tubes of natural gas and steam at 790°C (1454°F) and 2.4 MPa (348 psi) pressure. Single cavity, single aperture. "Pressure balanced," push-pull flue gas handling system. Aperture door for nighttime operation using fossil firing.
Heat Recovery	Recover heat from hot reaction products. Recovery heat from hot flue products. Preheat steam/natural gas feed. Preheat combustion air.	Flue gas exit temperature = 1150°C (2102°F). Process gas exit temperature = 843°C (1549°F). Process gas inlet temperature = 538°C (1000°F).

Scale Selection Methodology

The factors used to determine the appropriate scale for direct flux reactor design are as follows:

- The thermal input at the aperture of the receiver/reactor should be at the lowest end of the industrial scale for the thermal input of individual reactors. This strategy minimizes the risk in assessing problems related to the development of direct flux reactors while illustrating the potential technical feasibility and practicality of direct flux reactors.

- Reactor scale should roughly correspond to the thermal power levels available at solar test facilities such as the CRTF. Pilot-scale reactors are likely to be tested at the CRTF, and by reducing the gap in thermal power input between a pilot-scale plant and a commercial scale plant, scale-up problems are reduced.

- The scale should be selected at the low range of the thermal power levels that have been indicated as economic for solar central electric and industrial process heat applications. A study by Dellin[15] indicated that the levelized cost of thermal energy at a temperature of 288°C (550°F) was flat over a range of 10 to 1000 MWth (3.41×10^7 to 3.41×10^9 Btu/h). Another study[16] suggests that the costs of 288°C (550°F) process steam is insensitive to scale over the range 20 to 300 MW (6.83×10^7 to 1.02×10^9 Btu/h) because there are no large economies of scale associated with system components. Consistent with other factors considered in this methodology, a scale of 10 to 20 MWth (3.41×10^7 to 6.83×10^7 Btu/h) is appropriate.

Application of Scale Selection Methodology to Calcium Carbonate Calcination Reactor

Table 21 gives the distribution of plant sizes in the U.S. used for calcination of calcium carbonate. As indicated in the table, a plant size producing 9.07×10^6 kg/yr (10,000 ton/yr) of lime is the smallest commercial-scale calciner. Thus, a reactor capable of an annual production of 9.07×10^6 kg/yr (10,000 ton/yr) was used to determine the approximate thermal input scale of the reactor.

The thermal input scale for the calciner was based on the following:

- Reaction temperature = 1000°C (1832°F)

- Practical energy requirement = 8.6×10^6 Joules/kg (7.41×10^6 Btu/ton)

- Six hours per day of operation

- 365 days per year of operation

- A stream factor of 0.9. The stream factor is the fraction of the year the plant is operating, allowing downtime for maintenance and other foreseeable interruptions of production

- Thermal efficiency of reactor/receiver of 70% defined as net heat available to reaction ÷ thermal energy available at aperture of reactor/receiver.

Table 21. LIME SOLD OR USED BY U.S. PRODUCERS IN 1975 BY PLANT SIZE[17]

Size of Plant	Plants	Quantity,[a] 10^8 kg	(10^3 short tons)	Percent of Total
Less Than 9.07×10^6 kg/yr (10,000 tons/yr)	28	1.57	(173)	1
9.07×10^6 to 2.27×10^7 kg (10,000 to 25,000 tons)	35	5.76	(635)	3
2.27×10^7 to 4.54×10^7 kg (25,000 to 50,000 tons)	18	5.68	(626)	3
4.54×10^7 to 9.07×10^7 kg (50,000 to 100,000 tons)	28	18.30	(2,018)	9
9.07×10^7 to 1.81×10^7 kg (100,000 to 200,000 tons)	22	28.67	(3,161)	15
1.81×10^7 to 3.63×10^7 kg (200,000 to 400,000 tons)	33	83.38	(9,193)	12
More than 3.63×10^7 kg (400,000 tons)	9	52.96	(5,839)	27
Total[b]	173	196.33	(21,645)	100

a. Excludes regenerated lime, includes Puerto Rico.

b. Data do not add to total shown because of independent rounding.

The thermal input scale is thus:

$$\text{Thermal Input Scale (Joules)} = \frac{\text{Annual Lime Production (kg/yr)} \times \text{Practical Energy Requirement (Joules/kg)}}{\text{Thermal Efficiency of Reactor/Receiver} \times \text{Hours per Day of Operation} \times \text{Days Per Year} \times \text{Stream Factor}}$$

The calculated thermal input scale for a calcium carbonate calciner is thus 5.67×10^7 Joules/h (equivalent to 15.7 MW or 5.36×10^7 Btu/h).

The design was thus based on a 15 MW (5.12×10^7 Btu/h) thermal input to the reactor. The scale selected is only three times the size of the CRTF and is at the low end of the range at which thermal energy costs from central receiver systems are flat.

Application of Scale Selection Methodology to Steam Reforming of Methane Reactor

Hydrogen production was chosen as the process into which the example reformer was placed for several reasons. Hydrogen plants are commercial in a variety of sizes from small skid-mounted units to large refinery-scale, whereas commercial ammonia and methanol plants almost invariably require very large reformers. It is desirable that early installations of new technology be both commercially viable and relatively small in scale. Reformers for hydrogen production operate at a severity between that for ammonia and methanol production. Oxo-alcohol production is not as important economically as ammonia, hydrogen and methanol; operating conditions are severe and the carbon dioxide recycle would add an unnecessary complication to the study. This means that solar energy can potentially have a larger economic impact on hydrogen production than on the other processes.

Methane was chosen as a feedstock because natural gas, which is the most likely feedstock for future hydrogen plants is 90+% methane. Material and heat balances performed using methane can be easily applied to natural gas with minor corrections.

A size of 15 MW (thermal) (5.12×10^7 Btu/h) was chosen for the reformer duty because it corresponds to a small-to-medium sized hydrogen plant.

Process Design of Calcination Reactor

The conceptual design of the calcination reactor consisted of the following efforts:

- Process design — energy and material balances

- Components design — receiver/reactor and heat recovery.

In the process design effort, a steady-state model of reactor performance was developed. The model was developed by undertaking the following efforts:

- Review existing knowledge of solar kiln heat transfer processes

- Review of conventional kiln model literature

- Identification of system boundaries

- Identification of heat transfer, chemical, and kinetic parameters pertinent to calciner design

- Identification of assumptions used in the model

- Development of mass and energy balances of system components.

The scope of this effort was to develop a preliminary design of the calcination system. The outputs of this effort are the development of reactor technical specifications, the determination of design point receiver performance, the development of heat recovery technical specifications, and the mechanical design development of receiver and heat recovery components.

The original choice for a reactor concept was a windowless rotary kiln for the calcination of calcium carbonate. This is essentially the reactor type used industrially for this reaction.

As analysis proceeded on the design of the rotary kiln, a number of problems were identified that led to the selection of an alternative kiln concept: the conveyor kiln. The nearly horizontal rotary kiln has poor coupling of direct solar flux to the reactants.

The cylindrical rotary kiln appears to have a conflict between materials handling requirements and solar coupling. If the kiln axis is oriented horizontally (as is customary), the solar coupling may be poor with little direct irradiation of the burden and a very high flux incident on the kiln wall near the aperture. This may result in high radiation losses because the kiln wall will reach a high temperature and it has a good view factor for the

aperture. If the kiln is steeply inclined to improve coupling by allowing deeper penetration of flux within the kiln, the residence time will be too short for adequate reactant conversion. Slowing the kiln rotation rate improves residence time, but will exacerbate one of the critical problems identified for rotary kilns: expected short lifetime for the refractory liner due to periodic heating cycles. As an example, preliminary calculations for a 70% thermally efficient, 15 MW (5.12×10^7 Btu/h) (at aperture plane) kiln indicate kiln dimensions of 22.9 m (75 ft) length and 7.92 m (26 ft) diameter when heat recovery from hot gases and solids is practiced. Residence time will be 3.59 hours. For a typical kiln slope of 4.17 cm/m (0.50 in./ft), Perry's Handbook gives a 2.23 revolution per hour rotation speed for the kiln. A simple energy balance suggests these surfaces will be heated to temperatures near the limit of commercial refractories (1650°C/3000°F) and as the kiln rotates they will cycle to near the reaction temperature (980°C/1800°F). At a typical kiln rotational speed of two revolutions per hour, the kiln walls will cycle through more than 600°C (1080°F) every 30 minutes. This will lead to very short refractory liner lifetime.

The use of dams was briefly considered as a means of slowing the flow of reactants through a more steeply tilted rotary kiln. A steep tilt offers some potential for deeper penetration of flux into the reactor. However, such a kiln is still subject to periodic heating of the refractory wall. The "top" of the kiln will likely still experience high incident solar flux resulting in high refractory temperatures that would be expected to cycle down to approximately the reaction temperature. Although this decision is somewhat intuitive since time did not permit flux mapping of this alternative, the use of dams is not expected to resolve longevity concerns regarding the kiln liner.

The motion of the reactant bed in a rotary kiln, while providing good mixing, leads to dusting, which may impede penetration of solar radiation into the kiln.

The alternative design developed was the conveyor kiln. The cavity walls do not rotate. The design is mechanically simple.

The conveyor kiln appears to offer an attractive solution to the drawbacks of the rotary kiln. It offers the following features:

1. Reduced power consumption due to improved material handling efficiency

2. Enhanced flexibility and control of residence time by varying conveyor drive speed

3. Potential for improved solar coupling flexibility, which is achieved by relative freedom in selection of kiln axis inclination. The reactor can be tilted upward to almost any angle up to the limiting angle of repose of the reactants.

4. Reduced burden agitation minimizes dusting within the cavity to limit reflection and scattering losses at the aperture.

A conveyor kiln will be mechanically simple compared to the rotary kiln. It will be a compact design in the sense that its stationary walls make it less unwieldy to operate as a tower mounted reactor than the rotary kiln. The conveyor kiln is expected to be more thermally efficient than the rotary kiln because of better coupling of direct and reradiant flux to the burden and lower radiant losses. Constructed as a fixed container that allows the use of an ample thickness of lightweight refractories, the conveyor kiln can be cheaper to construct than the rotary kiln.

The conceptual nature of this study precluded detailed modeling of reactor performance. The model of the rotary kiln was well along at the time the conveyor kiln was finally selected. Detailed kinetics models to analyze the calciner are complex, proprietary programs owned by kiln manufacturers and available for use only at high fees (generally over $100K in the industry). The rotary kiln model used was developed at IGT from papers available on the subjects of kiln heat transfer and calcining dynamics. It is thus important to note that because configuration factors for radiation heat transfer within the reactor were established for the cylindrical geometry of a rotary kiln, kiln dimensions resulting from analytical calculations most closely represent those of a rotary kiln. For instance, whereas a conveyor kiln will have a flat bottom and a uniform burden depth, the rotary kiln has a crescent shaped burden cross section. In any case, values used in modeling of calciner performance should not be construed as optimum. The purpose of the modeling effort was to estimate physical dimensions and performance characteristics (thermal efficiency, throughput) of a direct flux solids reactor. Project scope does not permit optimization of design parameters such as geometry of kiln walls, aperture diameter, kiln length, and burden width.

The primary difference between the rotary kiln and conveyor kiln is that the conveyor kiln may permit a larger reactant bed width for a given aperture size than the rotary kiln. That is, a 7.92 m (26 ft) diameter rotary kiln modeled with a 3.8% solids fill factor gives a 4.33 m (14.2 ft) reactant width. The conveyor kiln would permit a broader reactant surface close to the 7.92 m (26 ft) dimension.

The results of the modeling effort included burden temperature profiles as a function of length in the kiln and throughput rates. These profiles were provided to Sanders where the radiant heat transfer balance in the kiln was modeled. The Sanders Model dealt with the radiant heat transfer within the kiln on a finite element basis. The results of the Sanders model was a cavity wall temperature profile and net flux to the burden as a function of length in the kiln.

Iteratively then, the Sanders results were fed to the IGT model; its results were fed back to the Sanders model until profile temperatures had converged to within several degrees ($< 50°C$).

The process yielded process temperatures and kiln temperatures sufficiently accurate to verify that the materials selection and design approach was feasible. In addition the model provides a means of estimating residence time and total burden weight.

As part of the reactor design effort the SRI International report on Design of an Experimental High Temperature Materials Processing System for the Solar Thermal Test Facility[18] was reviewed. The SRI report describes a windowless solar kiln designed for installation at the CRTF at Sandia Laboratory in Albuquerque, N.M. The report gives an overview of the use of rotary kilns in industry, and provides a useful introduction into some of the considerations in elucidating the heat transfer processes within the kiln and on materials of construction that will withstand the thermal and chemical environment within the kiln. The report falls short, however, on the development of an adequate model for kiln design. The kiln design developed by SRI was not sized by heat transfer and kinetics considerations, but rather by length constraints imposed by the site (CRTF).

A solar-heated rotary kiln differs from a fossil-fueled kiln in the way the solid is heated. In a fuel-fired kiln the solids are heated primarily by

radiation and convection from hot combustion products. Convection plays a major role in heat transfer. This is not the case in the solar kiln where radiation is the primary heat transfer mechanism for reactant heating. The rotary kiln designed by SRI would be 1.83 m (6 ft) ID, 3.66 m (12 ft) in length, with an aperture diameter of 1.22 m (4 ft). The aperture faces north toward the heliostat field of the CRTF. The focused light from the heliostat field enters the aperture and heats the rotating upper wall of the kiln. The hot upper wall of the kiln heats the solids by radiation and reflection. The cavity configuration allows the kiln walls to be heated directly by the focused light while keeping heat losses significantly lower than an externally heated receiver. Calculations by SRI indicate a thermal efficiency of 75% with 2 MWth (6.83×10^6 Btu/h) incident on the kiln aperture. Heat is also transferred by conduction to the solids as the hot wall rotates to the bottom. The SRI study anticipated almost uniform bed temperatures because the kiln rotation provides a tumbling motion to the solids to ensure good mixing.

The authors of the SRI study emphasize that modeling heat transfer processes in rotary kilns is very complex, and a completely satisfactory formulation is not available. They note that existing modeling studies of fuel-fired kilns have simplified the problem in order to seek solutions for understanding kiln behavior. Although the authors did not carry out a model of the solar kiln, they did identify the heat transfer processes within the kiln that are important to consider in model development. The SRI study merely based material throughput on the basis of an overall energy balance. This resulted in an overestimation of the possible processing rate because the overall reaction rate is slower than the rate implied by a gross energy balance, which leads to a requirement for longer residence times to achieve complete conversion.

As shown in Figure 8,[18] heat flow inside a solar heated rotary kiln can be divided into four principal steps:

1. The upper walls are heated by concentrated solar radiation and by reflected radiation from other parts of the kiln. The temperature of the wall surface is determined by the interplay of radiative heat transfer among the incoming radiation, the optical characteristics of the materials of construction and reacting solids in solar and infrared wavelengths, and the temperatures of the solids and kiln surfaces. The authors of the SRI study note that the absorbance for solar radiation of alumina bricks, the typical kiln liner material, is 0.35. Reflectance is 0.65. They use an IR "grey body" emittance of 0.8.
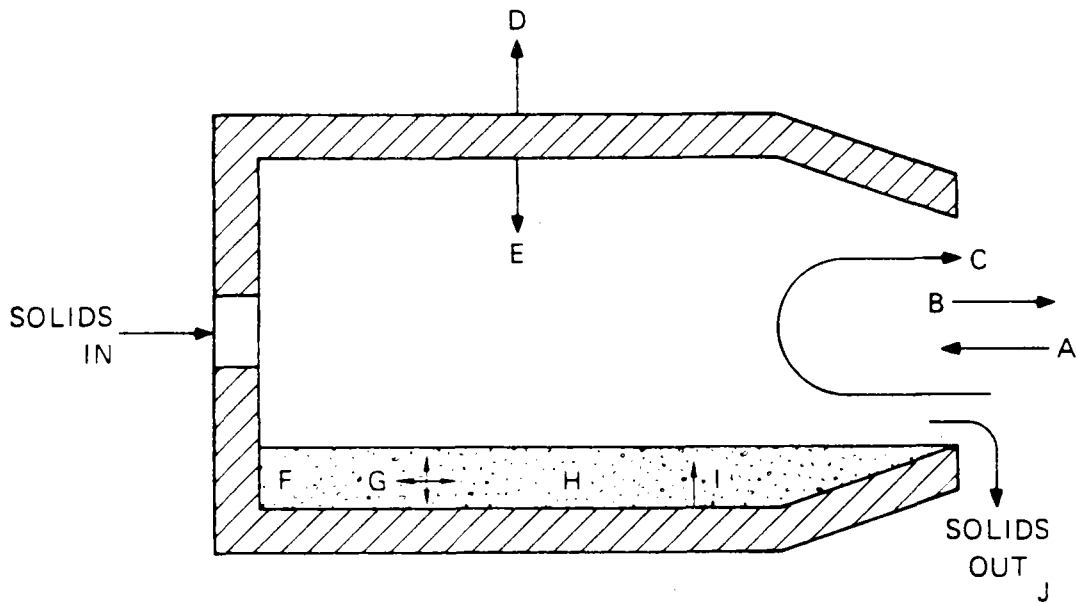
A	SOLAR RADIATION IN
B	RADIATION LOSS FROM CAVITY
C	GAS CONVECTION LOSS
D	CONDUCTION LOSS THROUGH WALL
E	RADIATION FROM UPPER WALL TO BED
F	PRE-HEATING OF SOLIDS
G	CONDUCTION AND RADIATION WITHIN BED
H	CHEMICAL REACTION HEAT
I	CONDUCTION FROM BOTTOM WALL TO BED
J	SENSIBLE HEAT IN THE HOT DISCHARGE SOLIDS

Figure 8.   HEAT TRANSFER PROCESSES IN A ROTARY KILN

2. The upper surface of the solid bed is heated by reflected solar radiation and emitted radiation from the hot kiln walls.

3. The lower surface of the bed is heated by conduction from the hot wall as it rotates under the bed. In a conveyor kiln this mode of heat transfer is not operative.

4. Heat transfer within the bed occurs due to the tumbling motion of the solids. Solids mixing in kilns is very good and leads to uniform bed temperature. The screw conveyors in the conveyor kiln can also provide good mixing.

A number of references on the modeling of kilns have been used to formulate the kiln model.[19-35]

System Boundaries

The system boundaries for characterization of calciner performance were identified. Kilns fired from fossil fuels typically have a preheater to heat the feed (limestone) while recovering heat from the combustion and product gases. A contact cooler is also used to preheat combustion and sweep gases by recovering heat from the product solids. As this auxiliary equipment is crucial for efficient and economic operation of a kiln, heat recovery is incorporated in the model. The system will include the use of preheaters as a means to recover the substantial sensible heat content in kiln off-gases (44 kg of CO_2 are produced for every 100 kg of $CaCO_3$ reacted). Contact coolers are included to recover the sensible heat in the product lime.

Air is used as a sweep gas to ensure that the partial pressure of carbon dioxide above the reactants is low, and to entrain fines and prevent their escape through the aperture. The sweep gas is heated in the contact cooler, injected around the kiln aperture, mixes with product gases and is pulled along the kiln axis to the feed end of the kiln where the hot gases contact the feed in the preheater. Finally, after cleanup, the sweep gas, laden with CO_2 is exhausted to the atmosphere through an induced draft fan. Figure 9 shows the solar calciner conceptual design.

Relevant Design Parameters

In the case of the solar kiln, the energy source for limestone decomposition will be reflection, reradiation, and conduction from the kiln walls to the limestone. In this approach, the upper inner walls of the kiln, heated by the solar flux, reflect and reradiate to the solids burden. Based

REACTANT BED

LENGTH = 22.9 m (75.0 ft)
WIDTH = 7.92 m (26.0 ft)
DEPTH = 0.40 m (1.3 ft)
(Not-to-Scale)
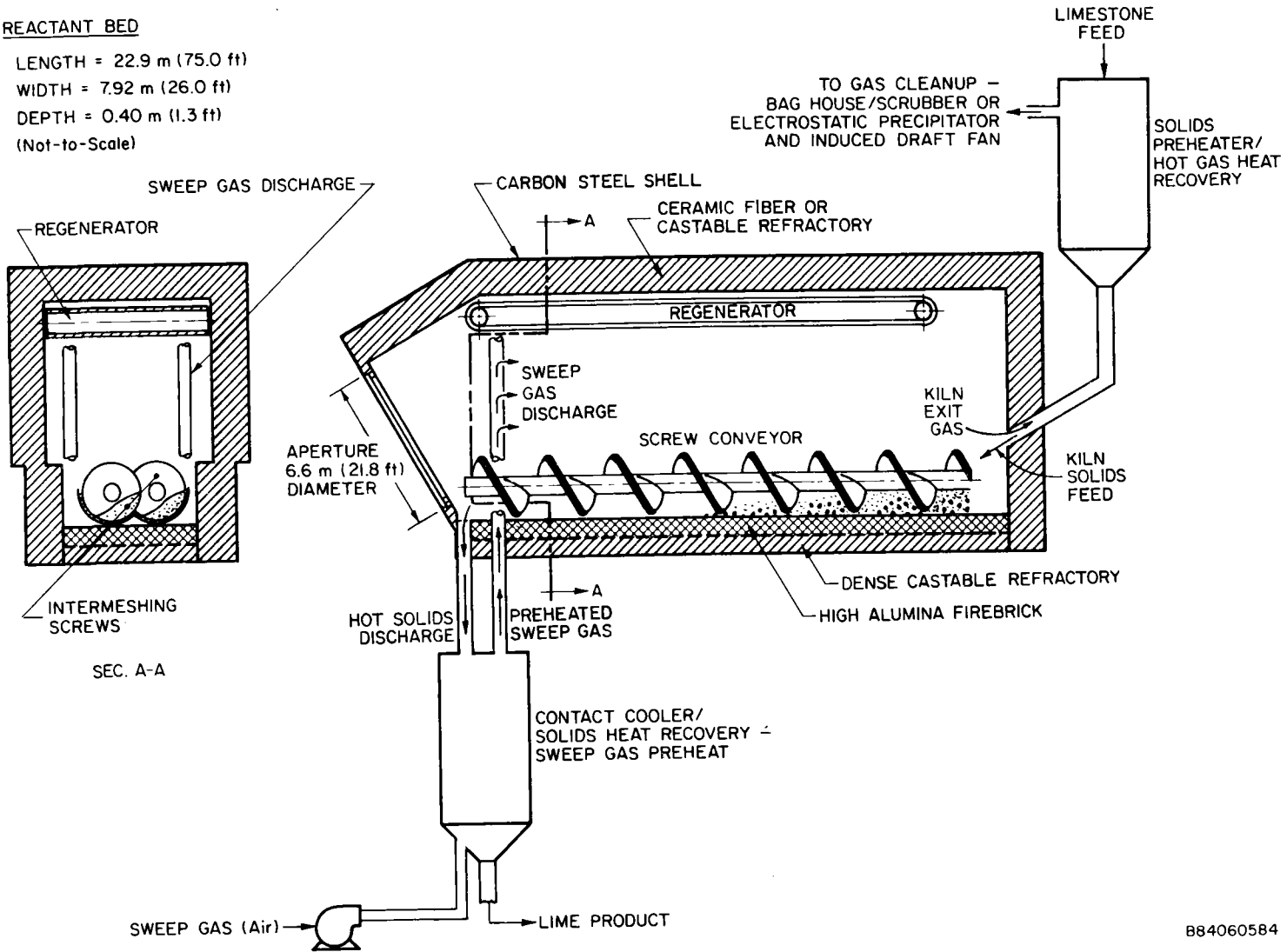
Figure 9.   SOLAR CALCINER CONCEPTUAL DESIGN

B84060584

on general heat transfer considerations for a solar calciner, an outline of the parameters pertinent to calciner design has been developed:

Heat Transfer Step	Critical Design Parameter/Design Issue
Solar Radiation to:	
1. Kiln aperture	Aperture orientation
Objective: Large power input consistent with low reradiation loss	Aperture diameter
2. Inner kiln walls	Kiln configuration/shape factors
Objective: Effective coupling of solar energy to reaction through achievement of good thermal efficiency	Burden slope angle
	Emissivity/absorptivity of refractory in solar and infrared wavelengths
3. Regenerator	Configuration/shape factors
Objective: Assess methods to improve kiln performance through improved solar heat utilization	Optical properties in solar and IR
4. Solids burden	Exposed surface area (length, width); kiln fill factor
Objective: Kiln performance modeling	Emissivity/absorptivity of burden in solar and infrared wavelengths
5. Kiln gases[**]	Composition (CO_2, N_2, O_2)
	Emissivity/absorption in solar and infrared wavelengths
Reradiation Losses	
Objective: Achieve low thermal losses	Aperture diameter
	Shape factors
	Kiln length
	Optical properties of interior of reactor: reactant, walls, regenerator

---

[*] Assume adiabatic walls.

[**] Neglect for this task.

Distance collector to aperture

Kiln gas reradiation[**]

.

Convective Transfer

General

Objective: Kiln modeling

Heat transfer coefficients

Temperature differences

1. To/from gases and solids burden

Diluent (air) flow rates

CO_2 evolution rates

Burden surface area

2. To/from gases and inner kiln walls[*]

Diluent (air) flow rates

CO_2 evolution rates

Kiln wall surface area (dependent on kiln length and cross section)

3. To/from kiln shell to ambient[**]

Wind speed

Kiln external dimension

4. Losses

Diluent flow rates

CO_2 flow rates

Percent recycle of exhaust gases[*]

Extent of heat recovery of exhaust gases for preheating feed

Dust losses[*]

Heat Recovery

Diluent flow rates

Objective: Analyze thermal performance of equipment to recover enthalpy of feed and products

CO_2 evolution rates

Heat transfer coefficients

Heat transfer contact areas

Heat transfer effectiveness

Conduction Heat Transfer**

1. General

Thermal conductivity values of kiln liner materials

Objective: Determine performance of insulation systems

Heat capacities of kiln liner materials and of burden*

Temperature differences

2. To/from firebrick and insulating brick

Thermal conductivities

Heat capacities*

Temperature differences

3. To/from insulator and outer shell

Heat capacities*

Temperature differences

4. End wall

Thermal conductivities

Heat capacities*

Temperature differences

5. From solids*

Particle size

Reaction kinetics

Objective: Determine reactor performance

Particle size

Nominal one-inch particle assumed. Typical of limestone kiln operations

Catalysts*

Assumptions

The assumptions used to facilitate the analysis of kiln performance were:

o   Burden is horizontal. The sensitivity of reactor performance to varying the tilt angle of the burden was not explored. The tilt angle of the burden affects the coupling of direct solar radiation to the reactants.

o   Sensitivity of reactor performance to the emissivity/absorptivity of the burden, refractory, and regenerator was not looked at. Considerable uncertainty exists in optical properties of materials, especially at high temperatures

- Constant (mean) heat capacities of reactants and products[†]

- Temperature dependent heat of reaction

- No interaction of kiln gases (N_2, O_2, CO_2, H_2O) with solar and IR radiation

- No dusting

- Reactor walls are perfectly insulated (adiabatic walls)

- No convective heat transfer from kiln walls to kiln gases

- No exhaust gas recycle

- 2.54 cm (1 in.) diameter feed. This is typical of industrial rotary kiln operation. Sensitivity to particle size was not investigated. Reaction rate is sensitive to particle size. Reaction rate varies as the reciprocal of the square of particle radius.

- Solids move in plug flow as a uniform bed (perfectly mixed; uniform temperature and composition at any given cross section)

- Gases flow countercurrently in plug flow (perfectly mixed; uniform temperature and composition at any given cross section)

- Reaction takes place in the bed of solids: $CaCO_3 \rightarrow CaO + CO_2$

- Pure $CaCO_3$ is fed in a constant rate and temperature

- Operates at constant pressure; gases are ideal

- 28.32 m^3/min. (1000 SCF/min.) sweep gas air flow. Model results indicate this sweep gas flow rate is adequate to recover heat from solid products, preheat solid feed, and maintain a moderate partial pressure of CO_2 in the reactor.

Calciner Mass and Energy Balances

As noted earlier, we assume that the walls of the kiln are perfect insulators. This enables us to neglect the effects of heat transfer from the walls on the temperature of the gas and burden. In addition, we assume

---

[†] We are using mean heat capacities, C_{pm}, where

$$C_{pm} = \frac{\int_{T_o}^{T_1} C_p \, dT}{T_1 - T_o}$$

and a value of $T_1 = 147.15$ K = 1200°C (2192°F) is used.

111

constant mean gas and solids heat capacities. A temperature-dependence is incorporated into the rate expression. The temperature dependent rate expression will be discussed in more detail later.

The mass and energy balances of the model developed are as follows:

Mass Balances

CaCO$_3$:
$$v_s \frac{dx_C}{dz} = R(x_C) \tag{1}$$

at $z = L$, $x_C = 1$

CaO:
$$x_D = 1 - x_C \tag{2}$$

CO$_2$:
$$\frac{d}{dz}(c_B v_B) = \frac{A_s}{A_g} c_{CO} R(x_C) \tag{3}$$

at $z = 0$, $c_B v_B = c_{BO} v_{BO}$

Air:
$$c_A v_A = c_{AO} v_{AO} \tag{4}$$

Energy Balances

Gases:
$$C_{pA} \frac{d}{dz}[c_A v_A (T_g - T_o)] + C_{pB} \frac{d}{dz}[c_B v_B (T_g - T_o)]$$
$$- \frac{A_s}{A_g} c_{CO} C_{pB}(T_s - T_o) R(x_C) - \frac{w}{A_g} h_{sg}(T_s - T_g) = 0 \tag{5}$$

at $z = 0$, $T_g = T_{go}$

Solids:
$$v_s c_{CO} C_{ps} \frac{d}{dz}(T_s - T_o) - c_{CO} C_{pB}(T_s - T_o) R(x_c)$$
$$- \frac{w}{A_s} h_{sg}(T_s - T_g) - \Delta H_r c_{CO} R(x_c) + \frac{w}{A_s} q_r = 0 \tag{6}$$

at $z = L$, $T_s = T_{so}$

Notation

c = molar density (mol/L^3)

v = speed of solids or gas species (m/sec, ft/sec)

z = distance (longitudinal from aperture end ($z = 0$) (m, ft)

L $\quad=\quad$ length of kiln (m, ft)

T $\quad=\quad$ temperature (°C, °F)

T_O $\quad=\quad$ datum temperature, 25°C (77°F)

r_w $\quad=\quad$ interior radius of kiln (m, ft)

w $\quad=\quad$ width of surface of bed (m, ft)

A_g $\quad=\quad$ cross-sectional area of gas filled portion of kiln (m^2, ft^2)

A_s $\quad=\quad$ cross-sectional area of solids filled portion of kiln (m^2, ft^2)

$\qquad \pi r_w^2 = (A_s + A_g)$. Fill factor = $A_s/(A_s + A_g)$.

C_p $\quad=\quad$ molar heat capacity (kcal/mole-°C, Btu/lb-mole-°F)

h $\quad=\quad$ heat transfer coefficient (cal/cm^2-s-°C, Btu/ft^2-h-°F)

x $\quad=\quad$ mole fraction

ΔH_r $\quad=\quad$ heat of reaction (kcal/mole, Btu/lb-mole)

θ_w $\quad=\quad$ 1/2 of the angle subtended by the solids bed (radians)

q_r $\quad=\quad$ radiant heat flux into surface solids (kW/m^2, Btu/h-ft^2)

$R(x_C)$ $\quad=\quad$ reaction rate (1/sec)

$$= \frac{3K_e \, \Delta T}{c_{CO}\Delta H_r r_0^2} \; \frac{1}{x_C^{-1/3} - 1}$$

k_e $\quad=\quad$ effective thermal conductivity of CaO (kcal/m-°C, Btu-in./ft^2-h-°F)

r_0 $\quad=\quad$ particle radius (cm, in.)

ΔT $\quad=\quad$ temperature difference between outside surface of particle and center (°C, °F)

Subscripts

A $\quad=\quad$ air

B $\quad=\quad$ CO_2

C $\quad=\quad$ $CaCO_3$

D $\quad=\quad$ CaO

g $\quad=\quad$ gas

s $\quad=\quad$ solids ($CaCO_3$ + CaO)

w = wall of kiln (interior)

O = initial.

The functional form of the reaction rate, $R(x_C)$, is not suitable for a realistic model because $R(x_C) \to \infty$ as $x_c \to 1$, that is, for pure, unreacted $CaCO_3$ where $x_c = 1$. Because the rate is limited by heat conduction through the ash (CaO) layer, a high (but not infinitely high) reaction rate is expected when there is not product layer (when $x_c = 1$). It was therefore necessary to reformulate the rate expression so it would behave more realistically at low conversions. In fact, the expression for $R(x_c)$ given above is a limiting rate law, valid only for conversions greater than about 50% ($x_c < 0.5$). So a revised rate expression should be accurate when $x_c < 0.5$, and should have a relatively high but finite value when x_x approaches 1.0. To satisfy these requirements, we obtained a least-aquares polynomial fit to the expression $f_1 = (x_c^{-1/3} - 1)^{-1}$ for $0 \leqslant x_c < 0.5$, with a numerically equivalent expression f_2 constrained to pass through the point $(x_c, f) - (0,0)$:

$$f_2 = x_c (10.5334 - 23.5704\, x_c + 36.3358\, x_c^2) \tag{7}$$

The rate expression used in our model is then —

$$R(x_c) = \frac{3k_e\, \Delta T}{c_{CO}\, \Delta H_r\, r_o^2}\, x_c (10.5334 - 23.5704\, x_c + 36.3358 x_c^2) \tag{8}$$

After introducing dimensionless variables and manipulating the energy balances, we are left with the following four differential equations:

$$\frac{dx_c}{d\zeta} = K(x_c) \tag{9}$$

at $\zeta = 1$, $x_c = 1$

$$\frac{dN_B}{d\zeta} = F(x_c) \tag{10}$$

at $\zeta = 0$, $N_B = N_{BO}$

$$\frac{d\theta_s}{d\zeta} = S_s (\theta_s - \theta_g) + G(x_c)\, \theta_s + H(x_c) - Q_r \tag{11}$$

at $\zeta = 1$, $\theta_s = \theta_{so}$

$$\frac{d\theta_g}{d\zeta} = \frac{S_g + F(x_c)}{\gamma + N_B} \left(\theta_s - \theta_g\right) \tag{12}$$

at $\zeta = 0$, $\theta_g = \theta_{go}$

Variables

$\zeta = z/L$ dimensionless axial position

$x_c = \dfrac{c_C}{c_C + c_D}$ mol fraction $CaCO_3$ in solids

$N_B = \dfrac{c_B\, v_g}{c_{BO}\, v_{go}}$ dimensionless molar flux of CO_2

$\Theta_s = \dfrac{T_s - T_o}{T_o}$ dimensionless solids temperature

$\Theta_g = \dfrac{T_g - T_o}{T_o}$ dimensionless gas temperature

Parameters	Physical Significance of Dimensionless Parameters
$K(x_c) = \dfrac{LR(x_c)}{v_s}$	ratio of rate of conversion of $CaCO_3$ to rate of transport of $CaCO_3$ through kiln
$F(x_c) = \dfrac{A_s\, c_{CO}\, LR(a_c)}{A_g\, c_{BO}\, v_{go}}$	ratio of CO_2 flue from solids into gas stream to CO_2 flux into kiln
$G(x_c) = \dfrac{C_{pB}\, LR(x_c)}{C_{ps}\, v_s}$	ratio of heat transfer by CO_2 evolving from solids to convective heat transfer by solids
$H(x_c) = \dfrac{\Delta H_r\, LR(x_c)}{v_s\, C_{ps}\, T_o}$	ratio of heat of reaction to heat content of solids
$S_g = \dfrac{wL\, h_{sg}}{A_g\, c_{BO}\, v_{gc}\, C_{pB}}$	Stanton number for gas — ratio of the capacity of the gas/solids interface to transfer heat, to the capacity of the gas stream to convect it
$S_s = \dfrac{wL\, h_{sg}}{A_s\, c_{CO}\, C_{ps}\, v_s}$	Stanton number for solids — ratio of the capacity of the gas/solids interface to transfer heat, to the capacity of the solids to convect it

$$\gamma = \frac{C_{pA}\, c_{AO}}{C_{pB}\, c_{BO}} \qquad \text{ratio of volumetric heat capacities of air to } CO_2$$

$$Q_r = \frac{wL\, q_r}{A_s\, c_{CO_s}\, v_s\, C_{ps}\, T_o} \qquad \begin{array}{l}\text{ratio of radiant heat flux to convective heat flux}\\\text{of solids}\end{array}$$

The solids heat capacity is given by

$$C_{ps} = x_c\, C_{pc} + (1 - x_c)\, C_{pD} \qquad (13)$$

Thus every parameter except S_g and γ is a function of x_c and so varies at each axial point in the kiln.

Preheater and Aftercooler Design

Kilns fired with fossil fuels typically have a preheater to heat the feed while recovering heat from the combustion and product gases. An aftercooler (also called "contact cooler") is also used to preheat combustion and sweep gases by recovering heat from the product solids. Because this auxiliary equipment is crucial for efficient and economic operation of a kiln, we felt we should try to incorporate heat recovery into our model. To simulate these processes in a straightforward fashion, we divided our kiln into three sections — an aftercooler section where product is cooled by incoming air; the kiln, which is the only section where heat is input; and a preheater section in which the feed is preheated by the exiting hot air and CO_2. Generally, in this equipment the solids and gases are contacted more intimately than in the rotary kiln, for example, by flowing the gas through a bed of solids rather than over the surface of the bed. To simulate this, we simply increased the heat transfer coefficient in the aftercooler and preheater section by some factor. This factor (a value of 10 was used in the model calculations) actually represents the increase in surface area of solids in the auxiliary sections, and seems to be a reasonable assumption. The lengths of the aftercooler and preheater sections should be interpreted as "effective" lengths, that is, the lengths they would have to be if they were operated as rotary kiln (though with high heat transfer coefficients). The lengths currently being used in the model evolved historically and are certainly not optimized. Nevertheless, they are suitable for illustrating the gross behavior of the heat recovery system.

Method of Solution

Equations 10 through 12 are coupled and nonlinear; therefore, they must be solved numerically. Equation 9 is independent of all the other variables and can be solved analytically. The solution, however, is a transcendental function of x_c that would have to be solved numerically at each ζ. In this particular case, as is often true, it is easier to integrate the differential equation numerically than it is to solve the nonlinear algebraic equation numerically. The differential equation was integrated numerically.

The four differential equations (9 through 12) are solved simultaneously using the so-called "shooting method" by which a Runge-Kutta method is used to solve the boundary value problem. The particular method used is the Runge-Kutta-England procedure.[36]

The rate expression developed by Turkdogan[37] for decomposition of $CaCO_3$ is:

$$R(x_c) = \frac{3k_e \, (T_{sp} - T_{ip})}{c_{CO} \, \Delta H_r \, r_o^2} \cdot \frac{1}{(x_c^{-1/3} - 1)} \tag{14}$$

where T_{sp} is the surface temperature of a particle, and T_{ip} is the center or reaction interface temperature. This expression was developed for a single spherical particle in a furnace at constant temperature. It is not completely consistent with our model, in which the "furnace," or gas temperature varies and where we assume the solids bed is at a uniform temperature at any point, z. Turkdogan found, however, that at 50 to 95% conversions, the temperature difference $\Delta T = T_{sp} - T_{ip}$ remained nearly constant (again, in a constant-temperature furnace) and that ΔT was a function of T_{sp}, varying from 3°C (5.4°F) when $T_{sp} = 803°C$ (1477°F), to 200°C (360°F) when $T_{sp} = 1120°C$ (2048°F). Higher surface temperatures result in larger ΔT's, and the relationship is nearly linear. We have exploited this observation and replaced ΔT in our rate expression with a linear least squares fit to some $(T_{sp}, \Delta T)$ data presented by Turkdogan:[37]

$$\Delta T = 0.629986 \, T_s - 514.286 \qquad (T_s \text{ in °C})$$

$$= 187.83 \, \Theta_s - 498.536 \tag{15}$$

ΔT is zero at 816°C (1501°F). Below this temperature, we set the reaction rate equal to zero.

Radiation Heat Transfer Modeling

The radiative heat transfer process inside the cavity was analyzed. A complete exchange of radiation, in the solar and infrared bands was calculated. This radiation exchange also included the energy reflected and radiated from each surface increment through the cavity aperture.

A "cavity receiver" is taken to mean any geometry that encloses or partly encloses a volume of space interior to surfaces that receive incident energy, whether directly from the heliostats or indirectly from other surfaces. Cavities may be constructed from combinations of intersecting planes and the surfaces of the planes that may potentially receive energy were divided into sets of nodes. The analysis allows determination of the total flux incident on each receiver node. The predicted incident flux on the nodes was used as input to radiation interchange and heat transfer programs to compute the rates of heat absorption into the reactants.

The basic steps in the calculation scheme are as follows:

1. Calculate configuration factors for the given receiver design

2. Calculate the distribution of solar energy in the cavity as a function of direct incident solar flux, and cavity geometry. Calculate solar reflective losses

3. Calculate the distribution of infrared energy to the receiver walls and reactant bed utilizing the solar flux distribution calculated in Step 2. Calculate temperature of walls and reactant bed and thermal radiation loses for the receiver

4. Calculate net heat flux absorbed by the reactants

5. Perform kinetic analysis of the reaction occurring in the bed of reactant

6. Print out all the calculated variables for thermal performance analysis of the receiver.

The basic assumptions and the calculation methodology are described below:

Basic Assumptions

Most materials are not gray, but selective; that is, their absorptivity, reflectivity, and emissivity vary with the wave lengths of incident energy. For simplicity, the electromagnetic spectrum will be divided into two segments: one corresponding to the solar band and one corresponding to the infrared band. An assumption was made that the materials are gray in each of

118

these regions. This assumption enables a separate calculation for heat flux distribution in the solar and infrared bands. Each incremental surface inside the cavity is assumed to be isothermal, with uniform thermooptical and physical properties and the radiant flux density reflected or emitted by each surface zone is assumed to be uniform and diffuse, neglecting the specular radiation component.

Configuration Factors Calculation

The configuration factors (or shape factors) represent the fractions of energy originating from one zone which is directly intercepted by any other zone in the cavity. They are a function of the geometry alone; that is, relative dimensions, form and spatial positions of each pair of zones.

Energy Balance in Solar Band

The solar flux intercepting the inner cavity walls will experience a series of multiple reflections and absorptions inside the cavity until it is totally absorbed or reflected back out of the aperture. This mechanism depends on the cavity geometry and the absorptivity and reflectivity in the solar band of each surface zone in the cavity.

The fraction of energy leaving a given zone, which reaches a node not only directly but also via all neighboring nodes, is usually termed the "total configuration factors." The evaluation of this factor enables the calculation of net solar energy incident on each zone.

The solar energy lost through the aperture is calculated by accumulating the products of emitted solar energy of each zone and the total configuration factors between the zones and the aperture.

Energy Balance in the Infrared Band

The infrared radiation interchange among all surfaces in the cavity is calculated following the calculation of the net solar energy incident to each surface zone. Calculations are made of the actual temperature of each zone, the net heat flux to the reactants and radiant energy losses through the aperture. In the infrared spectrum the surfaces are also emitting radiant energy.

The total configuration factors of the infrared radiation mechanism are calculated (this time with the emissivities and reflectivites corresponding to

119

the infrared spectrum) and are utilized in the thermal energy balance. The temperature of each refractory zone is determined and the computation of radiative losses through the aperture is done in a similar way as in the solar band.

The fluxes are fed into the chemical reaction model which performs, for each increment along the reactant bed, a complete mass and component balance, and reaction kinetics. Overall mass and energy balances were computed as a check on validity of solutions.

Model Implementation (Determination of Design Point Performance)

The parameters of the receiver/reactor design that were explored to meet the technical requirements of the system design and to prepare a conceptual design were:

— Reactant bed surface area

— Reactant bed arrangement/orientation, that is, long and narrow

— Refractory wall area

— Relative orientation of walls with respect to each other and to reactant bed

— Regenerator presence and characteristics/absence of regenerator.

The geometrical design of the reactor/receiver is an iterative process. Geometry changes influence the pattern of incident solar flux inside the cavity, influence overall efficiency, and affect the aperture sizing (to maximize input power, consistent with loss minimization).

The final solution to the model had to take into account reradiation from the burden. Because Sanders model of the flux distribution was developed independently of IGT's model of the kiln behavior, there was no direct link between the programs, so burden temperatures and net fluxes could not be computed simultaneously in the strictest sense. The net flux accounts for the IR and solar radiation to the reactants net of burden reradiation. Instead, temperatures and net fluxes were determined iteratively. IGT produced a simulated net flux which amounted to an initial guess of the actual net flux. IGT then provided Sanders with burden temperatures based on the assumed net flux, and Sanders calculated a new net flux distribution based on our burden temperatures. With this new flux distribution, IGT recalculated burden

temperatures as a second iteration. The actual net flux distribution was not radically different from the initially assumed flux, and the burden temperature was not highly sensitive to flux distribution so this procedure converged rapidly. Only three iterations were required to achieve a stable solution to the model.

Calciner Conceptual Design

Optimal design of the calciner must take into account such factors as burden tilt angle, aperture diameter, cavity configuration, use of regenerator, and reactant bed dimensions. Optimization of calciner design is outside the scope of this project. As a result, although the design is that of a conveyor kiln the "as modeled" cavity configuration is cylindrical as if a rotary kiln cavity was the design. No sensitivity to burden tilt angle explored. The kiln aperture diameter was 6.64 m (21.8 ft).

Two kiln lengths were explored: 10.7 m (35 ft) and 22.9 m (75 ft). Model results for a 10.7 m (35 ft) kiln indicated that such a kiln can obtain adequate conversion of feed limestone to product lime. The lengths were chosen somewhat arbitrarily; considerably more analysis is required to optimize the length. The primary consideration was to create some type of cavity shape inspite of the large ratio of aperture to kiln diameter. However, because reactor walls have good view factors for the aperture, the 10.7 m (35 ft) kiln has extremely high radiant losses leading to poor efficiency. Because the 10.7 m (35 ft) calciner had such poor efficiency (around 40% based only on aperture radiant losses) it was dropped from further consideration and design efforts concentrated on the 22.9 m (75 ft) long unit which had an 88.7% efficiency (based on radiant losses only). Although convective losses were not determined, Figure 4 suggests total losses of from 25% to 30% can be expected at operating temperatures in the range of 900° to 1000°C (1652° to 1832°F).

The lengths of the aftercooler and preheater sections (6.1 m and 9.1 m [20 ft and 30 ft], respectively) should be interpreted as "effective" lengths, that is, the lengths they would have to be if they were operated as rotary kiln (though with high heat transfer coefficients). The lengths used in the model are not optimized; since the solids still come out very hot, this section should be lengthened considerably, whereas, the preheater can probably be shortened. Nevertheless, they are suitable for illustrating the gross behavior of the heat recovery system.

121

Physical property data used in the analysis are summarized in Table 22.

Operating conditions used in the analysis of kiln performance are summarized in Table 23.

The calciner design is shown schematically in Figure 9.

The receiver technical specifications are summarized in Table 24.

For this study the field geometry was taken to be similar to that of the Central Receiver Test Facility (CRTF) at Albuquerque, New Mexico. The center of the CRTF beam is tilted upward at about 20°. Further, the relatively broad side angle of the field results in a rapid splaying out of the solar beam behind the receiver aperture. The bulk of the direct solar impinges on the cavity (kiln) wall near the front (output) end of the kiln and little solar energy reaches the back (feed) end of the kiln. Reradiation is the principal mechanism for heating the feed end of the kiln. Due to the Lambertion (diffuse) distribution of the reradiation significant losses occur at the aperture unless measures are taken to reduce temperatures on the front cavity walls. As a result, a regenerator was used in the conceptual design. (Regenerator design is discussed later in this section.)

Receiver aperture diameter is 6.64 m (21.8 ft). The aperture is of a circular cross section with an area of 34.7 m (373 sq ft). Aperture diameter was sized by scaling the CRTF (5 MW) to the size of the solar chemical application (15 MW). Mirror areas and field acreage are CRTF specifications multiplied by three. Linear dimensions of field extent, slant range from mirror(s) to aperture, and tower height are CRTF specifications multiplied by $\sqrt{3}$. The model then is run and the aperture sized to a near optimum.

The sizing is accomplished by sizing the aperture so that the incoming solar flux is equal to the cavity reradiation loss at the edge of the aperture. Within the aperture the incoming solar flux is more intense than the reradiation at the cavity temperature and the cavity <u>gains</u> energy. If the aperture is sized larger than optimum then reradiation near the edge exceeds solar and the cavity suffers net energy loss near the edge of the aperture. If these incremental energies are summed across the aperture, peak net cavity gain occurs (in this case) when the aperture radius is 6.64 m (21.8 ft) (See Figure 10). Field size is then iterated to yield at net power ≈ 15 MW. The aperture is tilted downward from the vertical at an angle of 20 degrees and

Table 22. PHYSICAL PROPERTY DATA USED IN ANALYSIS
OF SOLAR CALCINER PERFORMANCE

Molar Heat Capacity of Air	7.51 cal/mol °K (or Btu/lb-mole-°F)
Molar Heat Capacity of CO_2	12.32 cal/mol °K (or Btu/lb-mole-°F)
Molar Heat Capacity of $CaCO_3$	29.51 cal/mol °K (or Btu/lb mole-°F)
Molar Heat Capacity of CaO	14.04 cal/mol °K (or Btu/lb-mole-°F)
Heat of Reaction*	423.68×10^2 cal/mol (76441 Btu/lb-mole) at 25°C (77°F)
Effective Thermal Conductivity of CaO	1.2×10^{-3} cal/s cm °C (2.9×10^{-1} Btu/h-ft-°F)
Density of $CaCO_3$	2.50 g/cm^3 (1.56×10^2 lb/ft^3)

*$\Delta H_R(T) = 42368 - 3.15 (T_{solid} - T_o)$ cal/mol, where T_o — datum temperature of 25°C (77°F).

Table 23. OPERATING CONDITIONS USED IN THE ANALYSIS
OF SOLAR CALCINER PERFORMANCE

$CaCO_3$ Particle Diameter	2.54 cm (1.0 inch)
Total Pressure	1.01325 Bar (1.0 atmosphere)
Sweep Gas (Air) Flow Rate In	4.719×10^{-1} m^3/sec (1000 ft^3/min)
Inlet Air Temperature	25°C (77°F)
$CaCO_3$ Feed Temperature	25°C (77°F)
Fill Factor	3.8%
Inlet CO_2 Mole Fraction	3.3E-04
Reactor Solid/Gas Heat Transfer Coefficient*	9.5×10^{-4} cal/s cm^2 °C (7.0 Btu/hr ft^2 °F)
Heat Recovery Solid/Gas Heat Transfer Coefficient**	9.5×10^{-3} cal/s cm^2 °C (70 Btu/hr ft^2 °F)
Solar Power at Kiln Aperture	15 MW (5.12×10^7 Btu/h)
$CaCO_3$ Feed Rate	5.06802E01 mol/s (5.07258×10^3 g/s, 20.13 ton/h)
Aperture Diameter	6.64 m (21.8 ft)
Kiln Length	22.8 m (75 ft)
Kiln Diameter	7.92 m (26 ft)

* Assumed.

** As discussed in the section on "Process Design of Calcination Reactor" under
"Preheater and Aftercooler Design."

Table 24. LIMESTONE CALCINER DESIGN SPECIFICATIONS

Operating Mode	Production during day – feed and product storage
Receiver Type	Single cavity
Power at Aperture	15 MWth (5.12 x 10^7 Btu/h)
Power to Process	13.3 MWth (4.54 x 10^7 Btu/h)
Efficiency	89%
Limestone Process Flow	5.1 kg/sec (20.1 ton/h)
Reactor Inlet/Outlet Conditions	399°C (750°F) inlet/956°C (1753°F) outlet
Sweep Gas (air) Flow	0.47 m^3/sec (1000 ft^3/min)
Aperture	Circular 34.7 m^2 (373 ft^2). Tilted 20° from vertical facing north to heliostat field.
Reactant Bed	Length – 22.9 m (75 ft) Width – 7.9 m (20 ft) Depth – 0.40 m (1.3 ft) Residence time – 5.9 hours
Refractory Liner (sides and roof)	Fibrous refractory – 0.30 m (1 ft) thick.
Refractory Liner (floor)	High alumina firebrick over dense castable refractory – 0.30 m (1 ft) total thickness.
Material Conveyance	Intermeshing screw conveyors – Incoloy 800H.
Weight	748 metric tons (825 tons)
Heat Recovery	Conventional design

* Based only on receiver radiation heat loss through aperture. Based on Figure 4, total radiation convection losses may be estimated at 25% to 30% for a net design point receiver efficiency of 70% to 75%.
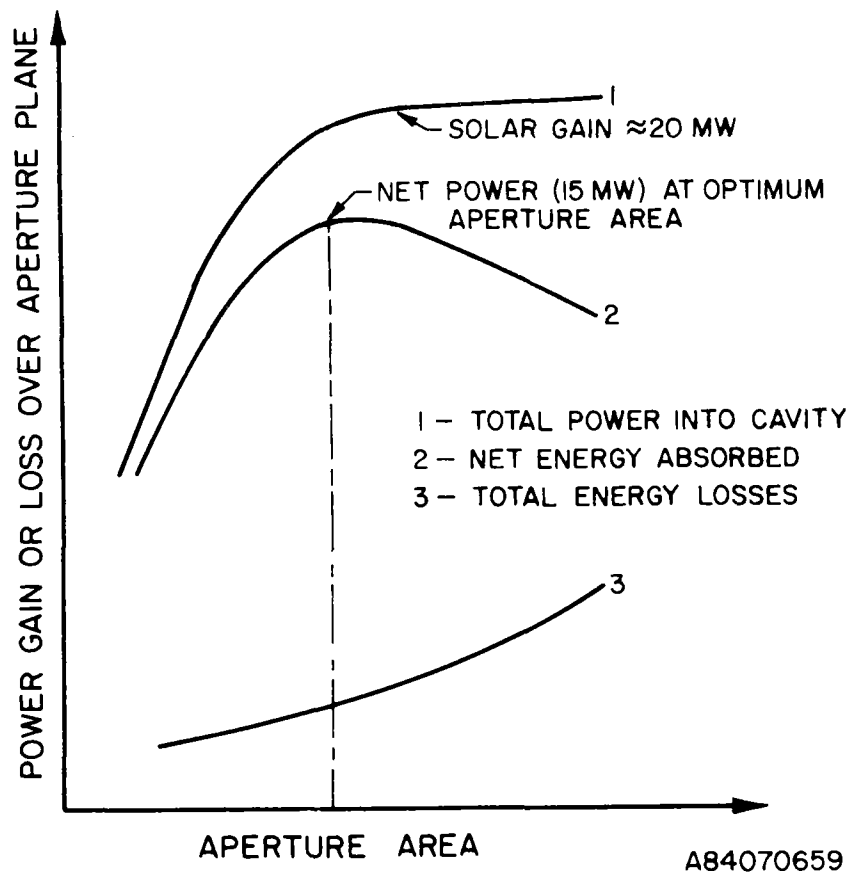
Figure 10. APERTURE SIZING

faces north towards the heliostat field. A shroud, looking somewhat like the brim of a baseball cap extends over the top and sides of the aperture could be used to help reduce convective loss from winds and to preserve a "bubble" of buoyant hot air which tends to reduce convective losses from the push-pull gas handling system. The operation and philosophy of the push-pull (forced draft-induced draft) process gas handling system are shown in Figures 11, 12, 13, 14, and 15. As shown in Figure 11, in an "unprotected" cavity that is closed except for the aperture, convection currents can circulate to rob heat from the cavity. The convection currents will rob heat from that portion of the cavity that is below the uppermost point of the aperture. Some mixing of the cold convection current and warm cavity air occurs due to inertial effects. As shown in Figure 12, in the protected or shrouded design, the "visor" is extended to a point where a hot/warm air bubble suppresses convective transfer almost completely. Secondary currents of much lower intensity become the primary convective loss mechanism. If we add a diluent stream as shown in Figure 13, the forced draft fan can cause a positive pressure at the aperture, overcoming the passive convection protection provided by the shroud, and cause heat loss. An induced draft causes infiltration by producing a negative pressure within the cavity, as shown in Figure 14. The combined push-pull process gas handling system shown in Figure 15 maintains the cavity at ambient pressure to significantly reduce convection losses. An aperture door is provided to minimize nighttime heat loss. A small fossil fired burner is used to offset conduction losses to maintain a high nighttime stand-by temperature.

The cavity is of substantially square cross section when viewed from the aperture or feed ends and is rectangular in cross section in top view. Cavity walls and roof are made up of a casing of carbon steel of 6.4 mm (0.25 in.) thickness. Side walls and roof are faced with fibrous ceramic insulation or castable refractory to a thickness of 0.30 m (1 ft). Wall and roof refractory areas are each estimated at 260 m^2 (2800 sq ft). The floor of the cavity is lined with high alumina firebrick to withstand erosion and the high temperatures in contact with the reactants. The firebrick is underlain by a layer of dense castable refractory to retard heat loss with an assumed total thickness of 0.30 m (1 ft). Refractory thicknesses are not optimized but merely reflect standard kiln practice. The reactants are moved through the kiln from the feed end towards the product discharge chute near the aperture by intermeshing, Incoloy 800H screw conveyors that are immersed in the burden

127
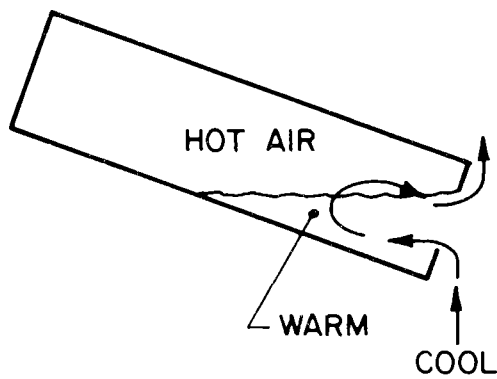
Figure 11. CONVECTION LOSSES IN UNPROTECTED CAVITY
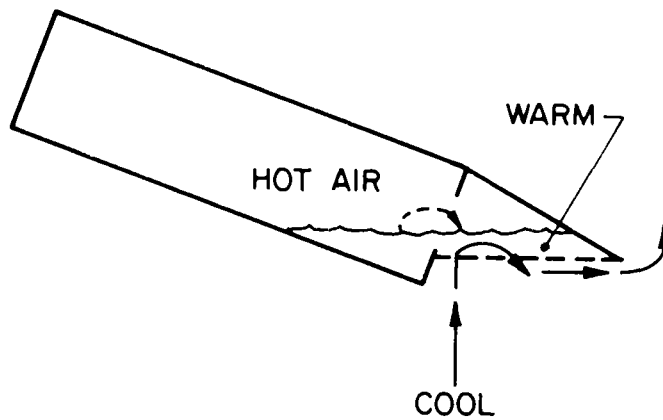
A84070643

Figure 12. CONVECTION LOSSES IN SHROUDED CAVITY

PREHEATED GAS "PUSHED" OUT BY
POSITIVE PRESSURE DIFFERENCE
AT APERTURE

HIGH
PRESSURE

AMBIENT
PRESSURE
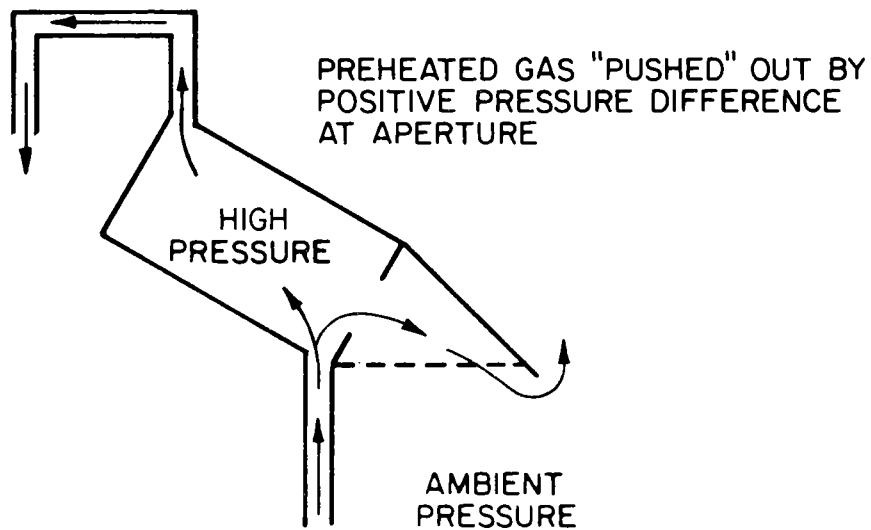
Figure 13.   CONVECTION LOSSES IN FORCED DRAFT PROCESS
GAS HANDLING SYSTEM

COLD AMBIENT AIR PULLED IN BY
NEGATIVE PRESSURE DIFFERENCE
AT APERTURE

LOW
PRESSURE

AMBIENT
PRESSURE
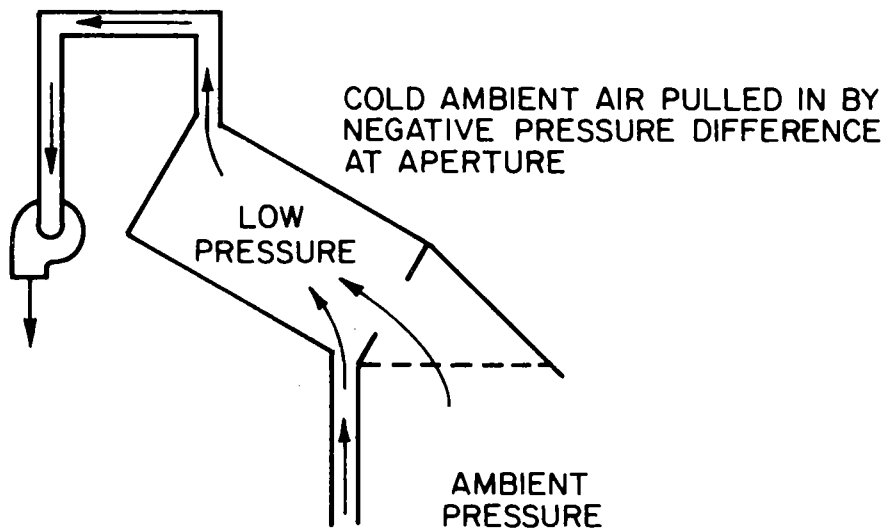
Figure 14.   CONVECTION LOSSES IN INDUCED DRAFT PROCESS
GAS HANDLING SYSTEM

IN PUSH-PULL SYSTEM,
EXHAUST PRESSURE RISE
AND FEED PRESSURE DROP
ARE BALANCED BY
THEIR RESPECTIVE FANS

AMBIENT
PRESSURE

AMBIENT
PRESSURE
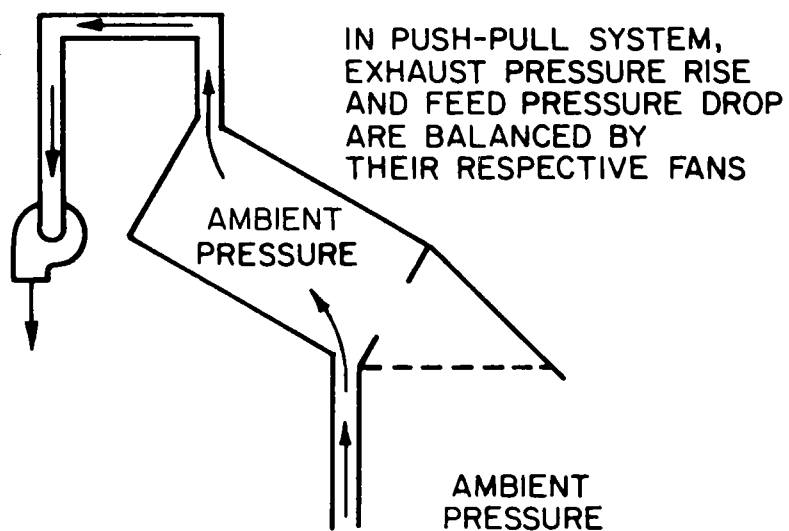
A84070642

Figure 15.   CONVECTION LOSSES IN PUSH-PULL PROCESS
GAS HANDLING SYSTEM

to avoid exposure to the solar and infrared radiation. Incoloy 800H will resist corrosion and erosion. The reactant bed is flat, on the cavity floor, and is of rectangular cross section. The flow length is 22.9 m (75 ft), width is 7.92 m (26 ft). Burden surface area is 181.2 m^2 (1950 sq ft). Burden residence time is 5.9 hours. Burden depth is 0.40 m (1.3 ft).

Ceramic honeycomb covered conveyors of thermal shock resistant alumina or silicon carbide line the roof and upper side walls of kiln. These conveyors act as counterflow regeneration that is, the conveyor surface that is exposed to the kiln interior moves from front (solar aperture) to back (feed) end contrary to the motion of the feedstock/product. The moving regenerator conveyors are heated at the aperture end of the kiln by concentrated solar radiation. The heated ceramic is transported aft in the kiln to reradiate to the relatively cool feedstock. Rotation rates of the regenerator conveyors are controlled to maximize radiant heat to the reactants and to minimize kiln reradiation losses at the aperture. Model results indicate that regenerators should move from front to back in about one hour. In principle, the approach is to run regenerators fast enough to minimize temperatures at the aperture end of the reactor (to minimize reradiation losses), but slowly enough to provide high enough regenerator temperatures to yield net energy gain to the reactants. Optimum regenerator operation is a tradeoff dependent on reactant flow rate, feed temperatures, cavity dimensions, etc. A total of 5 regenerator conveyors provide flexibility to differentially control rotation rates as the diurnal flux variations occur due to sun position. At noon, for example, the flux is most intense in the upper corners of the kiln. In the morning the flux is strongest on the east wall of the (north facing) kiln.

In practice, the upper side walls of the kiln may be tilted. In the conceptual design, upper side walls were was also shielded with the ceramic regenerators to create a better radiation shape factor and thermal efficiency. The lower side walls do not utilize moving side walls as these areas are both susceptible to potential dust and exposed to low solar flux levels. Furthermore, if this is desirable, the lower walls may be used as mechanical supports for flame lances and mixing augers. Fuel lances and mixing wind boxes may be provided to allow radiant fossil firing of the kiln during hours of reduced insolation or darkness.

Walls, roof, and floor are supported by the required load bearing structures to maintain the physical integrity of the receiver. Receiver weight is estimated as 748 metric tons (825 tons). Weight breakdown estimate is shown in Table 25.

The temperature profiles of reactants and gases flowing through the reactor and heat recovery sections are shown in Figure 16. The solids enter the 9.14 m (30 ft) long preheater (modeled as a rotary kiln) at a temperature of 25°C (77°F). After passing through the preheater in contact with hot CO_2 laden product/sweep gas the limestone feed is heated to a temperature of 399°C (750°F). The product/sweep gas exits the solids feed end of the kiln at a temperature of 790°C (1454°F). These gases flow countercurrent to the solids feed. The gases are cooled (based on model results, which do not reflect optimized heat recovery sizes) to 62.8°C (145°F), exchanging 2.3 MW (8 X 10^6 Btu/h) to the solids. As the solids pass through the kiln, they are exposed to a net IR and solar flux shown in Figure 17. Within 3.1 m (10 ft) of the solids feed end, the limestone feed begins reacting and this conversion to lime and carbon dioxide is shown in Figure 18. As the reaction proceeds solids and gases maintain a relatively flat temperature profile with the solids at about 843°C (1550°F) and gases at about 871°C (1600°F). As the conversion approaches 100% near the kiln discharge end, the solids temperature increases to 956°C (1753°F). The solids enter the solids heat recovery section at 956°C (1753°F). The solids flow countercurrently to the 28.3 m^3/min. (1000 cu ft/min) sweep gas flow of air through the 6.10 m (20 ft) heat recovery section (modeled as rotary kiln). Solids are discharged at 758°C (1396°F). The air is heated from 25° to 952°C (77° to 1746°F). The cooler section heat duty is 0.59 MW (2 X 10^6 Btu/h). The solids heat recovery section is not optimized. Complete conversion of limestone to lime is attained in the solids heat recovery section. However, 99.7% of conversion is attained in the kiln.

The assessment of the technical feasibility of the limestone calcination reactor is discussed in Section 4 under "Assessment of Solar Fired Limestone Calciner."

Table 25.   ESTIMATE OF CALCINER WEIGHT

Basis:

   Length – 22.9 m (75 ft)
   Side walls height and floor and arch width – 8.53 m (28 ft)

- Floor and arch area = 260.1 m^2 (2800 ft^2)

- Wall area = 260.1 m^2 (2800 ft^2)

- Shell at 6.35 m (1/4 in.) carbon steel density = 7865 kg/m^3 (491 lb/ft^3)

   Shell weight = 39,000 kg (86,000 lb)

- Wall and arch insulated with 288 kg/m^3 (17.98 lb/ft^3) block insulation to 0.30 m (1 ft)

   Weight = 68,500 kg (151,000 lb)

- Floor insulated with average 497 kg/m^3 (31.03 lb/m^3) firebrick and dense castable refractory to total 0.30 m (1 ft) thickness

   Weight = 39,400 kg (86,900 lb)

- Regenerator at same weight as floor

   Weight = 39,400 kg (86,900 lb)

- Burden at 0.30 m (1 ft) depth, 181.2 m^2 (1950 ft^2) at 3.50 g/cm^3 (219 lb/ft^3) as CaO

   Weight = 188,000 kg (415,000 lb)

- 100% safety factor for screw conveyor and heat recovery

Total Calciner Weight Estimated = 748 metric tons (825 tons)
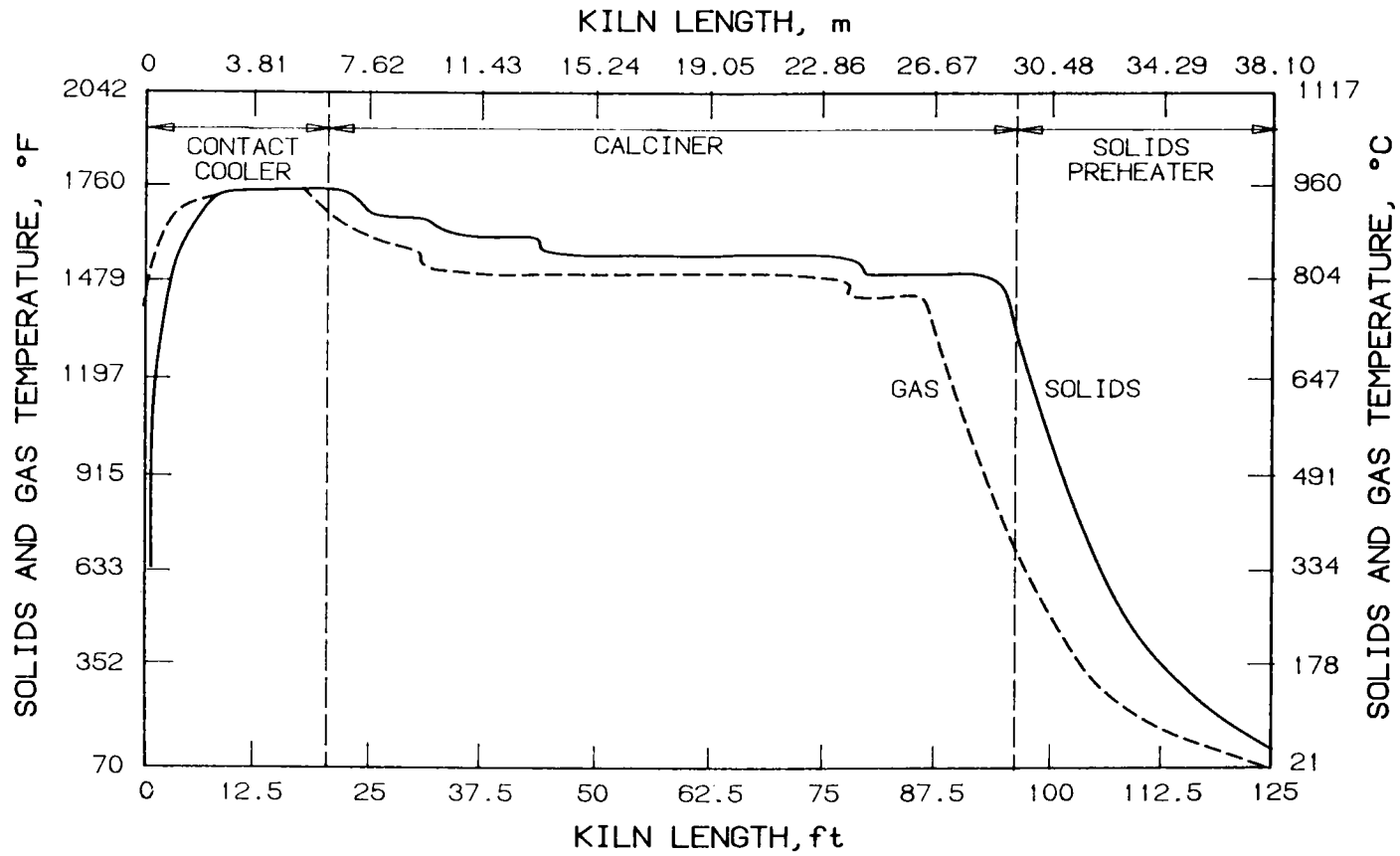
Figure 16. SOLAR CALCINER SOLIDS AND GAS TEMPERATURE PROFILES
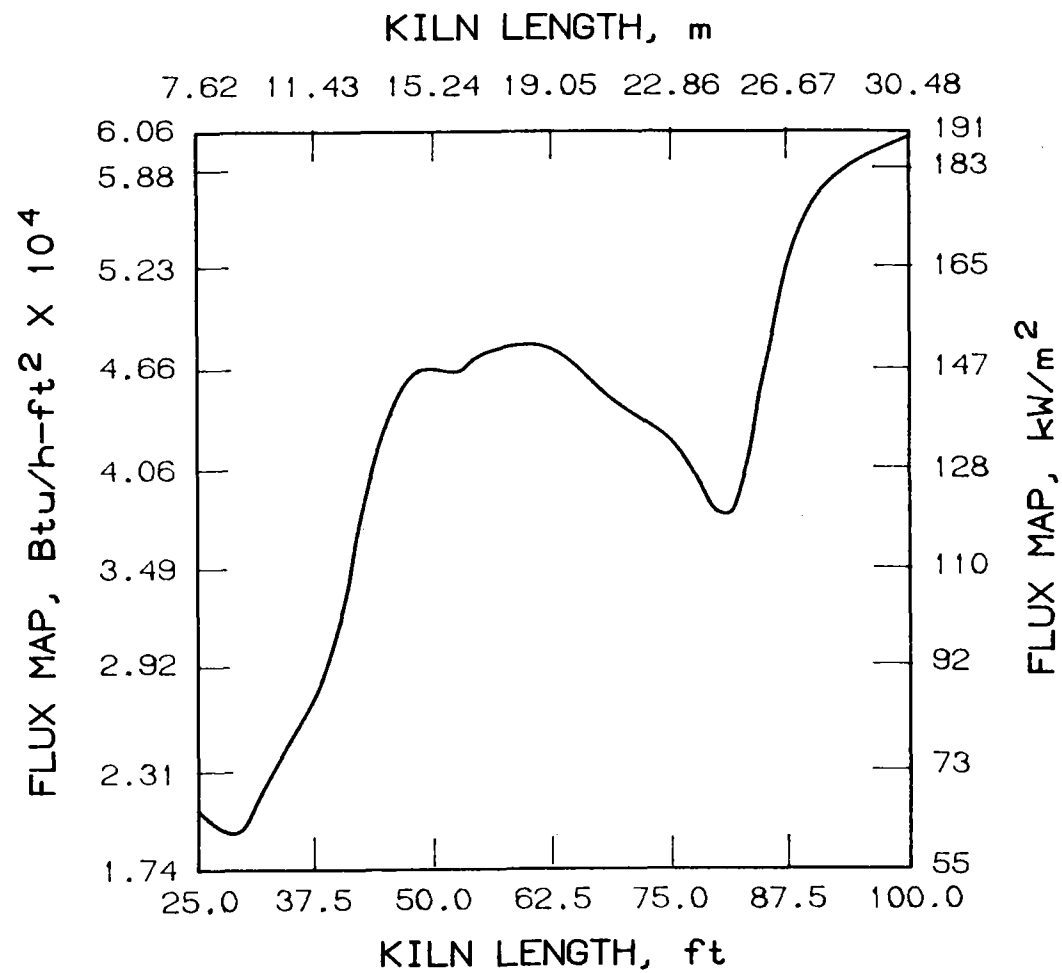
A84060607H

Figure 17.   SOLAR CALCINER NET FLUX ON REACTANT BED PROFILE
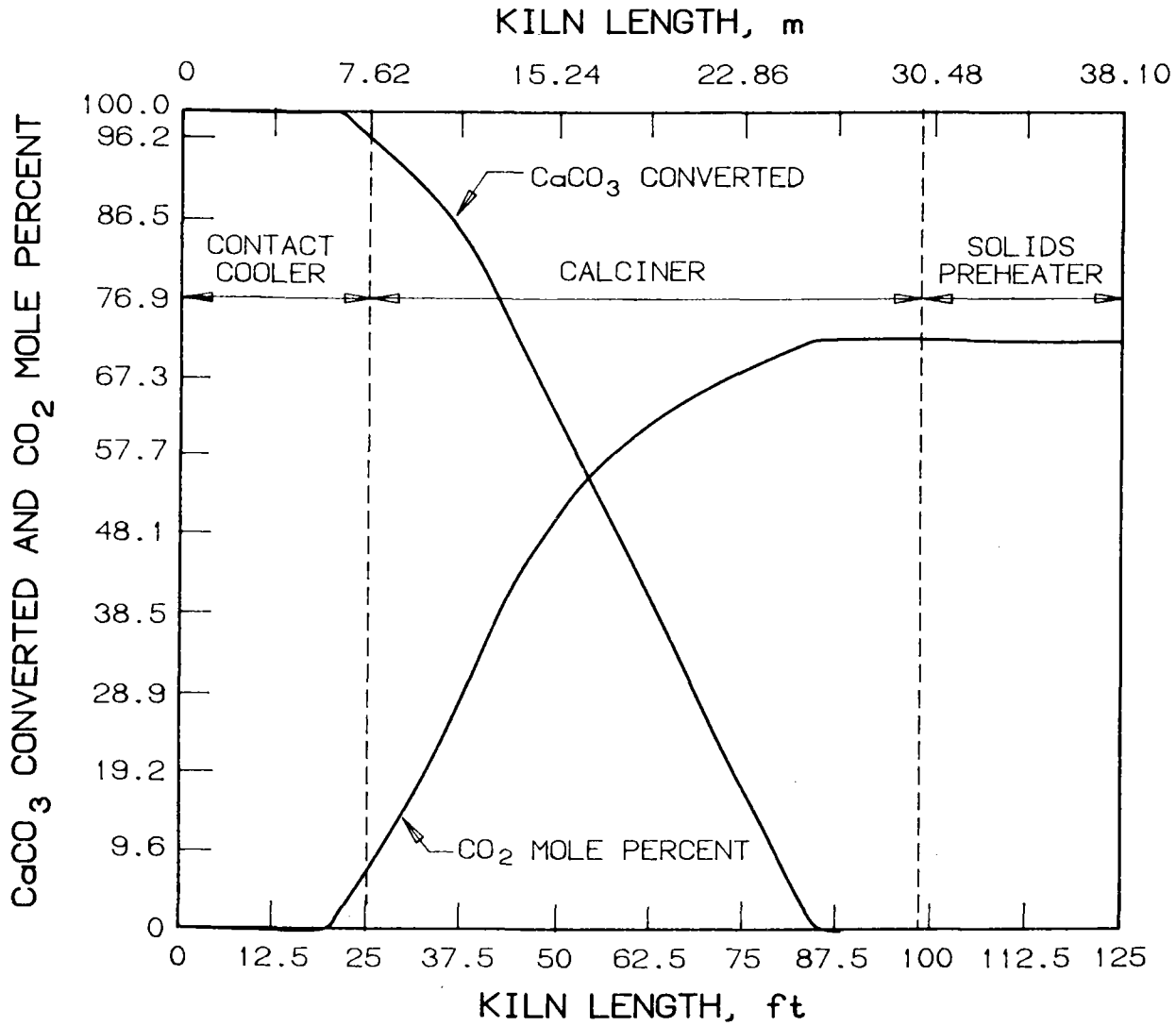
Figure 18. SOLAR CALCINER SOLIDS CONVERSION AND CO_2 MOLE FRACTION PROFILES

A84060606H

Steam Reformer Design Development

Introduction

The approach taken for the design of the steam reformer was influenced by information on the high cost and moderate performance of candidate transparent or translucent materials for a direct flux reactor (Table 26). All candidate transparent materials are significantly more costly than Inconel. Availability also is a problem. Typically, reformer tubes are 10.2 cm (4 in.) diameter and 9.14 to 12.19 m (30 to 40 ft) long. While candidate materials can be obtained in the desired diameter, lengths are limited by the size of fabrication equipment to less than 1.83 m (6 ft). With no market there is no incentive to develop fabrication facilities. A market has not been identified that might serve to bring the cost of transparent materials down.

Table 26. COST OF TRANSPARENT MATERIALS

Material	Cost/kg	(Cost/lb)	Cost Ratio
Inconel	$ 3.76	($ 8.3)	1.0
SiC	45.3	(100.0)	12
Quartz	49.9	(110.0)	13
Vistal	739	(1630.0)	196
Sapphire	1910	(4210.0)	507
Spinel	2240	(4930.0)	594

Will quartz work in a direct flux reactor? Unfortunately, quartz will not work adequately (Table 27). The basis for Table 27 is identical to the basis for Table 16. The assumption in the analysis represented in Table 27 is that heat transport is from the hot refractory liner. Research by PFR indicates that this approach is necessary to achieve the desired reformer axial flux distribution. Reformer tubes are inevitably spaced apart to permit more uniform circumferential irradiation. Uniform circumferential temperatures are necessary to avoid hot or cold spots and to avoid stress concentrations. Thus the projected area of the tubes is far less than the area of the refractory wall. As a result, tubes are primarily exposed to IR radiation emitted by cavity walls. Quartz is substantially opaque to IR. The lower temperature gradient associated with spinel and sapphire results in lower outer skin temperatures for these tubes and thus lower cavity temperatures to transport heat from the hot cavity walls by IR radiation to the tubes. The lower cavity temperature consequently results in lower radiation and convection losses through the aperture than cavity designs

137

Table 27. COMPARATIVE THERMAL PERFORMANCE OF OPAQUE TRANSPARENT MATERIALS

Solar Concentration at Aperture   1500:1
Cavity Ratio   10:1
Reaction Temperature   900°C (1652°F)
Cavity Wall is Perfectly Insulated
Tube Wall Thickness   6.35 mm (0.25 in.)

Material	SiC	Inconel	Quartz	Spinel	Sapphire
Conductivity, W/M°K (Btu/h-ft-°F)	7.7 (4.5)	7.7 (4.5)	2.2 (1.3)	8.0 (4.6)	13 (7.5)
Transmitted Flux, kW/m^2 (Btu/h-ft^2	0	0	150 (47600)	250 (79300)	225 (71300)
Conducted Flux, kW/M^2 (Btu/h-ft^2)	300 (95100)	300 (95100)	150 (47600)	50 (15900)	75 (23800)
Temperature Gradient, °C °F	248 (446)	248 (446)	434 (781)	39.8 (71.6)	36.7 (66.1)
Cavity Efficiency, %	62	62	52	73	73

involving tube materials with large temperature gradients and thus yields improved cavity thermal efficiency. It is thus lower cavity temperature that is the prime justification for direct flux reactors. The estimated receiver efficiencies for the various opaque and transparent materials are presented in Table 27. Receiver efficiencies for a windowless horizontal cavity have been estimated based on Figure 5 assuming that the cavity temperature can be approximated as the sum of the process temperature (900°C, 1652°F) and the temperature gradient and linearly extrapolating the curve to higher temperatures. A sapphire tubed receiver operating at 937°C (1719°F) might attain an efficiency of about 73% and an Inconel receiver would have an estimated efficiency of 62% at 1148°C (2098°F). A quartz based receiver operating at 1334°C (2433°F) would have an efficiency of 52% because of very large radiation losses at such a high cavity temperature. A gain of perhaps ten percentage points in efficiency may be realized by substituting a transparent material such as sapphire for an opaque metallic material.

Improved cavity efficiency allows reduction in heliostat field costs through reduction in heliostat field area. The increased cost of transparent materials must be recovered by savings in the costs of heliostats. Although the heliostat field is a costly component of the system, the very high current costs of transparent materials cannot be recovered by potential efficiency gains through use of direct flux tubular reactor configurations. As documented in section four under the "Assessment of Solar Steam Reformer," tube costs for a metallic steam reformer are about \$130,000 while Vistal costs about \$66 million. A 27,000 m^2 (291,000 ft^2) heliostat field will only cost \$2.4 to 6.3 million (@ \$90/m^2, \$8.36/ft^2 to @ \$235/m^2, \$21.84/ft^2).

As a result of the high cost of candidate transparent materials, the steam reformer design was based on the use of nickel alloy tubing. Nickel alloy tubing is the standard material of construction for conventional reformers. The basic design is derived from the PFR study.[1] The cavity shape gives uniform IR flux irradiation of the centrally located tubes. The shock wall blocks any direct flux irradiation of tubes. The 12.2 cm (40 ft) long tubes are packed with catalyst. Twenty percent of the daytime heat requirement is derived from fossil fuel to ensure uniform circumferential flux distribution and the desired axial flux distribution. Fossil fuel burners are integrated with the solar reactor to provide 100% of the heat requirements at night. Heat recovery equipment is used to recover heat from reaction products and combustion products. A forced draft/induced draft system is employed to minimize daytime aperture convection losses. The philosophy behind the use of a forced draft/induced draft flue gas handling system is the same as for the calcination reactor discussed on page 127. The aperture will be closed at night.

The basic receiver configuration (octagonal shape, double row of tubes arranged in a N-S line, shock wall, refractory lining) was accepted as given in the PFR design. The configuration was judged to be reasonable and well-thought out. There were no immediately obvious omissions or design errors and therefore the design was considered to be a good starting point. Tubes were arranged in a double row in order to minimize the length of the unit without unreasonably compromising the circumferential flux patterns. The octagonal shape was chosen to create the desired axial flux progression with as uniform tube-to-tube variations as possible in the receiver as in the PFR design. A

refractory brick liner was chosen for thermal inertia to minimize process disruptions due to transients and the shock wall was necessary to protect the tubes from direct insolation in the high flux region. The unit was scaled-down to the 15 MWth (5.12×10^7 Btu/h) size from the 35 MWth (1.19×10^8 Btu/h) design developed by PFR. The reformer general arrangement is shown in Figure 19.

Materials chosen were conventional tube material, refractory, and catalyst. No window was provided for the aperture. This was in the interest of near-term commercialization. Unresolved technology issues raised by this decision were presumed to be resolveable within the necessary time span. More exotic or transparent tube materials, or configurations that differ widely from current conventional technology, while worthy of investigation, could probably not be commercialized on a near-term basis. The design presented is therefore optimistic from a technical and economic standpoint. Thus this effort accomplished an independent evaluation of the PFR conceptual design effort for a metallic steam reformer, and also allowed development of target costs for transparent materials that would permit direct flux reactors to compete with metallic designs.

Design Procedure

With the above configuration set, the design proceeded as follows:

The solar energy available at the aperture plane was assumed to be 15 MWth (5.12×10^7 Btu/h). The solar efficiency of the receiver was assumed to be 78% (22% losses include re-radiation, spillage, convection). This was based on the performance estimate for the PFR receiver. It was further assumed that at peak solar duty 20% of the net solar energy available to the reaction would have to be added as fossil fired duty in order to provide the required flux pattern. The total radiant duty is therefore $15 \text{ MW} \times 0.78 \times 1.2 = 14.04 \text{ MW}$ (4.79×10^7 Btu/h).

It was assumed that solar power is turned on at 7 a.m. at 2.75 MWth (9.39×10^6 Btu/h). Solar power increases at a constant rate from 7 a.m. to 9 a.m. when the power level is 8.95 MWth (3.05×10^7 Btu/h). At this time the auxiliary burners in the convection section are fired. The auxiliary burner firing rate increases at half the rate of decrease of the main burners. Solar power increases at a constant rate from 9 a.m. to 10:24 a.m. at which time it

140
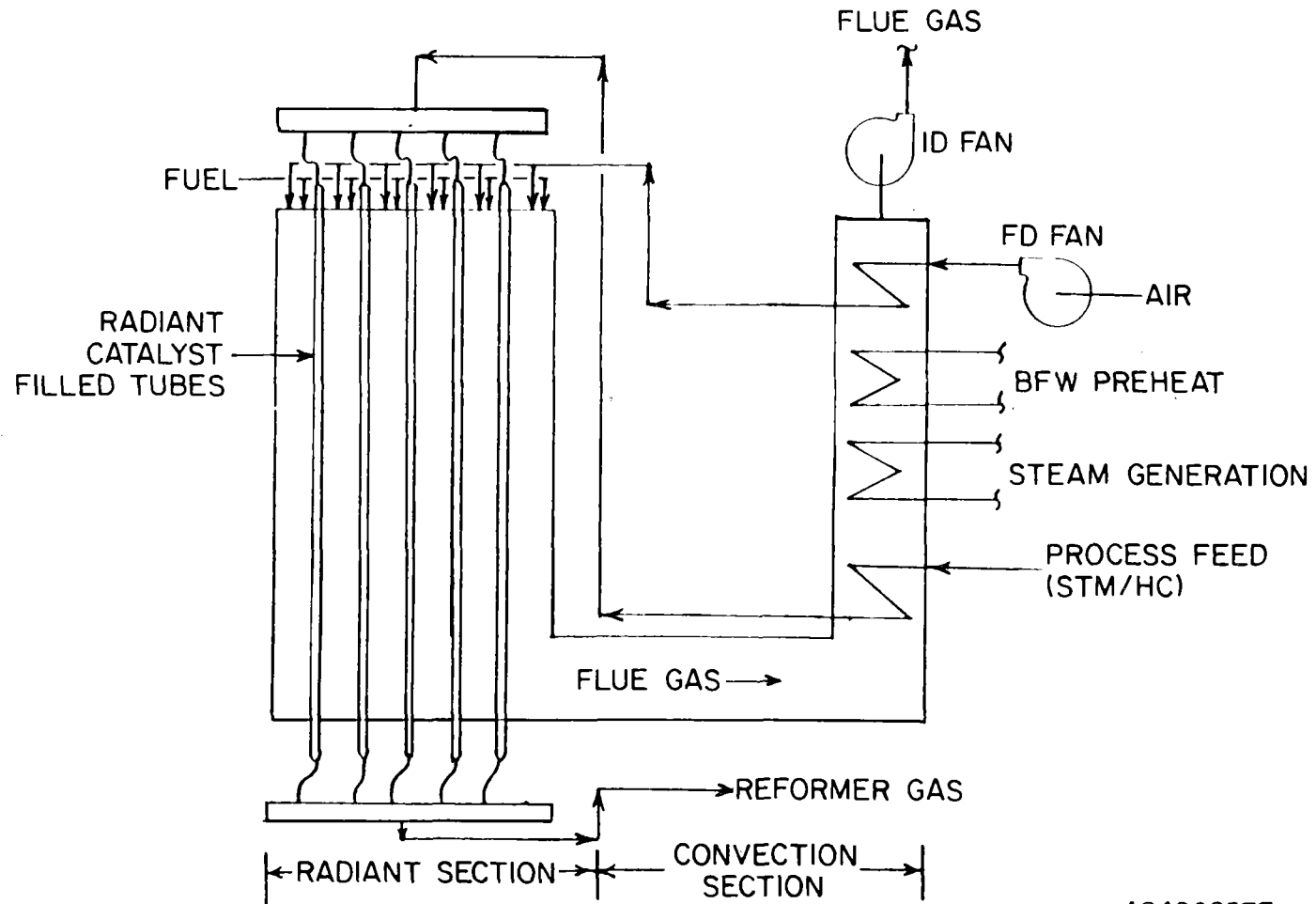
Figure 19. SOLAR STEAM REFORMER GENERAL ARRANGEMENT

reaches its peak level of 11.7 MWth (3.99 X 10^7 Btu/h). The solar power curve is symmetric around noon. This curve is illustrated in Figure 20. It was assumed that the by-product energy exported as steam was proportional to the main burner firing rate between solar turn-on and 9 a.m. and between 3 p.m. and solar turn-off. Export is at the maximum level throughout full fossil operation and at the minimum while auxiliary burners are being fired.

Tubes were assumed to be 102 mm (4.02 in.) ID, 11.6 m (38.1 ft) heated length (12.2 m [40.0 ft] total length); design average flux based on tube ID was taken as 63 kW/m^2 (2.0 X 10^4 Btu/h-ft^2). These are all standard parameters used in reformer design estimates. Sixty-two tubes are therefore required for this duty. Material balance programs for the HP-41C calculator were written for the steam reformer, the shift convertors and the overall hydrogen plant. Steam reforming material balances were run at reformer outlet conditions of 843°C (1549°F) and 2.17 MPa (315 psi). These are within the normal range for hydrogen plant reformers. These runs were each followed by an overall hydrogen plant run. The methane slip (that is, the amount of methane in the reformer product) on the reformer was varied until a 97% purity could be attained on the hydrogen product with reasonable conditions in the balance of the hydrogen plant. The results of this balance are shown in Table 28.

Heat balances were then run around the reformer and the following requirements were obtained:

Methane Preheat	25,828 kj/kmole (11105 Btu/lb-mole)	CH$_4$ feed
Boiler Feed Water Preheat	111,046 kj/kmole (47747 Btu/lb-mole)	CH$_4$ feed
Steam Generation	135,289 kj/kmole (58171 Btu/lb-mole)	CH$_4$ feed
Steam Superheat	71,081 kj/kmole (30563 Btu/lb-mole)	CH$_4$ feed
Radiant Duty	175,984 kj/kmole (75669 Btu/lb-mole)	CH$_4$ feed

Methane was assumed to be available at 15.6°C (60.1°F) and boiler feed water at 35°C (95°F). Reformer inlet temperature was taken to be 538°C (1000°F). The capacity of the reformer in terms of methane feed rate and ultimate hydrogen production rate were then calculated from the radiant duty requirement and the available radiant energy. These capacities were 183.2 X 10^2 mol CH$_4$/h (2.9 X 10^3 kg/h or 6.48 X 10^3 lb/h) and 3.871 X 10^5 m^3/day (13.67 X 10^6 SCF/day) 97% hydrogen respectively.
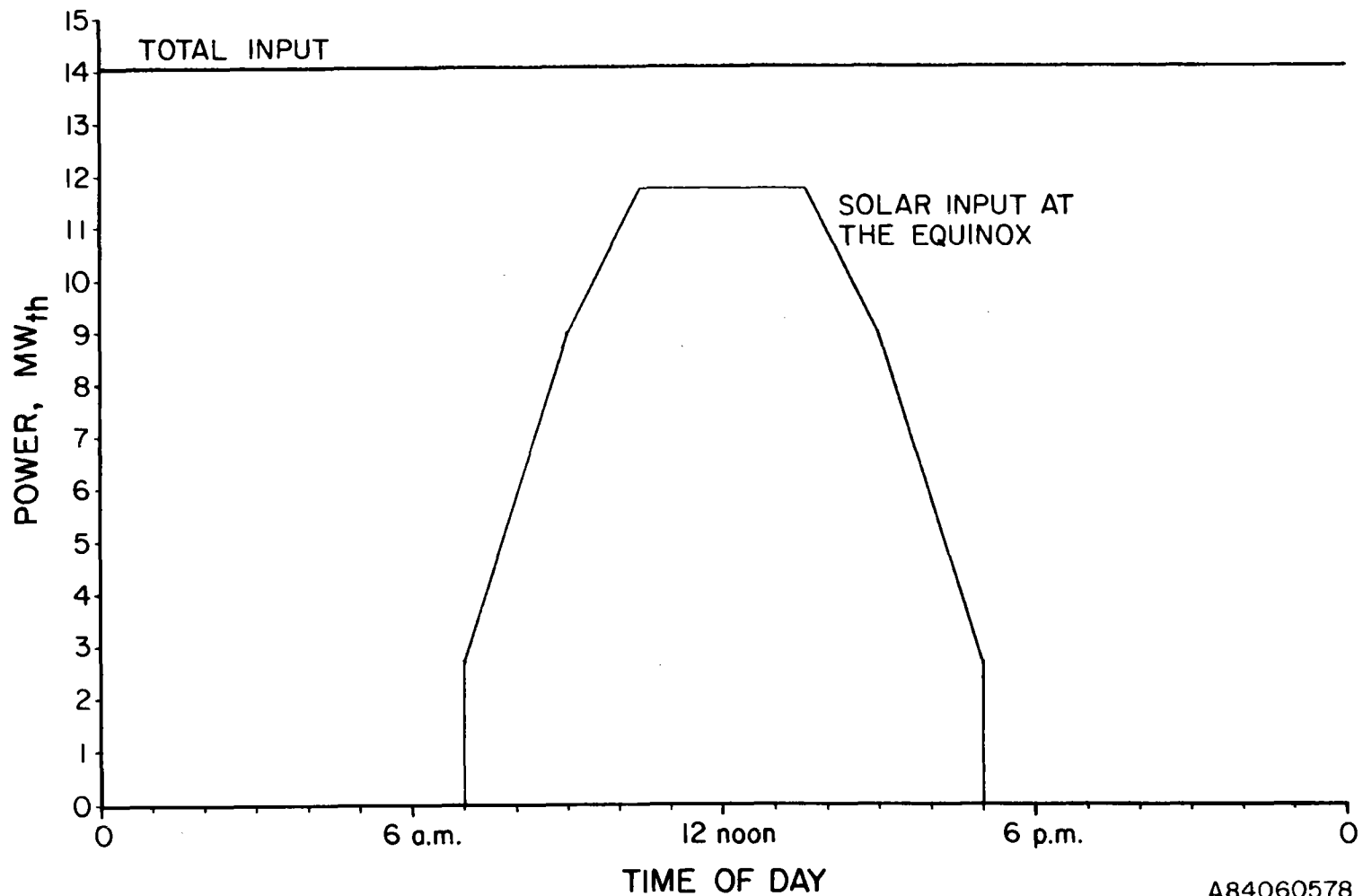
Figure 20. SOLAR STEAM REFORMER HEAT TRANSFER RATE INTO
REFORMER TUBES

A84060578

143

Table 28. STEAM REFORMER MATERIAL BALANCE

Feedstock	Methane
CH_4 Slip	2.1%
Outlet Temperature	843°C (1550°F)
Water Gas Shift Equilibrium Constant	0.89428
Steam-Methane Equilibrium Constant	3.4130 MPa^2 (332.43 atm^2)
Steam to Methane Molar Ratio:	5.07
Product in Moles/Mole of Dry Methane Feed	
CH_4	0.0882
CO	0.4488
CO_2	0.4630
H_2	3.1985
H_2O	3.6904
Ultimate H_2 Yield	3.608 moles/mole CH_4 feed

Material and heat balances were then run around both high and low
temperature shift converters in order to determine the heat energy available
in the product effluent. Below the low temperature shift the available energy
in the product was calculated down to 38°C (100°F). The outlet temperature of
the high-temperature shift was assumed to be 427°C (801°F). Shift inlet
calculations are shown on the process schematic diagram, Figure 21 and Table
29, and as the upper curve of Figure 22. Detailed heat and material balances
around the reformer are important in establishing the feed and fuel
requirements for the process. Heat and material balances serve as the basis
for sizing equipment, in this case, heat exchangers and fans.

One of the most important tasks in the design of a steam-hydrocarbon
reformer is matching the requirements for feed, boiler feed water and air
preheat as well as for generating and superheating process steam with the heat
available in the process effluent and the flue gas. The economic success of a
unit depends upon it. While one would like to recover heat as efficiently as
possible, there are practical limitations such as the cost of heat exchange
area and of exotic high-temperature service materials. Therefore, for
example, the first unit downstream of either the catalyst tubes or the firebox
is invariably a boiler. Although this is thermodynamically inefficient, it is
necessary to lower the gas temperature to a point where exotic materials are
not necessary. Also, since a boiler is always flooded with water, this
temperature drop is assured in spite of any possible flow failure. The boiler
itself need not be made of exotic materials because the boiling coefficient is
so high that the tube wall temperature is virtually at the steam
temperature. The channels of steam reformer process boilers are usually
protected with refractory and Incoloy 800 ferrules and the first 3 rows of the
first convection section boiler are usually made of Incoloy 800.

Another consideration is that temperature differences between the high
and low temperature sides of heat exchange equipment must be high so that heat
exchange surface area is not uneconomically large. Therefore the minimum
temperature difference or "pinch point" is limited to 10°C (18°F).

Since the reformer will undoubtedly be a net exporter of steam, the
export steam must be useful for generating power or driving turbines.
Therefore steam should be generated at about 7.5 MPa (1088 psi) even though
the process requires only about 1.7 MPa (247 psi). All steam is generated at
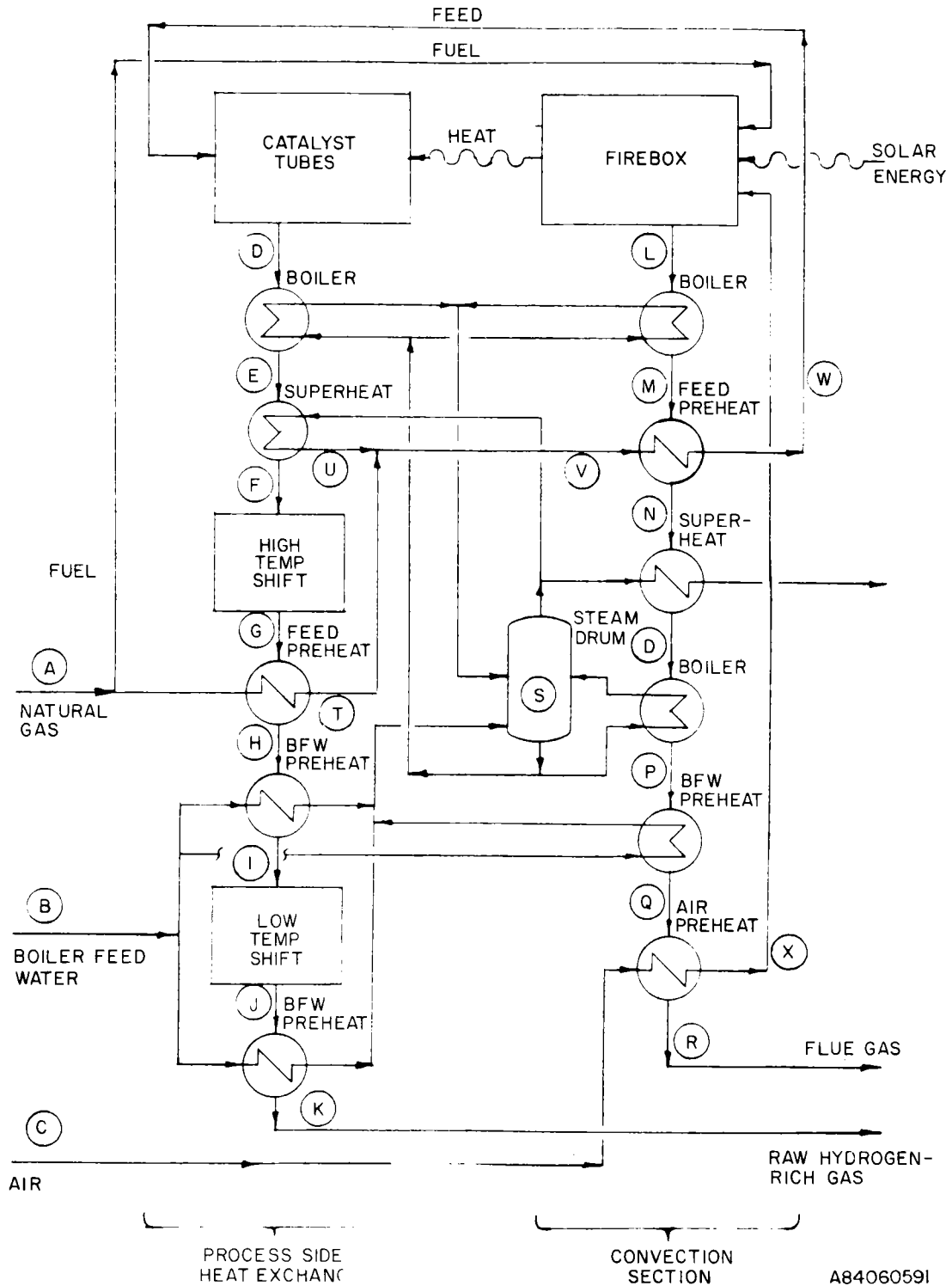
Figure 21. SOLAR STEAM REFORMER PROCESS SCHEMATIC DRAWING

146

Table 29. STATE POINTS FOR SOLAR STEAM REFORMER PROCESS
SCHEMATIC DRAWING

		Zero Solar				Full Solar			
		Temperature,		Pressure,		Temperature,		Pressure,	
Point	Preheated Combustion Air	°C	(°F)	MPa	(psi)	°C	(°F)	MPa	(psi)
A	Natural Gas Supply	15.6	(60.1)	2.76	(400)	15.6	(60.1)	2.76	(400)
B	BFW Supply	35	(95)	7.45	(1001)	35	(95)	7.45	(1001)
C	Ambient Air	15.6	(60.1)	0.1	(14.5)	15.6	(60.1)	0.1	(14.5)
D	Reformer Outlet	843	(1549)	2.17	(315)	843	(1549)	2.17	(315)
E	Process Boiler Outlet	510	(950)	2.14	(310)	510	(950)	2.14	(310)
F	High Temperature Shift In	378	(712)	2.10	(305)	378	(712)	2.10	(305)
G	High Temperature Shift Out	427	(801)	2.07	(300)	427	(801)	2.07	(300)
H	Feed Preheater Out	370	(698)	2.03	(294)	370	(698)	2.03	(294)
I	Low Temperature Shift In	221	(430)	2.00	(290)	221	(430)	2.00	(290)
J	Low Temperature Shift Out	234	(453)	1.97	(286)	234	(453)	1.97	(286)
K	Product	158	(316)	1.93	(280)	158	(316)	1.93	(280)
L	Firebox Out	1149	(2100)	0.101	(14.7)	1149	(2100)	0.101	(14.7)
M	First Boiler Coil Out	792	(1458)			815	(1499)		
N	Feed Preheat Coil Out	648	(1198)			425	(797)		
O	Superheat Coil Out	537	(999)			425	(797)		
P	Second Boiler Coil Out	537	(999)			330	(626)		
Q	BFW Preheat Coil Oil	345	(653)			175	(347)		
R	Stack	157	(315)	0.098	(14.2)	175	(347)	0.101	(14.7)
S	Steam Drum	289	(552)	7.35	(1066)	289	(552)	7.35	(1066)
T	Natural Gas Feed	371	(700)	2.69	(390)	371	(700)	2.69	(390)
U	Feed Steam	400	(752)	2.69	(390)	400	(752)	2.69	(390)
V	Mixed Feed	371	(700)	2.69	(390)	371	(700)	2.69	(390)
W	Hot Feed	538	(1000)	2.62	(380)	538	(1000)	2.62	(380)
X	Preheated Combustion Air	260	(500)	0.105	(15.2)	15.6	(60.1)	0.105	(15.2)
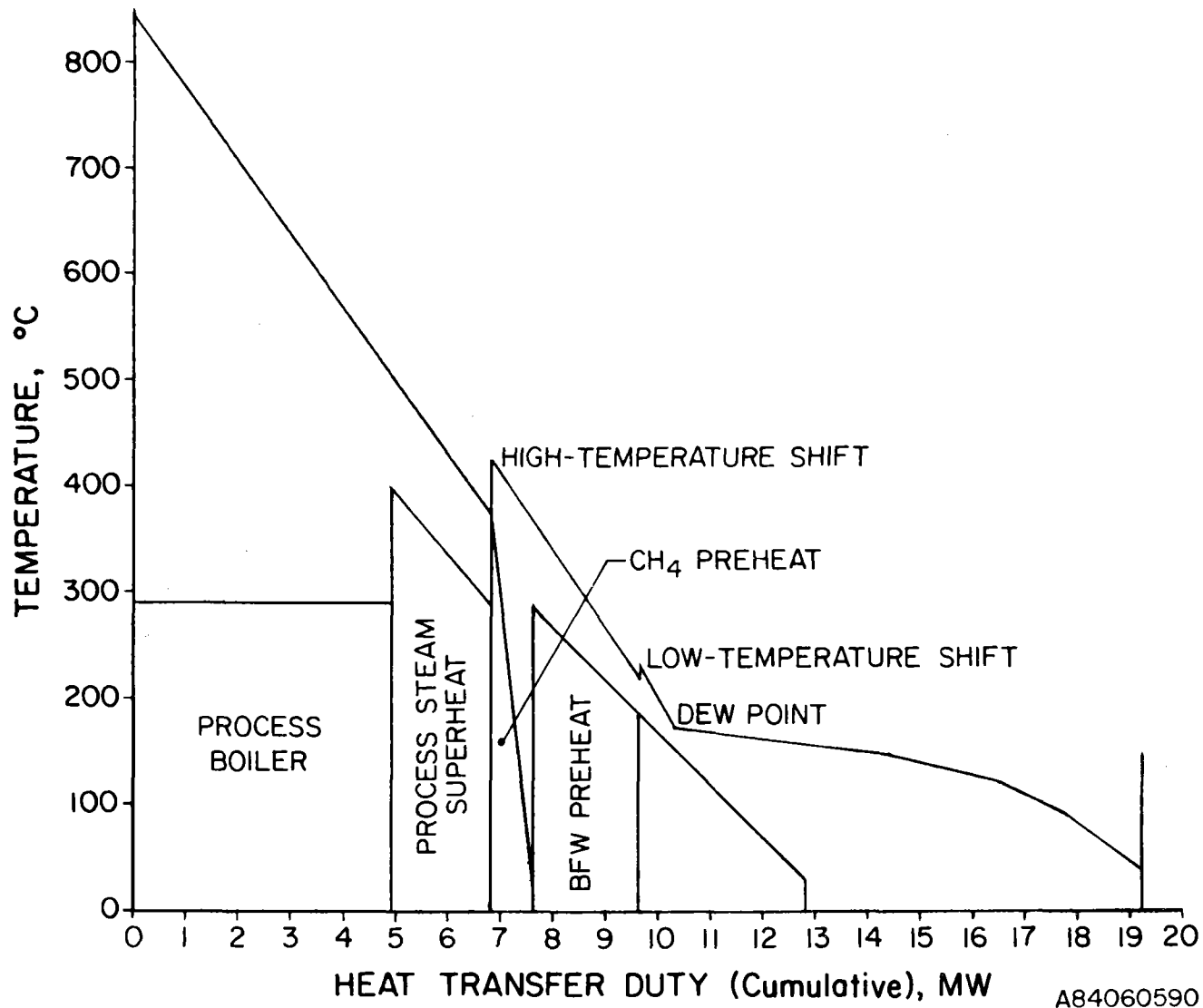
Figure 22. SOLAR STEAM REFORMER EFFLUENT HEAT TRANSFER DIAGRAM

the higher pressure in order to avoid the expense of two separate steam systems. Steam needed for the process is depressurized and superheated.

Within the above constraints, heat balances were developed around the reformer. After inspecting the available heat diagram for the reformer effluent, it was decided to heat the methane and process steam separately to 371°C (700°F) and 2.7 MPa (392 psi) (reformer inlet pressure) before mixing them and completing the feed preheat to 539°C (1002°F) in the flue gas convection section. The effluent temperature duty profile was such that it was obvious the methane should be preheated just downstream of the high-temperature shift and the process steam superheat just upstream. Note that at 7.23 MPa (1049 psi) steam must be superheated to about 400°C (752°F) in order to be at 371°C (700°F) when depressurized adiabatically to 2.5 MPa (363 psi). The remaining available duty from the reformer process effluent upstream and downstream are taken up by a process boiler and boiler feed water preheat respectively. These, however, do not fulfill the requirement for process steam. Additional steam must be generated in the flue gas convection section. Note that the boiler feed water is not a large enough heat sink for all the available heat in the reformer effluent. Some of this heat could be used for driving the carbon dioxide removal unit. This as well as further optimization of the boiler feed water preheat is certainly possible. This is, however, beyond the scope of this study. The purpose of the boiler feed water balance was to ensure that heat was available for fulfilling all of the boiler feed water requirements. The results of the reformer effluent heat balance are shown on Figure 22.

Similar heat balances were performed for the convection section for two cases; full solar, that is, 16.7% of radiant duty supplied by fossil fuel, zero solar. Minimum convection section requirements that is, process requirement remaining after reformer effluent available heat is used, were determined and these were matched with heat available in the flue gas. The temperature of the gases leaving the firebox was assumed to be 1149°C (2100°F). A rough check was made using radiation heat transfer curves for CO_2 and H_2O[38] and against a furnace temperature guide published in Perry's 5th Edition[39]. Both checks indicated the assumption to be reasonable.

149

In order to fulfill the minimum requirements of full solar conditions it is necessary to burn extra fuel in auxiliary burners located downstream of the main reformer firebox. This might be avoided by putting feed preheat coils in the firebox as in the PFR design. Trade-offs of this kind were not performed. It was also necessary to install a second convection section boiler and to export a small amount of steam in order to meet the heat balance restrictions and also recover as much heat as possible from the flue gas. Air preheat and steam superheat coils would not be used in this case. Figures 21 and 23 and Tables 29 and 30 depict full solar operation of the convection section.

At full fossil operation all process requirements are easily met and 2.152 kg/s (4.74 lb/s) of 7.0 MPa (1015 psi), 538°C (1000°F) steam is exported. All combustion air is preheated to 160°C (320°F), but the second convection section boiler is not used. Zero solar (that is, at night) convection section operation is shown in Figures 21 and 24 and Tables 29 and 30.

Table 30. SOLAR STEAM REFORMER CONVECTION SECTION SUMMARY

	Full Solar	Zero Solar
Radiant Section Fuel, kmol/s	7.06×10^{-3}	34.17×10^{-3}
Auxiliary Fuel, kmol/s	3.46×10^{-3}	None
Export Steam, kg/s (lb/s)	0.331 (0.73) (7.0 MPa [1015 psi], sat.)	2.152 (4.745) (7.0 MPa [1015 psi], 538°C [1000°F])
Air Preheat, °C (°F)	None	260 (500)

Equipment Conceptual Design

Operating Conditions

Selection of the appropriate reformer operating pressure is based upon the available pressure of the feedstock and the required product pressure. Pressure required in most applications is usually of the order of tens of atmospheres. For every mole of methane feed reacted, four moles of synthesis gas are produced. It is therefore far more economical to compress the feed to the required pressure than the products. Steam can be raised at whatever pressure is required up to the critical pressure (22.09 MPa [3204 psi]). Because the reforming reaction is favored by lower pressure, operating at higher pressures requires that higher temperatures be used in order to improve conversion.
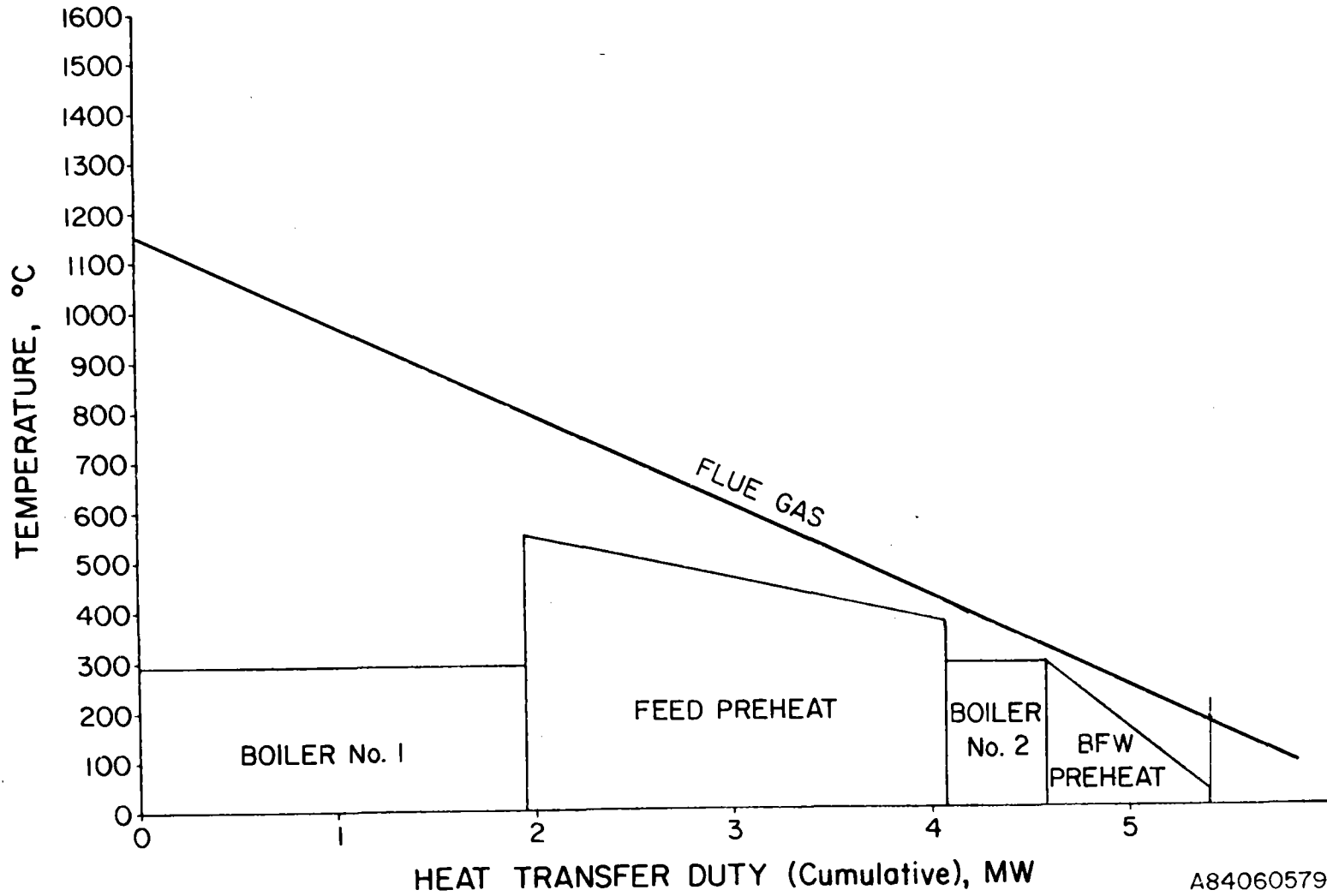
Figure 23. SOLAR STEAM REFORMER FLUE GAS HEAT TRANSFER DIAGRAM
(Full Solar Operation)
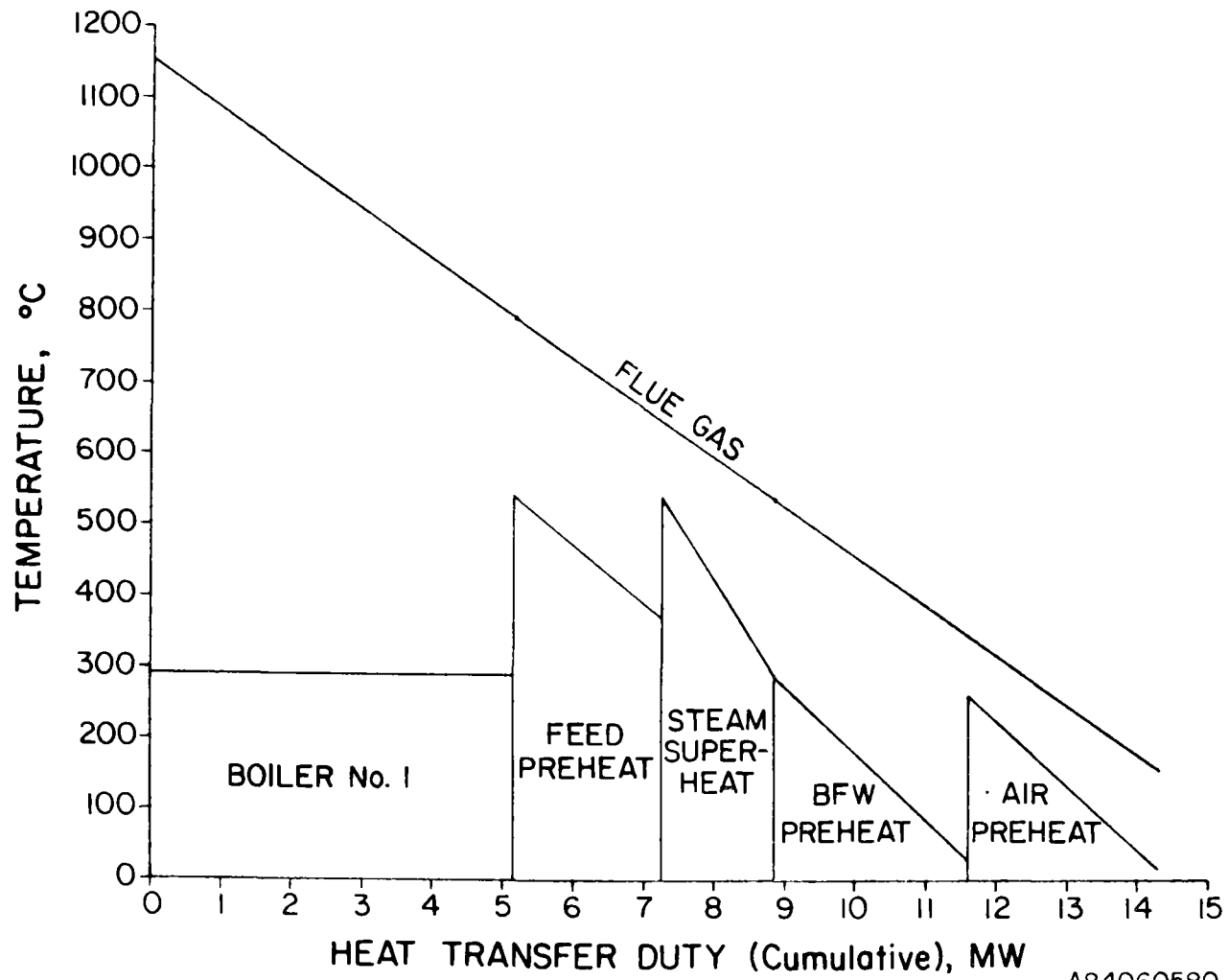
A84060579

Figure 24.   SOLAR STEAM REFORMER FLUE GAS HEAT TRANSFER DIAGRAM
(Zero Solar Operation)

Reaction Kinetics

Reaction kinetics are not of great importance in the overall mass and heat balance around a reformer. Catalyst activity declines with age and this is compensated for in design with a safety factor known as the equilibrium temperature approach. Catalyst volume is not determined by design space velocity or reactant residence time although obviously some minimum catalyst volume is necessary. Reaction rate is limited by the rate of heat transfer to the reactants. This is because the steam hydrocarbon reforming reaction is highly endothermic and the rate of heat absorption by the reactants is proportional to the reaction rate. Thus the limits set by heat transfer, economical pressure drop and construction material capabilities drive the reformer configuration towards parallel tubes of the usual commercial dimensions.

Importance of Heat Recovery

The operating temperature in a steam reformer is so high that about half the fired duty of the furnace cannot be used to supply heat of reaction. This heat must be recovered from the flue gas in order to make the process economical. In addition, the reaction products are at an elevated temperature and this heat must also be recovered. The schemes used for recovering heat from the flue gas and the process stream are therefore a major consideration in reformer design. The scheme used in the conceptual design presented in this report is typical of hydrogen plant reformers of this size. In conventionally fired reformers there is generally more heat available than is necessary for preheating feed, raising and superheating the steam required for the process, and combustion air preheat. Therefore high pressure superheated steam is usually exported for generating power or driving compressor or pump turbines.

Catalyst Tubes

Probably the most important component of a reforming furnace, both from operational and capital cost viewpoints, is the catalyst tubes. A schematic drawing of a typical reformer tube is shown in Figure 25. These tubes operate with skin temperatures of approximately 1040°C (1904°F) and contain a process fluid with high hydrogen partial pressure at 1.4 to 2.8 MPa (203 to 406 psi). These conditions are at the upper limits of presently available materials of construction.
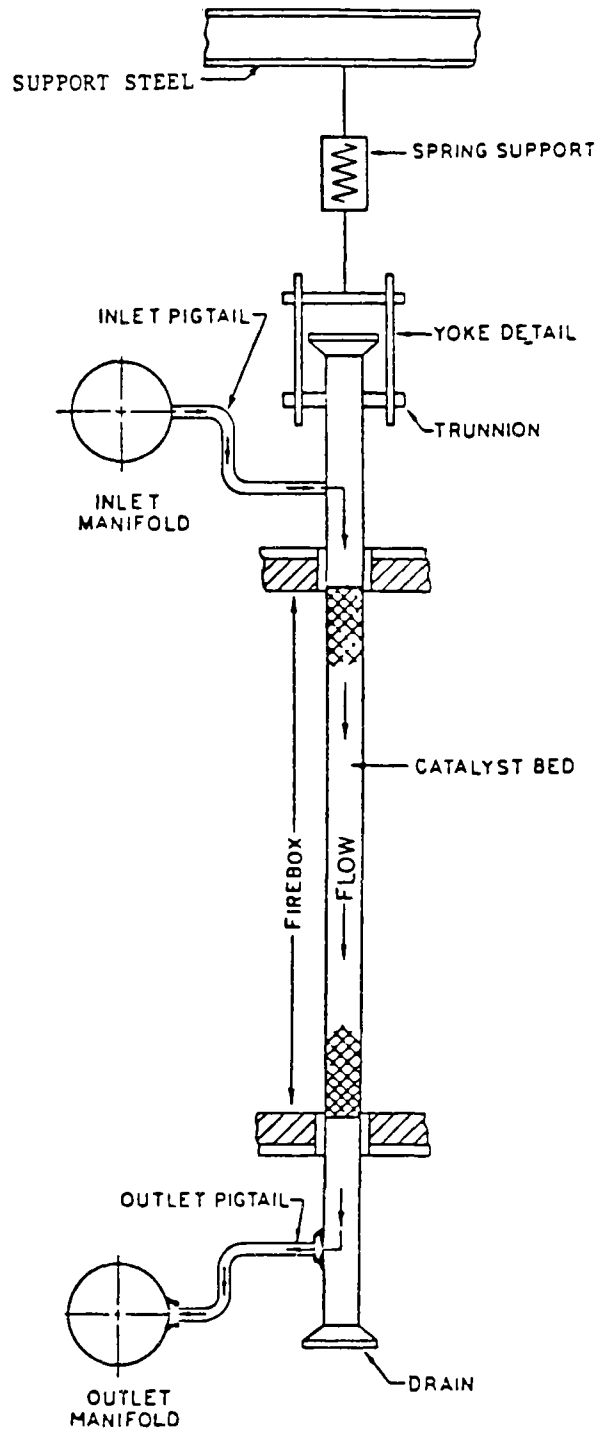
Figure 25.   SCHEMATIC DRAWING OF TYPICAL STEAM REFORMER CATALYST TUBE

154

Any metal subjected to operating temperatures greater than 540°C (1004°F) has to be designed for creep (permanent deformation) even at stress levels well below the yield stress. If the metal temperature is high enough for creep effects to be significant, the tube will fail by creep-rupture. Tube failures have been the main cause of downtime in steam reformers and so prevention of such failures usually determines tube/reformer design. Designs attempt to uniformly transfer the heat through the tube walls at a maximum rate without exceeding tube wall design temperatures. Usually catalyst tubes fail of localized overheating which causes creep-rupture. Such localized overheating can be caused by faulty burners, incorrect or poor furnace temperature control, inactive or poorly loaded catalyst, or plugging within the tubes or headers.

Reformer tubes are currently made of stainless steel known as HP-50 (35% Ni 25% Cr), HK-40 (35% Ni 25% Cr), or Manaurite 36X. The tubes are mounted vertically with support from top and bottom to prevent bowing or sagging. During operations such a tube will expand 150 to 300 mm (5.91 to 11.8 in.). The inlet and outlet connections must be flexible. These connections are usually made of Incoloy 800 and are known as "pigtails." Pigtail failure has also been a common cause of reformer downtime. Failure can be caused by overstressing of the pigtail through repeated expansion and contraction of the tube. These effects can be prevented by minimizing the thermal cycling of the reformer. Ideally, once a reforming furnace is brought up to operating conditions the status will be maintained for a year or more. Frequent start-up and shutdowns are usually avoided since such thermal cycling can dramatically increase the possibility of catalyst tube and pigtail failure. Since creep-rupture is time-dependent, catalyst tubes are typically designed for a lifetime of 100,000 hours. In some instances frequent thermal cycling has been known to reduce this lifetime to less than 20,000 hours. Clearly, thermal cycling inherent in solar operations is of critical importance as a design consideration for solar steam reformer development.

Flux Distribution

In order to achieve uniform radial heat transfer to the catalyst tube, the distance between tubes is carefully selected. Tubes should be located in a row with the hot radiant cavity walls equidistant on both sides. In this case if the tubes are located sufficiently far apart, the radial flux

distribution will be practically uniform. However, this will result in a long, narrow furnace which may not be the most economic design. Consequently, the inter-tube distance may be reduced which will result in less uniform radial flux (Figures 26 and 27).[40] In some cases the tubes are arranged in staggered double rows. Such designs permit a reduction in furnace length but can suffer from increased tube failure caused by the less uniform radial flux distribution.

Catalyst tubes are generally designed for the maximum tube wall temperature. For a given flow rate and conversion, a fixed amount of heat must be transferred to the reactants over the tube length. Since the reactants are further from equilibrium at the tube inlet, the reaction rate is highest there. As it decreases down the tube, the rate of heat absorption by the reactants decreases proportionately. If the heat flux were constant along the tube length, the maximum tube wall temperature would be at the tube outlet and the difference between the maximum and minimum tube wall temperature would be relatively large (Figure 28).[40] This leads to an inefficient tube design.

In the design of the fossil fired steam reformers the most efficient tube designs are executed by predicting the longitudinal tube wall temperature variation by simultaneously solving the heat transfer, fluid flow, mass transfer and reaction kinetics problems. Several reformer furnace vendors have computer models to solve the equations. Time variations are not normally taken into account.

Development of a detailed steady-state model of the steam reformer equivalent in detail to those used for conventional steam reformer design was outside the scope of this effort. The PFR study carried out extensive reformer modeling and demonstrated the capability of the solar heat source to achieve the required axial flux distribution and the desired, relatively uniform circumferential flux distribution. A typical down fired reformer process gas temperatures, tubewall temperature, and flux profile is shown in Figure 29. The PFR flux profile is shown in Figure 30. Comparing Figure 29 and 30 it is observed that a solar fired reformer can achieve a flux distribution comparable to fossil fired reformer practice.

Any departure of the achievable flux pattern from the optimum forces a departure of tube design from the optimum. Variation of furnace flux patterns with time would be particularly troublesome from a design standpoint.

156
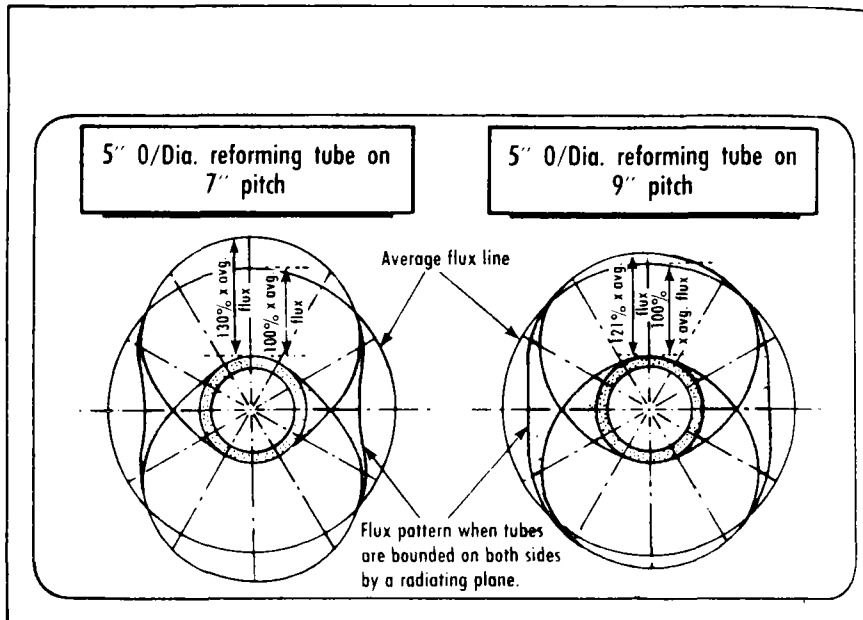
Figure 26. IMPACT OF INTERTUBE DISTANCE ON RADIAL FLUX UNIFORMITY
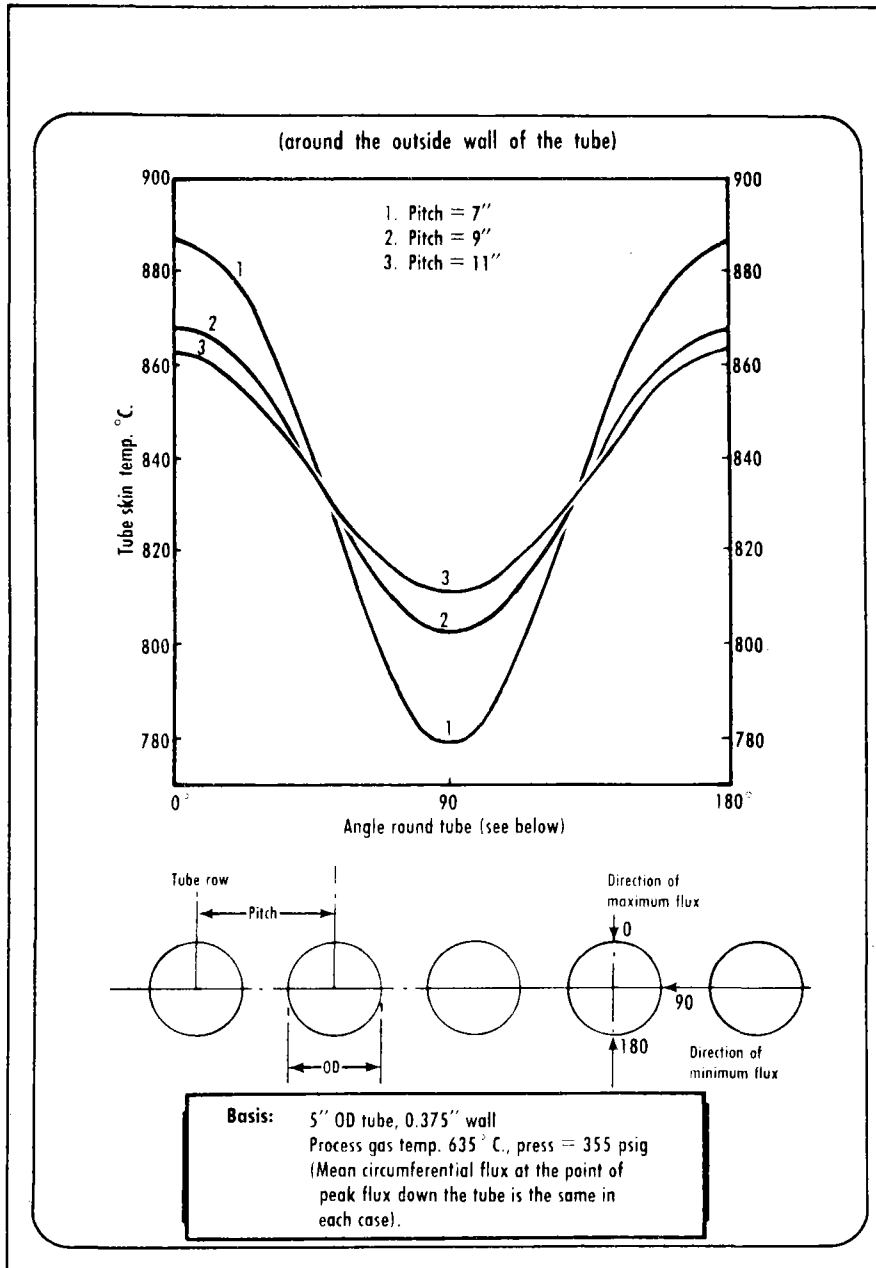
Figure 27. TUBE PITCH TEMPERATURE DISTRIBUTION
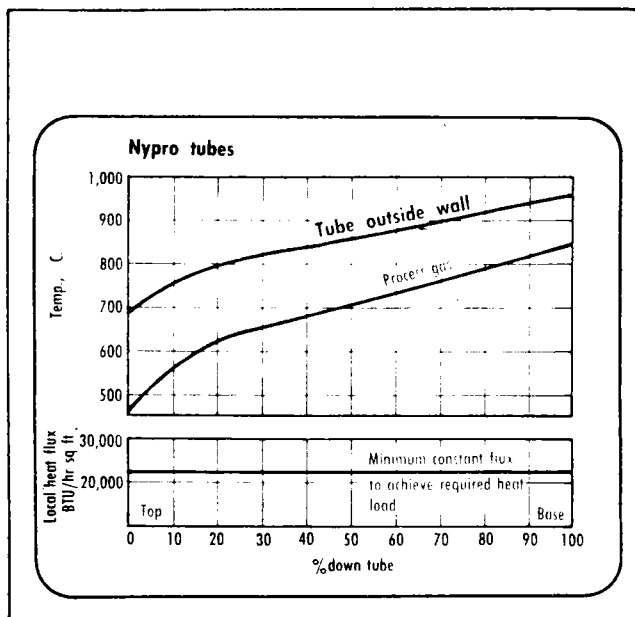
Figure 28. STEAM REFORMER TUBE PROCESS GAS AND TUBE WALL
TEMPERATURES FOR CONSTANT FLUX CONDITIONS

159
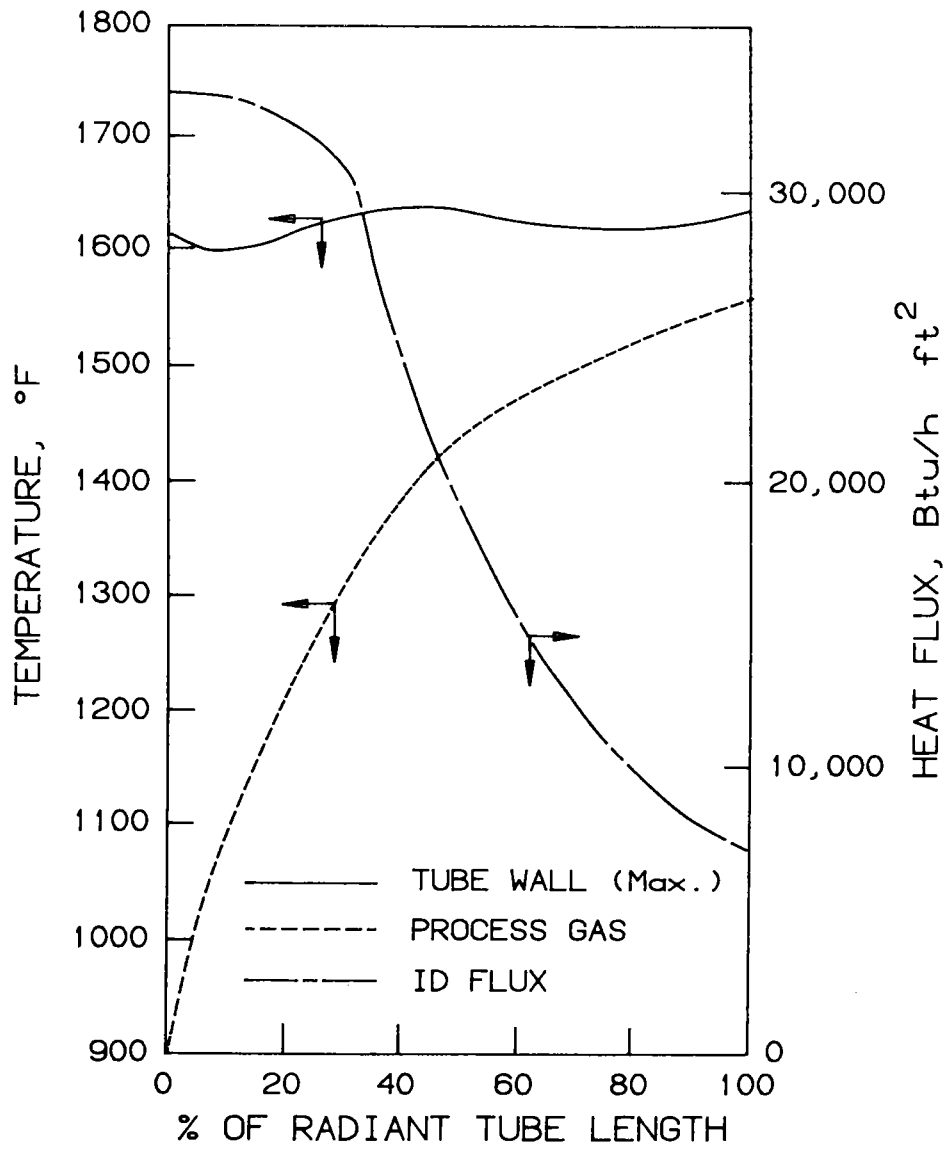
A84060588H

Figure 29. TYPICAL DOWN FIRED STEAM REFORMER PROCESS GAS TEMPERATURE,
TUBE WALL TEMPERATURE, AND AXIAL FLUX PROFILES

160
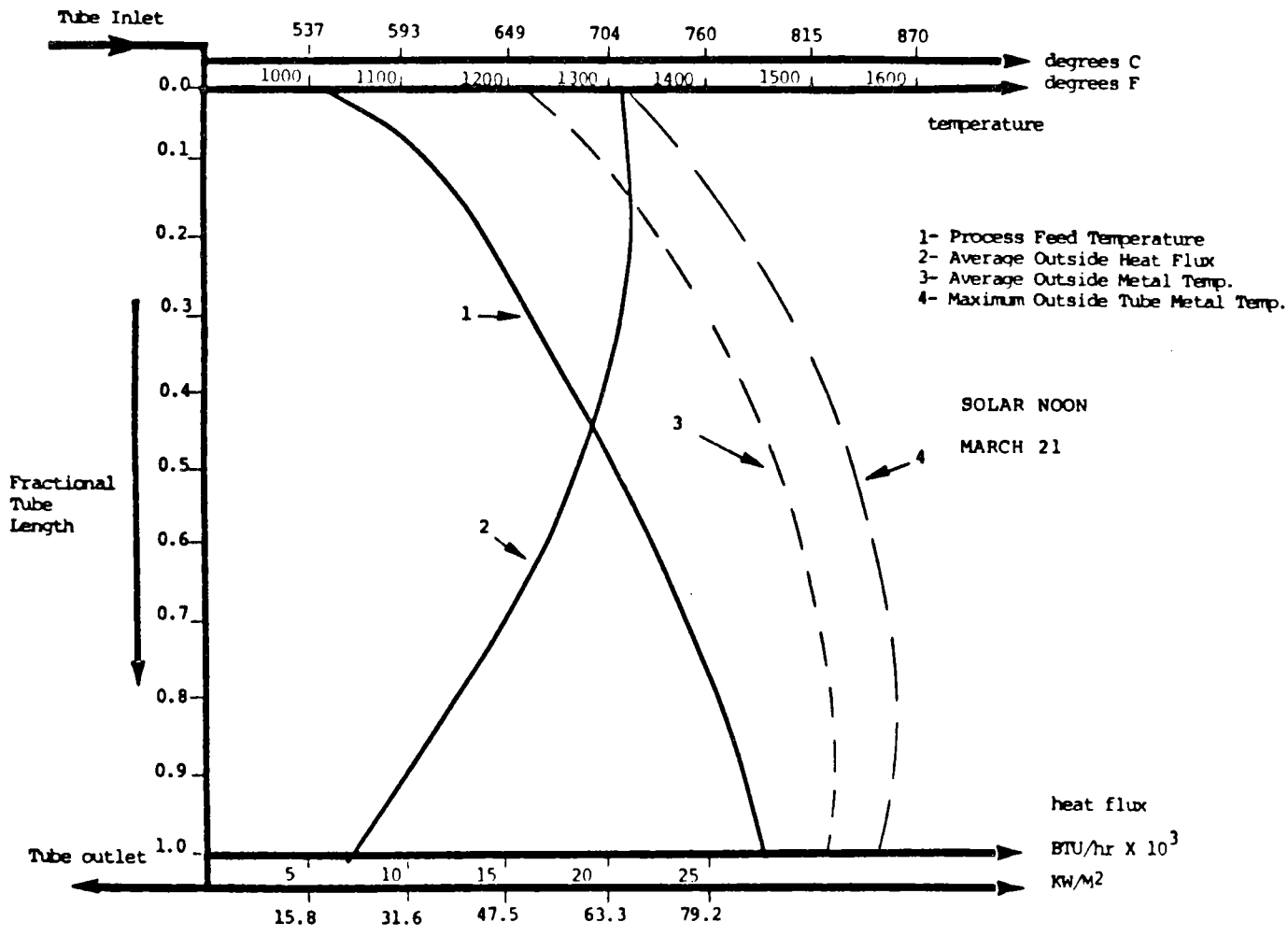
Figure 30. PFR SOLAR STEAM REFORMER NET HEAT FLUX, PROCESS GAS, AND
TUBE TEMPERATURE PROFILES ALONG CENTRAL REACTOR TUBES

-161

Excessive time variations of flux may render an economic tube design impossible due to the thermal cycling and stresses caused.

The firebox or receiver design used in this study is a scaled-down version of the PFR design. The tube length sets the height of the receiver; the number of tubes and tube spacing (2 X OD was used to ensure reasonable radial flux distribution) plus the distance from the front wall to the shock wall sets the length. By geometric similarity, the aperture angle, size, and distance to the shock wall were computed based on the following assumptions:

— Average flux at the aperture plane is the same as the PFR design: 1.23 MW/m^2 (3.90 X 10^5 Btu/h-ft^2)

— Aperture shape is the same as PFR design: elipse with major and minor axis ratio of seven to six

— Horizontal beam angle limits are ±55° from the vertical plane

— Vertical beam angle limits are +5° and +45° from the horizontal plane

— Center of the incident beam is normal to the aperture plane

— Maximum aperture heat flux is the same as PFR design: 3.46 MW/m^2 (1.10 X 10^6 Btu/h-ft^2)

— Maximum incident flux on shock wall is same as PFR design: 0.8 MW/m^2 (2.5 X 10^5 Btu/h-ft^2)

— Beam intensity decreases in inverse proportion to the area of the entire beam in a plane normal to the beam center

— Receiver width to length ratio are the same as the PFR design.

Furnace Construction

Reformer furnaces are designed to achieve the high temperature necessary over the length of the tubes with as little flux variation as possible and with maximum heat efficiency. The solar steam reformer conceptual design is shown in Figure 31. Solar steam reformer design specifications are summarized in Table 31.

To minimize heat losses through the furnace walls, to maximize radiation and to prevent overheating of the casing, insulation is provided on the interior of the steel casing. This refractory insulation may consist of firebrick, concrete, ceramic fiber batting or usually some combination of these. The insulation material will vary in the different section of the

162

Figure 31. SOLAR STEAM REFORMER CONCEPTUAL DESIGN

163
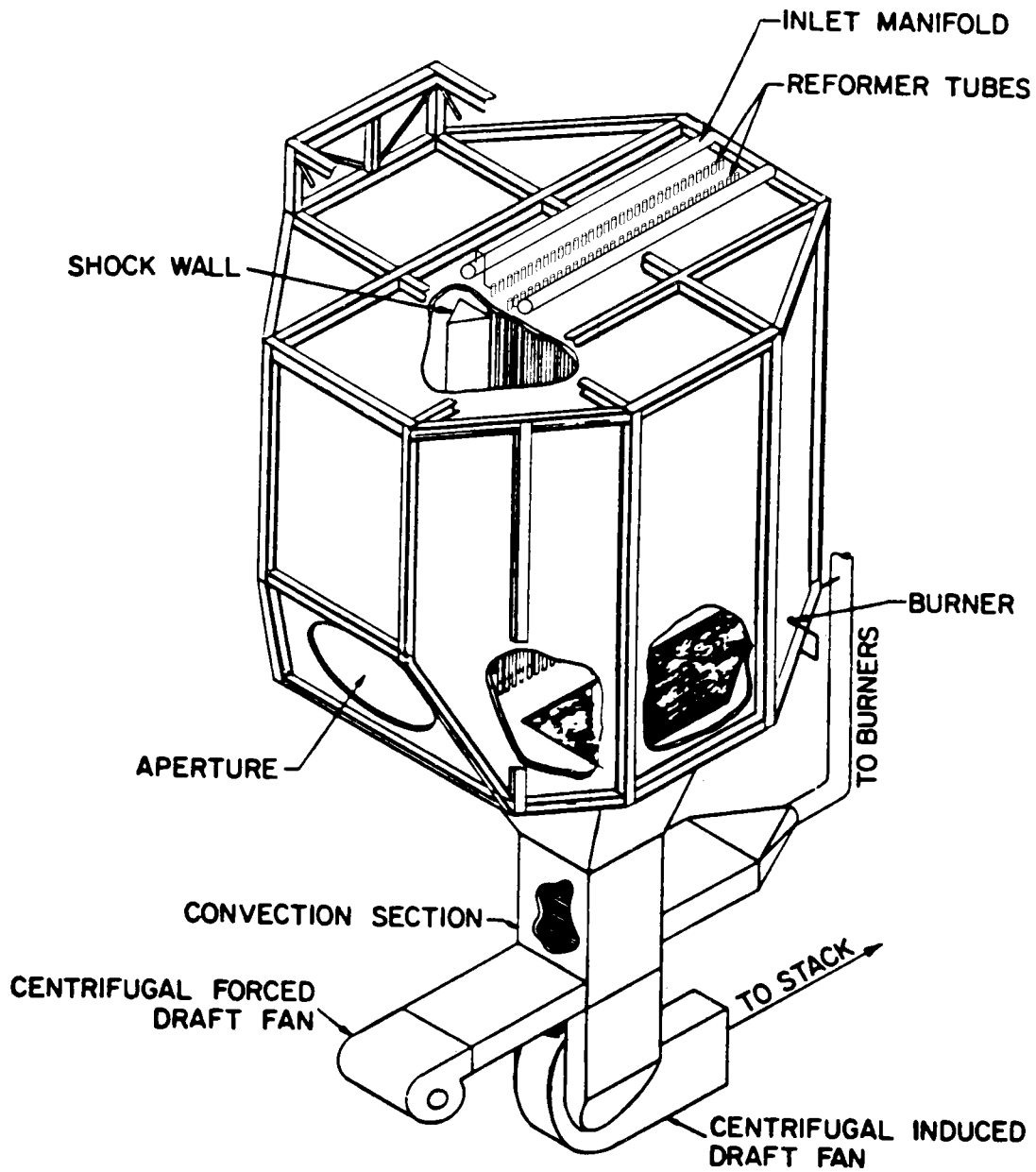
Table 31. SOLAR STEAM REFORMER DESIGN SPECIFICATIONS

Mode of Operation	Hybrid – part of daytime energy requirement by fossil fired combustion. Nighttime operation by fossil fuel combustion.
Power at Aperture	15 MWth (5.12×10^7 Btu/h)
Fossil Power at Design Point	2.34 MWth (7.99×10^6 Btu/h)
Power to Process ÷ Power at Aperture (Net of Fossil Fuel Use)	78%
Design Average Tube Flux	63 kW/m^2 (19980 Btu/h-ft^2)
Process Flow	2.93×10^3 kg/h (6.48×10^3 lb/h) of methane
Inlet/Outlet Conditions	538°C (1000°F) inlet/843°C (1550°F) at 2.7 MPa (392 psig)
Number of Cavities	1
Cavity Cross Section	Octagonal
Aperture Shape	Elliptical
Aperture Area	12.1 m^2 (130.2 ft^2)
Number of Tubes	62
Tube Length (heated)	11.6 m (38.1 ft)
Tube ID	102 mm (4.02 in.)
Tube Material	Manaurite 36X
Convection Loss Control	Forced draft/induced draft system for combustion air/flue gas
Receiver Weight	455.5×10^3 kg (501 tons) (includes heat recovery section)
Heliostat Field Area	27,000 m^2 (291,000 ft^2)

furnace depending on the temperature of operation in each section, the possibility of flame impingement and the extent of thermal cycling. Firebrick is not tolerant of thermal cycling and ceramic fiber may not be strong enough to withstand high gas velocities. For the sake of comparison, conventional reformer configurations are shown in Figure 32. With the reformer wall surface determined, refractory insulation and steel plate weights were estimated based on the parameters given in Table 32.

Table 32. SOLAR STEAM REFORMER FIREBOX DESIGN PARAMETERS

Outside Wall Temperature	49°C (120°F)
Inside Wall Temperature	1149°C (2100°F)
Conductivities: Block Insulation	0.10 W/m °C (5.8×10^{-2} Btu/h-ft-°F)
Firebrick	0.24 W/m °C (0.14 Btu/h-ft-°F)
Density: Block Insulation	288 kg/m^3 (18.5 lb/ft^3)
Firebrick	497 kg/m^3 (31.9 lb/ft^3)
Thickness: 76 mm (3 in.) Block Insulation 229 mm (9 in.) Firebrick	
Weight per m^2 (ft^2)	137 kg (28.0 lb)
Steel Plate: Thickness Density	6.4 mm (0.25 in.) 7865 kg/m^3 (505.6 lb/ft^3)

A summary of weights is given in Table 33.

Tube wall thickness, weights and catalyst requirements were calculated based on a simplified API formula and creep-rupture allowable design stress for Manaurite 36X at a tube wall temperature of 900°C (1652°F). The catalyst used was United Catalyst and Chemicals G-90D steam-methane reforming catalyst with a bulk density of 930 kg/m^3 (58.1 lb/ft^2).

A combination forced-induced draft system analogous to the process gas handling system used for the calcination reactor was decided upon so that air infiltration through the aperture might be minimized. It was then more reasonable to locate the convection section below the firebox where it could be more easily supported by the tower. The transition section was then designed in a "Y" shape so that the process boiler, outlet header, tube supports, pigtails, steam and boiler feed water headers and auxiliary burners could be accommodated. The weight of the transition section was then estimated in a manner similar to the firebox.

1.0 TOP FIRING

FUEL — I.D. F.D.

AIR PREHEAT
BFW
PROCESS
BOILER

2.0 SIDEWALL RADIANT

BFW
PROCESS
STEAM

3.0 SIDEWALL TERRACE

F.D.

AIR PRE HEAT
BFW
STEAM
PROCESS

4.0 BOTTOM FIRING BOX DESIGN

AIR PRE HEAT
BFW
PROCESS
BOILER

FUEL

5.0 BOTTOM FIRING CYLINDRICAL

BFW
PROCESS
STEAM

6.0 COMMON VARIATIONS

1. AIR PREHEAT AND V.F.O. FOR NO.2 FUEL OIL
2. AUXILLIARY FIRING IN CONVECTION SECTIONS
3. STEAM SUPER HEATER COILS
4. HORIZONTAL CONVECTION SECTION FOR NO. 1.
5. AIR PREHEAT FOR NO.5

Item	Type				
	Top Fired	Sidewall Radiant	Sidewall Terrace	Bottom Fired Box	Bottom Fired Cylinder
Shape	rectangular box	long and narrow	long and narrow	rectangular box	vertical cylinder
Tube Arrangement	several parallel	one or two rows	one or two rows	several parallel rows	circular around periphery
Convection Section	at grade or vertical alongside box	elevated above radiant section	elevated above radiant section	elevated above radiant section	elevated above radiant section
Draft	forced and induced	natural or forced	natural or forced	natural or forced	natural or forced
Fuel	gas or liquid	gas or vaporized liquid	gas or liquid	gas or liquid	gas or liquid
Air Preheat	normally provided	possible	possible	normally provided	possible

Figure 32.   COMMON ARRANGEMENTS FOR STEAM REFORMER FURNACES

166

Table 33. SOLAR STEAM REFORMER UNIT WEIGHT — WEIGHT SUMMARY

Material or Equipment	Solar Hybrid	
	metric tons	(tons)
Tubes and Catalyst	22-1/2	25
Refractory and Insulation	134	148
Firebox	102-1/2	113
Transition	20	22
Convection Section	6-1/2	7
Stack	5	5-1/2
Steel Plate	58-1/2	64-1/2
Firebox	35	38-1/2
Transition	7-1/2	8
Convection Section	4-1/2	5
Stack	11-1/2	13
Structure	72-1/2	80
Process Boiler	6	6-1/2
Super Heater	4-1/2	5
Steam Drum	10-1/2	11-1/2
Convection Section	43-1/2	48
Tubes	41-1/2	46
Piping	2-1/2	3
Preheat Coils	–	
Burners and Piping	36-1/2	40
Fans and Motors	7-1/2	8-1/2
Sub-Total	396	437
Safety Factor * 15%	57-1/2	64
TOTAL	455-1/2	501

The process boiler, process superheater,[41,42] and steam drum were sized using rough estimates of film heat transfer coefficients. Weights and envelope sizes were estimated from these designs. Convection section finned tube banks were sized based on both full solar and zero solar cases. Gas-side film heat transfer coefficients were estimated using simple correlations.[43] A summary of the convection section design is presented in Table 34. Flue gas pressure drop through the convection section was estimated for induced draft fan sizing.

A rough structural design was executed in order to estimate cost and weight. Stack, fans, and lines were also sized for weight.

Table 34. SOLAR STEAM REFORMER CONVECTION SECTION — DESIGN SUMMARY

Coil	Operation	Duty, MW (Btu/hx10^6)	Process Flow, kg/s (lb/s)	Flue Gas Flow, kg/s (lb/s)	LMTD °C (°F)	Design Temp., °C (°F)	Overall Heat Transfer Coef., W/m^{2}K (Btu/h-ft^2-°F)	Surface Area m^2 (ft^2) (Outside Finned)
Boiler #1	Full Solar	1.954 (6.669)	1.318 (2.906)	3.445 (7.595)	679.3 (1222.7)	390 (734)	27 (4.8)	
	Zero Solar	5.144 (17.56)	3.470 (7.650)	11.372 (25.071)	666.8 (1200.2)	390 (734)	46 (8.1)	168 (1808)
Feed Preheat	Full Solar	2.127 (7.259)	5.459 (12.04)	3.445 (7.595)	139.5 (251.1)	815 (1499)	15 (2.6)	1050 (11300)
	Zero Solar	2.127 (7.259)	5.459 (12.04)	11.372 (25.071)	266.9 (480.4)	815 (1499)	18 (3.2)	
Superheat	Full Solar	–	–	3.445 (7.595)	–	815 (1499)		
	Zero Solar	1.557 (5.314)	2.152 (4.744)	11.372 (25.071)	169.7 (305.5)	815 (1499)	22 (3.9)	425 (4570)
Boiler #2	Full Solar	0.491 (1.676)	0.331 (0.730)	3.445 (7.595)	77.4 (139.3)	320 (608)	25 (4.4)	255 (2740)
	Zero Solar	–	–	11.372 (25.071)	–	–		
BFW Preheat	Full Solar	0.834 (2.846)	0.720 (1.587)	3.445 (7.595)	80.6 (145.1)	330 (626)	15 (2.6)	539 (5800)
	Zero Solar	2.944 (10.05)	2.540 (5.600)	11.372 (25.071)	280.0 (504.0)	540 (1004)	35 (6.2)	
Air Preheat	Full Solar	–	–	3.445 (7.595)	–	330 (626)		
	Zero Solar	2.710 (9.249)	10.824 (23.863)	11.372 (25.071)	110.9 (199.6)	540 (1004)	31 (5.5)	849 (9140)

V. Evaluation of Reactor Concepts

Objective

The objective of this section (involves the evaluation of reactor concepts) was the assessment of the technical feasibility of the conceptual solar chemical reactor designs discussed in Section III. An essential output of this task is the identification of major problems/limitations of the concepts. This approach leads to identification of areas for research and development (discussed in Section V) that may lead to the successful demonstration and ultimate commercialization of direct flux chemical reactor technology.

Approach

The approach to the assessment of the technical feasibility of the solar calciner and steam reformer reactor concepts was based on the following activities:

● Review of reactor designs in the context of technical requirements and constraints identified in the reactor design effort to identify technology areas where there is uncertainty in meeting requirements and/or constraints

● Review of assumptions used in performance evaluation

● Review of mechanical design components that have been adapted to the reactor design to determine qualitative likelihood of successful use in the solar reactor

● Know-how of the project team

● Discussion with kiln manufacturer (Kennedy Van Saun Corporation).

Assessment of Solar Fired Limestone Calciner

The overall assessment of the conceptual design of a limestone kiln employing direct flux irradiation of reactants in a windowless reactor is that the technical feasibility is established. However, before addressing the positive features of the concept, the principal problems and limitations of the design and design analysis are reviewed.

The first issue is that the method of solids conveyance must be proved. That is, the screw conveyor is conceptually attractive and based on industrial experience and vendor discussions appears to be a workable technique. The screw conveyor must be proven out experimentally.

It is uncertain how a mechanical regenerator will be configured so that it will survive in the high flux, high-temperature environment. While the regenerator offers undeniable conceptual benefits in improving energy delivery to reactants and reducing aperture radiation losses, the regenerator will also be subject to periodic heating which always holds the prospect of failure due to thermal shock. Alternatives to a mechanical regenerator should be considered — such as heat pipes and run-around heat exchangers — which may avoid the potential thermal shock and mechanical design problems (that is, linking of the refractory bricks into a conveyor, driving the conveyor subject to high temperatures and dust) of the mechanical regenerator.

The kinetic data used in the modeling was evaluated under laboratory conditions that are, strictly speaking, not analogous to the conditions in the calciner. The primary artifact of this fact is that results indicate that the reaction takes place at temperatures less than those typical of industry practice. This may lead to an underestimate of kiln radiation losses and an overestimate of kiln efficiency. Future design work should use improved kinetic data (if available).

A catalyst for limestone to lime conversion has recently (Chemical Engineering, July 13, 1983, p.19) been revealed. The catalyst significantly promotes reaction rates at temperatures of 800° to 900°C (1472° to 1652°F). In this context, our results are consistent with the temperatures that would be used in a catalyzed limestone to lime process plant.

Since CO_2 is a good absorber and radiator of infrared energy and it is present in significant concentration in the gaseous products of the reaction, models of kiln performance should account for or at least estimate the extent of CO_2 radiation and absorption in kiln heat transfer. As a product of combustion and a reaction product, CO_2 radiative properties are important in modeling conventional limestone kilns.

Modeling accounted only for radiation losses. The adiabatic wall assumption neglected conduction losses. Aperture convective losses were also not determined. Of course, the principal source of energy loss in a solar receiver is radiation; however, convection and conduction losses are important and must not be ignored as kiln designs are developed.

Kiln design efforts did not emphasize the details of integration of heat recovery into the kiln. In particular, recovery of the heat content of the product solids as preheated sweep gas requires the distribution of these hot gases at or near the aperture so that these hot gases can contribute to heating of the solid reactants. However, excessive convective losses must be avoided. This creates the need for a pressure balanced design in which the induced draft fan withdrawing product gases from the kiln is balanced with the forced draft fan supplying hot air to the kiln so that there is little or no net flow of hot gases out of the reactor aperture. Combined with an aperture tilted down towards the heliostat field to mitigate stack effects and avoid excessive infiltration from wind, and a shroud around the aperture for further wind protection and to maintain a buoyant "bubble" of hot air to offset transport of hot gases out of the aperture, it is conceptually possible to successfully integrate heat recovery into the kiln. This must be proven in practice and the impact of convective losses arising from integration of heat recovery must be quantified. It must also be emphasized that the use of air windows appears promising as a method to achieve low convective losses from open apertured reactors. Air windows are effective convection and mass transfer suppression devices that are used in heat treating facilities and in heavily traveled public building entrances and exits. If the kinetic energy of the moving curtain has an equivalent pressure greater than the buoyancy pressures created by temperature differences, then natural convection or mass transfer through the air window is suppressed. An air window used in conjunction with the other convection reduction measures discussed would be very effective.

The presence of dust in the gas stream is an inevitable fact of life in kiln operation. The use of limestone that is nondecrepitating and without fines will minimize this problem. Screw conveyors will also minimize dusting compared to a rotary kiln approach to material conveyance. Dust will tend to scatter the incoming solar flux back out of the aperture leading to high reflection losses. The sweep gas flow will entrain these particles and if dusting can be confined to the back end of the kiln away from the aperture, the problem may not be that serious because reflected flux will not see the aperture and most of the solar flux is incident near the aperture. However, experiments must be done with various feeds, with and without fines, and with various sweep gas flows to observe the extent of this problem. As kiln models

172

are refined, the presence of dust in the sweep gas stream should be included to estimate the effect of dust on reflective losses and on kiln radiative heat transfer.

Operating strategies and process control methods must be developed for the kiln. These should be implemented into the kiln model and should be developed and validated by experiments. In particular, losses of reactant on start-up and shutdown, particularly in the form of unconverted feed in the lime product has a negative impact on product quality. Operating strategies and plant design will have to account for and accommodate (if necessary) this problem. The intention is, of course, to consume some fossil fuel to maintain reactor in a hot standby condition to minimize the start-up and shutdown product losses.

The kiln as designed has a nonwindowed aperture. Kiln applications are thus limited to reactants/products with low toxicity or environmental impact. While at a very preliminary stage of development, work by MSNW (Mathematical Sciences Northwest, Inc., Bellevue, Washington) under DOE contract suggests that air windows may allow control of the internal environment of nonwindowed reactors permitting the extension of the kiln design to air sensitive, toxic, or environmentally sensitive materials. This must be regarded as a tentative assumption.

By no means should the design concept developed in this study be regarded as optimal. It is merely exemplary to provide a basis for evaluation of technical feasibility and R&D needs. Optimization of the design involves further analytical and experimental work to identify optimal insulation thickness, aperture area and orientation, reactor cross section and length, bed area, etc.

Finally, the design effort was constrained by project scope to consider direct flux reactor design. Thus other concepts, perhaps involving transport of heat through opaque surfaces must be considered.

On the positive side, the similarity of reactor design to existing industrial designs should lend to potential industrial acceptance. The calciner is of similar configuration to rotary kilns with analogous patterns of flow of solids and gases. Feed and discharge methods for solids closely resemble methods used for industrial kilns. Kiln construction techniques are

similar employing a carbon steel shell and refractory lining. Of course the solar calciner offers potential for lower weight through use of fibrous refractories. Existing technology for heat recovery from hot solids and gases is applicable to the solar kiln.

The inherent cavity configuration of the calciner leads to moderate aperture radiant losses. If regenerator technology may be proven, the kiln should be capable of high efficiencies, commensurate with the high process temperature, through avoidance of high flux density on cavity walls and resulting hot spots near the aperture.

Development of the kiln appears straightforward due to the lack of complex chemistry, and derivation of design from industrial kiln design. While it must be stressed that reactor development is never a simple undertaking, development is within the state of the art in technology to model kiln performance, fabricate kiln and heat recovery devices and to control the process. As a result there is a good likelihood of calciner technology being developed in time for a 1995 pilot plant demonstration.

The calcination process in particular, and reactions with solid products and reactants in general lend themselves to a "solar batch" process. A key issue in the development of solar fuels and chemicals technology is the plant interface. The interface problem is generally one of creating circumstances in which the plant operations are disturbed as little as possible by the substitution of the solar heat source for the reaction for the typical fossil heat source. The essence of the problem is twofold: 1) economic amortization of plant components generally requires operation of plant components on a 24 h/d basis and 2) plant operations are run at steady-state and process disruptions are costly. In the case of a solids reaction such a limestone calcination a logical plant interface is to run the calciner only during sunny hours. Plant operations are maintained on their usual 'round-the-clock schedule by provision of storage of limestone feed and lime product. Batch operation results in a simplified reactor design without the complexity of integrating fossil heating components within the reactor for 24 hour operation (hot standby conditions are expected to be maintained by an aperture door and a limited amount of fossil fuel usage). The simplicity and expected economy of solids storage recommends that this approach be taken for the plant interface. The expected requirement that solar reactor systems shall

174

ultimately be required to operate without substantial fossil fuel use also suggests that solids storage and batch operation be developed for solids reactions such as calcination.

The kiln reactor has other attributes which may be briefly summarized:

o   The reactor uses direct flux irradiation of reactants through a combination of solar, reflected, and reradiate energy

o   The reactor is of relatively simple construction

o   It has high thermal efficiency because it functions as a cavity receiver

o   Offers potential for low cost design since it does not require exotic materials of construction.

It is useful to recapitulate the reasoning that had led to the evolution of the conveyor kiln concept.

The original choice for a reactor concept was a windowless rotary kiln for the calcination of calcium carbonate. This is essentially the reactor type used industrially for this reaction.

As analysis proceeded on the design of the rotary kiln, a number of problems were identified that led to the selection of an alternative kiln concept: the conveyor kiln. The nearly horizontal rotary kiln has poor coupling of direct solar flux to the reactants.

The cylindrical rotary kiln appears to have a conflict between materials handling requirements and solar coupling. If the kiln axis is oriented horizontally (as is customary), the solar coupling may be poor with little direct irradiation of the burden and — possibly — a very high flux incident on the kiln wall near the aperture. This may result in high radiation losses because the kiln wall will reach a high temperature and it has a good view factor for the aperture. If the kiln is steeply inclined to improve coupling by allowing deeper penetration of flux within the kiln, the residence time will be too short for adequate reactant conversion. Slowing the kiln rotation rate improves residence time, but will exacerbate one of the critical problems identified for rotary kilns: expected short lifetime for the refractory liner due to periodic heating cycles.

The use of dams was briefly considered as a means of slowing the flow of reactants through a more steeply tilted rotary kiln. A steep tilt offers some

175

potential for deeper penetration of flux into the reactor. However, such a kiln is still subject to periodic heating of the refractory wall. The "top" of the kiln will likely still experience high incident solar flux resulting in high refractory temperatures that would be expected to cycle down to approximately the reaction temperature. Although this decision is somewhat intuitive since time did not permit flux mapping of this alternative, the use of dams is not expected to resolve longevity concerns regarding the kiln liner.

The motion of the reactant bed, while providing good mixing, leads to dusting, which may impede penetration of solar radiation into the kiln.

The alternative design developed was the conveyor kiln. The cavity walls do not rotate. The design is mechanically simple.

The conveyor kiln appears to offer an attractive solution to the drawbacks of the rotary kiln. It offers the following features:

1. Reduced power consumption due to improved material handling efficiency

2. Enhanced flexibility and control of residence time by varying conveyor drive speed

3. Potential for improved solar coupling flexibility, which is achieved by relative freedom in selection of kiln axis inclination. The reactor can be tilted upward to almost any angle up to the limiting angle of repose of the reactants

4. Reduced burden agitation minimizes dusting within the cavity to limit reflection and scattering losses at the aperture.

The kiln itself is stationary; the product is moved through the kiln via conveyor. The upper side walls of the kiln may be tilted to create a better radiation shape factor for better coupling of IR radiation to the reactants while possibly avoiding hot spots near the aperture and this design approach is advantageous in terms of product processing and quality, simplified mechanical design, reduced system weight and cost, and full 24 hour operation.

The mechanical design of the kiln is simplified. The rotary gear drives, thrust mechanisms, riding rings, bearings, etc., are eliminated for the stationary kiln.

Most rotary kilns used in the United States avoid the use of multilayer insulation due to potential slippage between the layers during rotation of the

kiln. The insulating materials of the stationary kiln may be multilayer both radially and axially allowing for increase insulation and decreased kiln weight and cost.

The proposed kiln concept allows for operation at reduced temperatures and hence improved product quality. Lime burnt at low temperatures is highly porous and shows large internal free surface. Such lime, called soft-burnt, is usually preferred due to high chemical reactivity.

Operation at low temperatures will allow increased capacity/heliostat yield as well as reduce thermal stresses on materials.

Additionally, generation of fines/dust is minimized. This is of concern not only to the process but also to the downstream equipment (such as baghouses and scrubbers).

Discussions with a conveyor vendor indicate that the use of intermeshing screw conveyors will meet the requirement to transport solids at temperatures up to 1200°C (2192°F) quite adequately. There is experience in industry with solids conveying at temperatures up to 1100°C (2000°F). In the conceptual design the screws remain below the surface of the burden so they will not be subjected to high fluxes and thus to excessive temperatures. The likely material of construction would be Incoloy 800H. It should be a satisfactory material of construction up to 1316°C (2400°F) since it is not subject to stresses such as experienced in its more typical applications at high pressure Incoloy 800H will resist erosion and corrosion. Screw conveyors can be designed to provide good mixing. While requiring demonstration, the use of screw conveyors does not appear to require new technology but rather sound engineering design.

Summarizing, a conveyor kiln will be mechanically simple compared to the rotary kiln. It will be a compact design in the sense that its stationary walls make it less unwieldy to operate as a tower mounted reactor than the rotary kiln. The conveyor kiln is expected to be more thermally efficient than the rotary kiln because of better coupling of direct and reradiant flux to the burden and lower radiant losses. Constructed as a fixed container that allows the use of ample thickness of lightweight refractories, the conveyor kiln can be cheaper to construct than the rotary kiln. Integration of a fossil burner and use of aperture door permit maintenance of high standby nighttime temperatures to simplify daily start-up procedures.

The kiln reactor is of generic significance. The kiln reactor is applicable to a number of industrially significant chemical reactions. The list includes:

o   Portland cement manufacture

o   The SL/RN process for iron ore reduction

o   Roasting of gold and silver ores

o   Bauxite calcination

o   Gypsum drying

o   Production of titaniferous ore.

Because of potential environmental contamination, applicability to roasting processes producing substantial quantities of sulfur oxides is uncertain and dependent on proof of effectiveness of use of induced draft to minimize uncontrolled convective loss of gaseous reaction products while maintaining low convective losses to achieve high thermal efficiency.

Air window technology, if successful, will allow use of kiln technology in such process applications. The nickel alloys have limited high-temperature resistance to corrosive attack by sulfur oxides. Appropriate materials of construction or coatings on a nickel alloy substrate have to be identified and proven to allow use of kiln technology in applications where sulfidation resistance is important.

The reactor may also be a candidate for adaptation to a windowed design for reactions requiring isolation from the atmosphere, particularly where reactants or products are toxic or corrosive, or gaseous products must be recovered, as in zinc sulfate decomposition for thermochemical hydrogen production when sulfur oxides must be recovered and cycled through the process.

At the scale considered for this conceptual design, the reactor can produce a very significant amount of lime products. Using the 89% efficiency of the calciner based only on radiation losses through the aperture with a 6 hour per day production day and 330 days per year plant operation, at 5.07 X 10^3 g/s (20.13 ton/h) limestone feed rate, annual lime production would be 20230 metric ton/yr (22,300 ton/yr). At a more realistic efficiency of, say, 79% production would be 17960 metric tons lime/yr (19,800 tons

lime/year). Obvious limitations to scale-up involve mounting a heavy unit of large physical dimensions on a 100 meter (328 ft) tower. At a thermal input of 50 MWth (1.7 X 10^8 Btu/h) at the reactor aperture, production would be of the order of 59,870 metric tons lime/yr (66,000 tons lime/yr). While this is a somewhat small production capacity, approximately 15% of annual U.S. lime production is done in plants at or below the capacity. Thus, it appears that a solar fired limestone kiln can produce lime at a capacity comparable to existing production facilities.

Assessment of Solar Steam Reformer

The overall assessment of the direct flux solar steam reformer is that the technical feasibility of such a reactor concept is not established. Primary requirements to establish technical feasibility involve significant materials development to produce materials in required lengths and diameters with confidence of performance reliability comparable to nickel alloys currently used as reformer tube materials of construction while achieving significant cost reductions on the order of a factor of 100 over todays per kilogram (pound) costs.

The principal problems and limitations involved in the design of a direct flux solar steam reformer may be identified as follows.

A key limitation is that a direct flux reformer has a very low likelihood of being sufficiently developed for 1995 demonstration at the pilot stage. Thus a gas phase reactor in a direct flux configuration will not be available to demonstrate this aspect of solar fuels and chemicals technology. Development of direct flux gas phase reactor technology is thus inconsistent with the stated DOE programmatic objective of a 1995 technology demonstration and must be regarded as a high risk undertaking for a later generation of solar reactor designs.

Current ceramic tube receiver designs are limited to four atmospheres for Brayton cycle applications. This low operating pressure limitation is not consistent with the much higher operating pressure of conventional reformers.

The use of transparent materials instead of metals is unfamiliar to industry. The lack of similarity of a direct flux reformer to industrial practice using metallic materials for reactor tubes incurs a requirement for extensive operating experience with at least pilot scale hardware to prove the capabilities of this technology to industry.

179

Even if the higher heat transfer rates that may be possible through the use of direct flux reformer technology permits the use of shorter tubes, tubes are only available in 1.83 m (6 ft) lengths. To use shorter tubes, a more than six to one increase in average flux from typically 63 to 420 kW/m^2 (19,975 to 133,172 Btu/h-ft^2) would be required and would imply drastic redesign of reformers that now would likely be subject to kinetically limited reaction rates rather than heat transfer limited rates. In any case, these high fluxes exceed solar superheater design practice of around 350 kW/m^2 (110,977 Btu/h ft^2) and would result in catastrophic overheating of catalyst should process flow be interrupted. A much more likely scenario of development would use tubes of length the same as or near to current practice in which the principal benefit of direct flux is derived through the reduction in cavity temperature. After this is proven through extensive operating experience, the benefits of higher fluxes and shorter tubes to permit more compact reformer designs could be explored.

Transparent ceramics are subject to thermal shock which leads to catastrophic failure of the reformer tube. Of course, the use of pigtails allows a reformer tube to be taken out of service and replaced during maintenance procedures.

Candidate ceramic materials are subject to corrosion. The opacity of transparent tubes will be increased by corrosion and even a small amount of carbon deposition will reduce the coupling of direct flux into the catalyst bed. This will tend to increase receiver operating temperature and require longer tube lengths for adequate conversion.

The most critical problem in the development of direct flux steam reformer technology is that material costs are very high. These high costs are inherent in current manufacturing processes due to purity requirements, high temperatures and thus large energy requirements required for fabrication, and the close temperature control required for manufacturing. The current economics of transparent ceramics may be briefly summarized:

o   Age of product technology

   —   5 to 20 years old

   —   Designed for radically different environments and applications

o   Additional processing steps than standard ceramics

- — Remove impurities from raw materials

- — Modify bulk chemistry

- Complexity of fusing, sintering, or melting processes

  - — Control grain growth

  - — Prevent environmental contamination

  - — Prevent devitrification or phase changes

- High energy costs to fuse or sinter Al_2O_3/SiO_2

- Low demand prevents economies of scale

- Low product yields as compared to raw material input

- Inability to model ceramic properties at this time.

How high is the cost of transparent tubes? An estimate is given here. The weight of the metallic tubes and manifolds is estimated at 18,400 kg (40,600 lb). The cost of Manaurite 36X is approximately $7/kg ($3.17/lb). Ignoring fabrication costs and density and strength of material differences (a transparent reformer may require thicker walls than a metallic design), the cost of material for metal tubes is about $130,000, while Vistal, the lowest cost alternative material, at $3600/kg ($1630/lb) would cost $66 million in material alone. A 27,000 m^2 (291,000 ft^2) heliostat field will only cost $2.4 million (@ $90/m^2$, $8.36/ft^2$) to $6.3 million (@ $90/m^2$, $21.84/ft^2$). Thus, at current costs, transparent materials cannot compete with metallic materials as a material of construction for a solar steam reformer. Even as an approximation, a possible efficiency improvement in solar energy utilization will not affect high material costs.

Compounding the issue of high material costs is that the already high efficiency of solar utilization of metallic reformers leads to a limited capability for efficiency improvements through the use of direct flux reactor design. As has already been noted, it is from efficiency improvements and as a consequence (primarily) heliostat field size (and thus cost) reduction that the increased transparent tube costs must be recovered.

Thus the target that a direct flux steam reformer must beat is the metallic steam reformer. The metallic steam reformer has a good likelihood of being sufficiently developed for a 1995 pilot plant scale demonstration. The

metallic steam reformer design holds significant promise for successful development and potential industrial acceptance through use of a similar configuration to down fired reformer design practice, the use of similar materials of construction, similar heat recovery techniques from process gases and flue gases, and the ability to achieve (at least at the design point) flux distribution comparable to conventional reformer design practice.

Importantly, the metallic steam reformer design is of generic applicability to gas phase reactions such as naphtha reforming, ethane cracking, and sulfuric acid decomposition. Since steam reforming is conducted under severe process conditions of high temperature and pressure, the technical feasibility of this reactor concept leads to a good measure of confidence in the potential for technical success of gas phase reactor designs for fuels and chemicals processes.

The technical feasibility of the metallic steam reformer has been established over a range of scales appropriate to hydrogenation plants (around 15 MWth [5.12×10^7 Btu/h] at aperture plane) and to ammonia plants (around 30 MWth [1.02×10^8 Btu/h]). Thus at this conceptual stage of development, the reactor technology appears appropriate to supply the synthesis gas requirements of typical chemicals process plants.

Although operating at high temperatures, the cavity configuration shows the promise of good receiver efficiencies. An efficiency of 78% was used as a design basis in this study. This efficiency value is based on detailed calculations by PFR for their reformer conceptual design of substantially the same configuration (the version reported on here is essentially a scaled down version of the PFR conceptual design).

The use of fossil fired integration as a means for low insolation and nighttime reformer operation is an intermediate step on the road towards development of solar fuels and chemicals plants that require minimal use of fossil fuels. This fossil fired hybridization allows the plant to operate as a "fuel saver," permitting a single reformer to supply synthesis gas to the plant 'round-the-clock. As a result, the reformer can follow diurnal and instantaneous variations in insolation, the cycling of components can be minimized leading to increased component lifetimes then if cyclic operation is practiced, and the reformer minimizes effects on plant hardware and plant operation. Minimum impacts on plant hardware and plant operation is essential

182

to rapidly introducing solar technology to industry because it is responsive to the question: What happens when the sun goes down?

The principal problems and limitations of the metallic steam reformer may be briefly outlined as:

⊙ Uncertainty in the combination of fossil and solar firing to achieve assumed axial flux distribution, especially due to absorptivity of IR flux from cavity walls by combustion products

⊙ Uncertainty in capability of achieving desired flux distribution under off design conditions

⊙ Uncertainty in locating burners for desired flux distribution

⊙ Prevention of convective loss through aperture during combined fossil/solar operation is uncertain

⊙ Creep/rupture failure in the solar operating environment may lead to premature tube failure. (Excessive thermal cycling may be a problem.)

⊙ Catalysts, catalyst supports, and flow valves must be proven out in an environment of repeated thermal cycling

⊙ To achieve adequate response to transient conditions, control of burners and process flow must be proven, especially in view of possible rapid flux variations and the high temperature, hydrogen rich process fluid

⊙ Refractory choices are influenced by conflicting needs for thermal inertia to facilitate transient control while reducing weight to minimize tower costs.

The design and estimates presented were carried out on the basis of the major assumption that a hybrid solar steam reformer can be made to work. Concepts include technology that has neither been proven nor designed in detail.

The hybrid receiver design solves the primary solar design problem by firing fossil fuel in the receiver itself to supply for any insolation deficiencies. The hybrid avoids the expense of dual units and presumably the problem of thermal cycling. Process dynamics problems involve firing burners quickly enough and at the proper rate with due consideration to the use of thermal mass in the receiver to moderate process response to transients. There are, however, a myriad of design problems that are raised by this approach and that require investigation.

The first questions regard the mutual influences of wall radiation and the combustion gases: Will wall radiation be absorbed by combustion gases? What will be the effect on the furnace temperature? Will radiation be primarily from the walls as in the case of a reactor exclusively heated by solar radiation or from the body of gas as in fossil-fired furnaces? These questions can probably be addressed analytically with a minimum of experimentation.

The most obvious problem with the hybrid concept is that it must simultaneously admit solar radiation and prevent the infiltration of ambient air. Furnace efficiency is destroyed by the influx of even relatively minor amounts of air. A push/pull fan system as proposed in the conceptual design is only a preliminary step in the engineering solution of this problem. However, Sanders has extensive experience in the control of push/pull system based on their 1/4 MWth (8.53 X 10^5 Btu/h) receiver development. Their work suggests this problem is resolvable through shrouding of the aperture to maintain a hot gas bubble that tends to prevent convection and sensing of the bubble temperature to control the flow and balance forced and induced draft fans. The ability of air window technology now under development to suppress convective losses is pertinent as a method to control infiltration losses.

Probably the most important component of a reforming furnace, both from operational and capital cost viewpoints, is the metallic catalyst tubes. These nickel alloy tubes operate with skin temperatures of approximately 1040°C (1904°F) and contain a process fluid with high hydrogen partial pressure at 1.4 to 2.8 MPa (203 to 406 psi). These conditions are at the upper limits of presently available materials of construction.

Any metal subjected to operating temperatures greater than 540°C (1004°F) has to be designed for creep (permanent deformation) even at stress levels well below the yield stress. If the metal temperature is high enough for creep effects to be significant, the tube will fail by creep-rupture. Tube failures have been the main cause of downtime in steam reformers and so prevention of such failures usually determines tube/reformer design. Designs attempt to uniformly transfer the heat through the tube walls at a maximum rate without exceeding tube wall design temperatures. Usually catalyst tubes fail of localized overheating which causes creep-rupture. Such localized overheating can be caused by faulty burners, incorrect or poor furnace

temperature control, inactive or poorly loaded catalyst, or plugging within the tubes or headers.

Reformer tubes are currently made of stainless steel known as HP-50 (35% NI 25% Cr), HK-40 (35% Ni 25% Cr), or Manaurite 36X. The tubes are mounted vertically with support from top and bottom to prevent bowing or sagging. During operation such a tube will expand 150 to 300 mm (5.9 to 11.8 in.). The inlet and outlet connections must be flexible. These connections are usually made of Incoloy 800 and are known as "pigtails." Pigtail failure has also been a common cause of reformer downtime. Failure can be caused by overstressing of the pigtail through repeated expansion and contraction of the tube. These effects can be prevented by minimizing the thermal cycling of the reformer. Ideally, once a reforming furnace is brought up to operating conditions the status will be maintained for a year or more. Frequent start-ups and shutdowns are usually avoided since such thermal cycling can dramatically increase the possibility of catalyst tube and pigtail failure. Since creep-rupture is time-dependent, catalyst tubes are typically designed for a lifetime of 100,000 hours. In some instances frequent thermal cycling has been known to reduce this lifetime to less than 20,000 hours. Therefore, appropriate tube material selection and minimization of thermal cycling are essential to reliable solar reformer operation.

In order to achieve uniform radial heat transfer to the catalyst tube, the distance between tubes must be carefully selected.

Catalyst tubes are generally designed for the maximum tube wall temperature. For a given flow rate and conversion, a fixed amount of heat must be transferred to the reactants over the tube length. Since the reactants are further from equilibrium at the tube inlet, the reaction rate is highest there. As reaction rate decreases down the tube, the rate of heat absorption by the reactants decreases proportionately.

Flux patterns required to give this result are highest at the tube inlet (about 126 kW/m^2 [40,000 Btu/h-ft^2]). The flux pattern achievable in the reformer and any variation of the pattern with time are critical in reformer design.

The most efficient tube designs are executed by predicting the longitudinal tube wall temperature variation by simultaneously solving the

heat transfer, fluid flow, mass transfer and reaction kinetics problems. Time variations are not normally taken into account.

Any departure of the achievable flux pattern from the optimum forces a departure of tube design from the optimum. Variation of furnace flux patterns with time would be particularly troublesome from a design standpoint. Excessive time variations of flux may render an economic tube design impossible due to the thermal cycling and stresses caused.

The shape and dimensions of the hybrid receiver were chosen to provide as even a flux pattern as possible on the tubes with solar radiation. This shape is much wider than conventional reformers. Preliminary checks indicate that this is not detrimental to fossil furnace design, but this should be investigated in detail. An optimum configuration that will serve the needs of both solar and fossil heat sources should be found.

The fossil burners are presumed to be able to adjust for any irregularities in the solar flux pattern. To what extent is such adjustment required? Can the burners be placed in a practical way to accomplish the leveling function? If it is in fact advantageous to have a flux pattern which varies along the tube length, can the solar radiation and the burners be designed to accomplish this? The answer to each of these questions may have a profound effect on a hybrid receiver design.

The primary problem of any solar design is caused by the time variability of the energy source. This includes three aspects: The diurnal and annual cycles, the irregular variation of insolation intensity because of atmospheric conditions, and the continuing possibility of sudden interruptions due to weather. A secondary problem for a central receiver design is that the reformer must be mounted on a tower unless an intermediate heat transfer medium is employed. Both the remote location, that is, on top of a tower, and rapid and continuous response to insolation changes indicate that automatic control of heat input, feed rate or both is required. Hybrid receivers will require automatic control of the tube outlet temperature.

The firing rate will be varied for the hybrid reformer. The temperature of each steam on the tube side of the convection section will have to be controlled. This will be done by dampers on the flue gas side. Temperature control of process effluent and steam preheat are also necessary and will be

186

automatic. Each of these is a potential reliability problem. If burners need to be used to adjust flux on the tubes, accurate tube wall temperature measurements must be made continuously or semicontinuously at many points on the tube bundles and the temperatures used as control signals for the burners. Success of this approach depends upon reliable temperature measurements at 843°C (1549°F) and in a hydrogen-rich environment. This has been a long-term reliability problem in commercial reformers and therefore some development work in this area in anticipated.

There are two possible types of material that can be used for reformer furnace lining: firebrick and ceramic fiber. Ceramic fiber is much lighter, much less expensive and much less subject to damage due to thermal cycling than firebrick. It has two major disadvantages for solar hybrid application: it has a very low heat capacity and it is easily damaged by high velocity combustion gas. Because neither the burner locations nor their time response is known at this stage, it was judged that either the erosion resistance or the heat capacity or both of the firebrick would be required in the hybrid design and it was sized and priced accordingly. There is potentially substantial savings in this area and this should be investigated. The comparative optical properties of firebrick and ceramic fiber ought also to be studied.

V. Research and Development Plan

Objective

The ultimate objective of the DOE Solar Fuels and Chemicals Program, of which this work is a part, is the establishment of a technical design data base for the use of solar chemical reactors in industrial process applications. The specific objective for this section (involves the creation of a research and development plan for solar chemical reactors) is the identification of research and development areas and the preparation of a development plan that will lead to the evolution of the technical design data base.

The primary input was the evaluation of the reactor design concepts as reported on in Section IV. The development plan will identify activities that establish the advantages of the design concept while resolving disadvantages and problems.

Primary areas in which research and development activities are likely to by necessary are in the areas of chemical engineering, materials development and testing, window and tube design and testing, systems integration, and systems analysis.

Chemical engineering includes such areas as materials selection and testing; reactor performance modeling, especially in consideration of the solar environment with its transients, diurnal cycling, and high thermal flux; materials handling; model validation; interface of collector and reactor; and pilot-scale reactor construction, testing, scale-up, and demonstration. Of course, chemical engineering activities address the issue of selecting an appropriate reactor design for the reaction of interest and include reactor cost analysis and optimization.

Systems integration addresses issues that may be required to demonstrate and commercialize solar reactor technology as an integrated part of chemical process plant operation. System integration may include the further development of conceptual designs of baseline solar fuels and chemical plants for specific reactor/reactants and involve the evolution of the conceptual design to pilot plant and demonstration scale. Systems integration may also focus on the firming of economics for the integrated solar reactor/chemical process plant.

Systems analysis is oriented to the larger view of solar reactors for chemical process applications. Issues to be addressed include the need for or appropriateness of direct flux reactors or the alternative use of intermediate heat transfer fluids to supply thermal energy to ground-mounted reactors of conventional design. Systems analysis may also consider developing target costs for reactors and processes that would make them competitive with conventional process methods.

The research activities oriented to the establishment of direct flux reactor technology in particular and solar reactor technology development in general may be broken out in the following categories of research activities:

- Calciner research and development

- Metallic steam reformer research and development

- Direct flux materials research and development

- Development of air window technology

- Direct flux tubular (steam reformer) research and development

- Window technology research and development.

Calciner Research and Development Program

The development of a direct flux reactor for limestone calcination using a conveyor kiln may be accomplished through the execution of a conceptual design study of a commercial scale reactor design giving consideration to the integration of the reactor in limestone plant operations. The logical next step is a downsizing of the commercial scale design to the range of 0.5 MWth to 1 MWth (1.7×10^6 to 3.4×10^6 Btu/h) (at the aperture plane) with this design executed as an experimental reactor to be installed at the CRTF to prove the technology embodied in the conceptual design, gain operating experience, and provide a validation to industry of the capability of solar technology to produce an industrially significant chemical commodity. The reactor design study should consider the use of batch feed and product storage as means to integrate solar reactor operation with the plant. Economic analysis and trade-offs should also be studied.

The existing model of the conveyor kiln is of significant utility in reactor design, but makes simplifying assumptions that are commensurate with the project scope and level of effort of the project. The primary drawback is

that process chemistry and heat transfer models at IGT are physically separated from the radiation heat transfer models executed at Sanders Associates. Merging of the process chemistry and radiant heat transfer programs will allow parametric assessment of reactor design alternatives to be carried out quickly. The model will be improved if better kinetic data that reflects actual commercial kiln operating temperatures is found and can be incorporated into the model. The adiabatic wall assumption should be relaxed and the actual model should reflect the geometry of the conveyor kiln with a flat burden profile rather than the crescent shaped burden profile of the rotary kiln. In order to identify process control requirements a time dependent, rather than the current steady-state model, should be developed. This model will permit assessment of daily, monthly, seasonal, and annual performance of the kiln. The model will guide development of the experimental reactor, will identify the experiments to be conducted and provide a feedback mechanism to improve and validate the model based on experimental findings. Further model improvements involve the impact of carbon dioxide in the gas stream on infrared heat transfer from cavity walls and regenerator surfaces and the gas itself to the reactants and incorporation of the effects of dust in the gas stream on solar radiation heat transfer. System operation will be established through development and implementation of a computer model representing the dynamic operation of the solar calcination system.

The outputs of the conceptual effort will be to develop component technical specifications, including plant layouts and process flow schematics, develop mechanical design specifications of the receiver, heat recovery, and material conveyance.

The parameters of the receiver/reactor design that should be explored to meet the technical requirements of the system design and to prepare the facility design are:

- Aperture area, orientation, and configuration

- Reactant bed surface area

- Reactant bed arrangement/orientation: that is, long and narrow

- Refractory wall area and composition

- Relative orientation of walls with respect to each other and to reactant bed

190

o   Regenerator presence and characteristics/absence of regenerator

o   Sweep gas flow rate

o   Sensitivity of performance to variations in nominal gas/solid heat
    transfer coefficient

o   Sensitivity to reactant particle size ranging from 0.25 mm to 38.1 mm
    (0.01 in. to 1-1/2 in.), nominal of 25.4 mm (1 in). Particle size of
    25.4 mm (1 in.) typical of conventional rotary kilns. The short
    residence times characteristic of small particles may dictate the use of
    a shorter residence time reactor configuration.

The geometrical design of the cavity is an iterative process. Geometry
changes influence the pattern of incident solar flux inside the cavity,
influence overall efficiency, and affect the aperture sizing (to maximize
input power, consistent with loss minimization).

The object of the component mechanical design effort will be to
characterize physical aspects of the reactor, heat recovery devices, and
material transport components. The critical design issues to be considered
for the reactor system and components are summarized below.

The method of conveying solids through the reactor needs to be
finalized. This must be done in view of the high-temperature environment in
the reactor, potential exposure of conveyance components to high thermal
fluxes, and potential erosion, corrosion of conveyance components. The
current choice of the screw conveyor must be reviewed and the details of
conveyor design developed. The details of material conveyance integration
with reactor feed and product removal must be specified.

The regenerator component must be designed. The need for the regenerator
must be reviewed as the parametric study of the cavity shape and the
interaction of cavity geometry with the reaction and radiant heat loss
characteristics is investigated. The additional complexity, cost, and
technical uncertainty of the regenerator design must be considered in the
context of its potential improvement in the thermal efficiency of the reactor
through avoidance of hot spots with good view factors for the aperture.
Besides the mechanical regenerator conceived of for this conceptual design,
heat pipe and run-around loop approaches may also be identified as a means to
provide the regenerator function.

The methods for integration of the heat recovery from hot solids as the hot sweep gas must be reviewed and a method selected. This problem is intimately connected with the problems of design of means to minimize convection losses that may arise through the use of the forced draft/induced draft approach used in the current conceptual design. The use of air window technology is pertinent and should be included in design studies to permit (at least conceptually) heat recovery integration without excessive convective heat losses.

Operating strategies and control requirements must be identified. The objective is to describe the strategy for operating receiver/reactor, material transport, and heat recovery systems under conditions of:

Steady-state daytime solar operation

Daily start-up (hot start-up)

Normal shutdown

Cold start-up

Cloud transients

The approach is to utilize the transient simulation to evaluate system behavior (temperatures, conversion, mass flow) to achieve 100% conversion of feed to product under conditions of:

Steady-state daytime solar operation

Hot start-up

Normal shutdown

Cold start-up

Cloud transients.

The main process variable to be controlled is the mass flow rate of limestone. Typically, in batch operations limestone flow would commence shortly after sunrise, rises to its maximum value at solar noon, and then decreases to zero at sunset. Material conveyance flow rates are tied to the throughput of the reactor. The flow of sweep gas into the reactor and the flow of product gases and sweep gas through the heat recovery components and exhausted to the atmosphere are also dependent on mass flow of reactant. The extent of flow rate variations allows assessment of turndown requirements of

components such as the solids conveyance system within the reactor, material transport components and the induced draft fan handling product gas.

Control loop functions shall be identified. That is, measured and controlled variables will be identified. As much as possible, control methods shall be derived from methods used in conventional rotary kilns. Measured variables typically are solid product temperature; gaseous product temperature and composition.

The transient simulation will allow assessment of the impacts of cloud transients (typically modeled as a step change in receiver input power of specified duration) on reactor performance including consideration of the mass of solids and refractories within the receiver/reactor.

Based on the foregoing assessment, system response to transient and diurnal solar power variations the following information should be developed:

* Operating strategies

* A summary of control system requirements, that is, controlled variable, manipulated variable, and the controller

* An overall process and instrumentation diagram for a control system meeting process requirements and constraints such as need for 100% feed conversion

* Control methods for material conveyance and heat recovery

* Identification of instrumentation so that heat and mass balances will be performed around system components to monitor component performance for correct operation.

An essential output of the receiver design study is the development of receiver technical specifications. A partial list of factors for receiver specification are as follows:

Nominal process flow at design conditions

Receiver drawings

    Three-dimensional view of receiver cavity

    Solar central receiver calciner elevations and sections

    Structural representation of calciner

Identification of major reactor components

Cavity walls, including roof (arch), floor (hearth), and side walls

Support structure consisting of required beams, cross members, roof support, and aperture door for nighttime radiation convection loss prevention

Regenerator

Material transfer components

Cavity dimensions

Reactor section: that is, cylinder

Aperture area

Aperture shape

Reactant bed design: that is, flat bed at bottom of cavity

Total reactant bed exposed area

Optical properties of reactants and materials of construction in IR and solar bands

Particle size

Bed material conveyance: that is, screw conveyor

Regenerator type: that is, heat pipe

Total heat transfer area

Heat transport material

Receiver weight breakdown

Heat duty on receiver: that is, 25 MWth (8.53×10^7 Btu/h)

Design point receiver efficiency

Annual field performance

Monthly energy collection by process fluid

Design point field performance — spring equinox noon

Incident solar flux over aperture

Flux maps of cavity interior (incident solar flux, net IR and solar flux)

Aperture sizing energy trade-offs

Receiver radiation heat loss through aperture

Receiver convection losses through aperture

Receiver conduction loss through cavity walls

Refractory wall and regenerator equilibrium design temperatures

Reactant bed and process gas temperature profiles

Reactant conversion map

Heat recovery technical specifications

     Heat duty

     Heat recovery effectiveness.

Following the conceptual reactor design study, an experimental scale reactor should be developed for installation and demonstration at the CRTF. The objectives of this experimental reactor are to validate the conceptual design and to gain operating experience with this solar chemicals technology. The reactor should be designed with sufficient flexibility to demonstrate application to the closely analogous Portland cement manufacture although this should not be a primary technical requirement. Emphasis should be to prove solar limestone calcination technology.

The experimental unit will validate:

- Solids transport methods

- Regenerator performance

- Integration of heat recovery

- Convection loss suppression

- Operating strategies and process control

- Extent of dust problems/development of dust control techniques.

After completion of the conceptual design study for a conveyor kiln approach to limestone calcination, other conceptual design efforts should be carried out. These studies should look at alternative tower mounted reactor designs such as fluid beds, and should not be constrained to direct flux solid heating. The use of process fluids heated in a tower mounted receiver and conveyed to a ground mounted reactor such as a rotary kiln or fluid bed should also be analyzed in a conceptual design study. This will allow a thorough examination of alternatives and provide a data base of design technology that

should illuminate, if not resolve, the approach to be taken for a pilot scale reactor design study.

Assuming that the conveyor kiln approach to limestone calcination continues to show engineering feasibility and promising economics, a detailed design study for a pilot scale reactor of approximately 30 MW (1.02×10^8 Btu/h) should be carried out. This will build upon the detailed conceptual design study carried out before the experimental reactor design and demonstration, and will incorporate the lessons learned from operation of the experimental reactor at the CRTF. If the potential promise of solar batch operation is realized at an early stage in design studies, the pilot scale reactor should be configured as an integrated pilot plant or located adjacent to an existing calcination facility so that integrated operation can be demonstrated.

The detailed conceptual design study could start and be completed in 1984. The design of the experimental 1 MW (3.4×10^6 Btu/h) experimental reactor could begin in 1985 and be complete by 1987. Reactor construction could begin simultaneously in 1986 and be completed by 1988. The start-up and operation of the experimental reactor would run for four years through 1992. The 30 MW (1.02×10^6 Btu/h) pilot plant design would commence in 1990 and be completed by 1993. Pilot plant construction could begin in 1992 and be ready for start-up by 1995. The conceptual assessment of alternative reactor and plant configurations can begin in 1985 and be complete by 1987. The schedule is shown in Figure 33.

Metallic Steam Reformer Research and Development Program

There is little or no basic research that is required for near-term development of a solar powered steam-hydrocarbon reformer. Short-term development is almost exclusively in the area of engineering design studies and materials and equipment development. Design efforts should begin with hybrid reformer development and later consider the design of stand-alone reformers integrated into process operations. Periodically an economic comparison of hybrid and stand alone reformer plants should be carried out. This will indicate which concept appears to warrant more emphasis.

The development of the steam reformer can be accomplished through the execution of a commercial scale reactor design conceptual study giving

196

Task 84 85 86 87 88 89 90 91 92 93 94 95

Detailed Conceptual Design
 of Commercial Scale Lime-
 stone Calcination Reactor

Design of Experimental 1 MW
 Limestone Calcination
 Reactor

Construction of Experimental
 1 MW Limestone Calcination
 Reactor

Start-up and Operation of
 Experimental 1 MW Lime-
 stone Calcination Reactor

Design of 30 MW Limestone
 Calcination Pilot Plant

Construction of 30 MW
 Limestone Calcination
 Pilot Plant

Start-up and Operation of
 30 MW Limestone Calcin-
 ation Pilot Plant

Conceptual Assessment of
 Alternative Reactor and
 Plant Configurations

197

Figure 33. SOLAR FIRED LIMESTONE CALCINATION REACTOR TECHNOLOGY
DEVELOPMENT PROGRAM SCHEDULE

consideration to the integration of the reactor into plant operations. A reasonable application is hydrogenation. This will build upon existing design efforts by IGT and PFR. The conceptual design study will provide receiver technical specifications and will guide design of experimental reactors and design of experiments that will prove the hardware.

After completion of the conceptual design study for a hybrid solar fired steam reformer, other conceptual design efforts should be carried out. These studies should look at alternative tower mounted reactor designs such a fluid beds. The use of process fluids heated in a tower mounted receiver and conveyed to a ground mounted reactor should also be analyzed in a conceptual design study. This will allow a thorough examination of alternatives and provide a data base of design technology that should illuminate, if not resolve, the approach to be taken for a pilot scale reactor design study.

However, the primary effort should be directed toward testing and proving design and fabrication methods for tubes and refractories in an environment of repeated thermal cycling. Once these issues are resolved a small (about 1 MW to 1.5 MW [3.4×10^6 to 5.1×10^6 Btu/h]) hybrid solar steam reformer could be built. Temperature measurement and flow control hardware problems should be solved for the construction of this experimental reactor. Once some experience is gained with an operating plant, the problems of process dynamics might be addressed more readily.

Simultaneously, analytical studies should be done on the effects of flue gases on IR radiation and vice-versa, and on the optimum shape of a hybrid receiver. Flux pattern details and positioning of burners should be included in these studies. If the results are positive, an engineering and testing program should be undertaken to solve the aperture convection loss control problem. A small unit should be designed, built and tested with the aperture design at the Central Receiver Test Facility (CRTF) in Albuquerque. There is no point in testing on the scale of the CRTF unless a design for controlling ambient air influx is included. The next step is the development of reliable and economic valves and instrumentation for automatic control. Vendors should be invited to participate at an early stage.

Once there is some assurance that hardware problems such as thermal cycling of tubes and refractories, temperature and flow measurements and control, and control of ambient air influx can be solved, a detailed design of

a small plant (1 MWth to 1.5 MWth [3.4 X 10^6 to 5.1 X 10^6 Btu/h]) including a hybrid receiver should be executed. Many problems that can be overlooked in early development stages are brought out in high relief when a detailed design is attempted. The plant should be built and run in a commercial environment. Only after these steps are taken should the design and construction of a plant in the range of 30 MWth (1.0 X 10^8 Btu/h) duty be attempted. Even at that, further development of instrumentation and valves will probably be required.

The initial development efforts of metallic reformer technology may be presented in more detail as the following efforts with the objective of experimental demonstration of solar fired methane steam reformer technology for synthesis gas production.

Experimental investigations may be conducted as three tasks: 1) laboratory experimental studies, 2) analytical studies, and 3) experimental studies at 1 MWth (3.4 X 10^6 Btu/h) power level using a central receiver heat source. The first two phases will be conducted substantially in parallel. Experiments at a central receiver facility will be conducted after completion of analytical studies.

Laboratory Experimental Studies

Objective

Investigate performance of single tube reformer using an electrically heated radiant heat source.

Design basis shall be conventional reformer design practice for temperature and pressure, methane-steam ratio, catalysts and catalyst supports, tube length, tube ID, and OD.

Activities

o   Investigate steady-state performance simulating axial flux distribution typical of down fired reformer design practice

●   Investigate sensitivity of steady-state performance to axial flux variations and (if possible) to circumferential flux variations

●   Investigate transient response (investigate response to step changes in power)

●   Determine limits to reformer turndown guided by standard reformer practice with goal to achieve 10:1 turndown of methane process flow

- Develop hot standby procedures for rapid startup as insolation (power at aperture) increases

- Evaluation of potential problems and approaches to avoiding coking (carbon deposition) under transient conditions and under turndown conditions

- Development, implementation, and evaluation of operating strategies

- Evaluation of flow control components

- Evaluation of process gas temperature measurement methods

- Conduct tube cycling experiments to evaluate issues of tube, catalyst, and catalyst support longevity and failure modes and initial determination if solar steam reformer problems due to diurnal and transient cycling may be severe (that is, greater incidence of failures than experienced in conventional reformer practice).

Analytical Studies

Objective

- Support efforts of establishing technical feasibility of solar fired steam reformer

- Guide design and operation of the solar fired steam reformer

- Validate and improve analytical model through feedback from experimental studies.

Activities

The major activity involves modeling of a single tube reformer to be installed in a cavity receiver (approximately 1 MWth [3.4×10^6 Btu/h] at aperture) at a central receiver heat source.

- Conduct analytical reformer tube positioning and cavity shape studies with tube side heat transfer and kinetics to:

  — Validate model with experimental data

  — Identify steady-state component performance at design and off-design insolation/flux distribution conditions

  — Guide experimental design (that is, process flow versus apertured power)

  — Evaluate tube side pressure drop

- Evaluate burner positioning and performance for nighttime and low insolation operation

- Evaluate dynamic response to define control requirements and to begin control system development

- Size forced and induced draft fans (assuming no flue gas heat recovery for simplicity)

- Conduct tube stress analyses.

Experimental Studies at 1 MWth (3.4 X 10^6 Btu/h) Scale at CRTF (or Equivalent)[*]

Objective

Overall objective is to establish technical feasibility of continuous operation of the solar fired steam reformer. The secondary objective is to gain experience in solar reformer design and operation.

Activities

Primary activities will involve:

- Cavity design and construction

- Integration of burners to allow continuous operation under low insolation and nighttime conditions while protecting burners from damage from high solar flux

- Single tube experiments with typical reformer tube length and ID and linear configuration (straight tube).

Upon construction of the single tube in cavity receiver/reactor experiments will be conducted to determine reactor performance characteristics such as:

- Conversion versus length

- Conversion versus process flow

- Conversion versus apertured power

- Process fluid temperature versus length

- Pressure drop

- Energy balances evaluations of cavity efficiency versus apertured power and versus process flow based on efficiency as net power to process ÷

---

[*] Note that 1 MWth scale corresponds to an experiment of about 4 tubes based on linear extrapolation of IGT reformer with 62 tubes at 15 MWth (5.1 X 10^7 Btu/h) (note that IGT conceptual reformer consumes an additional approximately 20% of net power to the process as fossil fuel).

201

aperture power. Also determination of nighttime energy use to maintain system under continuous operation at maximum turndown

● Response to cloud transients, including incorporation of thermal mass versus use of lightweight refractories

● Tube and catalyst lifetime or failure experience

● Development and verification of control strategies and development and verification of standby and start-up methods.

The detailed conceptual design study could start and be completed in 1984. Thermal cycling studies and laboratory experimental studies using a radiant heat source can begin in 1984 and be completed in 1986. Analytical studies can be completed by the beginning of 1986. Experimental and analytical work will lead to the development of a single tube, hybrid receiver design. The design work can commence in 1985 and be completed in 1986. Beginning in 1986 the unit may be constructed and begin start-up and operation in 1987. The one tube unit will also be designed to look at convection suppression using the forced draft/induced draft approach with sufficient flexibility to permit integration of an air window if this technology looks promising for this application. A two year test program can be completed by the end of 1988. A 1 MW unit (3.4×10^6 Btu/h) can be designed beginning in 1988 with design completed by 1989. Reactor construction can begin in 1989 and completed by 1991. The unit can be operated for 3 years until 1994. The design of the pilot scale plant can begin in 1989 and be complete by 1991 with integrated plant construction beginning in 1990 and operation beginning in 1992. Plant design studies should evaluate the appropriate end use product: hydrogen, ammonia, or methanol. The 30 MWth (1.0×10^8 Btu/h) plant design can begin in 1991 with plant construction commencing in 1993. The plant will come on line in 1995. The schedule is shown in Figure 34.

Direct Flux Reactor Materials Research and Development

The result of this effort indicates that the technology for construction of windowed limestone reactors or transparent steam reformers is not available for reasons of high materials cost and technical uncertainty in window and tube fabrication and surviveability under conditions of high temperature, flux and chemical contamination. However, there is hope that new materials coming from the more generalized area of ceramic technology will offer potential for construction of direct flux reactors. It must be understood that the
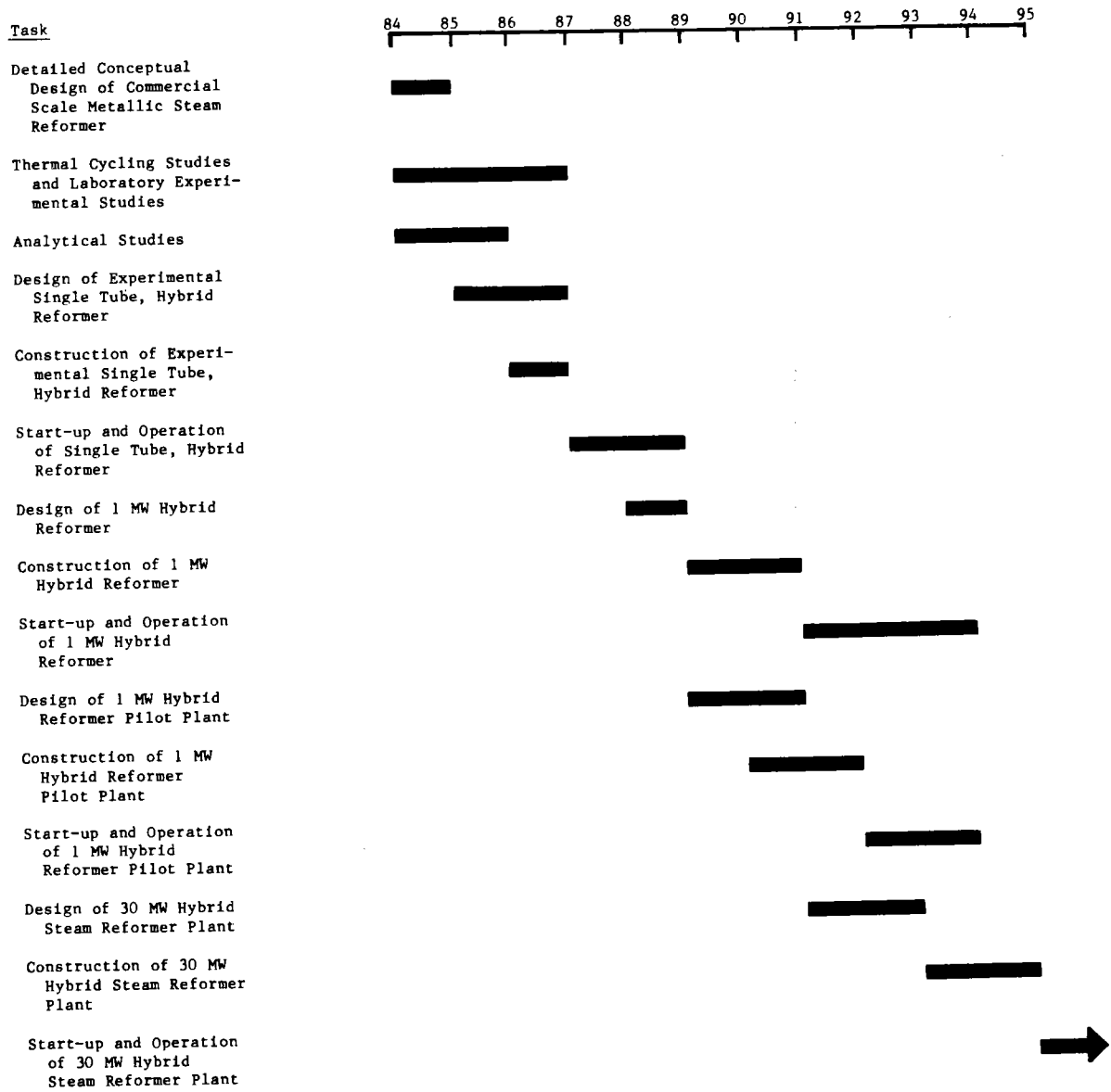
Figure 34. SOLAR FIRED METALLIC STEAM HYDROCARBON REFORMER
DEVELOPMENT PROGRAM SCHEDULE

development of direct flux reactor technology is a high risk undertaking with only moderate payoff in terms of system efficiency improvements and system cost reductions.

Better models must be developed to understand transparent material behavior in the solar environment. This environment is severe with high thermal energy fluxes, corrosion, erosion and high-temperature oxidizing and reducing atmospheres.

Raw materials must be purified to a high degree to achieve transparency. Techniques that may be explored to achieve lower costs to obtain high purity raw materials are:

— Freeze drying

— Coprecipitation

— Sol-gel

— Plasma deposition.

There are new classes of materials worthy of investigation. These include the development of transparent forms of SiC and SiN_4. The processing of present materials by the Sol-gel process can be attempted to develop the transparency and strength required for direct flux applications.

The application of new fabrication techniques such as

— Hot isostatic pressing

— Injection molding

— Sol-gel

— Microwave sintering

— Laser sintering

are worthy of investigation to produce strong, moderate-cost materials of proper dimensions for direct flux applications.

The application of developments in the design of composite materials and of developments in structural design may lead to surviveable, moderate-cost tube and window components.

Finally, target costs for windows and tubes must be updated so that R&D objectives can be refined as new materials and fabrication techniques pertinent to construction of direct flux reactors become available.

Air window technology is proven in high-temperature furnace infiltration reduction and commercial building convection suppression applications. Air windows can reduce convective losses. They also offer potential to isolate the reactor environment from the external environment. This may permit non-windowed reactors to be used with toxic reactants or with air sensitive reactants. Air windows can be coupled with optical windows as a means to keep windows clear of contaminants and for window cooling. Air windows are viewed as a much lower risk technology than optical windows. Air windows should be integrated with existing small scale receivers and tested at the ACTF or the CRTF. Calciner and steam reformer designs should be capable of utilizing air windows, either from the start of the design or incorporated as the designs are tested. Analytical models of air windows should be developed and validated. The mechanical design of air windows in terms of parasitics or performance particularly as applied to toxic or air sensitive reactions should be determined.

As tubes become available at moderate costs, they should be applied to the steam reforming reaction. The single tube cavity reactors used for metallic reformer development can be used for testing. Importantly, models of the performance of direct flux tubular designs should be developed to quantify the precise degree to which the performance improvements through direct flux utilization can be realized.

The desirability of windowed reactors is predicated on both the modest efficiency improvements possible using windowed receivers, and the high cost and uncertain performance of transparent materials in a high flux, high-temperature environment where they will be subject to erosive and chemical attack. The design of windowed reactors should be based on multifaceted windows since it is unlikely that monolithic windows can be fabricated. A low level program should be carried out to model, develop, and test one or two meter diameter windows. This will permit investigation of performance improvements attributable to the use of windowed receivers and allow observation of problems in using windows. This will lead, at moderate risk, to an assessment of R&D activities for further window development.

REFERENCES

1. PFR Engineering Systems, Inc., "Solar Central Receiver Reformer System for Ammonia Plants," Final Report DE-AC03-79SF10735. Marina Del Ray, CA, July 1980.

2. Wu, Y. C. and Wen, L. C., "Solar Receiver Performance in the Temperature Range of 300 to 1300°C," Jet Propulsion Laboratory, October 1, 1978.

3. Assessment of Fuels and Chemicals Production Using Solar Thermal Energy DOE/SF/11496-1, January 25, 1982 under Contract No. DE-AC03-81SF11496.

4. Noring, J. E. and Fletcher, E. A., "High Temperature Solar Thermochemical Processing — Hydrogen and Sulfur from Hydrogen Sulfide" Energy, 7, 651 (1982).

5. Perry, H. "The Gasification of Coal," Scientific American, Vol. 230, No. 3, 19, March (1974).

6. Gregg, D. W., Taylor, R. W., Campbell, J. H., Taylor, J. R. and Cotton, A., "Solar Gasification of Coal, Activated Carbon, Coke and Coal and Biomass Mixtures," Solar Energy, 25, 353 (1980).

7. Taylor, R. W., Berjoan, R. and Coutures, J. P., "Solar Gasification of Charcoal, Wood, and Paper." Proceedings of Annual Meeting Technical Sessions of Solar Thermal Test Facilities Users Association, SERI 9020/12, Preprint UCRL-84411, Las Cruces, New Mexico, April 15-17, 1980.

8. Stinson, S. C., "Ethylene Technology Moves to Liquid Feeds" Chemical and Engineering News, 32, May (1979).

9. Kniel, L., Winter, O. and Tsai, C., "Ethylene," Encyclopedia of Chemical Technology, Vol. 9, 407.

10 Krikorian, O. H. and Shell, P. K., "The Utilization of $ZnSO_4$ Decomposition in Thermochemical Hydrogen Cycles," Int. J. Hydrogen Energy, 7, 463 (1982).

11. Shell, P. K., Ruiz, R. and Yu, C. M., "The Thermal Decomposition of Zinc Sulfate — A Detailed Report," Lawrence Livermore National Laboratory, December 1, 1982.

12. Mol, A., "Industry Trends Indicate Need to Optimize Propylene Yield Will Grow" Oil and Gas J., 78, March 28, 1983.

13. Kunii, D. and Levenspiel, O., Fluidization Engineering. New York: John Wiley, 1969.

14. Lothar R., "Auswahlkriterien for Nichtkatalytische Gas/Feststoff-Hochtemperaturreaktoren," Chem.-Ing. Tech. 49, 786-95 (1977).

15. Dellin, T. A., "The Solar Central Receiver in Perspective." Proceedings of the 1980 Annual Meeting of the American Section of the International Solar Energy Society, Inc., June 2-6, 1980, Phoenix.

16. Fish, J. D. et al., "Solar Receiver Steam Systems," Chem. Eng. Progress, 48 (1983) January.

17. U.S. Department of the Interior, Bureau of Mines, Minerals Yearbook, 1975, Vol. 1: Metals, Minerals, and Fuels, 844. Washington, DC, 1977.

18. Krishnan, G. N. et al., "Design of an Experimental High Temperature Materials Processing System for the Solar Thermal Test Facility," Final Report for SRI International Project No. PYU 8291, prepared for Solar Energy Research Institute under Contract No. EG 77-C-01-4042 (Subcontract No. XJ-9-8017-1), Menlo Park, CA, November 1979.

19. Venkateswaran, V. and Brimacombe, J. K., "Mathematical Model of the SL/RN Direct Reduction Process," Metallurgical Trans. 8B, 387 (September) 1977.

20. Gorog, J. P., Brimacombe, J. K. and Adams, T. N., "Radiative Heat Transfer in Rotary Kilns," Metallurgical Trans. 12B, 55 (March) 1981.

21. Brimacombe, J. K. and Watkinson, A. P., "Heat Transfer in a Direct-Fired Rotary Kiln: 1. Pilot Plant and Experimentation," Metallurgical Trans. 9B, 201 (June) 1978.

22. Pearce, K. W., "A Heat Transfer Model For Rotary Kilns," J. Inst. of Fuels, 363 (December) 1973.

23. Gilbert, W., "Heat Transmission in Rotary Kilns," Cement and Cement Manufacture 5, 417 (December) 1932.

24. Ibid., 6, 79 (March) 1933.

25. Ibid., 189 (June) 1933.

26. Ibid., 262 (August) 1933.

27. Ibid., 327 (October) 1933.

28. Ibid., (December) 1933.

29. Ibid., 7, 1 (January) 1934.

30. Ibid., 123 (May) 1934.

31. Ibid., 196 (July) 1934.

32. Ibid., 295 (October) 1934.

33. Ibid., 8, 89 (April) 1935.

34. Ibid., 9, 1 (January) 1936.

35. Ibid., 27 (February) 1936.

36. England, R., "Error Estimates of Runge-Kutta Type Solutions to Systems of Ordinary Differential Equations," Comput. J., 12, 166-170 (1969).

37. Turkdogan, E. T., Olsson, R. G., Wriedt, H. A. and Darken, L. S., "Calcination of Limestone," *Trans. Soc. Min. Eng. AIME* 254, 9-12 (1973).

38. Kern, D. A., *Process Heat Transfer*, 5th Ed., 693, New York: McGraw Hill, 1950.

39. Perry, H. R. and Chilton, C. H., *Chemical Engineer's Handbook*, 5th Ed., 9-38, New York: McGraw Hill, 1973.

40. Blythe, B. M. and Sampson, R. W., "Modular Steam-Reformer Design — 2," *Oil and Gas J.*, 60, April 29, 1974.

41. Babcock & Wilcox, *Steam*, 39th Ed., 4-9.

42. Ganapathy, V., "Charts Give Quick Estimates of Heat Transfer Coefficient," *Oil and Gas J.*, 98f, December 13, 1983.

43. Ganapathy, V., "Charts Simplify Spiral Finned-Tube Calculations," *Chem. Eng.*, 117-122, April 25, 1977.

APPENDIX.   Review of High-Temperature Receiver/Reactor
            Concepts and Experiments

REVIEW AND EVALUATION OF HIGH-TEMPERATURE RECEIVER/REACTOR
CONCEPTS AND EXPERIMENTS

Introduction

This Appendix to Section I of this report presents a more detailed review and evaluation of high-temperature receiver/chemical reactor concepts and experiments which use concentrated solar radiation to drive endothermic chemical reactions. This review forms the basis for characterizing and evaluating solar receiver/reactor designs which may be suitable as direct flux solar chemical reactors. Reaction heat in a direct flux reactor can be supplied by any single or combination of sources including direct solar radiation, reflected solar radiation, or reradiant solar energy from hot surfaces within the reactor. Potential benefits of developing a direct flux reactor include smaller reactor sizes, higher heat transfer rates, and higher thermal efficiencies. The literature was reviewed and personal contacts made taking into consideration the numerous facets of direct flux solar reactor design.

Receiver/Reactor Designs

A direct flux solar reactor represents the integration of a solar receiver and a chemical reactor. Although the temperature levels of concentrated solar energy from parabolic dish collectors and central receiver heliostat fields represents a good match to many chemical reactions, control and distribution of this heat makes reactor design difficult. This is because reactor design is greatly influenced by the specific chemical reactions which are desired. The general goal of the receiver design is to maximize the utilization of solar radiation (that is, attain high thermal efficiency — maximize delivery of solar energy to the process) while providing the desired heat flux profile to the chemical reaction as consistently as possible. Frequently, the ideal receiver design does not coincide with the ideal reactor design.

For the receiver design, an externally heated or cavity configuration can be used. The cavity configuration offers potentially greater thermal performance by minimizing reradiative energy losses through the receiver aperture. Transparent vessels or a window can also be incorporated into the receiver design. Windows may be necessary to reduce heat losses by convection and/or radiation or to prevent reactants from escaping. Important criteria

used to evaluate transparent materials include, whether used in a vessel or window, high spectral transmissivity to solar radiation. Windows should have low IR transmissivity but tubes should have high IR transmissivity. This must be coupled with a relative inertness to the reactants and products as well as the thermal conditions prevailing. Depending on the type of design, window sealing and cleaning methods may also be critical.

The reactor design should take advantage of the solar radiation and efficiently process the reactants. The reactor design must also consider the scale of application, flux requirements, operating temperatures and pressure, materials handling, transient performance and diurnal cycling capability. The reactor design is further complicated by the desirability of mounting the reactor on a tower at or near the focal point of the heliostat field and orientating the reactor at such an angle as to accept the solar radiation. In order to minimize reactor costs the design should ideally be easy to fabricate, and relatively easy to control and operate.

Chemical reactors used in industry form the basis for any direct flux solar reactor design. These chemical reactors are broadly classified by the type of operation or the design features of the reactor. Reactors classified by the type of reaction can be described as batch, continuous, and semicontinuous types. Batch type reactors are typically in the shape of a tank and are principally used for small scale production. Commonly used for homogeneous reactions, the batch reactor is defined as a reactor where no reactant or products leave during the reaction process. Continuous reactions simultaneously introduce reactants and withdraw products from the reaction vessel. These reactors are frequently used in large-scale applications. Semicontinuous reactors cover the remaining reactor types where some reactants or products are continuously or intermittantly introduced or removed.

A more refined reactor classification technique is by the reactor features. These features commonly describe the operation or physical properties of the reactor. Reactor feature classification include tank, tubular, and tower reactors, as well as fixed, moving, entrained and fluidized bed reactors. Rotary kilns are a type of moving bed reactor. These reactor designs encompass the gamut of chemical reaction systems from gas-phase to solid-phase reactions. Of particular relevance to the high-temperatures available from solar energy and industrially significant reaction, are the

catalytic gas phase reactions and gas-solid reactions. For these two reaction categories packed bed (tower), fixed, moving, rotary kiln, entrained, and fluidized bed reactor designs can be used to carry out the desired reactions. The applicability of various reactor configurations for solid catalyzed gas phase reactions and gas-solid reactions is given in Table 1. The reactor configurations are also compared, in qualitative terms, as to the temperature distribution in the bed, particle size, pressure drop, heat transfer, and conversion that may be obtained in each type of reactor.

Packed bed reactors are a subset of a broad range of reactors known as tower reactors. Typically they have a vertical cylindrical shape with a large height-to-diameter ratio. Commonly employed in large scale continuous heterogenous reactions, these reactors may be configured as an empty tower, packed bed with catalysts, reactants or inert solids or trays as in the case of distillation operations. Tower reactors are used for numerous types of reactions ranging from gas phase to solids. Packed bed reactors loaded with catalyst are commonly used in large-scale industrial gas-phase reactions.

Fixed, moving, entrained, and fluidized bed reactors are frequently used for reactions involving gas-solids phases. Fixed bed reactors are typically loaded with solids or packed with catalysts and are used in gas-solid decomposition reactions. This type of reactor usually requires relatively large and uniformly sized solids and is generally unsuitable for continuous types of operations involving solids decomposition. They are more appropriate for gas phase reactions. Large axial temperature gradients are characteristic of fixed bed reactors. When proper temperature control can be maintained, the plug flow of gaseous reactants through the bed can result in nearly complete conversion. Additionally, due to the requirements for large particle sizes, pressure drop across the fixed bed reactor can be low. In high-temperature operations that are anticipated with direct flux solar radiation, fusion properties of solid phase reactants should be considered to avoid particle agglomeration.

Moving bed reactors are similar to fixed-bed reactors except that continuous operation is possible and both solids and gas movement within the reactor are more pronounced. Temperature control within the bed is somewhat more controllable in the moving bed reactor relative to the fixed bed reactor due to potential for higher gas flows and some solids circulation within the

Table 1. COMPARISON OF TYPES OF CONTACTING FOR REACTING GAS-SOLID SYSTEMS[1]

	Solid Catalyzed Gas Phase Reaction	Gas Solid Reaction	Temperature Distribution in the Bed
Packed Bed	Suitable for a large range of catalytic solids from powders to large uniformly sized packings with high surface areas. Ideal for many gas phase as well as gas-liquid phase reactions. Large-scale operation possible.	Not applicable.	Where much heat is involved large temperature gradients can occur. May be minimized by proper gas flow.
Fixed Bed	Only for very slow or nondeactivating catalyst. Serious temperature control problems limit the size of units.	Unsuited for continuous operations, while batch operations yield non-uniform product.	Where much heat is involved large temperature gradients occur.
Moving Bed	For large granular easily deactivated catalyst. Fairly large-scale operations possible.	For fairly uniform sized feed with little or no fines. Large-scale operations possible.	Temperature gradients can be controlled by proper gas flow or can be minimized with sufficiently large solid circulation.
Rotary Kiln	Not applicable.	For fairly uniform sized feed with little or no fines. Large-scale operations are possible. Suited to batch-scale operation.	Where much heat is involved large temperature gradients may occur. Temperature gradients can be controlled by proper flow of combustion products and by proper location of burners.
Fluidized Bed	For small granular powdery nonfriable rapidly deactivated catalyst. Excellent temperature control allows large-scale operations.	Can use wide size range of solids with much fines. Large-scale operations at uniform temperature possible. Excellent for batch operations, yielding a uniform product.	Temperature is almost constant throughout. This is controlled by heat exchange or by proper continuous feed and removal of solids.
Entrained Flow	Suitable only for rapid reactions.	Suitable only for rapid reactions.	Temperature gradients in direction of solids flow can be minimized by sufficient circulation of solid.

Table 1, Cont.   COMPARISON OF TYPES OF CONTACTING FOR REACTING GAS-SOLID SYSTEMS

	Particles	Pressure Drop	Heat Exchange and Transport of Heat	Conversion
Packed Bed	Catalyst solids size and packing should be uniform to minimize flow velocity gradients. Not applicable to solid reactants.	Can be very low for large catalyst materials and low gas flows. Pressure drop increases with smaller catalyst sizes and increased gas flow.	Heat exchange can be regulated somewhat with gas flow. This is often the limiting factor with scale-up.	Continuous operations and proper reactor design allow for near 100% conversions.
Fixed Bed	Fairly large and uniform. With poor temperature control these may sinter and clog the reactor.	Because of low gas velocity and large particle size, pressure drop is not a serious problem, except in low pressure systems.	Inefficient exchange, hence large exchanger surface needed. This is often the limiting factor in scale-up.	With plug flow of gas and proper temperature control (which is difficult) close to 100% of the theoretical conversion is possible.
Moving Bed	Fairly large and uniform; upper limit governed by convenient application of gas lift in circulation system, lower limit by minimum fluidizing velocity in reactor.	Intermediate between fixed and fluidized bed.	Inefficient exchange but because of high heat capacity of solids, the heat transported by circulating solids can be fairly large.	Flexible and close to ideal countercurrent and cocurrent contacting allows close to 100% of the theoretical conversion.
Rotary Kiln	Fairly large and uniform.	Because of large cross section for gas flow, gas velocities may be low so that pressure drop is low.	Heat transport is somewhat inefficient. This leads to large heat transfer areas.	Flow of gas and solid close to plug flow. Allows close to 100% of the theoretical conversion.
Fluidized Bed	Wide size distribution and much fines possible. Erosion of vessel and pipelines, attrition of particles and their entrainment can be serious.	For deep beds pressure drop is high, resulting in large power consumption.	Efficient heat exchange and large heat transport by circulating solids that heat problems are seldom limiting in scale-up.	For continuous operations, backmix flow of solids and poor performance than other reactor types. For high conversion, staging is necessary.
Entrained Flow	Same as fluidized bed. Upper size limit governed by minimum transport velocity.	Low for fine particles, but can be considerable for large particles.	Intermediate between fluidized and moving bed.	Flow of gas and solid is close to cocurrent plug flow, hence high conversion possible.

217

bed. Fairly uniform solids loading is still required for this type of reactor. Increased operating flexibility in this design allows for near perfect cocurrent or countercurrent contacting which makes almost complete conversion possible.

A subset of the moving bed reactor is the rotary kiln reactor. This reactor consists of a slightly inclined horizontally oriented tube with a large length-to-diameter ratio. It is primarily used in industrial applications for high-temperature solid decomposition reactions. The tube or shell of the reactor is of welded construction with diameters exceeding 3.1 m (10 ft) and length longer than 91.4 m (300 ft) not uncommon. Due to the typically high-temperature of operation the kiln is lined with refractory and possibly a second course of insulating brick to protect the metal walls. Feed is introduced at the upper end of the kiln and tumbles down the length of the reactor which is slowly rotating. Since the solid material is retained in the lower part of the cylinder, gas-solids contacting is less efficient than in other reactor designs. For industrial applications hot combustion gases flowing through the reactor provide reaction heat. Heat transfer to the exposed bed material is through radiation and convection from the hot gases and radiation from the kiln brickwork.

A third type of gas-solid or gas-liquid reactor is the entrained bed reactor. In this design solids or liquid are entrained with the gas stream. This type of reactor is only suitable for rapidly occurring reactions since the residence time of the reactants in the reactor is short. With sufficient circulation within the reactor temperature gradients in the direction of the gas flow can be minimized. Due to the rapid reaction rate requirements and near cocurrent plug flow of gases and solids in the reactor, high conversion rates are possible. When fine particles are involved in the reaction, the pressure drop in the entrained flow reactor can be low.

The last type of reactor discussed here utilizes the fluidized bed principle. A fluidized bed is made up of small granular or nonfriable powdery solids or catalyst which are suspended in a stream of gas. The gas velocity is maintained at a sufficient level to suspend the particles yet keep them from being entrained in the exit stream. Due to the high degree of circulation within the bed, temperature distribution within the bed can be very uniform. Thus, the fluid bed acts as a well-mixed reactor for solids

reactions (as opposed to plug-flow) A wide range of solids can be introduced into the bed for reaction. Both continuous and batch operations are practical in this reactor. The pressure drop characteristics of fluidized bed reactors are usually higher than other types of reactors. Depending on the bed depth, pressure drops can be very high. Another drawback of the fluidized bed reactor is the backmixing flow of solids and poor contacting patterns which can reduce the conversion rate of gaseous reactants.

Review of Previous Solar Receiver/Reactor Designs

Research on high-temperature receiver/reactor concepts and experiments was reviewed and categorized. Categorization is based on the reactor types as presented above. This review indicated that much of the past high-temperature receiver/reactor work does not shed new light on the problems of commercial scale direct flux reactor design. Although the primary heat transfer mechanism for both types of reactors is radiation, most of the conceptual designs or experiments were confined to small scale reactors in the 2 to 100 kW (6800 to 3.41 X 10^5 Btu/h) range. In addition, very little work has been done on commercial scale high-temperature solar receiver/reactor designs for commercially significant chemical reactions. Much of the past work has focused on thermochemical hydrogen applications and not commercially significant reactions. Exceptions to this include a steam-methane reforming reactor design by PFR Engineering Systems and calcination experiments in small-windowed rotary kiln and fluidized bed reactors that have been done in France. The remaining discussion presents a review and evaluation of past high-temperature receiver/reactor research based on reactor types.

Packed Bed Reactor Summaries for Gas Phase Reactions

A number of packed bed receiver/reactor configurations were found in the literature. All of the designs reviewed in this reactor category were for gas phase applications with the majority designed to operate at the focal point of a parabolic dish collector. The gas phase reactions included in these designs are:

$$SO_3 \rightarrow SO_2 + O_2$$
$$CO_2 + CH_4 \rightarrow 2CO + 2H_2$$
$$2NH_3 \rightarrow N_2 + 3H_2$$
$$CH_4 + H_2O \rightarrow CO + 3H_2$$
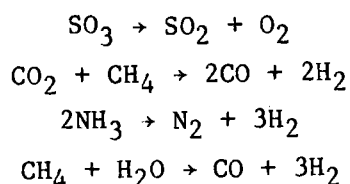
The advantage of all the packed bed reactors analyzed is that they have continuous processing capabilities. They are particularly appropriate for gas or liquid phase catalytic reactions. A problem encountered in the design of these reactors is that the direct flux illumination and/or radiation of solids nearest to the outside of the reactor can lead to nonuniform cross-sectional temperature within the packed beds due to the absorption of flux on the exposed surface of solids. The results of this temperature gradient is a variable reaction rate over the cross section of the bed. Through the uniform control of flux within or around the packed bed and the proper selection of bed width, this problem can be minimized. For packed bed reactors using parabolic dish collectors, reactor design is less complicated due to the independence of the flux profile from time dependent effects within the reactor cavity. On the other hand, packed bed reactors designed for central receiver applications are more complex in design due to the time-dependent and directionally dependent flux variations on the multiple tubes comprising the reactor. In the much larger central receiver/reactor design larger mass flows, multiple flow paths and potentially different reactant temperatures further complicate the reactor design. The remainder of this section presents the eight packed bed receiver/reactor designs reviewed in Section I.

Configuration I

Naval Research Laboratory (NRL) Sulfur Trioxide Reactor[1]

This receiver/reactor was designed to carry out the dissociation of sulfur trioxide to sulfur dioxide and oxygen at the focus of a parabolic dish reflector. It was developed by and technical analysis performed by Chubb et al. at the Naval Research Laboratory (NRL).[1] Bench or experimental testing has been done. The reaction is part of a chemical heat pipe system of transporting energy as well as several other thermochemical hydrogen cycles. The receiver/reactor is shown schematically in Figure 1.

The reactor design is comprised of spiral passages wound around a cylindrical cavity into which the concentrated sunlight is reflected. The reactor walls are opaque. The design is based on ceramic extrusion technology to form the flow passages for reactant inflow and product outflow. Ceramics have been considered preferably to metals in this work because of their resistance to sulfidation and oxidation. However, NRL has also considered metallic and transparent reactors.
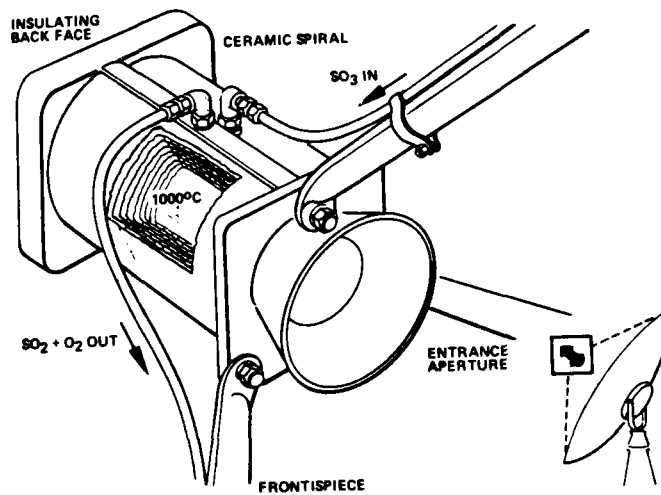
Figure 1. SULFUR TRIOXIDE DECOMPOSITION REACTOR BY NRL[1]

The reactor cavity is formed by using a toroidal ceramic body closed off front and back by insulating ceramic plates with the front plate incorporating a 0.20 m (0.66 ft) aperture. The innermost passage serves as the chemical reactor and has the catalyst deposited on the walls of the ceramic. The inner wall of the cavity is irradiated by the sunlight and the remaining outer passages serve as a heat exchanger. Thermal conduction through the ceramic permits heat exchange between inflow and outflow gas streams. These so-called "thick wall" designs, as shown in Figure 2, have been evaluated by NRL and the Rocket Research Company.[2]
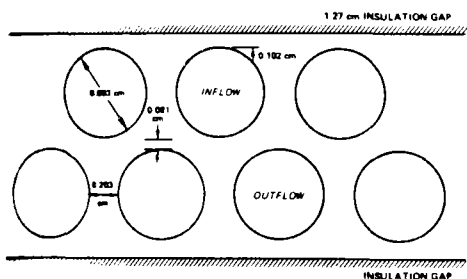
Figure 2. HEAT EXCHANGER CONFIGURATION

In this design the inflow and outflow passages are aligned along two separate rows. A high-temperature ceramic fiber insulation fills the gap separating the layers. The inside cavity has a diameter of 30.45 cm (12.0 in.) and a length of 45.7 cm (18.0 in.). Pressure drop across the reactor was estimated at 1.6% of operating input pressure.

A thin walled design was also subjected to technical evaluation. This design was based double layers of ceramic tape wound around a mandrel. No insulation was used between layers. Pressure drop was estimated at 1.2% of operating pressure.

Configuration II

Westinghouse Sulfur Trioxide Reactor[3]

This reactor concept, as shown in Figure 3, consists of a cavity receiver that can be mounted at the focus of a parabolic dish collector. The receiver cavity that Westinghouse used is formed by 20 coiled tube modules assembled

222
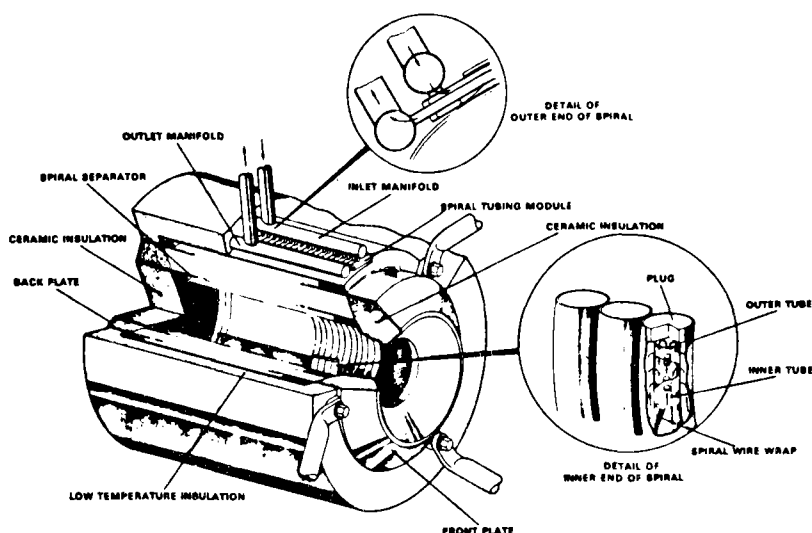
Figure 3.   WESTINGHOUSE SULFUR TRIOXIDE DECOMPOSITION REACTOR[3]

side by side to form a parallel flow circuit. The aspect ratios and aperture
sizing of the cavity may by varied to achieve the desired flux pattern on the
inner surface of the cavity to avoid hot spots and to facilitate the
reaction. As a result of the use of coils rather than the continuous passage
as used by NRL, the tubes are subject to nonuniform irradiation, with the
irradiated "front" of the tubes hotter than the nonirradiated "back" of the
tubes. This leads to variable reaction rates across diameter of tube. This
effect is somewhat reduced because of small tube diameters and because of
radiative heat transfer across the tubes.

    Each module consists of eight coils. Only the innermost coil acts as the
chemical reactor, having a wall deposited catalyst for conducting the
reaction. The remaining coils recover the sensible heat in the reaction
products to heat reactants to near reaction temperature. The incident flux in
the innermost coil provides additional sensible heat and provides the heat to
drive this endothermic reaction. The module tube uses a 9.5 mm (3/8 in.) O.D.
tube concentrically located inside a 15.9 mm (5/8 in.) O.D. outer tube. A
spacer wire on a 25.4 mm (1 in.) pitch is used to maintain concentricity and
to aid in heat transfer. Reactants enter through the annulus and exit via the
inner tube. Pressure drop was estimated at 7% of operating pressure.
Figure 4 presents the temperature profile of the reactor and fluid passing
through the reactor. Temperatures range from just under 700°C (1292°F) to
approximately 860°C (1580°F) at the reactor walls.
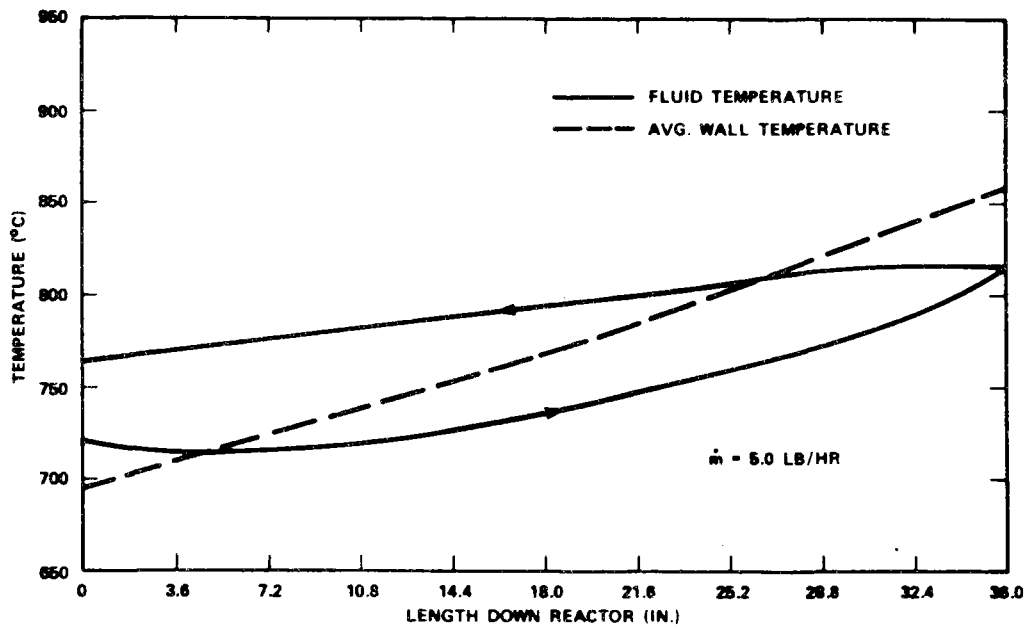
Figure 4. WESTINGHOUSE SULFUR TRIOXIDE REACTOR ZONE THERMAL PERFORMANCE

The material of construction was 316 stainless steel. For the areas of the coil where the reaction occurred and which were exposed to high-temperature products, a treatment called "Alonizing" (Alonized is a trademark of Alon, Inc.) was used. The Alonizing process diffuses aluminum into the base metal at high-temperatures to form an alumide surface layer. The inter-metallic compound formed by this process provides heat and corrosion resistance as well as strength and rigidity and also provides a suitable substrate for deposition of the platinum catalyst. However, Westinghouse experienced coil fabrication problems with the 316 SS Alonized material and they have suggested the use of a stabilized stainless steel such as 318 or 347, or a low carbon stainless steel such as LC 304 or LC 316.

Problems with SO_3 feed occurred during bench scale testing of a single tube reactor. However, testing with gaseous sulfuric acid at 670°C (1238°F) and 304 kPa (3 atm) was reasonably successful in demonstrating this design and suggests that such designs are also suitable for sulfuric acid decomposition.

Configuration III

Jet Propulsion Laboratory (JPL) Sulfur Trioxide Reactor[4]

This configuration encompasses two metallic reactors used for sulfur trioxide decomposition in an electric furnace designed to simulate a solar

heat source. Electric input was eight 750W (2560 Btu/h) electrical resistive heaters capable of producing reactor temperatures up to 1100°C (2012 °F). The first reactor was made from Kanthal A-1 tubing. Kanthal is a stainless steel with aluminum added for additional corrosion resistance. The second reactor was made from 316 stainless steel and was fabricated by JPL. The stainless steel did not receive a surface treatment such as that given to the Westinghouse reactor. Both designs include a spiral tube-in-tube heat exchanger surrounding a single turn reactor which contains the catalyst which is coated onto alumina spheres or rings. The reactants enter through the annulus and products exit through the center tube.

According to Reference 4:

> "The Kanthal reactor is fabricated entirely from welded*
> Kanthal A-1 tubing. The O.D. of the outer tube is
> 25.4 mm; that of the inner tube is 15.9 mm. The heat
> exchanger spiral has four turns. The converter is a
> circular ring of 25.4 mm O.D. tubing whose ends are mani-
> folded to the annulus and the inner tube as the end of
> the innermost turn of the heat exchanger. The configur-
> ation is similar to that shown in Figure 1. The inner
> diameter of the converter rings is 30.5 cm. Surrounding
> the converter ring is a 5 cm wide IR reflector. The
> reflector is made of thin stainless steel covered with
> white fiberglass fabric. The platinum catalyst in the
> Kanthal reactor is carried by alumina Raschig rings whose
> dimensions are 17 mm O.D. by 6 mm I.D. by 10 mm thick.
> Seventy five of these rings are tightly packed in the
> coverter with their axes alternately perpendicular and
> parallel to that of the converter tube."

High-temperature fibrous insulation was packed between adjacent turns of the heat exchanger to minimize turn-to-turn heat losses. The JPL reactor contained 5 5/8 turns and was packed with 3 mm (0.12 in.) diameter catalyst coated spheres. No IR reflector was used.

In tests with a simulated solar heat source, the Kanthal reactor performed adequately in terms of conversion of sulfur trioxide. However, the researchers expressed reservations about the value of metallic reactors in long term operation. The stainless steel reactor experienced considerable corrosion.

Configuration IV

Jet Propulsion Laboratory Sulfur Trioxide Quartz Reactor

In addition to the two metallic reactors for sulfur trioxide decomposition that were used experimentally and discussed in Reference 4, two quartz reactors were also constructed and tested.

These quartz reactors benefit from the impingement of flux directly on dark catalyst coated alumina spheres. They are described in Reference 4:

> "Quartz I reactor. The quartz reactors used in this work were fabricated by the Wm. A. Sales Co. of Wheeling, Illinois. Both quartz reactors are configured as six-turn flat spirals, tube-in-tube over the entire length. The outer tube is 25.4 mm O.D.; the inner tube is 13 mm O.D. by 10 mm I.D. The catalyst is contained by the inner tube over the length of the innermost 1 1/8 turns (the converter) of the spiral. Feedstock gas flows through the heat exchanger section through the annulus between the inner and outer tubes. At the innermost end of the spiral, the heated SO_3 enters the inner tube where it encounters the catalyst. The platinum catalyst in the Quartz I reactor is coated onto 3 mm diameter (nominal) alumina spheres. These spheres are tightly packed throughout the volume of the 10 mm I.D. inner tube over the length of the converter. Swagelok fittings with Teflon ferrules are used to connect the quartz reactors to the stainless steel tubing of the test loop.
>
> Quartz II reactor. The Quartz II reactor is identical with the Quartz I reactor except that the platinum catalyst is coated onto 7-8 mm diameter alumina spheres instead of 3 mm spheres. The Quartz II converter contains 194 of these catalyst beads."

In practice, only the inner turn of the reactor, which comprises the areas where the reaction occurs, needs to be made of quartz. It is only in this turn where direct flux irradiation is of value in conducting the reaction. The term "direct flux" used in this connection means that packing materials were directly heated and they transferred heat to reactants by convection. The heat exchanger may be made of ceramic or metal. However, for these experimental reactors, it was easier to fabricate the whole reactor out of a single material. In addition, reactor designers had reservations about joining quartz to other materials in parts of the reactor that were at elevated temperatures, particularly in view of the toxic nature of possible leaks of sulfur trioxide. Such problems must be solved for commercial direct

226

flux reactors. As a result, glass to metal seals were placed outside the hot zone of the reactor where reactants and products were relatively cool.

The quartz reactors performed extremely well during tests. The quartz stood up to reactants and products, and near equilibrium conversions were obtained at 900°C (1652°F). Because of concerns with safety and potential pressure limitations, these reactors were run at lower pressure (101 kPa vs 304 kPa [1 atm vs 3 atm]) than the metallic designs. The authors expressed confidence that a successful, practical reactor could be developed using transparent, direct flux components.

Configuration V

Methane-Steam Reforming Reactor Design

Another metallic reactor was developed and tested at the WSSF.[5] This reactor is a derivative of the metallic reactors used for sulfur trioxide decomposition and were described as "Configuration III." The reactor is shown schematically in Figure 5. This reactor is configured to conduct the methane reforming reaction:

$$CO_2 + CH_4 \xrightarrow{\text{catalyst}} 2CO + 2H_2$$
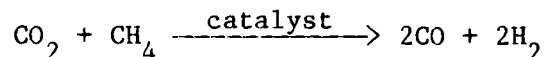
This reaction is part of a chemical heat pipe means of transporting solar energy.
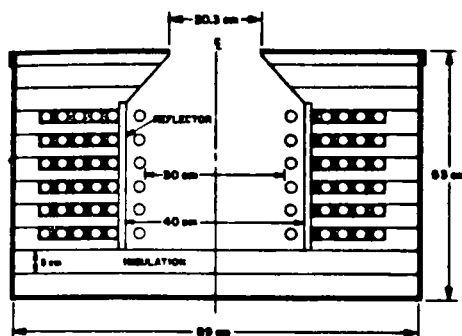
Figure 5. METHANE REFORMING REACTOR

The reactor uses six elements in parallel. Each element is constructed of four turns of tube-in-tube construction operating as a counterflow heat exchanger. The innermost turn is heated by the solar energy and consists of a single tube loaded with ruthenium catalyst coated metal saddles. Material of

227

construction is 316 stainless steel. To prevent turn to turn heat transfer Fiberfrax insulation is packed between turns. Front and back faces of the receiver use ceramic fiberboard insulation. The reactor is enclosed in an aluminum housing. In this reactor configuration, reactor elements are spaced apart from each other and also spaced away from the cavity wall. This is in contrast to the Westinghouse design with reactor elements placed immediately adjacent to one another. In this case, the thinking is to allow the flux to irradiate reactor walls as well as the tubes, and to thereby permit more uniform heating of reactor tubes by reflected and reradiated flux. This reduces stress on the tubes and by providing more nearly isothermal conditions around tube perimeter permits a uniform reaction rate at any given cross section within the tube. Apparently this design issue has not been examined very intensively with different reactor developers exploring either configurations with reactor elements adjacent or with reactor elements spaced apart from each other and apart from the walls of the cavity.

In tests at the WSSF in 1981 the reactor operated quite well. At a mass flow rate of gas of 12 g/s (1.6 lb/min), pressure of 405 kPa (4 atm) absolute, and receiver elements operating from 625° to 1025°C (1157° to 1877°F), a reactor efficiency of 62% was obtained for a power input of 26 kW (88,738 Btu/h). The nonuniform element operating temperatures result from nonuniform flux distribution within the cavity. Modifications in cavity geometry and positioning of elements is viewed as a method to obtain a more nearly uniform reaction temperature. A temperature of 900°C (1652°F) is the preferred reactor operating temperature.

Configuration VI

Ammonia Dissociation Reactor Design

This reactor[6] was developed for the dissociation of ammonia according to the catalytic reaction:

$$2NH_3 \longrightarrow N_2 + 3H_2$$
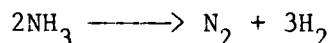
The reaction is envisioned as part of a chemical heat pipe means of transporting thermal energy. The design is purely conceptual and is shown in Figure 6.

The design is a cavity type receiver configured to accept an input of 10 kWth (34,130 Btu/h) with a maximum material temperature of 700°C (1292°F)
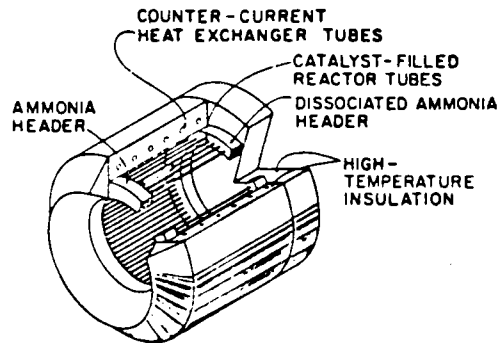
Figure 6.   AMMONIA DISSOCIATION REACTOR

and 650°C (1202°F) reaction product exit temperature. Operating pressure of
this packed bed reactor is 30 MPa (4350 psi). Such high operating pressures
preclude the ammonia dissociation reaction as a candidate reaction because the
limited strength of transparent materials create a requirement of excessive
wall thickness to contain the reaction. The cavity design is windowless and
uses Inconel 617 alloy to contain the reaction. As in the previous
configurations a cavity design was selected for the high-temperature reaction
because it permits relatively large heat transfer surface areas while
accepting high fluxes at the aperture.

A number of configurations including both helical tubes and parallel
straight tubes were evaluated to provide adequate residence time, minimal
pressure drop, and high heat transfer rates. A design using eight manifolded
parallel coils was found to produce moderate heat transfer coefficients, and a
pressure drop of 0.2% of system operating pressure. The design used was a
30.5 cm (12 in.) cavity diameter with a tube I.D. of 6.35 mm (0.25 in.) and a
cavity length of 20.3 cm (8 in.). No spacing between tubes was provided. A
single helical tube reactor was also evaluated with a coil length of 15.2 m
(50 ft). With cavity dimensions of 30.5 cm (12 in.) diameter, and a length of
22.9 (9 in.) with no spacing between tubes, pressure drop was 12% of system
operating pressure, but very high heat transfer rates were obtained. High
heat transfer rates minimized the necessity for high wall temperatures to
transport heat to reactants: this minimizes heat loss from the reactor while
reducing stresses on the tubes.

The helical coil designs were rejected from further consideration because the experimental nature of Lenz's work required access to tubes for catalyst removal which would be facilitated by a reactor consisting of parallel straight tube along the walls of the reactor as in Figure 6. It should be emphasized however that the multiple helical tube design appears desirable from a performance standpoint because of low convective film temperature differences and lower stress values at the reactor tube to header interface. The straight tube design concept uses forty-three 6.22 mm (0.245 in.) I.D. Inconel 617 tubes with a wall thickness of 1.65 mm (0.065 in.). Tube length and cavity diameter are 30.5 cm (12 in.), and tubes are spaced 22.2 mm (0.875 in.) on center. The 12.7 mm (0.5 in.) spacing between the tubes permits some of the incident flux to be reflected and reradiated to the back of the tubes which should reduce circumferential heat flux variation on the tubes thus reducing material operating temperatures and stresses. Lenz notes that use of fewer, wider spaced tubes reduces stresses in the ligaments between tubes in the manifold plus access for fabricating tube to manifold welds is facilitated. While this design has a very low pressure drop of only 0.0017% of operating pressure, significantly higher convective film temperature differences result in higher reactor tube material operating temperatures.

The reactor is insulated by ceramic fiber insulation contained between two light gauge Inconel cans. A 5.1 cm (2 in.) thickness of high density insulating material is used at the top with an additional 10.2 cm (4 in.) of fibrous insulation. Conduction losses are estimated at 6% of the 10 kWth (34,130 Btu/h) input power.

The principal design problems relate to nonuniform flux illumination on reactor elements and uncertainties in estimates of heat and mass transfer rates. Nonuniform flux illumination may lead to nonuniform temperature along the tube and corresponding variations in reaction rates as reactants pass down the tube.

Configuration VII

Williams Ammonia Dissociation Reactor[7]

Williams has also developed a reactor concept for ammonia dissociation to interface with a 10 kWth (34,140 Btu/h) parabolic dish reflector. Because the

conceptual design effort was a look at potential process economics rather than an experimental demonstration, a helical coil design was adopted, and is shown in Figure 7.

The design configuration was determined by modeling the roles in determining reactor performance of the flux distribution profile within the cavity, reaction thermodynamics and kinetics, and heat transfer. The conceptual reactor employs a cavity configuration to minimize thermal losses. The reactor is designed to operate with a wall temperature of 750°C (1382°F). With an ammonia flow rate of 2.2 g/s (0.29 lb/min), a conversion of 0.85, and an operating pressure of 20 MPa (2900 psi), a cavity with an 8 cm (3.2 in.) aperture would operate at an efficiency of 90%. Pressure drop is calculated as 10% of operating pressure. The process temperature profile is shown in Figure 8.

The design uses a single helical coil. A significant innovation is the shaping of the coil to match the incident flux profiles to the needs of the reaction. In general, one desires to maintain the highest uniform temperature along the length of the coil. Results of modeling efforts indicate that shaping the coil can reasonably meet this requirement. Mass flow distribution and control may also be used. In contrast to the previous ammonia dissociation reactor configuration, this reactor design has the tubes adjacent to each other. The impact of nonuniform illumination of the tubes is explicitly considered in the design.

Configuration VIII

PFR Engineering Systems Methane-Steam Reformer Design

The objective of the PFR conceptual design was to study the feasibility of retrofitting a 34.5 MW (1.18 X 10^8 Btu/h) (at aperture plane) receiver/reactor in parallel to a conventional methane-steam reformer at an existing ammonia plant. The study included a detailed look at the reformer design and involved extensive cavity, heat transfer and kinetic modeling of the reactor. The design considered trade-offs in such areas as aperture sizing, insulation thickness and weight, tube materials and wall thicknesses as well as control methods.

The design developed was for a cavity receiver with a single elliptical aperture. The basic system configuration consists of the solar reformer
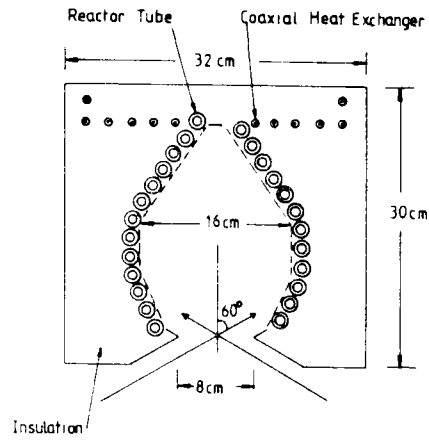
Figure 7. WILLIAMS' AMMONIA DISSOCIATION REACTOR[7]
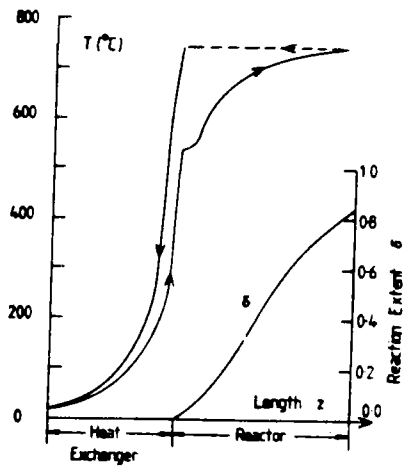
Figure 8. AMMONIA DISSOCIATION REACTOR
PROCESS TEMPERATURE PROFILE

operating in parallel to a fossil reformer. The process feed flow (steam and natural gas) is split into two parallel streams, one flowing to the solar reformer and the other to the existing fossil reformer. Both reformers preheat the process flow to reaction temperatures and the process flow is directed to the catalyst filled reaction tubes. The solar reformer contains solar heated preheating and chemical reaction sections. The existing fossil reformer is fired continuously during operation of the solar reformer. As the solar reformer assumes the duty requirements, the firing of the fossil reforming is reduced. This constitutes the savings that the solar retrofit provides.

The functional requirements of providing preheating and reforming energy was accomplished by a design very similar to fossil fired reformer design. A prime design condition met by the receiver configuration is maintenance of tube temperature uniformity because temperature conditions in the reformer are at the upper limit of metallurgical applications. Reformer design characteristics are:

o   Cavity receiver

o   Centrally located rows of tubes

o   No direct solar irradiation of metallic tubes

o   Tubes absorb reflected and reradiated energy from cavity walls

o   Uniform heat flux distribution for all tubes with heat flux levels
     comparable to fossil reformers

o   Refractory walls capable of heat storage

o   Fossil auxiliary burners to maintain night standby temperatures.

The design developed, as shown in Figure 9, was for a cavity receiver with a single elliptical aperture. The receiver/reactor is an octagonal shape with metallic reaction tubes located in the middle. A shock wall positioned in the longitudinal axis of the receiver/reactor and recessed from the aperture plane protects the tubes from direct solar radiation. The tubes are heated by solar and thermal radiation reflected and reradiated from the cavity interior surfaces. The shape and size of the walls and aperture provide uniform heat flux to all the tubes and minimal variations in circumferential flux distribution around the tubes. Reaction tubes are arranged eight panels
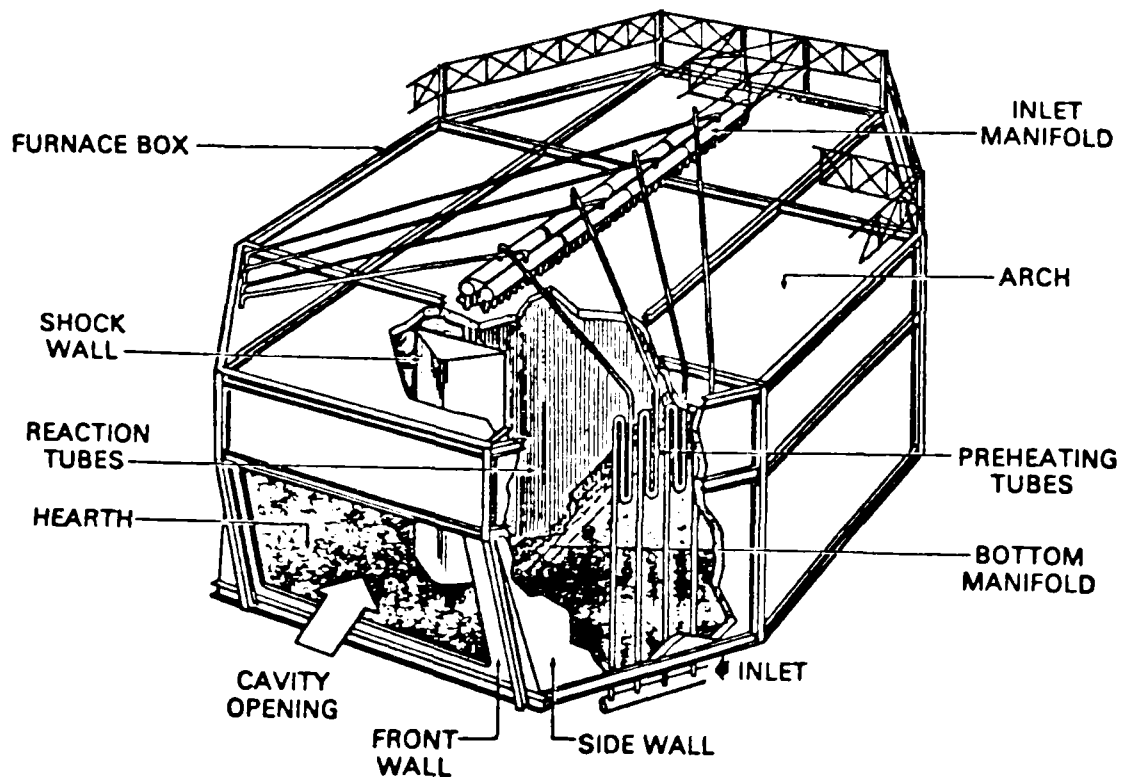
Figure 9.   THREE-DIMENSIONAL VIEW OF THE PFR CAVITY

234

placed in two rows along the longitudinal axis of the receiver. Flow to each panel is controlled by a valve upstream of the preheat coils. The two row design was selected to limit receiver depth. The pitch ratio was a compromise between the desire for uniform circumferential heat flux distribution around each tube and receiver depth. A conceptual design of the receiver/reactor piping system is presented in Figure 10. Part of the solar energy concentrated at the plane of the aperture directly penetrates the reactor cavity, striking portions of the inner reactor walls with the remainder striking the shock wall. The energy directly entering the cavity is reflected, absorbed and reradiated to all surfaces within the reactor. The optimal shape of the cavity was calculated to control the energy distribution to the reaction tube surfaces. Several shapes were investigated in terms of heat flux, distribution and receiver heat loss. The octagonal shape proved to be an optimal configuration. Figure 11 presents the equilibrium temperatures of wall segments in the reactor. Peak incident flux at the reactor walls is 113 kW/m^2 (35,840 Btu/h-ft^2) and peak temperature is 1043°C (1909°F). Figure 12 presents the net heat flux and temperature profile along the central reactor tubes behind the shock wall. The peak absorbed flux at the reactor tubes is 99.66 kW/m^2 (31,610 Btu/h-ft^2) with the maximum local temperature being 862°C (1584°F). The peak incident flux on the shock wall is 808 kW/m^2 (2.56 E05) with a peak temperature of 1260°C (2300°F).

Tube and manifold material selection for this design were based on conventional methane-steam reformer materials. The design basis included a maximum wall temperature of 871°C (1600°F) and a working pressure of 2.76 MPa (400 psig). Material selection criteria included cost, weldability, fabricability; and good stress, creep, and rupture characteristics. In view of the thermal cycling inherent in solar operations, particular emphasis was paid to stress, creep, and rupture characteristics. The material also had to have a high chrome and nickel composition which has proven to be resistant to oxidation, carbonization, and embrittlement which have posed problems in conventional steam reformers in the past. The results indicated that Manaurite 36X and Manaurite 900 were acceptable materials for the tube and manifolds, respectively. Tube life was estimated to be about 5 years which is typical for conventional methane-steam reforming reactors.
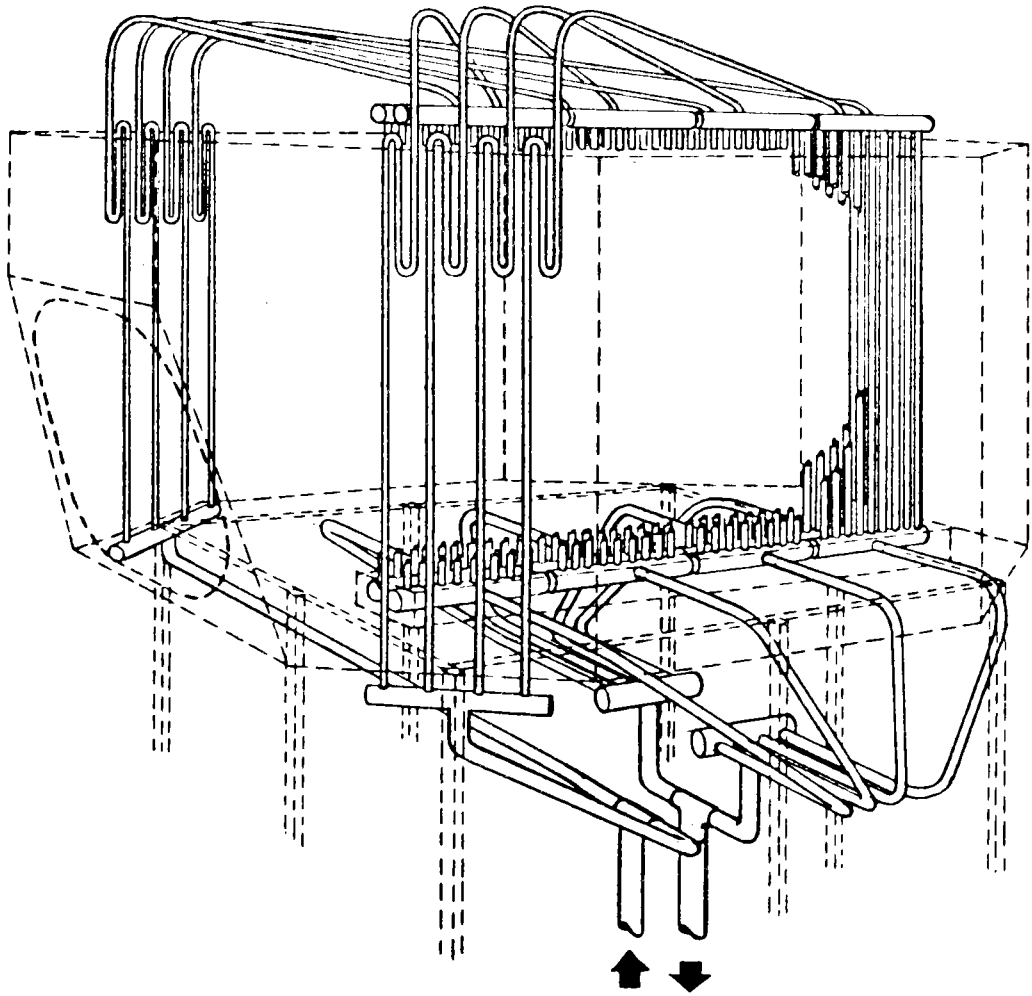
Figure 10. CONCEPTUAL DESIGN OF PFR RECEIVER PIPING SYSTEM

SOLAR NOON

MARCH 21

ARCH

1006 1006

987 992 992 987
940 984 984 940
976 946 946 976
999 955 955 999
1007 957 957 1007
1021 963 963 1021
1021 977 977 1021

WEST SIDE WALL

EAST SIDE WALL

993 Preheat coil location 1000 1012 1014 1043 1024 1034 989 989 1034 1024 1043 1014 1012 1000 Preheat coil location 993
984 976 970 969 996 996 1007 981 981 1007 996 996 969 970 976 984
968 945 943 944 941 941 953 956 956 953 941 941 944 943 945 968

BACK (SOUTH) WALL

963 958 958 963

958 955 955 958

HEARTH

955 954 954 955

990 990

Figure 11.   REFRACTORY WALLS EQUILIBRIUM TEMPERATURES
(°C) OF PFR REACTOR DESIGN
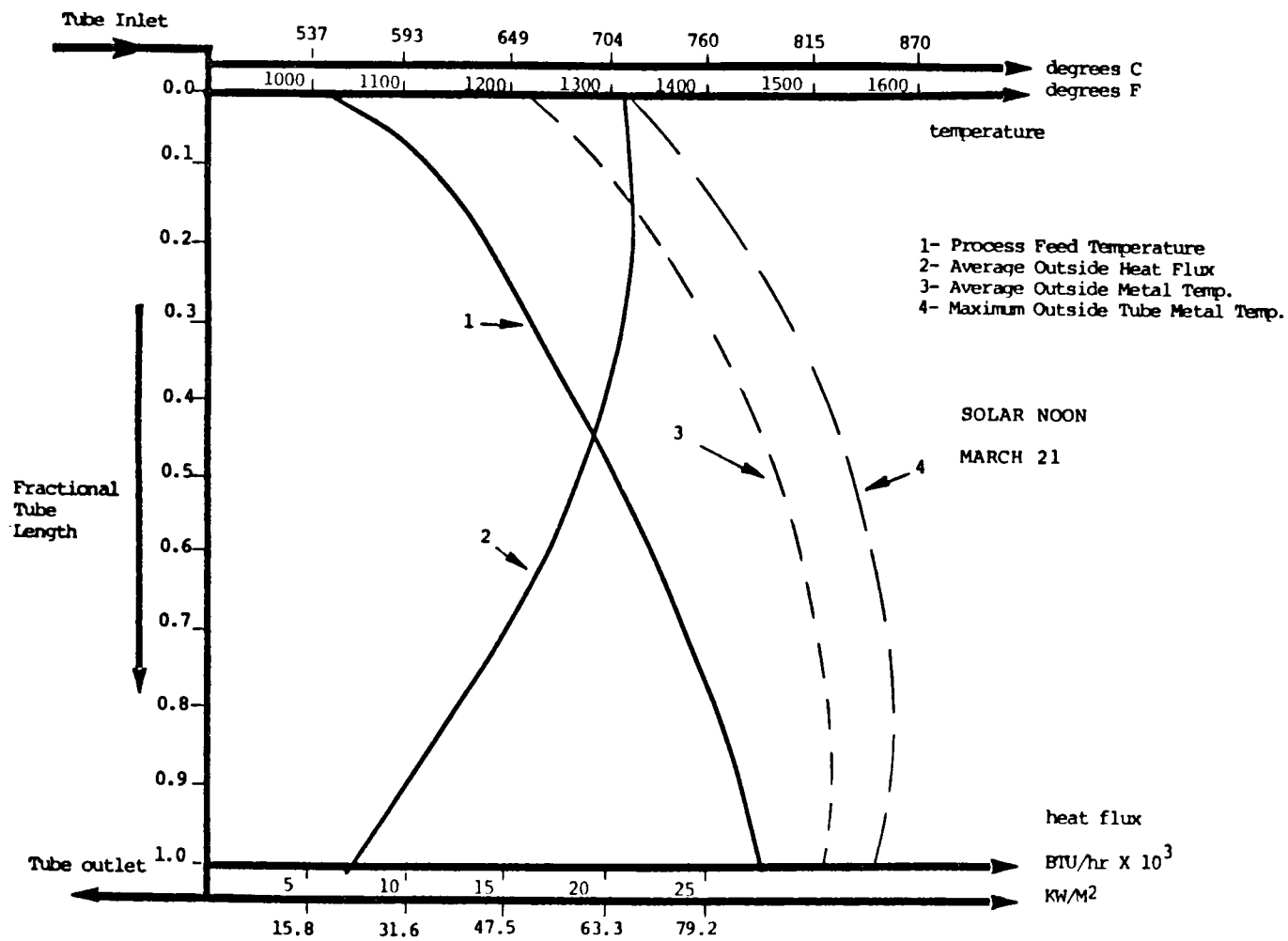
Figure 12. PFR SOLAR STEAM REFORMER NET HEAT FLUX, PROCESS GAS, AND
TEMPERATURE PROFILES ALONG CENTRAL REACTOR TUBES

Another important issue addressed in the PFR conceptual design study was reactor performance during transients. To maintain reactor performance, a thermal storage technique was desirable. A compromise of the thermal storage weight on the reactor tower and the amount of storage was made. Although a lightweight insulating refractory material such as Kaowool (product of Babcock and Wilcox) had excellent properties in respect to solar exposure conditions, thermal storage capabilities to maintain process flow were less than one minute when the material was used to line the cavity walls. Thermal storage time was increased to allow approximately 11 minutes of process flow before shutdown by using a combination of heavy refractory brick and castable Purotab N (product of Kaiser Refractories) on the cavity walls. This increased reactor performance but also increased the cost of the reactor and support tower by increasing reactor weight.

Packed Bed Reactor Review Summary

Tables 2 through 4 present a summary of the eight packed bed receiver/ reactor experiments and conceptual designs which were reviewed in this section. Table 2 presents a summary of the four gas phase sulfur trioxide decomposition reviews. For this reaction only small scale, parabolic dish mounted, cavity receiver/reactors were proposed. Design scales ranged from 6 to 25 kWth (20,480 to 85,325 Btu/h). Materials of construction included ceramics, high performance steels and a transparent quartz reactor. For the sulfur trioxide reaction operating temperatures were 900°C (1652°F) and pressures ranges from 152 to 304 kPa (22 to 44.1 psig).

Tables 3 and 4 present the summary of findings for two ammonia dissociation studies and two methane reforming studies; one using carbon dioxide and the other using steam. Both ammonia dissociation conceptual design studies were for cavity type receiver/reactors for parabolic dish applications operating at 650° to 700°C (1202° to 1292°F) at pressure levels of 20 to 30 MPa (2900 to 4350 psig). Design scales were in the range of 10 to 12.5 kWth (34,130 to 42,660 Btu/h). Both designs used Inconel 617 as the reactor material of construction. For the methane reforming reactions presented in Table 4 one study involved the construction of a small scale 15 kWth (51,200 Btu/h) experimental proof of principle reactor for the carbon dioxide/methane reforming reaction. This experimental receiver/reactor was designed for parabolic dish applications and uses a cavity design

239

Table 2. REACTOR TYPE: PACKED BED/GAS PHASE CATALYTIC
(Sulfur Trioxide Decomposition)

Reaction	SO_3 Decomposition	SO_3 Decomposition	SO_3 Decomposition	SO_3 Decomposition
Researcher	Chubb/Naval Research Laboratory	Westinghouse	New Mexico State University/NRL/JPL	NMSU/NRL
Reference Number	1	3	4	4
Scope of Effort	Conceptual Design	Conceptual	Experimental	Experimental
Objective	Outline of Technical Features of Concept	Proof of Principle	Proof of Principle	Proof of Principle
Design Scale	25 kWth (85,300 Btu/h)	12.5 kWth (42,700 Btu/h)	6 kWth (20,500 Btu/h) (Elec. Resistance Heat)	6 kWth (20,500 Btu/h)
Scale of Intended Application	Parabolic Dish Heat Source	Parabolic Dish Heat Source	Parabolic Dish Heat Source	Parabolic Dish Heat Source
Flux Coupling Method	Indirect/Opaque Heat Transfer Surfaces	Indirect/Opaque Heat Transfer Surfaces	Indirect/Opaque Heat Transfer Surfaces	Transparent Heat Transfer Surfaces
Material of Construction	Ceramic	Alonized 316 Stainless Steel	Kanthal A-1/316 Stainless Steel	Quartz
Configuration	Cavity	Cavity	Cavity	Cavity
Windowed Aperture	No	No	No	No
Schematic Figure Number	1	3	Similar to 1	Similar to 1
Principal Dimensions:				
Aperture Diameter	0.20 m (0.66 ft)		Not Applicable	Not Applicable
Cavity Diameter	30.45 cm (11.99 in.)	25.4 cm (10 in.)	30.5 cm (12.0 in.)	30.5 cm (12.0 in.)
Cavity Length	45.7 cm (18.0 in.)	31.8 cm (12.5 in.)	102 cm (3.35 ft)	152.4 cm (5.0 ft)
Thermal Efficiency	93% (Calculated)	64% (Assumed)	Not Applicable to Laboratory Model	Not Applicable to Laboratory Model
Flux Capability:				
Basis	Not Available	Assumed	Not Applicable	Not Applicable
At Aperture		Not Available	Not Applicable	Not Applicable
In Reactor		Uniform Flux Assumed	Not Applicable	Not Applicable
Temperature of Operation	900°C (1652°F)	900°C (1652°F)	900°C (1652°F)	900°C (1652°F)
Process Fluid Temperature Profile	Not Available	Figure No. 4	Not Available	Not Available
Refractory Temperature	Not Applicable	Not Applicable	Not Applicable	Not Applicable
Window Temperature	Not Applicable	Not Applicable	Not Applicable	Not Applicable
Operating Pressure	304 kPa (44.1 psi)	304 kPa (44.1 psi)	304 kPa (44.1 psi)	152 kPa (22 psi)
Pressure Drop ($\Delta P/P$, %)	1.6 (Calculated)	7 (Calculated)	13 (Measured)	36 (Measured)
Evaluation	Conceptual Design Only.	Single tube lab experiment successful. No test of conceptual design.	Adequate conversion. Stainless Steel corrosion problems.	Concept proved. Technical feasibility not established.

Table 3. REACTOR TYPE: PACKED BED/GAS PHASE CATALYTIC
(Ammonia Dissociation)

Reaction	Ammonia Dissociation	Ammonia Dissociation
Researcher	Lenz/CSU	Williams
Reference Number	6	7
Scope of Effort	Proof of Concept	Proof of Concept
Objective	Conceptual Design	Conceptual Design
Design Scale	10 kWth (34,100 Btu/h)	12.5 kWth (42,700 Btu/h)
Scale of Intended Application	Parabolic Dish Heat Source	Parabolic Dish Heat Source
Flux Coupling Method	Indirect/Opaque Heat Transfer Surfaces	Indirect/Opaque Heat Transfer Surfaces
Material of Construction	Inconel 617	Inconel 617
Configuration	Cavity	Cavity
Windowed Aperture	No	No
Schematic Figure Number	6	7
Principal Dimensions:		
Aperture Diameter	12.5 cm (4.92 in.)	8 cm (3.15 in.)
Cavity Diameter	30.5 cm (12 in.)	16 cm Maximum (6.30 in.)
Cavity Length	20.3 cm (8 in.)	30 cm (11.81 in.)
Thermal Efficiency	Not Available	90% Calculated
Flux Capability:		
Basis		
At Aperture	Not Available	Not Available
In Reactor	Not Available	8.0 w/cm^2 Average (25,400 Btu/h-ft^2)
Temperature of Operation	650°C (1202°F) Product Exit Temperature	Wall Temperature 750°C (1382°F)
Process Fluid Temperature Profile	Not Available	Figure No. 7
Refractory Temperature	Not Available	Not Applicable
Window Temperature	Not Applicable	Not Applicable
Operating Pressure	29.99 MPa (4350 psi)	19.99 MPa (2900 psi)
Pressure Drop ($\Delta P/P$, %)	0.2	10
Evaluation	Conceptual Design Only. Explored a number of tube configurations.	Conceptual Design Only

Table 4.   REACTOR TYPE: PACKED BED/GAS PHASE CATALYTIC
(Methane Reforming)

Reaction	Carbon Dioxide/Methane Reforming	Steam Reforming of Methane
Researcher	NRL	PFR
Reference Number	5	1
Scope of Effort	Experimental	Conceptual
Objective	Proof of Principle	Technical Feasibility Study
Design Scale	15 kWth (51,200 Btu/h)	34.5 MWth (1.18 X 10^8 Btu/h) at Aperture
Scale of Intended Application	Parabolic Dish Heat Source	Same as Design Scale
Flux Coupling Method	Indirect/Opaque Heat Transfer Surfaces	Indirect/Opaque Heat Transfer Surfaces
Material of Construction	316 Stainless Steel	Manaurite 36X Nickel Alloy
Configuration	Cavity	Cavity
Windowed Aperture	No	No
Schematic Figure Number	5	5
Principal Dimensions:		
Aperture Diameter	20.3 cm (7.99 in.)	33 m^2 (355 ft^2) (Elliptical)
Cavity Diameter	30 cm (11.8 in.)	Octagonal Shape
Cavity Length	Approximately 50 cm (19.7 in.)	Tubes are 12 m (39.4 ft) Heated Lengths; 10.16 cm (4.0 in.) ID; 11.8 cm (4.65 in.) OD
Thermal Efficiency	62%	78.2%
Flux Capability:		
Basis		Calculated
At Aperture	Not Available	1.23 MW/m^2 (3.90 X 10^5 Btu/h-ft^2) Average
In Reactor	Not Available	Pk Tube Flux 99.66 kW/m^2 (3.16 X 10^4 Btu/h-ft^2) Pk Wall Flux 113 kW/m^2 (3.58 X 10^4 Btu/h-ft^2) 80 kW/m^2 Avg. Tube Flux (2.54 X 10^4 Btu/h-ft^2) (ID Basis) - Figure 9
Temperature of Operation	900°C (1652°F) (Range 625°C to 1025°C, 1157°F to 1877°F)	538°C (1000°F) Inlet/790°C (1454°F) Outlet
Process Fluid Temperature Profile	Not Available	Figure 9
Refractory Temperature	Not Available	Figure 10
Window Temperature	Not Applicable	Not Applicable
Operating Pressure	405 kPa (58.8 psi)	2.61 MPa (379 psi) (Inlet)
Pressure Drop ($\Delta P/P$, %)	Not Available	8.31
Evaluation	Concept proved. Technical feasibility not established.	Technical feasibility of of conceptual design established.

The primary problem preventing continuous operation of the reactor was the buildup and fusion of ash in the focal zone. The ash buildup prevented effective feeding of coal and blocked direct flux input. A practical reactor for coal and other materials producing ash or other solid products must provide a means to remove reaction products.

Yudow Cadmium Oxide Fixed Bed Reactor

Figure 14 is a cross-section of the cadmium oxide reactor developed by Yudow at the Institute of Gas Technology.[9] This reactor is strictly a batch reactor for direct flux irradiation of cadmium oxide at temperatures up to 1500°C (2732°F). It was designed for use at WSSF. The reactant-bed design that was adopted consisted of a set of "shelves" onto which the CdO was loaded. The shelves were made from ceramic tubes slit in half, lengthwise, to form a trough or channel. The channels were supported in a vertical array and separated from each other by a small gap to allow a carrier gas to sweep the O_2 and Cd vapor away from the reaction zone. (See Figure 15.) Each channel was tipped forward toward the concentrated sunlight. The channels were made of zirconium oxide stabilized with 3% magnesium oxide, a material chosen for its superior resistance to thermal shock. This property was necessary because, as the CdO disappeared, the channels themselves would have to bear the full brunt of the solar flux.
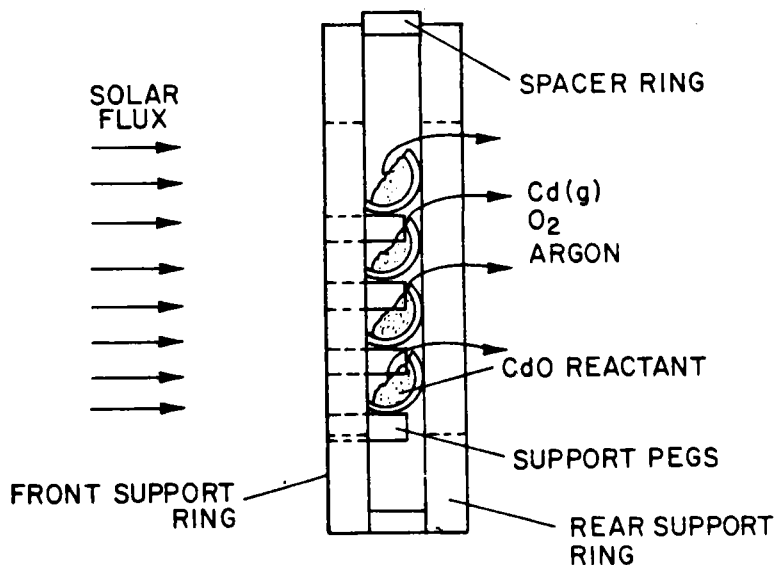
Figure 15. SIDE VIEW OF REACTANT BED AND SUPPORTS

243

configuration. The reactor was constructed of 316 stainless steel and operated at 625° to 1025°C (1157° to 1877°F) and at 405 kPa (58.8 psig). The second methane-steam reforming design reviewed was of a conceptual technical feasibility nature. The design scale was 34.5 MWth (1.18 X 10^8 Btu/h) for use with a central receiver/heliostat field. Materials of construction were envisioned to be Manaurite 36X nickel alloy operating at up to 790°C (1454°F) and 2.61 MPa (379 psig) pressures.

The distribution and utilization of the flux is critical in all the designs reviewed. All conceptual designs appear capable of accepting up to 2000 kW/m^2 (6.34 E05 Btu/h-ft^2) flux rates at the aperture of the reactor. However, proper cavity design was of utmost importance to provide large heat transfer areas that reduced local flux levels in order to match conductive and convective heat transfer rates to the incident radiant heat flux. For instance, typical steam reformer flux levels average 60 kW/m^2 (19000 Btu/h-ft^2).

Control of flux rates is not only important from the standpoint of controlling reaction rates, but also from the standpoint of material compatibility. Materials used in the designs evaluated include transparent quartz, high strength steel alloys and ceramic materials.

The transparent quartz laboratory reactor for sulfur trioxide decomposition has successfully operated at temperatures up to 900°C (1652°F). Stainless steel and Kanthal sulfur trioxide reactors did not perform well at 900°C (1652°F) due to corrosive attack. Quartz appears to be an appropriate material for sulfur trioxide decomposition. Based on tests using the concentrated flux at the ACTF, Georgia Institute of Technology (GIT) researchers have observed, as to be expected, serious devitrification of fused quartz after 12 to 15 hours at temperatures of 1000° to 1200°C (1832° to 2192°F). GIT research has suggested possible methods to protect quartz. These methods include operation only in reducing atmospheres and the avoidance of contact with water vapor. This may limit the use of quartz as either a tube or window material should reactor applications involve window or tube temperature conditions above 1000°C (1832°F).

Another limitation of quartz relative to metallic construction materials is its lack of strength. Quartz is not as strong a material as most high-temperature metals and a tubular packed bed reactor may require moderately thick walls in order to operate under pressure. The equation:

$$t = \frac{P \cdot d}{2(S-0.6P)}$$

may be used to estimate wall thickness, where:

t = minimum wall thickness, inches

P = operating pressure, psi

S = tensile strength of quartz, 1000 psi at room temperature

d = internal diameter of tube.

Wall thicknesses are summarized in Table 5:

Table 5. WALL THICKNESS vs. PRESSURE FOR TUBULAR QUARTZ VESSEL

Pressure, MPa (psig)	Wall Thickness, cm (in.)[*]
0.30 (44.1)	0.30 (0.09)
1.03 (150)	0.84 (0.33)
2.65 (385)	2.54 (1.0)
4.31 (625)	5.08 (2.0)

[*] Assumes a 10.2 cm (4 in.) internal diameter.

Values are based on room temperature strength. Cyclic operation, elevated operating temperature and thermal gradients will cause an increase in required wall thickness. On the other hand, quartz is a moderate cost material with excellent solar spectral transmissivity and good high-temperature performance in terms of hardness and chemical resistance. However, quartz does have poor IR transmissivity compared to such materials as sapphire or polycrystalline alumina. If transparent materials such as sapphire are required for direct flux reactors because of resistance to corrosion or high IR transmissivity, cost factors may make metallic or ceramic materials more attractive. Based on our review, little information is available on fabrication techniques for these transparent materials. Although a small scale quartz reactor has been successfully fabricated, techniques to fabricate long, large diameter transparent reactor tubes; gas to metal, and glass to ceramic joints that will survive severe chemical and thermal environments still require research. Transparent windows larger than one foot diameters have not been demonstrated. Solar experiments with windows reactors have frequently encountered quartz devitrification, and corrosion.

Packed bed reactors have continuous processing capability. In operation they typically exchange the sensible heat contained in products in a counter-flow heat exchanger against reactants to preheat feed. The heat exchanger may be located within the container housing the reactor or it may be external.

Packed bed reactors have limited versatility. As considered in this discussion they are particularly appropriate for gas or liquid phase catalytic reactions. Direct flux illumination of solids within the reactor will lead to nonuniform temperatures within the bed due to absorption of the flux at the exposed surface of the solid and consequently variable reaction rates over the cross section of the bed. This should be accounted for in practical reactor designs. Corrosion and erosion always pose problems. For instance, some chemicals will react with quartz at high temperatures. Quartz is moderately hard (Moh's hardness of 9) so that erosion may be a problem with a fixed bed of solids.

Packed bed reactors are suitable for both dish and central receiver applications. Most existing design work involves the use of parabolic dishes as the flux concentrators. The existing conceptual designs of tubular receivers for gas heating using central receivers are similar in configuration to packed bed reactor concepts as currently envisioned. The design experience for development of gas heating receivers is most relevant for reactor scale-up considerations and heliostat field interface as suggested by the PFR design. Direct flux reactors may be envisioned as consisting of multiple transparent tubes containing catalyst coated packing over which reactants are passed. The flux impinging on the packing heats it up and heat is transferred to reactants by conduction and convection.

As a result of the stable flux distribution within the cavity of packed bed reactors for dishes, designs are relatively simple. Packed bed reactor designs for central receiver applications may be anticipated to be more complex because of time-dependent flux variations on the tubes comprising the reactor. The complexity of the design results from the need to control reaction rates through management of mass flow, flow distribution, and reactant temperature.

The issue of thermal storage incorporated within the receiver/reactor as a management technique to maintain reactor performance during transients will require more detailed study as reactor designs evolve to the point of hardware

construction. Weight limitations on tower mounted reactors may limit the use of thermal storage. Trade-off studies of the sensitivity of different reaction types to transient operation are still required. Reactions with temperature dependent reaction paths such as steam reforming of methane may have problems such as carbon deposition when operated outside the desired temperature range. It is expected that a combination of close control of mass flow, flow distribution and use of thermal storage will be necessary to accommodate daily flux variations and transients.

As mentioned earlier, nearly all studies of packed bed reactors were directed at small scale concepts or experimental reactors for parabolic dish applications. Although information on transparent materials and materials of construction are somewhat applicable to direct flux reactor design, these designs have been conceived for under 100 kW (3.41 E05 Btu/h) inputs and as a result are generally not applicable for scale up to large commercial scale central receiver facilities. An exception to this is the central receiver/reactor conceptual design work on methane-steam reforming that PFR Engineering Systems performed.

Fixed and Moving Bed Reactor Summaries for Solid Phase Reactions

Introduction

Several small scale experiments involving fixed and moving bed reactors using direct flux irradiation of reactants have been operated. Reactions carried out in these types of reactors include:

- Steam or carbon dioxide gasification of coal, coke, activated carbon and biomass

- Dissociation of cadmium oxide

- Elemental phosphorus production.

Fixed and moving bed reactors can be used for continuous, semi-continuous and batch type of operations where solids decomposition occurs. Moving bed reactors are applied to continuous processes. Generally, fixed bed reactors are applied to batch and semi-continuous processes. Although total decomposition of the solids is desirable, ash or slag can be removed from the reactor if necessary. These types of reactors are also acceptable for reactions producing solid and gaseous products, such as zinc sulfate decomposition. Although there is limited experience with fixed or moving bed

247

Figure 14. LONGITUDINAL CROSS-SECTION OF CdO REACTOR

The high temperature required for CdO dissociation necessitated the use of refractory materials for the hot areas of the reactor, particularly in the vicinity of the reactant bed. The rings and pegs that support the zirconia channels were made of alumina, as was the spacer ring. Another alumina ring of the same diameter as the spacer ring was positioned in front of the reactant bed support; this inner liner served both to help locate the reactant-bed assembly inside the containment vessel and to shield the vessel from radiation. The reactant bed and inner liner were enclosed in a mullite outer liner, another radiation shield. This assembly of ceramic parts was contained with a shell of type 304 Stainless Steel. Although the shell was shielded from the high temperatures within, additional protection was provided by a water-cooled jacket around the portion of the reactor exposed to the high solar flux.

A window at the front of the reactor was necessary to keep air out and to keep toxic cadmium and cadmium oxide fumes in, while admitting concentrated sunlight into the reactor. A 1.27 cm (0.50 in.) thick quartz window was used because of its high transmissivity for solar radiation and its resistance to thermal shock and chemical attack. The reactor operating pressure was 27.6 kPa (4.0 psig). However, despite its toughness, the window was the weakest point in the containment vessel; and because its strength decreases as it becomes hotter, it was essential to keep the window cool. This was accomplished by injecting inert gas (argon) through ports arrayed around the window perimeter. Inert gas injection served several purposes. First, it cooled the window by simple convective heat transfer. Second, it prevented cadmium and cadmium oxide vapor and particulates from accumulating near the window. If these substances condensed or settled onto the window, clouding it, the window would quickly absorb radiant heat that it would normally transmit if clear, possibly resulting in temperature induced failure. Third, the inert gas swept the decomposition products away from the reaction zone, as pointed out earlier, and carried them to a cold-quench area at the rear of the reactor, where cadmium and CdO were condensed. Finally, the inert gas carried the oxygen out of the reactor to an analyzer.

A quench heat exchanger was located in the rear of the reactor to provide a cold surface for condensation of the product vapors and for rapid cooling of the products to prevent back reaction. It also prevented condensable reaction

products from being carried out of the reactor, where they could plug gas lines or interfere with the gas analysis.

The design of an efficient receiver for solar radiation was not the intention of this work. With a holdup of less than 30 g (1.103) of reactant and power levels of 30 kWth (1.02 E05 Btu/h) available at the WSSF, there was no need to consider designing an efficient reactor. The experiment called for reaction rate determination at elevated temperatures, but not for evaluation of reaction energy balances. The resultant reactor design is clearly not the most efficient. The reactor has large radiant losses from a large aperture, and the uninsulated shell is cooled by water jackets and an air blower. The sensible and latent heats of reaction products and sensible heat of the argon are recovered at low temperatures and are essentially wasted. However, the final design was quite reliable and provided data useful in the evaluation of the CdO dissociation rates.

The gasket used to seal the window was an asbestos material with a styrene-butadiene binder. The binder degraded when exposed to high temperatures emitting acrid fumes. Window sealing was not a problem as the gasket retained structural integrity, and each run used a new gasket.

Windows suffered from problems of devitrification and clouding. In the first experiment, when argon flow became too low as the quartz wool plug at the reactor outlet became clogged, the window rapidly became clouded by material condensing on the inside surface. This buildup must have caused a significant rise in the temperature of the glass, because subsequent observation showed clouding (devitrification) inside the window material. In other experiments, material condensed around the outside of the diameter of the water-cooled aperture, but where the solar radiation penetrated, the window was generally clear. These results indicate although inert gas injection around the window helped, it was not completely effective in keeping the window clear. Improvements in distribution patterns may resolve the problem. Solar radiation penetrating the window will vaporize reactant material in its path, but material may condense on parts of the window that are not being irradiated.

250

Yudow Elemental Phosphorus Fixed Bed Reactor[10]

The reactor for cadmium oxide dissociation was modified for batch production of elemental phosphorus.[10] A graphite boat and crucible were fabricated to take the place of the zirconia channels resulting in a windowed reactor in which reactants were heated by conduction through the walls of the reactant container. The system was not sealed so that the window was exposed to reaction products.

One of the most vexing problems was the evolution of fumes that clouded over the window. The source of the fumes must be determined and the window fogging eliminated, perhaps by a design change that prevents the fumes from reaching the window. These severe window-fogging problems encountered with all the solar furnace runs essentially precluded lengthy runs at the requisite temperatures. These results indicate that diluent injection around the window is not completely effective in keeping the window clear. Solar radiation penetrating the window may vaporize reactant material in its path, but material may condense on the window possibly losing heat by radiation to the water-cooled aperture used to shield the window flange, and it is possible that the flux may cause heated reactants to react with the window rather than to be vaporized. Thus, diluent injection around the window apparently helps keep it clear, and radiation penetrating the window may cause reaction or vaporization of material condensing there.

Gregg Moving Bed Coal Gasification Reactor[11]

Gregg has patented a moving bed reactor, shown in Figure 16.[11] It is a direct flux reactor for coal gasification. However, as is shown in the figure, it relies on the use of a secondary mirror to provide a downwardly focused beam to irradiate the top of the packed bed. The reactor employs the essential elements of a direct flux reactor including use of a window and suggests a means of solids transport such as a screw feeder or piston. However, the use of a secondary mirror whose design is subject to enormous uncertainties in performance, cost, materials, and optical design, preclude the specific concept as a serious candidate for a direct flux reactor design.

Summary of Fixed and Moving Bed Reactor Designs

A summary of the fixed and moving bed reactors reviewed in this study is presented in Table 6. All designs were for a cavity type configuration with a
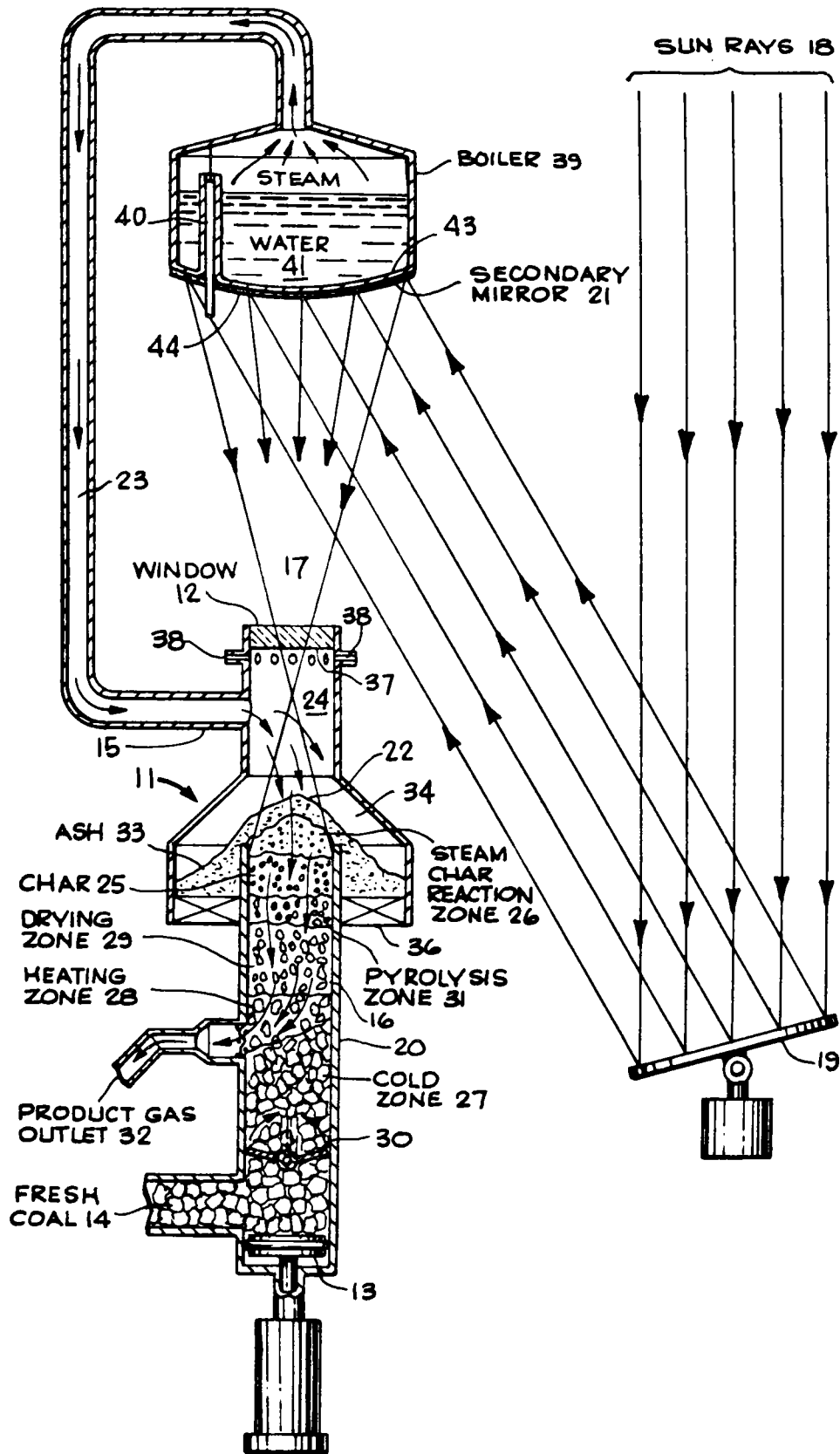
Figure 16. MOVING BED REACTOR FOR COAL GASIFICATION

252

Table 6. FIXED AND MOVING BED REACTORS FOR SOLID PHASE REACTIONS

	Steam Gasification of Coal	Cadmium Oxide Dissociation	Elemental Phosphorus Production	Coal Gasification
Reaction	Steam Gasification of Coal	Cadmium Oxide Dissociation	Elemental Phosphorus Production	Coal Gasification
Researcher	Gregg	Yudow	Yudow	Gregg
Reference Number	8	9	10	11
Scope of Effort	Experimental	Experimental	Experimental	Conceptual (Patent)
Objective	Proof of Principle	Proof of Principle	Proof of Principle	
Design Scale	30 kW	30 kW	30 kW	
Scale of Intended Application	Not Applicable	Not Applicable	Not Applicable	Central Receiver Heat Source
Flux Coupling Method	Direct	Direct	Indirect	Direct
Material of Construction	Stainless Steel/ Refractory Lined	Stainless Steel/ Refractory Lined	Stainless Steel/ Refractory Lined	Metal Shell/Refractory Liner
Configuration	Cavity	Cavity	Cavity	Cavity
Windowed Aperture	Yes (Quartz)	Yes (Quartz)	Yes (Quartz)	Yes (Unspecified, Could be Quartz)
Schematic Figure Number	A13	A15 and A16	A15	A17
Principal Dimensions:				
Aperture Diameter	20 cm	6 inch.	6 inch.	Not Available
Cavity Diameter	30 cm	6 inch.	6 inch.	Not Available
Cavity Length	1 m	4 inch.	4 inch.	Not Available
Thermal Efficiency	19 to 48%	Not Available	Not Available	Not Available
Flux Capability:				
Basis				
At Aperture	Not Available	Not Available	Not Available	Not Available
In Reactor	Not Available	Not Available	Not Available	Not Available
Temperature of Operation	1175 to 1425°K	1500°C	1500°C	1100°K
Process Fluid Temperature Profile	Figure A14	Not Available	Not Available	Figure A14
Refractory Temperature	Not Available	Not Available	Not Available	Not Available
Window Temperature	775 to 975°K (1075°K Max.)	Not Available	Not Available	Not Available
Operating Pressure	1 atm	4 psig	4 psig	Not Available
Pressure Drop ($\Delta P/P$, %)	Not Available	Not Available		Not Available
Evaluation	Proof of principle. Window remained rather clear. No thermal shock problems.	Proof of principle. Considerable problems with window devitrification and corrosion.	Proof of principle. Problems with window corrosion and devitrification.	Conceptual only. Requires a downward focusing heat source.

windowed aperture. Three of the four studies reviewed were of an experimental proof of concept nature performed on a 30 kWth (1.02 E05 Btu/h) scale. The fourth represents a preheated conceptual design which requires a down focusing heat source. The three experimental studies used a refractory lined stainless steel reactor. Operating temperatures ranged approximately 900° to 1500°C (1652° to 2732°F) with pressures from 101 kPa to 136 kPa (atmospheric to 5 psig).

For application to large scale processing of solids, fixed or moving bed reactors may be conceived of as a large number of vertical, transparent tubes arrayed in a generally circular pattern around the receiver periphery to intercept the concentrated flux from a heliostat field. The material is fed from the top of the tubes. The radiation impinges upon the reactant and the reaction occurs as heat is transferred to the material by direct absorption, by conduction through the bed of solids, and by convection from product gases. In direct flux applications, it is the surface of the bed where direct irradiation of reactants occurs, and where potentially high heat transfer rates are possible. Because conductive and convective heat transfer rates are relatively slow compared to radiative heat transfer, significant temperature gradients and variable reaction rates across the cross section of the bed are likely to occur. In may be speculated that a thin bed of extensive surface area is desired to expose the bulk of the reactant to direct flux rather than heat conducted or convected through the bed. Conceptually, this may be accomplished by such approaches as small diameter tubes, confining the reactant to a narrow annular space, or actively stirring the solids to augment the exposure of solids to direct flux. Design of the reactor includes consideration of proper dilution of flux over a sufficiently large surface area as in a cavity design to match flux absorption to reaction rate while attempting to avoid severe temperature gradients across the bed. Use of a cavity to provide proper dilution of flux impinging on reactants should allow high thermal efficiencies.

To make best use of direct flux heating of reactants, thin beds of solids are necessary. It is expected that the low thermal inertia of a thin bed of solids will make fixed and moving bed reactors responsive to transient variations in incident flux. For reactions without temperature-dependent side reactions, transients may be accommodated by control of reactant flow. More

temperature-sensitive reactions that may produce unwanted products may require the use of additional thermal mass in addition to flow control to help maintain reaction temperature at the desired level. Thick beds provide additional thermal mass but will have the problem of variable reaction rates with depth and poor control over undesired reactions across the reactor cross section. The low thermal inertia of the thin beds will result in relatively short start-up and shutdown times. Detailed analytical calculations must be carried out to investigate these qualitative speculations.

The temperature capability of a direct flux packed bed reactor is limited by corrosion of the transparent container. With a quartz container, operating temperature is limited to about 900°C (1652°F) with 1000°C (1832°F) possible in a dry, reducing atmosphere. Sulfates and carbonates may react with quartz at high temperatures. A tubular reactor may require moderately thick walls to operate under pressure since quartz is not a strong material. Based on room temperature strength a 10.2 cm (4 in.) ID tube requires a wall thickness of 0.84 cm (0.33 in.) at 1.03 MPa (150 psi), and 5.1 cm (2.0 in.) at 4.3 MPa (625 psi).

A packed bed reactor for solids will be of moderately complex design and will probably be more applicable for central receiver/heliostat applications due to the materials handling problem associated with small scale, distributed parabolic dish applications. Because of the daily and seasonal flux variations on reactor components within the cavity, feeding and collection of reactants and products may be a major problem due to the need for proper distribution and control of flow to the multiple tubes comprising the reactor.

Summary of Rotary Kiln Reactors for Solid Phase Reactions

Introduction

Many kinds of industrial processes can be performed in a rotary kiln. Some of the more common metallurgical and chemical processes that use the rotary kilns are:

a. **Direct Reduction of Iron Ores.** Crushed iron ore or iron ore pellets are mixed with excess coal/coke and heated to 1100°C (2012°F) to reduce the ore to metallic iron. The metallurgical product is further processed in electric furnaces to produce steel.

b. **Calcination of Limestone.** Limestone ($CaCO_3$) is calcined at 1100°C (2012°F) to produce lime (CaO). Dolomite ($CaCO_3 \cdot MgCO_3$) is calcined at 900°C (1652°F) to produce dolomitic lime.

c.   Oil Shale and Tar Sands. Retorting by solar heating is possible using
pebbles as a heat exchange media; this is much like the TOSCO process,
which uses hot pebbles to retort crushed oil shale.

d.   Roasting. Ores of gold, silver, iron, etc., containing sulfur and
arsenic are roasted at 530° to 1370°C (986° to 2498°F) in air to convert
them into oxides. Mercury is recovered by retorting ores in rotary
kilns.

e.   Calcining. Alumina (Al_2O_3) is produced by calcining either bauxite or
aluminum hydroxide at temperatures of 1000° to 1400°C (1832° to 2552°F)
in rotary kilns. Magnesite ($MgCO_3$), brucite ($Mg(OH)_2$), etc., are
calcined at 780° to 1760°C (1436° to 3200°F) to produce magnesia for
ceramic applications.

f.   Titaniferrous Ore. Ilmenite is mixed with carbon and heated in rotary
kilns to produce sponge iron and titania (TiO_2).

g.   Production of Portland Cement. Limestone, clay, and shale (wet slurry or
dry powder) are calcined at 830°C (1526°F) and agglomerated at 1400°C
(2552°F) in rotary kilns to produce cement clinkers.

Many of these processes operate in the range of 700° to 1200°C (1292° to

2192°F) and the amount of process heat required is significant. The heating

is usually accomplished industrially by a central burner using either natural

gas or oil. Use of solar energy to provide the heat requirements for these

processes can save substantial amounts of energy. The following sections

present a summary of the three solar rotary kiln designs reviewed.

Odeillo Limestone Calcination Rotary Kiln Design[12]

The Odeillo kiln was used with a horizontal solar furnace for heating of

inert material and for calcining calium carbonate. Materials to be processed

are heated by direct flux as well as by reflected and reradiated flux from the

hot kiln liner walls. As the hot walls rotate beneath the reactants, the

reactants are heated by conduction. It is not clear how rotary motion is

applied to the kiln.

The kiln can be described as follows:

"The scheme of the rotary furnace is given in
Figure 17. Inclination with respect to the
horizontal axis of the concentrator is 5°. The main
features are the following:

(a) Metallic frame is water cooled and rotates
inside the fixed shell.
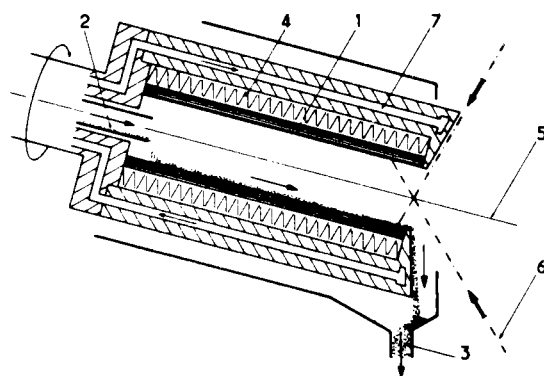
Figure 17. SCHEME OF THE ROTARY KILN
1 — refractory tube (Al_2O_3 or $LaCrO_3$);
2 — powder inlet; 3 — powder outlet;
4 — insulator; 5 — axis of the kiln (may be tilted);
6 — concentrated solar rays;
and 7 — water cooled metallic shell

(b) Internal lining at the wall is made of refractory tubes — alumina or lanthanum chromite 0.09 m (3.54 in.) in length and 0.02 m (0.79 in.) and 0.024 m (0.94 in.) in diameter respectively, exhibiting quite different radiative properties.

(c) Particles are continuously fed through a distributor along a vibrating pipe down to the back entrance of the tube.. Particle input was between 0.01 and $0.5 \cdot 10^{-3}$ kg·s-1."

Of course, although water cooling facilitates performance measurement in an experimental reactor, it results in significant thermal losses through the kiln walls and would not be appropriate to commercial scale reactors.

The kiln functions as a cavity absorber having, according to Reference 12, an absorbance of 0.9 to 1.0 regardless of wall material and feedstock. As determined by reflectometry with a xenon lamp, absorbance at 20°C (68°F) for the alumina (Al_2O_3) wall material was 0.15 ± 0.02; and for the lanthanum chromite ($LaCrO_3$) wall material absorbance was 0.95 ± 0.03. Measured emittance of lanthanum chromite at 1000°C (1832°F) at a wavelength of 0.63 μm by laser reflectometry was 0.90 ± 0.03.

The Odeillo kiln shown in Figure 17 is for small scale experiments with a 2 kW (6826 Btu/h) horizontal solar furnace. It was used for the calcination of limestone $CaCO_3 \longrightarrow CaO + CO_2$ to produce lime. This is of course a large scale industrial reaction that is commonly carried out using rotary kilns. In the Odeillo kiln particles were fed through a distributor along a vibrating pipe down to the rest of the kiln. Feed rates ranged from 0.01 to 0.0005 kg/sec (1.3 to 0.07 lb/min).

SRI International Rotary Kiln Design[13]

The SRI kiln was developed as a conceptual design for possible use at the CRTF. In operation, the focused solar beam enters the open aperture of the tower mounted kiln and heats the upper wall of the kiln. The bed of reactant solids is heated by reflection and reradiation from the walls. In contrast to the Odeillo kiln that is heated by a horizontal solar furnace, the SRI kiln is to interface with the 5 MW (1.7E07 Btu/h) CRTF. Since the flux from the heliostat field is angled upwards, it irradiates the upper wall of the kiln rather than heating the kiln walls and reactants as in the Odeillo kiln. Thus reactants are not heated by direct solar radiation, although the reactor still

258

meets the definition of a direct flux reactor since no intermediate heat transfer fluids or surface are involved. A diagram of the SRI rotary kiln is presented in Figure 18.

The SRI kiln dimensions are conceived to be 1.83 m (6 ft) ID, 3.66 m (12 ft) long, with a 1.22 m (4 ft) nonwindowed aperture. Specifications for kiln insulation are 15.2 cm (6 in.) 70% alumina brick for interior lining that contacts reactants with an additional 11.4 cm (4.5 in.) of insulating brick between the outer shell and the alumina brick. Insulating brick material specifications are undefined. The unit is operated under a slight negative pressure and the gases evolved during processing of reactants pass through a gas filtering system to remove particulates. Seals and associated gas containment apparatus are important issues in kiln reactor designs. A labyrinth seal is used to prevent escape of gas evolved during reaction. The approach to sealing and gaseous reaction product (and/or reactant) containment appear to be of conventional industrial kiln design practice and may be appropriate for commercial scale solar kiln reactors.

The drive mechanism shown in Figure 19 (Reference 13) appears to be a scaled down version of an industrial kiln drive and as a consequence, scaling up should not be a problem.

SRI presented an analysis of the thermal performance of a kiln for the CRTF. Their analyses are presented in Table 7 and Figure 20. Thermal efficiencies of greater than 70% at 1200°C (2192°F) and 80% at 1100°C (2012°F) kiln temperature are possible. Spillage losses due to a mismatch between the heliostat field image size and aperture size have not been determined.

The SRI kiln uses a 0.51 m^2 (18 ft^3) hopper with a vibratory feeder to deliver solids to the kiln. As shown in Figure 18, a discharge hopper collects products, allows them to flow through a 0.30 m (1 ft) diameter discharge chute to 0.21 m^3 (55 gal) steel barrels for final collection.

Shell Zinc Sulfate Rotary Kiln Reactor[14]

In the Shell design shown in Figure 21, the reactor is a rotary kiln contained in an outer can. A containment can is used to overcome the usual problem of moving seals which would be required for the drive system entrance, the zinc sulfate entrance, and exit points for the solid and gaseous products. The only seals made in this system are confined to the relatively

259
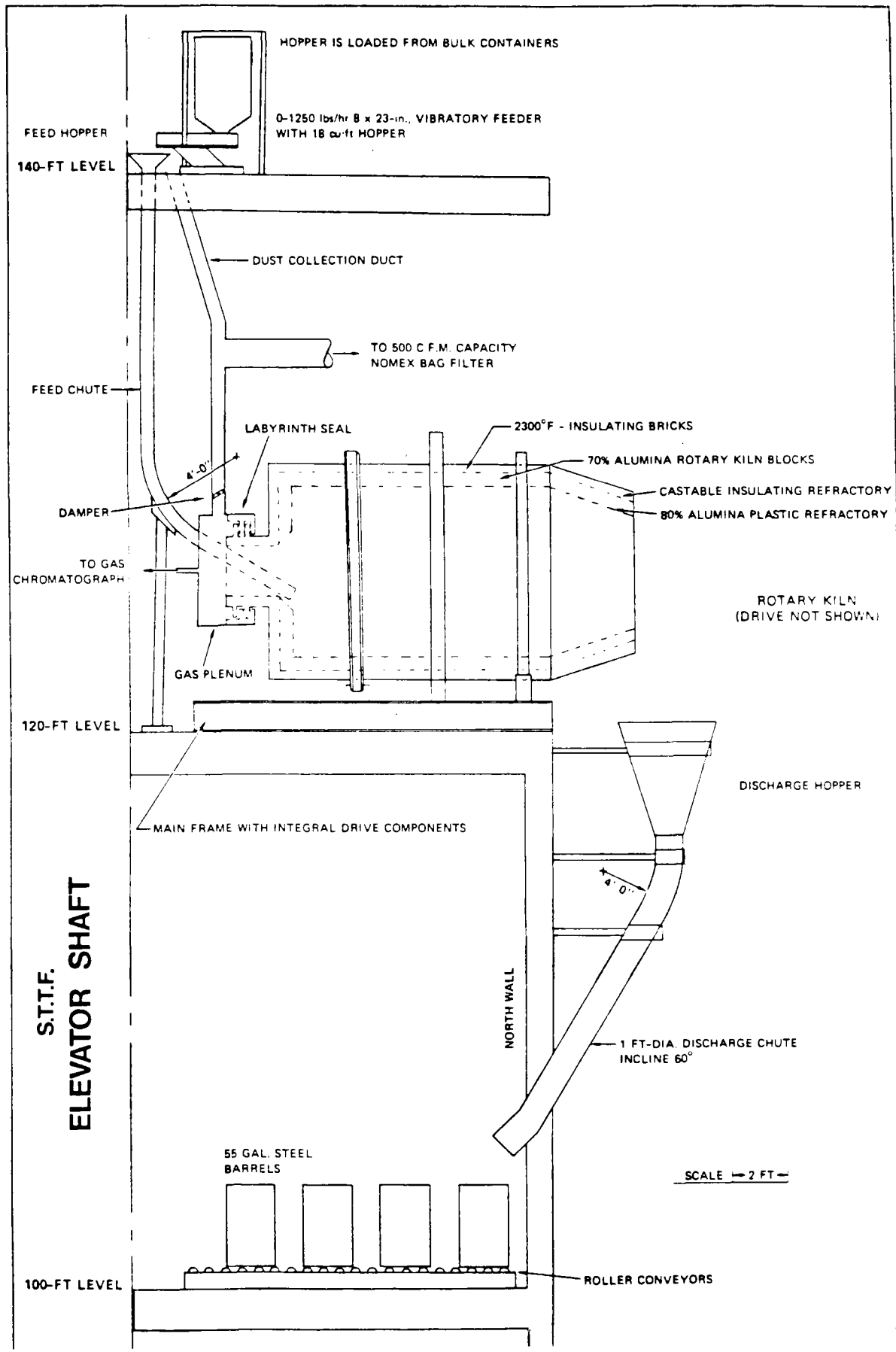
Figure 18. ROTARY KILN FOR CRTF

260
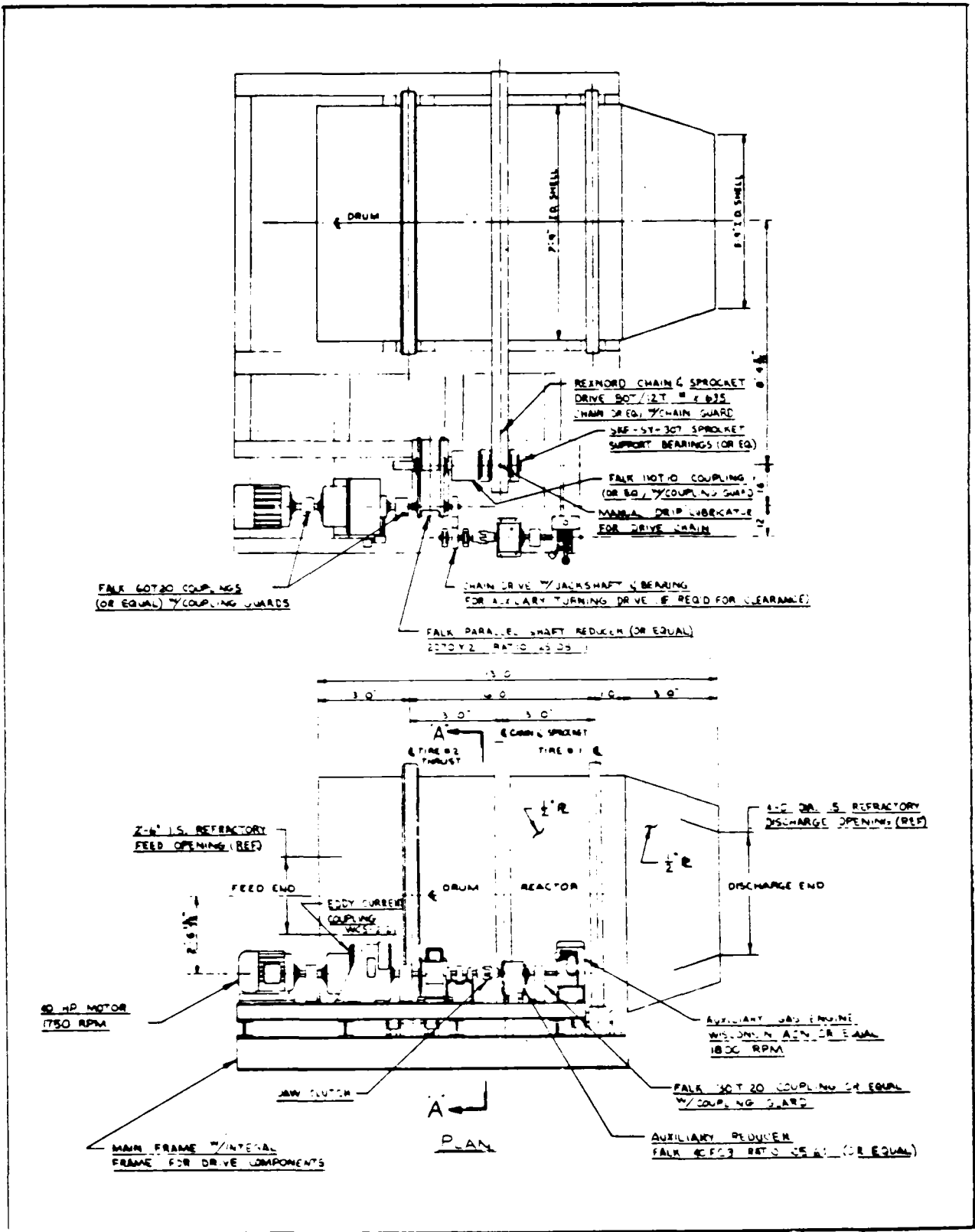
Figure 19.   SOLAR HEATED ROTARY KILN FOR THE CRTF AND ITS DRIVE MECHANISM

Table 7. SOLAR POWERED COLLECTED[1] AND HEAT LOSS FOR
VARIOUS KILN MOUTH OPENING SIZES[2]

Opening Diameter, m (ft)	Solar Power Collected, 10^6 Watts (10^9 Btu/h)	Average Flux, kW/m^2 (Btu/h-ft^2)	Heat Loss at 1200°C, 10^6 Watts (10^8 Btu/h)	Net Power, 10^6 Watts (10^9 Btu/h)
2 (0.61)	0.60 (2.05)	2055 (6.52E05)	0.16 (5.46)	0.44 (1.50)
3 (0.91)	1.14 (3.89)	1735 (5.5E05)	0.29 (9.9)	0.85 (2.90)
4 (1.22)	1.86 (6.35)	1593 (5.05E05)	0.48 (16.4)	1.38 (4.71)

1. Using the CRTF at Albuquerque.

2. The heat losses were based on a kiln of 3.66 m (12 ft) long, a burden depth of 0.30 m (1 ft), a kiln temperature of 1200°C (2192°F), 15.2 cm (6 in.) deep alumina refractory lining and 11.4 cm (4.5 in.) deep insulating lining.
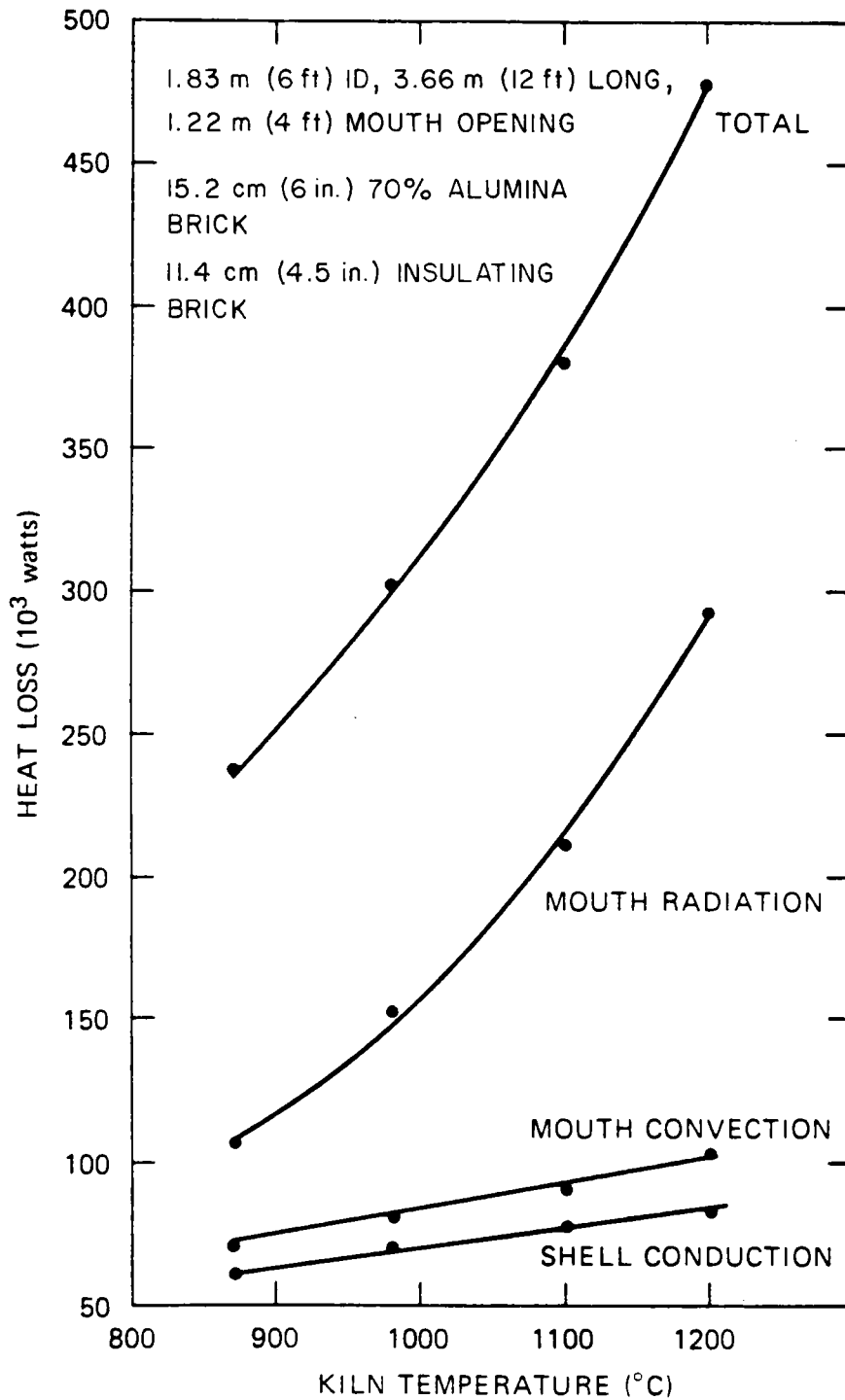
Figure 20. HEAT LOSSES FROM A ROTARY KILN FOR THE CRTF
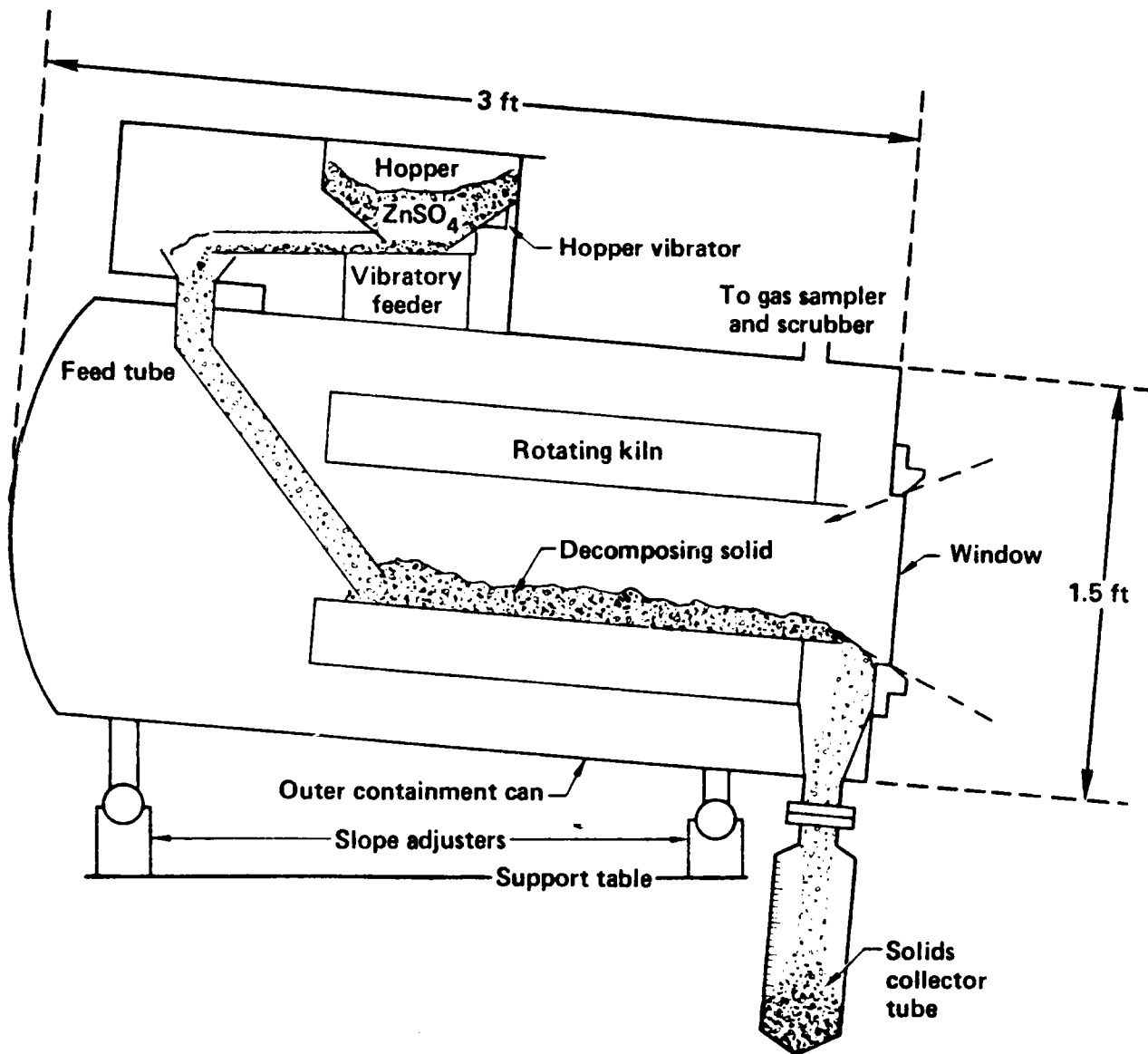
Figure 21.   ROTARY KILN FOR ZnSO$_4$ DECOMPOSITION

cool containment can. This approach greatly simplifies the problem of working with sealed hot systems.

The kiln is shown schematically in Figure 22, and consists of three main components: an inner liner, thermal insulation, and an outer wall. The liner is designed to be the primary surface exposed to the beam. The insulation is used to retain energy in the kiln in the form of heat. The outer wall, which is 304 stainless steel, serves two purposes, that is, to hold the kiln together and to receive the rotary motion from the drive train.

The liner material must have both high thermal stress resistance and good thermal insulating properties. The first criterion of thermal stress resistance requires a material with high thermal conductivity, while the second criterion of good insulating properties requires a material with low thermal conductivity, so some trade-off of properties is necessary. The liner material must also be resistant to the corrosive gases generated and be compatible with the solids involved. On the basis of these criteria the researchers selected alumina and mullite as liner candidates for service with zinc sulfate. In addition, it was reported that in a laboratory test Inconel-600 appears to be relatively inert to both the solids and gases involved.

The kiln was constructed with a mullite liner because it was expected to have better shock resistance yet it has comparable thermal conductivity compared to alumina. As a backup, there is an insertable liner of Inconel-600 that can be placed inside the mullite. The mullite liner is 61 cm (2 ft) long with a 15 cm (6 in.) outer diameter. Its walls are 0.5 cm (3/16 in.) thick.

The liner's outer surface is surrounded with basically two forms of insulation; cast and fibrous. Each end of the liner is supported by two cast alumina rings, although the rings are recessed 5 cm (2 in.) from the window end of the liner, as shown in Figure 22. Each ring is cast in two to four radially sectioned parts, which are secured into place around the liner with sufficient room between the individual pieces to allow for thermal expansion. Each ring is roughly 5 cm (2 in.) thick and leaves about 2-3 cm (1 in.) of space to the outer kiln wall. This space is filled with fibrous insulation, that is, Fiberfrax.

Between the alumina end rings the liner is covered with approximately 4 cm (1-1/2 in.) of a castable insulating cement which is primarily alumina
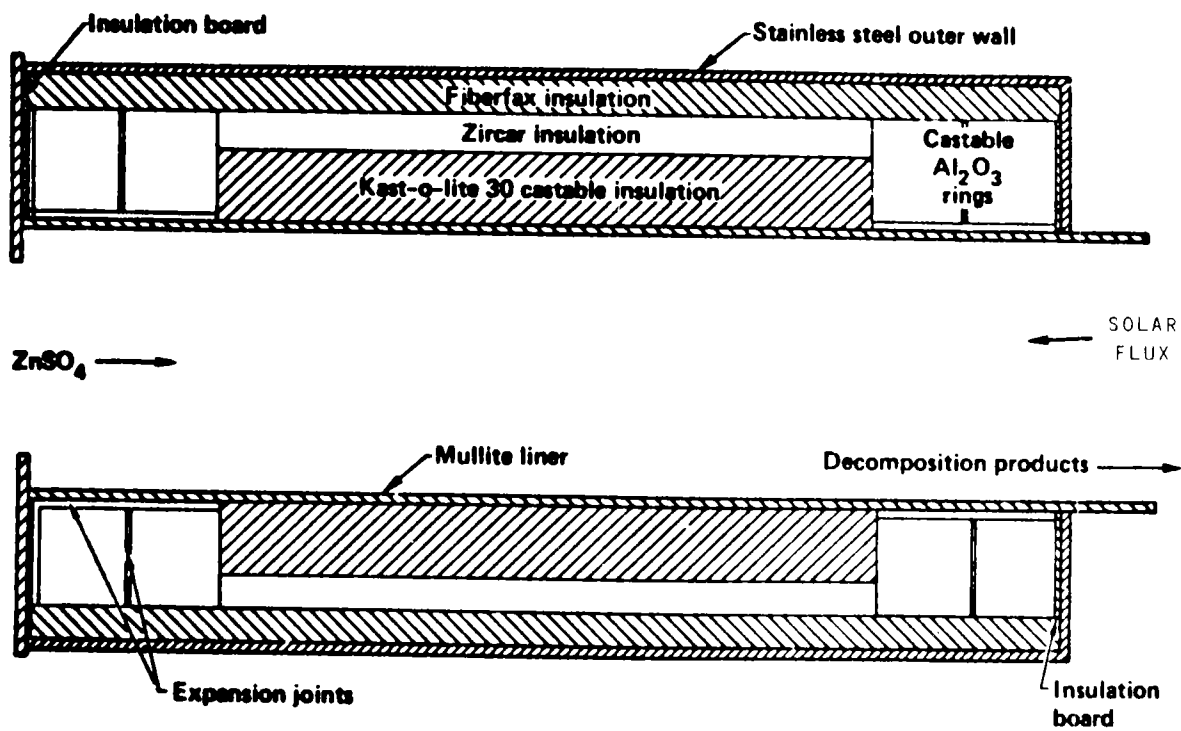
Figure 22.   DETAIL OF ROTARY KILN FOR ZINC SULFATE DECOMPOSITION

with some silica (Kast-o-Lite 30). The rest of the inner area between the castable and the outer kiln wall is filled with fibrous insulation (half Zircar, half Fiberfrax). This arrangement of insulation, although only 7.6 cm (3 in.) thick, is equivalent to approximately 23 cm (9 in.) of firebrick.

As shown in Figure 22, there is a 5 cm (2 in.) liner lip which protrudes from the insulating can. This lip prevents the decomposing solids from getting into the drive mechanism, and protects the outer kiln wall from seeing the beam. However, the lip would serve as a radiating source of energy loss if it were unprotected. Therefore, it is surrounded on the outside with approximately 2-3 cm (1 in.) of Zircar sheet insulation held loosely in place with a stainless steel collar.

Window design details are not explicitly discussed. The reactor uses a quartz window and operates at atmosphere pressure. The window is positioned at a point before (on the converging side) of the focal plane to reduce window heating because of reduced flux. Diluent flow is directed around the window for cleaning and cooling. A practical commercial design must carefully consider proper means to use diluent as it will affect reactor energy balance since as it is heated, it will take energy away from the process. Also the diluent may have to be separated from the other gases. (It may be possible to use reactant or product gases as window cooling/cleaning gas.) Efficient reactor operation demands that the product gas stream be used to preheat reactants or that recovered heat be used elsewhere in the process.

The drive train for turning the kiln is shown schematically in Figure 23, while Figure 24 shows an end-on view emphasizing the driver roller arrangement. The use of gears was avoided due to the high-temperatures of operation, as well as the corrosiveness of the product gases and the presence of gas borne particulate matter. Instead, the kiln is turned by friction against drive rollers. The kiln rests on top of two drive rollers placed end to end along a central drive shaft. The drive rollers have been specially grooved to increase the friction with the kiln and are firmly attached to the drive shaft by a series of locking collars. The kiln is kept from rolling off the drive rollers by four idling side rollers, two of which are located on either side of the kiln.

There is some question as to whether this drive method will scale. There is some question as to the necessity of a containment can when reactor is
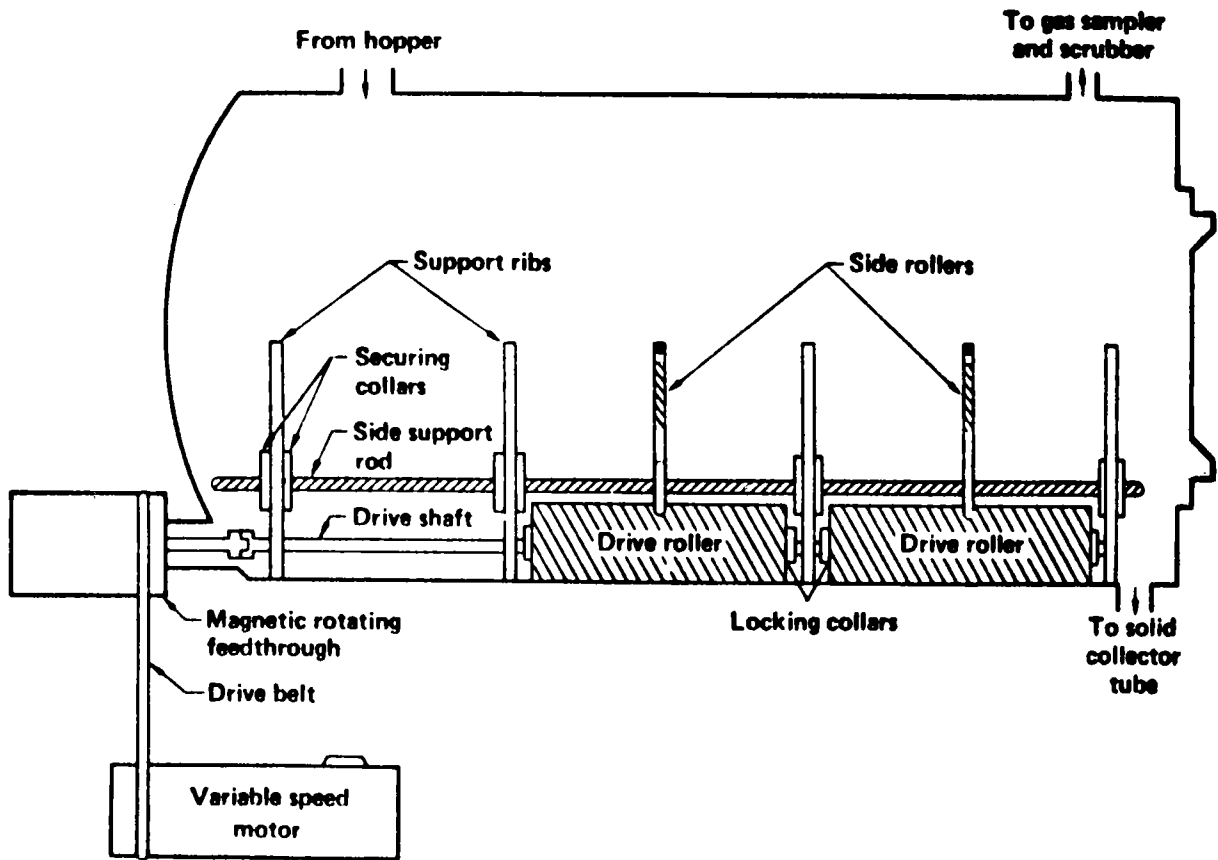
Figure 23. ZINC SULFATE KILN DRIVE MECHANISM
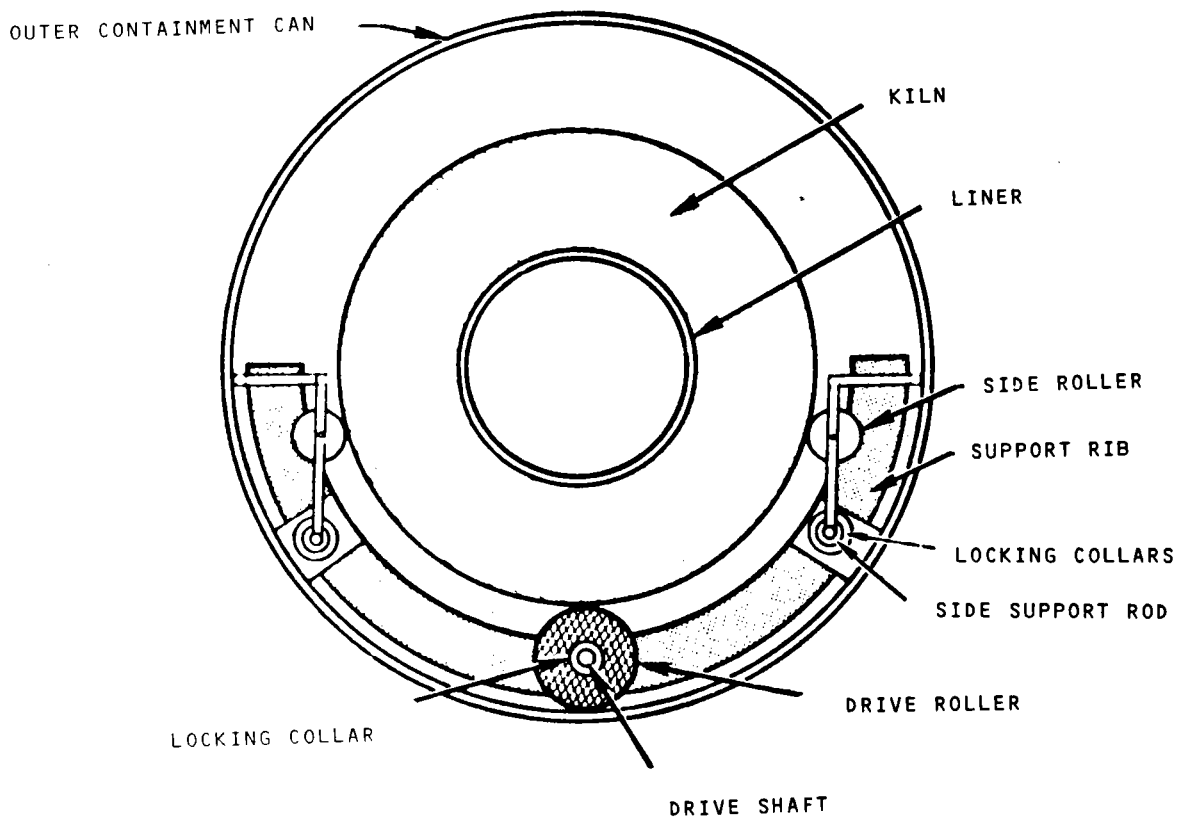
Figure 24. SCHEMATIC DRAWING OF END VIEW OF DRIVE MECHANISM OF
ZINC SULFATE KILN

scaled to commercial size since conventional method of gas and particle containment as applied to industrial kilns may be used. However, use of a "can" may be appropriate to isolate products from contacting the window and to allow gaseous products to be safely contained.

The motion to the drive shaft is provided with a magnetic rotary feed-through which is located on the outer containment at the lower rear corner of the back flange. The remote location of the feedthrough relative to the solar beam helps assure a low operating temperature for the feedthrough. The method of driving the kiln seems appropriate to the small scale experiment for which it is designed. However, the drive train for the SRI kiln appears more appropriate for larger scale kiln reactors.

The method for material handling described for the Shell rotary kiln is as follows:[14]

> "The zinc sulfate will enter the kiln through a feed tube which comes from a vibratory feeder located above the outer containment can. It will then tumble down through the rotating kiln, absorbing energy through both conduction and direct radiant heating, and decompose to form zinc oxide, sulfur dioxide, oxygen, and sulfur trioxide. The retention time within the kiln is easily controlled by varying the rotation rate and/or the angle of tilt of the kiln. The solids will leave the kiln and fall into a graduated quartz collection tube. Being transparent, the quartz tube will allow visual observation of the collection solids. The gases will be carried out through an exhaust system at the top of the containment can to a ground-based operations unit. There they will be sampled for later analysis by gas chromatography and/or mass spectometry, scrubbed, and then released.

> "Figure 25 shows a schematic drawing of the feed mechanism in more detail. The zinc sulfate is contained in a hopper (0.5 ft3 or ~14 liter capacity) which is sealed to prevent the anhydrous zinc sulfate feed material from absorbing moisture from the air. A vibrating device on the side of the hopper keeps the feed moving from the hopper to a vibratory feeder. As the zinc sulfate leaves the end of the feeder it falls into the feed tube which empties into the kiln."

It thus appears that standard materials handling methods for rotary kilns will be appropriate to solar kilns. However, since the kiln may be windowed, a modified design similar to this design may be appropriate to isolate products from the window and allowing gaseous products to be safely con-
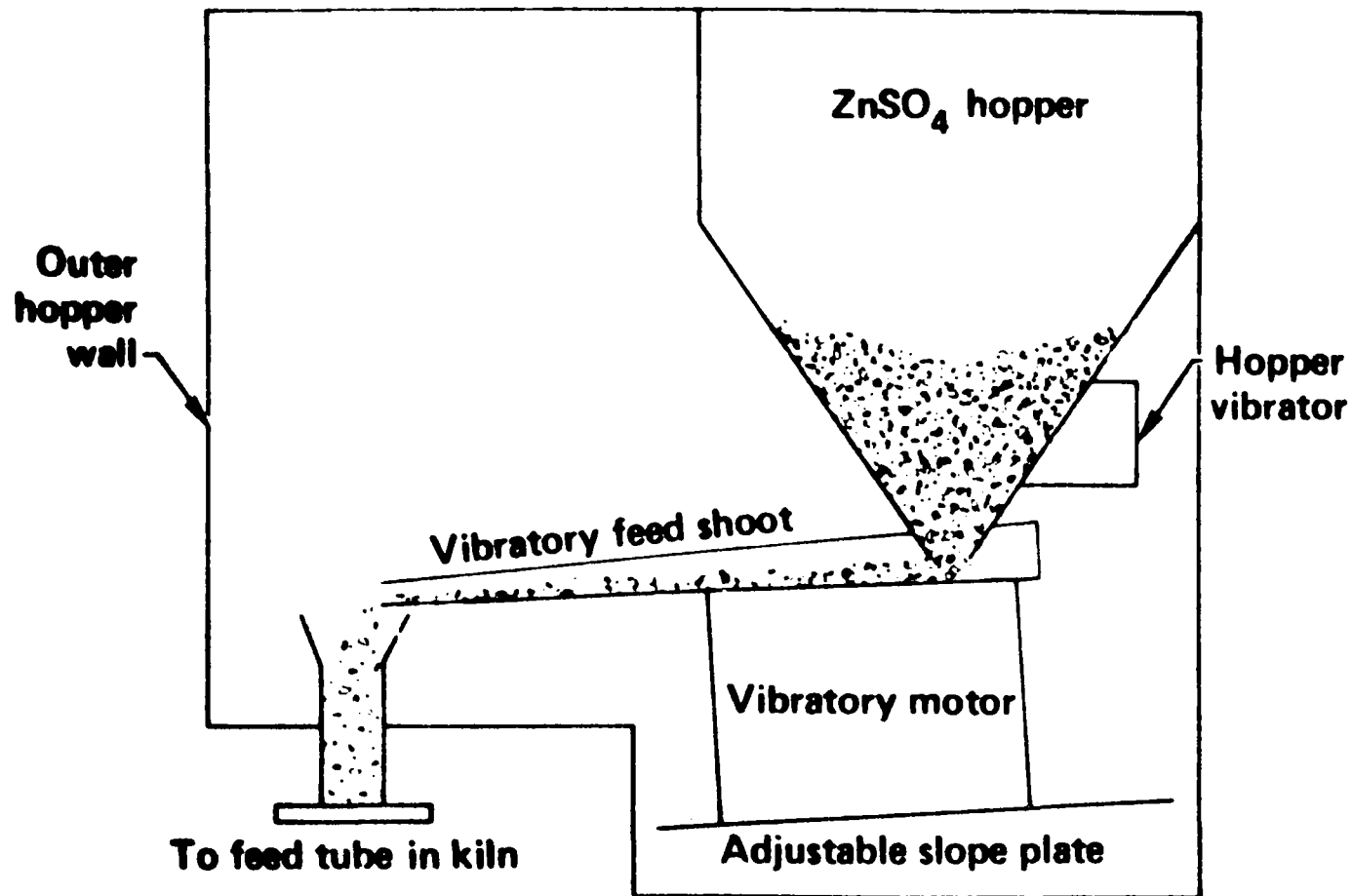
Figure 25. SCHEMATIC DRAWING OF SOLIDS FEED MECHANISM TO ZINC SULFATE KILN

tained. Essentially, this requires a "can" or containment vessel around the kiln through which feed and discharge (gas and solid) ports are passed. The containment vessel may have the windowed aperture as part of its structure.

Summary of Rotary Kiln Designs

In contrast to a conventional kiln, a solar rotary kiln need not be extremely long in order to process solids. Kilns are ordinarily heated by combustion gases and the long length is required because convective heat transfer rates from the gas to the solid are slow. In the solar kiln the radiative heat transfer processes are very effective in transporting heat to the reactants so an extremely long kiln is not required.

Kilns are primarily used for solids. It is conceivable that a bed of inerts or catalyst coated inerts might be used for gas phase reactions, but solid-gas contact will not be as good as in a packed bed or fluidized bed unit. With proper selection of materials and material handling devices corrosives and abrasives may be handled. It is also possible that the kiln may be able to handle liquid products such as slag.

Rotary kilns are not suited for distributed collector systems. The flow of materials through the reactor would be negatively affected by the traveling focus. Solids handling for a distributed collector field would be extremely difficult and almost certainly uneconomic.

Rotary kilns are expected to have the capability of accepting flux of 2 MW/m^2 (6.34 E05 Btu/h-ft^2). The cavity effect reduces flux impinging on solids by exposing them to reflected and reradiated flux (for the case of a tower mounted kiln) allowing the matching of heat transfer rate to reaction rate. Retention time may be adjusted by varying the tilt angle of the kiln, kiln length, using flights or chains to hold up material, and adjusting rotational speed to allow sufficient time at reaction temperature so that desired conversions may be achieved. There is no question that commercial kilns are capable of extremely high-temperature operation. The main constraints on solar kiln operation are expected to be materials limitations that result from the need to achieve very high temperatures at the refractory surface that is directly exposed to the flux so that it may reradiate to the cooler reactants. Because the kiln rotates, the hot refractory will continuously rotate in and out of the flux thus exposing it to cyclic

272

temperature variations greater than 500°C (900°F) causing potential thermal shock and fatigue problems.

As expected, the key design issue for scale-up is the design of the transparent aperture. Of course a windowed aperture is not always necessary in cases where gaseous products are nonexistent or inocuous and they need not be collected for further processing. However, products frequently are toxic (that is, carbon monoxide) or they must be processed further (that is, sulfur dioxide from zinc sulfate decomposition). This requires a sealed system and hence a windowed aperture. A window may be necessary to prevent solids from drifting out the aperture and blocking the flux. It may be possible to operate a slight negative pressure to sweep air through the open aperture and collect gases at the feed end if this will not impede downstream processing or significantly reduce collection efficiency. A potential advantage of the kiln is that the window may be positioned away from the reaction zone where it may avoid contact with gases or solids or at least be exposed only to relatively cool solids and gases with the reduced likelihood of chemical or physical interaction that would impede continuous operation.

Based on the literature reviewed, it appears that standard materials handling methods for rotary kilns will be appropriate to solar kilns. However, since the kiln may be windowed, a modified design may be appropriate to isolate products from the window and allowing gaseous products to be safely contained. A possible approach is the use of a "can" or containment vessel around the kiln through which feed and discharge (gas and solid) ports are passed. The containment vessel may have the windowed aperture as part of its structure.

Designs reviewed do not use the flights or chains commonly used in conventional kilns. These devices may throw up a cloud of solids which will "see" the aperture and reduce the cavity effect while also possibly permitting solids to contact the window. Experiments with zinc sulfate decomposition also experienced considerable problems with agglomeration. It may be possible through judicious use of flights and chains within the region of the reactor where this occurs to avoid agglomeration and limit the formation of a cloud of particles.

Rotary kilns have fairly high thermal inertia due to holdup of materials within the kiln. They should have reasonable transient performance in that

273

kiln rotational speed and feed rates may be adjusted to compensate for reduced flux while maintaining the reaction. Due to the significant thermal inertia, start-up times may be long. However, start-up time can be manipulated by adjusting feed rates and rotational speed. Some fossil fuel use may be required to maintain hot standby conditions for rapid start-up. Downstream process equipment must accommodate a varying mix of products and unconverted reactants. Thermal shock is considered to be a principal materials problem due to rotation of refractory surfaced in and out of regions of very high flux. An insulated aperture shutter may be desirable to reduce heat loss and lower cooling rates.

Table 8 presents a summary of the three rotary kiln research efforts which were reviewed. Experimental reactors ranged in size from 2 to 4 kWth (6826 to 13,650 Btu/h). The largest reactor dimensions were .30 m (1 ft) in diameter by 0.91 m (3 ft) long. Operating temperatures ranged from 800° to 1000°C (1472° to 1832°F) with operating pressures near atmospheric conditions. A conceptual design of a 2 to 3 MW (6.8 E06 to 1.02 E07 Btu/h) rotary kiln reactor for use at the CRTF was also reviewed. The conceptual design reactor is 1.83 m (6 ft) in diameter and 3.66 m (12 ft) long with a 1.22 m (4 ft0 aperture diameter. Flux at the aperture is expected to be 1593 kW/m^2 (5.50 E05 Btu/h-ft^2) and the operating temperature 700° to 1200°C (1292° to 2192°F).

Many uncertainties still exist in solar kiln design. Long-term window performance is unknown. It is unknown at this time if large windows can be constructed. Thermal performance of kilns, especially as tied to reaction kinetics is poorly defined. Versatility of reaction capability is apparent from industrial use but not established for the solar environment. Considerable development in regards to windows, transient effects, materials and thermal shock, and performance modeling and scale-up will be required.

Entrained Flow Reactors Summary for Solid Phase Reactions

Entrained flow reactors are used in industry where reaction rates are high and material residence times are short (<5 sec). This continuous operation reactor is capable of fast response times due to the low inventory of material in the reaction zone. The reaction zone is contained within the reactor walls where reactants are either dropped in or injected. For solid reactions the material must be finely ground both to increase its surface area

Table 8. REACTOR TYPE: ROTARY KILNS AND SOLID PHASE REACTIONS

Reaction	Limestone Calcination	Zinc Sulfate Decomposition	Test Facility
Researcher	Odeillo	Shell	SRI International
Reference Number	12	14	13
Scope of Effort	Experimental	Experimental	Conceptual
Objective	Proof of Principle	Proof of Principle	Proof of Principle
Design Scale	2 kW	9 to 14 kW	2 to 3 MW
Scale of Intended Application	Not Available	Not Available	CRTF at Sandia, Albuquerque
Flux Coupling Method	Direct	Direct	Direct
Material of Construction	Metal Shell/Refractory Lined	Metal Shell/Refractory Lined	Metal Shell/Refractory Lined
Configuration	Cavity	Cavity	Cavity
Windowed Aperture	No	Yes (Quartz)	No
Schematic Figure Number	A18	A22	A19
Principal Dimensions:			
Aperture Diameter	0.02 m	Not Available	4 ft.
Cavity Diameter	0.02 m	1 ft.	6 ft.
Cavity Length	0.09 m	3 ft.	12 ft.
Thermal Efficiency	15% (Overall)	Not Available	70% at 1200°C; 80% at 1100°C (Calculated)
Flux Capability:			
Basis	Not Available	Not Available	Average (Calculated)
At Aperture	Not Available	Not Available	1593 kW/m^2
In Reactor	Not Available	Not Available	Not Available
Temperature of Operation	800 to 1400°C	1000°C	700 to 1200°C
Process Fluid Temperature Profile	Not Available	Not Available	Not Applicable
Refractory Temperature	Not Available	Not Available	Not Available
Window Temperature	Not Applicable	Not Available	Not Available
Operating Pressure	1 atm	1 atm	1 atm
Pressure Drop ($\Delta P/P$, %)	Not Available	Not Available	Not Available
Evaluation	Proof of principle. Batch operation only.	Proof of principle. No serious problems with window. Serious materials handling problems with agglomerating reactant.	Appears technically feasible based on conceptual design.

for the reaction and for rapid dispersement throughout the reaction zone. Reactants may also be injected with catalytic material which becomes entrained in the flow and promotes the reaction.

Two types of entrained flow configuration reactions were found in the literature. Both feature external receiver design configurations which involved carbonaceous material gasification in quartz tubes. In one approach, solids were entrained in an upwardly flow of steam. In the second method, solids were introduced into the top of the reactor where they fell downward countercurrently through an upwardly flow of steam. In both designs the reactants are directly irradiated by solar flux. These single tube reactors may be considered prototypes of commercial designs involving a cavity lined with such tubes.

The entrained flow reactor design configuration developed by GIT involves a vertical, tubular, ceramic downcomer through which solids pass (Figure 26). The solids are entrained in a gas stream (such as steam) and flow upwards confined in the annular space between the downcomer and a one-inch diameter, tubular, quartz outside envelope. The concentrated flux impinges on the vertical sides of the reactor directly irradiating the reactants. The upper part of the reactor is covered by a cavity to reduce heat losses.

Antal has used a quartz entrained flow reactor of tubular design In laboratory experiments, a vertically oriented 25 mm (0.98 in.) O.D. quartz tube was used.[15] Biomass solids feed through the focal zone under gravity. The gas flowed upwards to maintain particle residence time in the desired range. This variant of the entrained flow reactor is sometimes called a "drop tube", "falling bed", or "free fall" reactor. At the 1 MWth (3.41 E06 Btu/h) solar furnace at Odeillo, Antal used a 50 mm (1.97 in.) O.D. Amersil TO8 quartz tube in a vertical orientation. Steam entrained solids and carried them downward through the focus.[16] Reactants are directly irradiated by the flux. However, the horizontal furnace only heats the reactor from one side. At the 400 kWth solar furnace (ACTF) at GIT, Antal used a quartz tube with solids falling by gravity with a countercurrent (upward) flow of steam.[17] This is a "falling bed" reactor. Reactants are directly irradiated by flux. In contrast to the experiments at Odeillo, the reactor configuration used at the ACTF permits the entire perimeter of the reactor to be irradiated. The upper part of the reactor was covered by a cavity to reduce heat losses.
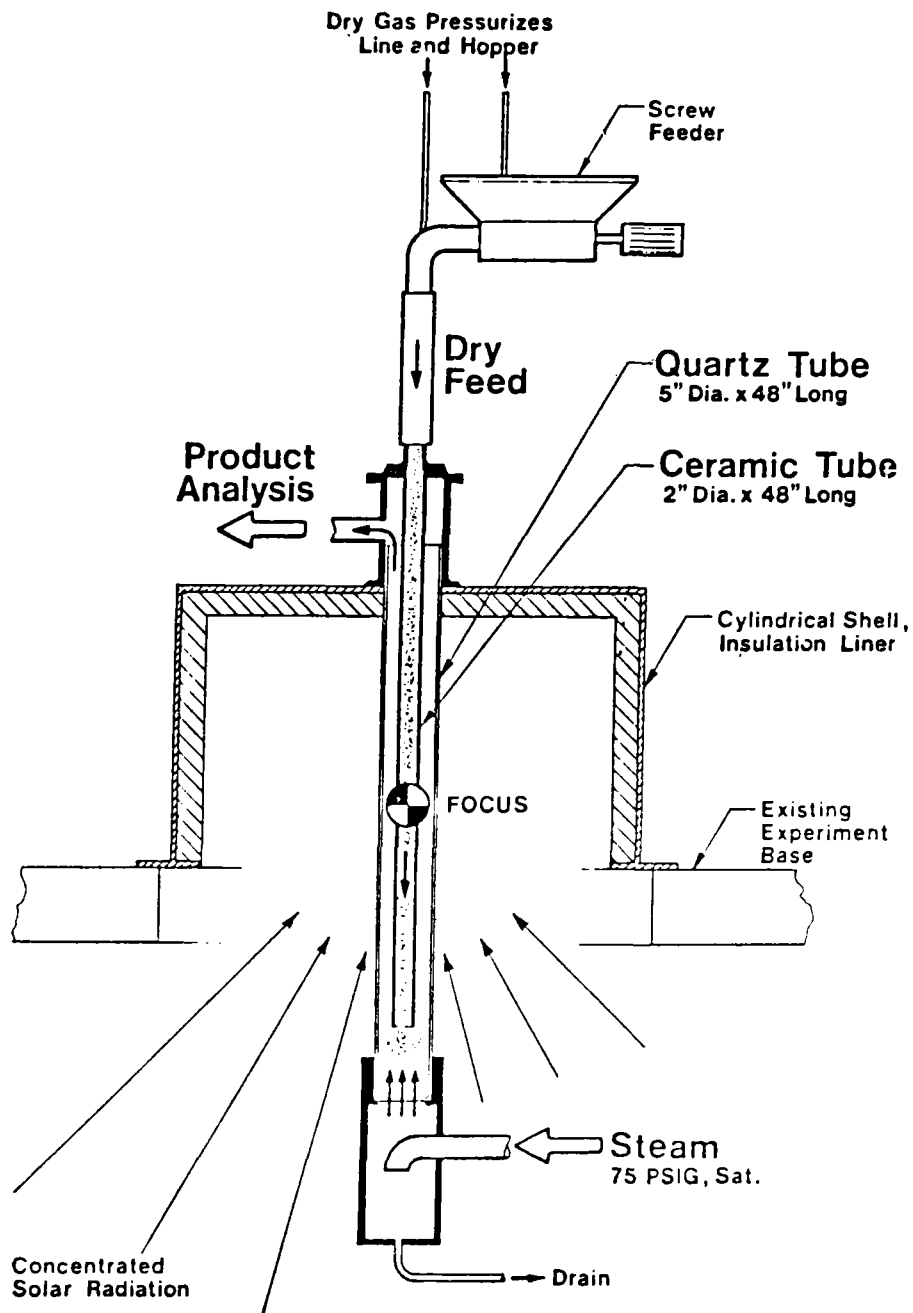
Figure 26.   SCHEMATIC DRAWING OF AN ENTRAINMENT REACTOR

GIT's entrained flow reactor program is using 70 to 80 μm particle sizes for carbon gasification. Particles are not ground to around the wavelength of light which would augment light absorption and reduce particle density requirements to achieve high absorptivities. In personal communications, Cassanova of GIT has observed that grinding to <1.9 μm is very energy-intensive and may have negative impact on economics. Antal used a range of sizes 75 to 700 μm at Odeillo.

The configurations used by GIT (Figure 26) and Antal are a compromise between externally heated reactor and a large cavity configuration with frequent tubes lining the cavity walls. These single tube reactors may be considered prototypes of a commercial scale design involving a cavity lined with such tubes. A full cavity-type configuration is expected to be necessary to achieve high thermal efficiencies in high-temperature reactor applications. In the entrained flow reactor concept the window will be in thermal balance with reaction and flux input.

It is probable that the tubes will not be subject to deposition of reactants or products or to corrosive attack. In Antal's laboratory experiments "a thin film of yellowish material...collected on the wall of the reactor...".[15] In his experiments at GIT he experienced "...pyrolytic carbon deposited on the interior of the reactor".[16] In his laboratory experiments he also noted "...solid and liquid materials that adhere to the quartz wall of the reactor." Thus problems with "fogging" of the tube are likely to occur. Cassanova at GIT suggests that hydrodynamic management of flow can avoid this but methods are unclear and certainly unproven.

Quartz may have limited usefulness as a reactor material of construction. Only limited materials evaluations have been done in terms of potential corrosive attack on window materials. For instance, the quartz literature suggests that carbon will reduce fused quartz at temperatures as low as 1200°C (2192°F). Where carbon may be present, this indicates problems with possible interaction of carbon with the quartz containment vessel in an entrained flow reactor. GIT will use a pure carbon for initial tests of carbon-steam gasification. Reaction temperatures are expected to be below 1200°C (2192°F). Future work involving char may lead to deposition of tars or other substances, or sticky materials may adhere to window (because char is composed of carbon and organics and ash). Gasification temperatures must be chosen to avoid ash fusion.

278

Erosion of the tube seems to also be a possibility. Although quartz is relatively hard, char particles may scratch the quartz. Scratches will reduce transmissivity and can lead to structural failure. Short-term experiments may not experience this problem to a great degree but may be a problem for commercial designs.

If quartz is cooled to the phase change temperature (~250°C [482°F]) during daily cycling there may be problems with devitrification. No information was identified in the literature on thermal shock problems with either Antal's or GIT's entrained flow reactors. Of course quartz is quite resistant to thermal shock due to its low coefficient of expansion.

Scale

GIT's reactor is designed for use at GIT's ACTF (Advanced Component Test Facility). As presently configured, it is capable of using the maximum available flux but is physically too small to absorb all power. Antal used his biomass pyrolysis reactor at 1 MWth (3.41 E06 Btu/h) facility at Odeillo. Antal's material flow was about 36 g/h (0.08 lb/h). He also used the reactor at GIT's ACTF.[16] At ACTF Antal fed cellulose at 8.6 g/min (1.14 lb/h); corn cobs at 225.0 g/min (29.7 lb/h); and hardwood at 3.2 g/min (0.42 lb/h). Entrained flow reactors are used at industrial scales. If problems with corrosion, erosion, and deposition can be solved it should scale to industrial capacities. It is not applicable to distributed collector systems because of operating problems such as solids handling.

Flux Capability

Antal used the 1 MWth (3.4 E06 Btu/h) solar furnace at Odeillo. Only a small fraction of the available power was used. The reactor was exposed to flux levels 0.2 to 1.6 MW/m^2 (6.34 E04 to 5.08 E06 Btu/h-ft^2). Absorption by relatively small particles is widely considered to be a useful way to absorb flux. Entrained flow reactors should be capable of absorbing high fluxes, especially when used in a cavity configuration.

Temperature Capability

High temperatures may be achieved in entrained flow reactors as long as quartz tube avoids devitrification or corrosion. Materials such as Vistal or Spinel may be required for higher temperature or greater corrosion resistance. Since the quartz tube absorbs some long wavelength energy

279

reradiated from the materials inside the reactor it will become quite hot. The net energy balance on the quartz tube will determine the maximum reaction temperature that may be conducted within the reactor. A 900°C (1652°F) material temperature is permissible, with 1000°C (1832°F) possible in a dry, reducing atmosphere.

Thermal Performance

No information is available on the thermal efficiency of experimental entrained flow reactor designs. Cavity or externally heated configurations made of a number of tubes (similar to steam boilers or air heaters for central receivers) will have thermal performance characteristics associated with their operating temperature, flux input, and cavity and aperture dimensions.

Operating Pressure

GIT and Antal's reactors operate at atmospheric pressure. Wall thickness may be varied to permit reaction pressure up to at least 1.03 MPa (150 psig).

Materials Handling

Small-scale systems have used vibratory and screw feeders for solids handling. Since a large scale entrained flow reactor is likely to be made of many tubes, significant attention will have to be made to ensure proper flow of solids and entrainment gases to each tube. Variable flow conditions must be provided to handle transient flux conditions, start-up and shutdown, and varying flux patterns on portions of the reactor as the sun transverses the sky (such as in early morning and late evening hours). Gas side pressure drops are dependent on particle loading and gas flow rates. Entrained flow reactors generally have moderate pressure drop.

Continuous Processing Capability

The entrained flow reactor has excellent continuous processing capability.

Versatility

Entrained flow reactors are limited to relatively fast reactions because reactants are not in the reaction zone very long (<5 sec). They are applicable to solid phase reactions with gaseous and/or solid products. They may be applied to heterogeneous reactions where solid and gaseous materials must be contacted. They may be used for reactions involving gaseous reactants

280

that may have solid catalyst particles entrained in the gas flow. Limitations primarily involve corrosion and/or erosion of the containment vessel. Material of construction could be quartz, Vistal, or Spinel. Antal has suggested that:[17]

> "The concentrated radiant energy can be used to establish two characteristic temperatures within the reactor: the temperature of the radiation ($\sim 6000°K$) and the temperature of the transparent gas ($\sim 400°K$). Opaque solid particles exposed to such an environment are rapidly heated to a high temperature; whereas the gaseous material present in the reactor remains relatively cold (depending upon solids loading and the solid-gas heat transfer rate). Very hot gaseous products evolved by the reaction may be quenched almost instantaneously in such an environment."

This may be advantageous for reactions such as biomass pyrolysis. Hunt[18] suggests that this effect is particle size dependent. Particles less than $1\mu m$ heat rapidly and transfer heat effectively to their surroundings and thus are very close in temperature to surrounding gas and in fact may be used to heat gases to high temperatures. It is implied that larger particles tend to heat faster than the rate of heat transfer to the surrounding gas and may therefore achieve higher temperatures than the surrounding medium. This may lead to a means to exploit the "two temperature" phenomenon. It is uncertain whether this effect may be exploited in commercial scale reactors.

Orientation Flexibility/Sensitivity

Reactor design should be able to accommodate the various heliostat field types. The vertical orientation and solids handling problems indicate this reactor concept is unsuitable for distributed collector fields.

Ease of Fabrication

Commercial reactors will be of multi-tube design because of heat transfer limitations within the bed and the current manufacturing limits on tube OD. Since the flux is absorbed by the solid particles, the thickness of the cloud of particles in the reactor (and thus tube diameter) is constrained by the requirements to directly absorb the flux rather than to heat particles by conduction and convection.

Design Complexity

Entrained flow reactors will be complex because of the multi-tube design and the problems of controlling solids and gas flows to the individual tubes.

Transient Performance Capability

Entrained flow reactors are of low thermal inertia. They will respond quickly to transients by a reduction in reaction rate and reactant conversion. If controls may respond quickly this will not be a major problem. Some thermal buffering such as preheating of gas and solid feed or including thermal mass in the reactor may be desirable to allow maintenance of good reactant conversions. Provisions in downstream processing equipment will have to be made to process a varying mix of products and unconverted reactants to accommodate variations in reactor performance due to transient conditions.

Diurnal Cycling Capability

As a low thermal mass design, entrained flow reactors should have short start-up and shutdown times. As with any quartz reactor, provisions must be made to avoid cooling of quartz below 250°C (482°F) to prevent devitrification. Designs must accommodate varying flux patterns on various parts of the reactor as the sun moves across the sky.

Summary of Entrained Flow Reactor Design

The entrained flow reactor is used in industry. It has been used for experiments involving biomass pyrolysis and is currently under development by GIT for biomass pyrolysis and carbon-steam gasification. A reactor capable of absorbing even a substantial fraction of the power available at the 400 kWth (1.37 E06 Btu/h) ACTF has yet to be constructed. Many uncertainties exist in entrained flow reactor design. Erosion/corrosion of quartz is a major potential problem that may force the use of more expensive materials such as Vistal or Spinel. Thermal performance, especially as tied to reaction kinetics is poorly defined. Material handling and control of a multitube reactor will be difficult. Development requires scale-up from small diameter, single-tube reactors to large diameter, multitube reactors. Development of a successful multi-tube entrained flux reactor is significant. Table 9 presents a summary of the entrained flow reactor design.

Table 9.   REACTOR TYPE: ENTRAINED FLOW

	Carbon/Steam Gasification	Biomass Pyrolysis
Reaction		
Researcher	Georgia Institute of Technology	Antal
Reference Number	Personal Communication with R. Cassanova	4 & 6
Scope of Effort	Experimental	Experimental
Objective	Proof of Principle	Proof of Principle
Design Scale	Less than 100 kW	Less than 100 kW
Scale of Intended Application	Not Applicable	Not Applicable
Flux Coupling Method	Direct	Direct
Material of Construction	Quartz	Quartz
Configuration	External	External
Windowed Aperture	Yes: Transparent Tube	Yes: Transparent Tube
Schematic Figure Number	A27	A27
Principal Dimensions:		
Aperture Diameter		
Cavity Diameter	Tube Diameter = 5 in.	Tube Diameter (Laboratory) = 25 mm OD; Tube Diameter (Odeillo) = 50 mm OD
Cavity Length	Tube Length = 40 inch.	Not Available
Thermal Efficiency	Not Available	Not Available
Flux Capability:		
Basis	Measured	Measured
At Aperture	Not Applicable	Not Applicable
In Reactor	Approx. 50 to 100 kW/m^2	20 to 1600 kW/m^2 at Odeillo
Temperature of Operation	1000°C	700 to 1000°C
Process Fluid Temperature Profile	Not Available	Not Available
Refractory Temperature	Not Available	Not Applicable
Window Temperature	Not Available	Not Applicable
Operating Pressure	75 psig	Not Available
Pressure Drop ($\Delta P/P$, %)	Not Available	Not Available
Evaluation	Low conversion experiments. Walls of tube are covered with carbon reducing transmissivity. Quartz devitrifies.	Qualitative demonstration successful. Product mix different from expected. Considerable deposition of materials on quartz reactor wall.

From the literature it is clear that the transparent tubes may be subject to deposition of reactants or products or to corrosive attack. Reports of yellowish films, carbon deposits, as well as solid and liquid adhesion has been cited in the literature. Therefore, "fogging" of the material may be a problem. Suggestions to cure this "fogging" include the hydrodynamic management of flow. However, this method is still unproven. Only limited materials evaluations have been done in terms of the corrosive attack on the quartz material. For instance, the quartz literature suggests that the presence of carbon will reduce fused quartz at temperatures above 1200°C (2192°F). This indicates that carbonaceous material gasification may be restricted to this upper temperature limit.

Erosion of the tube seems to also be a possibility. For instance, although quartz is relatively hard, char particles may scratch the quartz. Scratches will reduce transmissivity and can lead to structural failure. Short-term experiments have not experienced this problem to a great degree but it may be a problem for commercial designs. Another problem not clearly resolved in the literature is the devitrification of quartz due to daily thermal cycling below the phase change temperature of ~250°C (482°F). Quartz tubes or windows may have to be maintained at high temperatures to avoid devitrification.

In the proof of principle experiments reviewed involving entrained bed reactors, flux levels up to 1600 kW/m^2 (5.08 E05 Btu/h-ft^2) were tested in reactor sizes of less than 100 kWth (3.41 E05 Btu/h). Operating conditions in the quartz reactors were maintained at temperatures up to 1000°C (1832°F) and pressures in one of the experiments of up to 0.52 MPa (75 psig).

An interesting phenomena observed in the quartz entrained reactor experiments is the dual temperature condition. This occurs when the concentrated radiant energy rapidly heats up the opaque solid particles in the reactors to temperatures over 1727°C (3140°F). The transparent gaseous material in the reactor remains relatively cold depending on the solids loading and solid to gas heat transfer rate. Particles less than 1 μm have been shown to heat rapidly and transfer heat effectively to their surroundings. Thus, they are very close in temperature to the surrounding gas and in fact may be used to heat gases to high temperatures. Larger particles, on the other hand, may heat faster than the rate of heat transfer to the

surrounding gas and may therefore achieve higher temperatures than the surrounding media. The possibility thus exists that through material sizing product characteristics can be changed. Volatile matter flashed from the solids may be quenched before being cracked to lighter hydrocarbons. This would facilitate the production of liquid products. Unfortunately, grinding and sizing costs to produce very small size particles or obtain uniform material characteristics may exclude certain reactions from consideration.

Review of Fluidized Bed Reactor Designs

Introduction

When a gas is passed upward through a bed of solid particles at a sufficient rate that the drag force matches the weight of the particles, a suspension, or fluidized bed, of particles results. The fluidized bed is characterized by large local instabilities in flow fields that result in bubbles similar in appearance to those that occur when bubbling a gas through a liquid. These bubbles rise through the bed causing the surrounding suspended particles to circulate around them, and making the solids in the bed well-mixed. Mixing increases with increased gas flow.

Reasons for the use of fluidized bed technology for chemical processes are:

● The high solids-gas interfacial area results in excellent heat and mass transfer between these two phases

● The excellent mixing results in a bed of very uniform temperature for good control of reaction yields and selectivity

● The solids movement acts to disturb boundary layers on containing walls and immersed heat transfer surfaces, reducing film heat transfer resistance, and causing rapid heat transfer between these surfaces and the bed

● The fluidized solids behave like a liquid and can be easily transported into or out of the bed during continuous processing.

A commercial scale fluidized bed reactor may be conceived of as a large number of vertical, transparent tubes arrayed in a generally circular pattern to intercept the concentrated flux from a heliostat field. The radiation impinges upon the fluidized solids and the reaction occurs as heat is transferred to the bed by direct absorption, by the mixing action of the bed, and by convective heat transfer between solids and the fluidizing gas. The

fluidized bed reactor may be configured as a cavity for good thermal performance at high temperatures or externally heated for lower temperature applications.

Westinghouse/Georgia Tech Fluidized Bed Receiver

Westinghouse, in cooperation with Georgia Tech, has investigated the suitability of a fluidized bed as a solar thermal receiver.[19] In this design concentrated solar energy is transmitted by a transparent vessel containing a bed of particles that absorb the energy, are mixed, and transfer heat by convection to the gas stream.

The fluidized bed receiver concept is shown in Figure 27. Figure 28 is a schematic drawing of the receiver system. The fluidized bed was contained in a 0.30 m (1 ft) OD by 1.22 m (4 ft) long by 2.5 mm (1 in.) thick wall transparent fused silica cylinder. The bed was supported on a gas distributor/air plenum assembly made of stainless steel. An instrument tube containing thermocouple and pressure sensor leads penetrated into the bed.

According to Reference 20:

> "The receiver was exposed to over 75 hours of focused solar radiation during 23 tests at the ACTF. Receiver mechanical performance was excellent, with instrumentation, seal, cooling/shielding system, and support structures all performing well. A variety of bed materials with different optical and physical properties representative of several applications were tested with bed depths from 0.3 to 0.46 m (11.8 to 18.1 in.). Included were copper beads (high heat capacity), silicon carbide (high absorptivity), sand (inexpensive heat transport and storage), alumina (catalytic processes), crushed quartz (translucent), steel mill slag, lava, and mixtures of these. Mean particle sizes ranged from 1000 to 3000 μm, large enough to allow the large air flow rates that are desirable in air heaters."

Table 10 summarizes the results of the test program as reported by Westinghouse.

The Westinghouse team found that the fused silica vessel proved durable and not subject to thermal shock or abrasion, but became extremely discolored (brown-black) when silicon carbide or copper shot were used as the bed material. The apparent cause was a chemical interaction since no discoloration occurred when the other bed materials (oxides or carbides) were used.

286
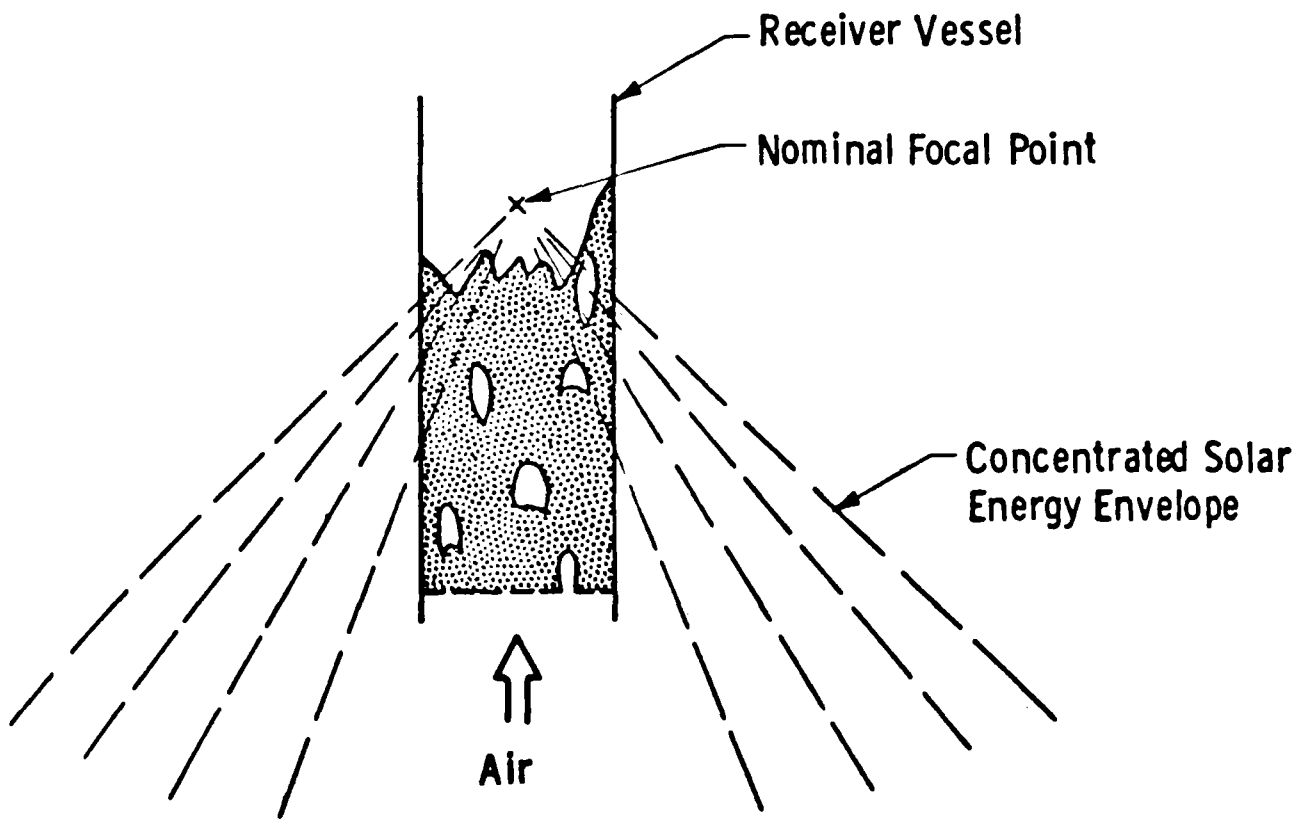
Figure 27. FLUIDIZED BED RECEIVER CONCEPT
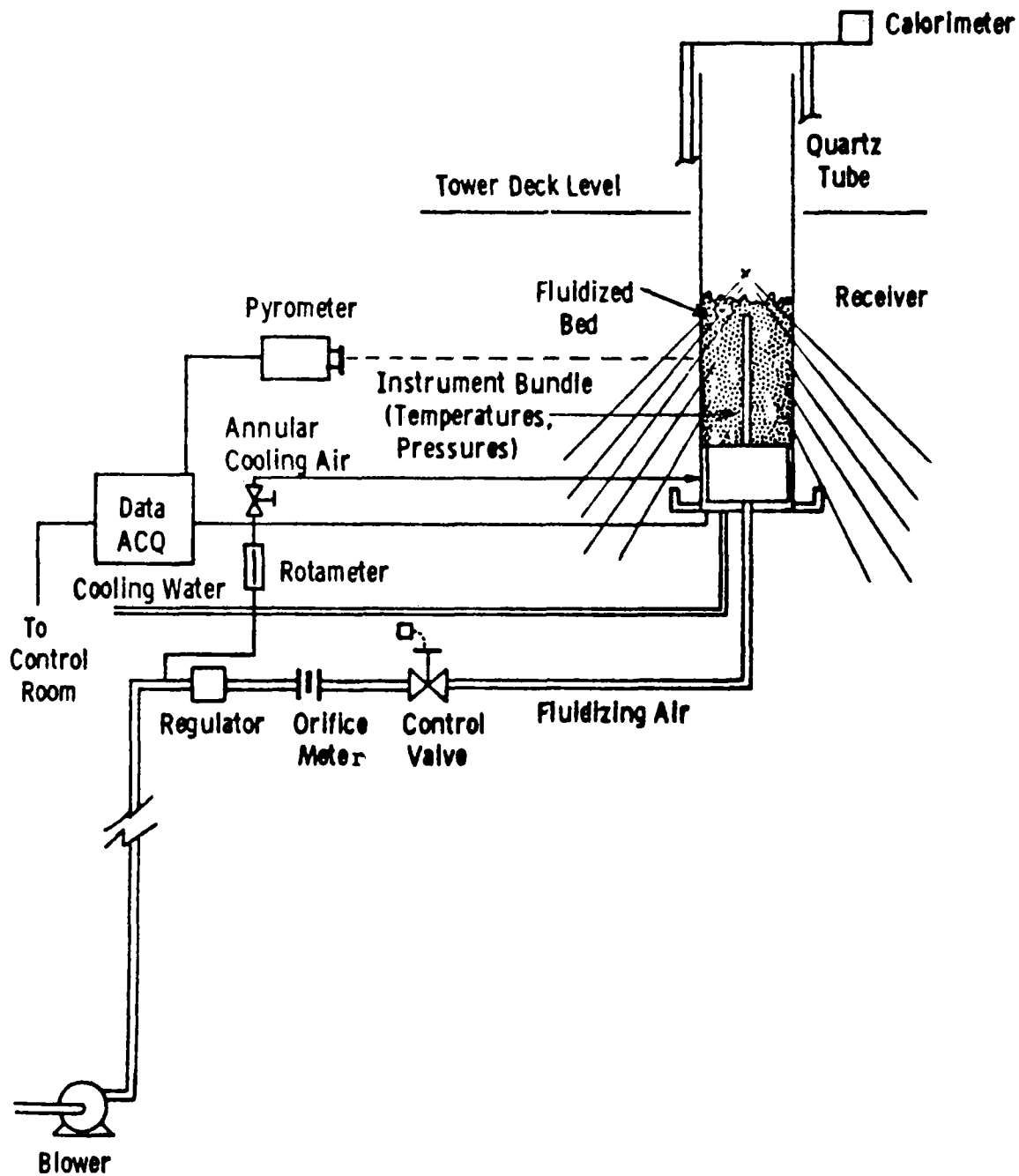
Figure 28.   SCHEMATIC DRAWING OF A FLUIDIZED BED RECEIVER

Table 10. TEST CONDITIONS AND RESULTS

Material	Bed Temp. °C	Incident Power kW	Energy to Air kW	Mean Bed Absorptance
Copper Beads	176 - 289	36 - 42	14.7 - 19.1	0.50
Silicon Carbide	160 - 476	32-- 72	11.7 - 29.5	0.58
Alumina	227 - 390	45 - 58	13.7 - 17.4	0.43
Fused Silica	310 - 324	51 - 54	17.8 - 24.9	0.54
Sand - Large	131 - 184	34 - 43	13.3 - 18.0	0.49
Sand - Medium	182 - 479	37 - 79	10.9 - 18.9	0.38
Sand - Small	202 - 563	42 - 80	8.1 - 15.9	0.47
Sand - Fine	465 - 544	28 - 36	5.9 - 8.6	0.50
Steel Mill Slag	223 - 233	50 - 58	23.9 - 30.5	0.58
SiC/Sand Mix	269 - 388	34 - 39	16.2 - 20.6	0.64
SiC/Silica Mix	266 - 287	44 - 49	24.2 - 25.6	0.70
SiC/Lava Mix	317 - 353	48 - 54	20.1 - 25.9	0.58

The effect of the discoloration was to form a very thin absorbing layer on the inner vessel wall. This layer apparently did not damage the tube mechanically, nor did it drastically effect receiver performance since it was a good absorber and was so thin that heat could be effectively removed by the mixing bed material. The discoloration did cause the expected differences in radiation properties of the bed materials to be obscured.

One surprising result noted by the researchers was the pronounced vertical temperature gradient which was normally observed within the bed. (Normally a fluidized bed will be uniform in temperature.) Figure 29[19] is typical. With air fluidizing a bed of sand at 2.74 E04 cm^3/s (58 SCF/min) only the upper half of the bed (depth is 0.46 m [18 in.]) is at a uniform temperature. When the flow was increased to 3.3 E04/cm^3/s (70 SCF/min) a much larger portion of the bed is fairly uniform in temperature. These results are attributed to poor mixing of solids because air flow rates were limited to values near minimum fluidizing conditions by excessive carryover of bed material. Also, the lower portion of the bed did not see the same flux intensity as the upper portion of the bed. Excessive carryover can be avoided by allowing a larger disengaging height, collecting entrained solids with a cyclone, or continuously feeding solids.

Transient behavior is shown in Figure 30[19]. About 20 to 30 minutes were typically required for a new thermal steady-state to be reached when the air flow was suddenly decreased (or increased).

French Fluidized Bed Reactor

Research at Odeillo has demonstrated the feasibility of both gas heating and chemical reaction of calcium carbonate in a small, transparent, fluidized bed reactor.[12] The scheme of the fluidized bed reactor is shown in Figure 31. Its main components are (a) a transparent, silica wall (cross-sectional area $10^{-3}m^2$ [1.08 E02/ft^2], height 0.3 m [0.98 ft]) allowing concentrated solar flux to enter the reactor and also visualization of the bed; (b) a gas distributor made either of metallic beads or of zirconia particles laying on a metallic grid; (c) a reflector surrounding the tube in order to decrease radiation losses. Different kinds of reflectors were tested, either specular or diffuse, in order to reduce radiation losses. The gas flow rate across the bed, total pressure drop and temperature inside the bed were continuously controlled. Figure 32 presents temperature profiles in the fluidized silica bed versus bed depth.
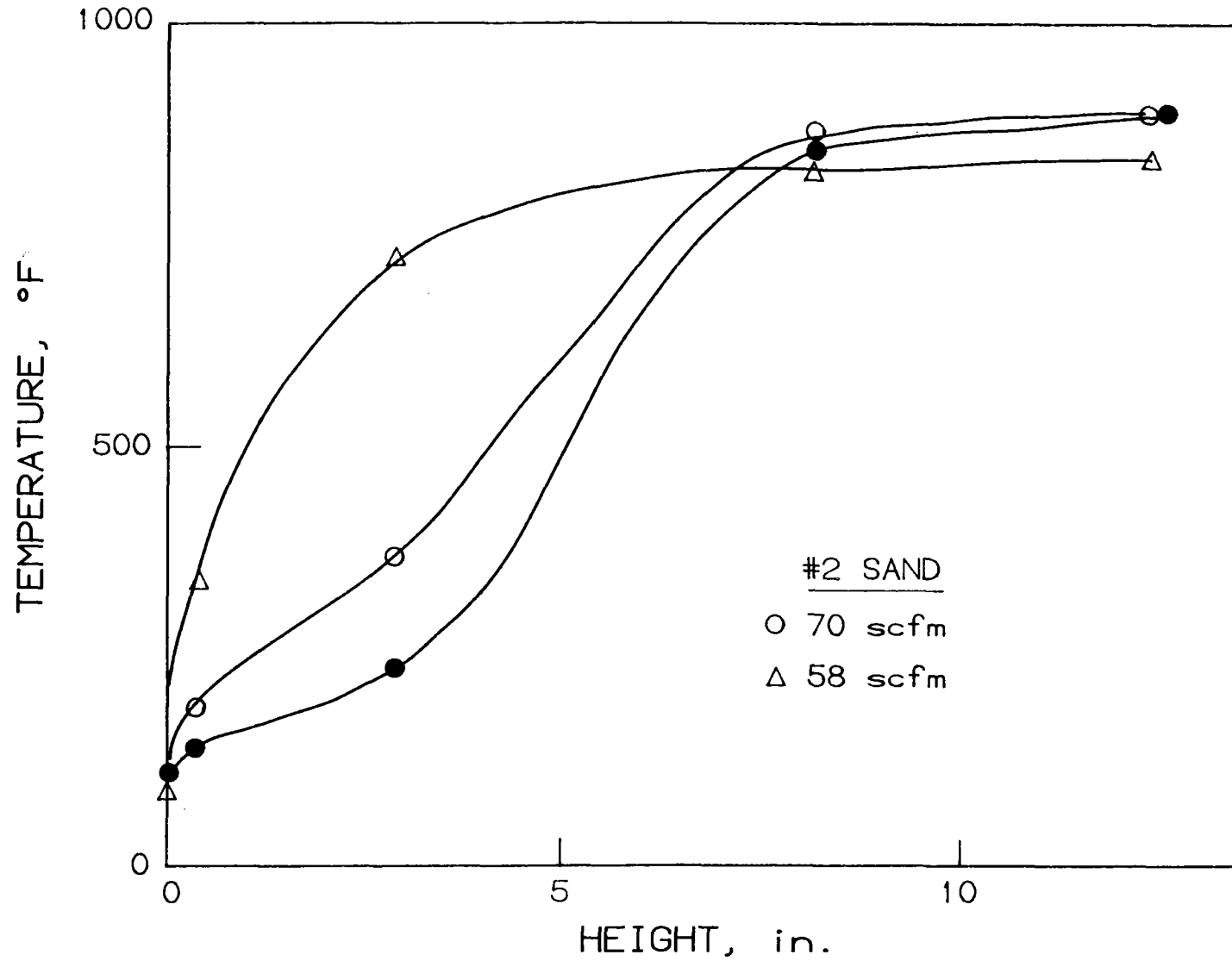
Figure 29. BED TEMPERATURE PROFILE
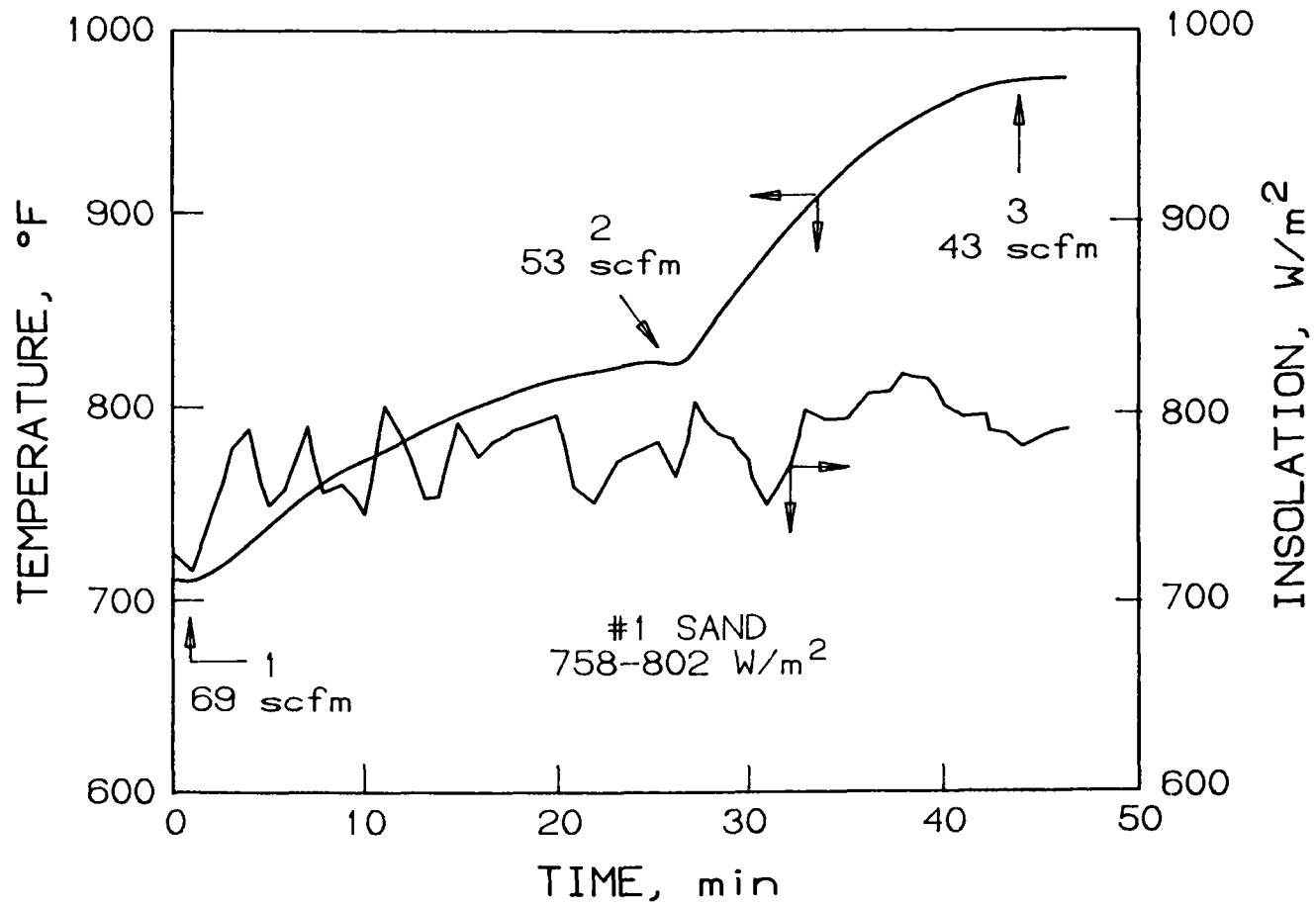
A84070622H

Figure 30. BED RESPONSE TO FLOW CHANGE

A84070623H
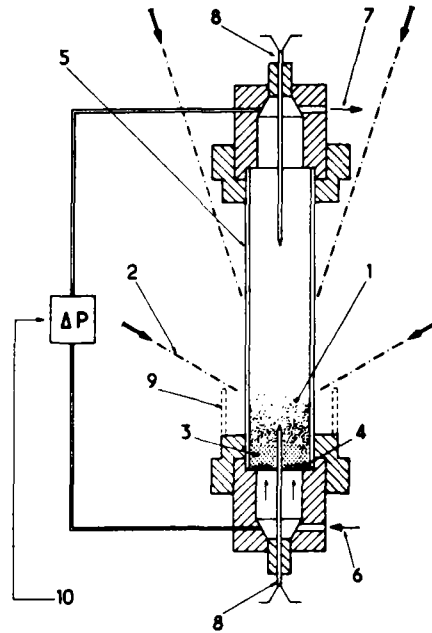
Figure 31.   SCHEME OF SOLAR FLUIDIZED BED REACTOR
1 — fluid bed; 2 — concentrated solar rays;
3 — gas distributor consisting of glass, iron or zirconia beads;
4 — grid; 5 — transparent silica tube; 6 — gas inlet;
7 — gas outlet; 8 — thermocouples; 9 — reflectors; and
10 — pressure loss measurement
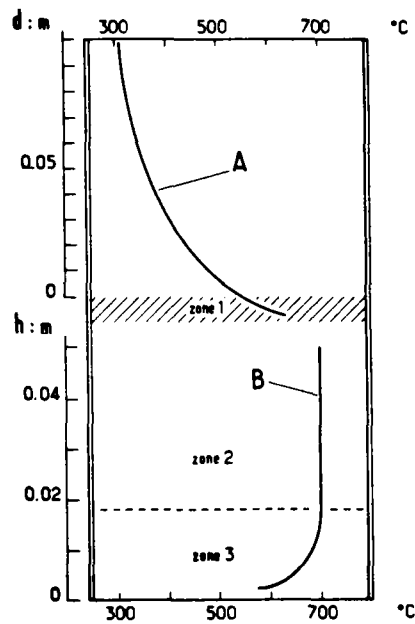
Figure 32.   TEMPERATURE (Distribution) PROFILES
IN THE FLUIDIZED SILICA SAND (Thermocouple
Measurements).   Cure A: Gas Temperature
and Curve B: Bed Temperature

No problems were found with chemical attack of the quartz vessel. There were no problems with erosion or thermal shock.

Fluidized bed reactors should scale-up to commercial sizes quite readily based upon extensive industrial experience. The Westinghouse receiver absorbed power levels ranging from 28 to 80 kW (9.56 E04 to 2.73 E05 Btu/h). Bed temperatures ranged from 160° to 563°C (320° to 1045°F). A considerable range of efficiencies were observed consistent with variations in bed materials, particle sizes, air flow rate, and bed temperature. The range was roughly 20% to 40% thermal efficiency. The small scale French reactor was scaled to a downward focusing solar furnace producing an input of power of 1.75 kW (5972 Btu/h). At 600°C (1112°F) an efficiency of 40% was observed when operating as a gas heater. Operating at temperatures ranging from about 850° to 950°C (1562° to 1742°F), the reactor efficiency in reacting calcium carbonate was 20%. Efficiency varies as the reaction proceeds because the radiative properties of the system are continuously modified due to the chemical reaction. The radiative properties of the bed are determined by the bed porosity and bubbling behavior as affected by fluidization velocity; particle type, and particle diameter.

Summary of Fluidized Bed Reactor Designs

Experiments reviewed demonstrated the heating of gases in the fluidized bed reactor and the calcination of limestone. All designs used a transparent quartz reactor vessel in an externally heated configuration. These experiments in small 1.75 kW to 80 kW (5972 Btu/h to 2.73 E05 Btu/h) reactors indicate that bed material selection is important both from the perspective of solar absorption with and chemical reaction with the quartz container. Discoloration of the reactor walls were observed with silicon carbide and copper shot bed materials. However, reactor performance was not dramatically affected by the discoloration possibly because of the thinness of the layer or its heat transfer qualities. Another interesting result observed in the experiments was a pronounced vertical temperature gradient which is not normally associated with fluidized bed reactors. This condition was attributed to the low gas fluidization velocity used in the experiments and the flux intensity which was directed primarily at the bottom of the fluidized bed. Increased fluidization gas velocity can minimize these temperature gradients. The possibility also exists through gas velocity control and bed

material density variances to establish different temperature zones within the reactor.

Fluidized bed reactors have demonstrated capability to absorb high flux levels in direct flux component configurations because of excellent bed mixing, continuous exposure of fresh material to direct flux heating, and very high heat transfer rates within the bed. The temperature capability of a direct flux fluidized bed reactor is limited by corrosion of the transparent container. For instance, operating temperature of a quartz container is limited to about 900°C (1652°F), with 1000°C (1832°F) possible in a dry, reducing atmosphere. Although quartz is quite hard, it may also be subject to erosion.

When operated in a cavity configuration, fluidized bed reactors are capable of high thermal efficiencies. However, operated as an externally heated reactor, reflection losses may be excessive because of the angle at which flux impinges on the wall. Externally heated designs are simpler and more compact than cavities, but have lower thermal efficiency. Compared to packed bed and rotary kiln reactors, fluidized beds may have significant parasitic power requirements. The fluidizing gas is heated as it passes through the bed. This is acceptable and desirable if the gas participates in the reaction. If the gas does not react, then it is taking energy away from the process. In any case, heat recovery from process gases is essential to maintain efficiency.

In the Westinghouse/Georgia Tech experiments reviewed, which is summarized in Table 11, the receiver absorbed power levels ranging from 28 to 80 kW (9.56 E04 to 2.73 E05 Btu/h). Bed temperatures ranged from 160° to 503°C (320° to 1043°F). A considerable range of efficiencies were observed consistent with variations in bed materials, particle sizes, air flow rate, and bed temperature. The range was roughly 20 to 40 percent thermal efficiency. In the other two Odeillo experiments summarized in Table 11, the reactor was scaled to a downward focusing solar furnace producing an input of power of 1.75 kW (5972 Btu/h). At 600°C (1112°F) an efficiency of 40% was observed when operating as a gas heater. Operating at temperatures ranging from about 850° to 950°C (1562° to 1742°F), the reactor efficiency in reacting calcium carbonate was 20%. Efficiency varies as the reaction proceeds because the radiative properties of the system are continuously modified due to the

Table 11. FLUID BED REACTORS

	Air Heating	Air Heating	Limestone Calcination
Reaction			
Researcher	Westinghouse/Georgia Institute of Tech.	Odeillo Solar Facility	Odeillo Solar Facility
Reference Number	19	12	12
Scope of Effort	Experimental (Series of Experiments)	Experimental	Experimental
Objective	Proof of Principle	Proof of Principle	Proof of Principle
Design Scale	28 to 79 kW	1.75 kW	1.75 kW
Scale of Intended Application	Central Receiver Heat Source	Central Receiver Heat Source	Central Receiver Heat Source
Flux Coupling Method	Direct	Direct	Direct
Material of Construction	Quartz	Quartz	Quartz
Configuration	External	External	External
Windowed Aperture	No	No	No
Schematic Figure Number	A28 and A29	A32	A32
Principal Dimensions:			
Aperture Diameter	18 inch. Bed Depth Unexpanded	10^{-3} m^2 Cross Section	
Cavity Diameter	1 ft. OD Tube	10^{-3} m^2 Cross Section	10^{-3} m^2 Cross Section
Cavity Length	4 ft. Length/ 2.5 mm Wall	0.3 m Length	0.3 m Length
Thermal Efficiency	Range 19 to 53%; Dependent on Bed Temperature	40%	20%
Flux Capability:			
Basis	Measured		
At Aperture	Not Applicable	Not Available	Not Available
In Reactor	5 to 10 W/cm^2	Not Available	Not Available
Temperature of Operation	404 to 836°K	600°C	850 to 950°C
Process Fluid Temperature Profile	Figure A30	Figure A33	Not Available
Refractory Temperature	Not Available	Not Available	Not Available
Window Temperature	Not Applicable	Not Available	Not Available
Operating Pressure	1 atm	1 atm	1 atm
Pressure Drop (ΔP/P, %)	Not Available	Not Available	
Evaluation	Proof of principle. Quartz suffered erosion/corrosion. No chemical reaction studied.	Proof of principle. No erosion/ corrosion observed.	Proof of principle. Batch process only. No corrosion/ erosion observed.

chemical reaction. The radiative properties of the bed are determined by the bed porosity and bubbling behavior as affected by fluidization velocity; particle type, and particle diameter.

Fluidized beds have high thermal inertia and should not be subject to wide temperature swings during transients. Feed rate and gas flow rate may be used to control temperature. Because of inertia, start-up and shutdown times may be long. However, use of smaller tubes with less solids holdup may be considered to speed start-up, if appropriate. Since fluidized beds require a vertical orientation and also need considerable support equipment for feed and discharge, they are strictly applicable only to central receiver applications.

Summary of High-Temperature Solar Receiver/Reactor Designs

This review of high-temperature solar receiver/reactor research has highlighted the various reactor and reaction types that may be applicable to direct flux reactor design. However, due to the fact that most of the designs reviewed were for small scale applications, especially with parabolic dish receiver, little direct knowledge can be gained from these designs which is relevant to large scale central receiver direct flux reactor design. The primary criteria that can be used to judge applicability of each design reviewed includes:

o   The closeness to a commercial scale design

o   The use of radiant energy

o   The use of direct flux coupling.

Although most of the designs reviewed utilized radiant solar energy, few employed direct flux. Of the experimental reactors that have undergone testing only the rotary kiln reactor concept developed for the CRTF design reviewed could be considered as having a commercially scalable basis. Even this experimental reactor conceptual design was several orders of magnitude away in size from rotary kilns commonly used in industrial applications. The closeness of all reactor designs reviewed to industrial reactor designs is important in order to minimize the risk of scale-up and take advantage of the know-how and technical experience gained in industry through the design and operation of industrially used reactor configurations.

297

Two of the conceptual designs reviewed; the PFR Engineering Systems steam-methane reforming reactor; and the direct flux rotary kiln developed for the CRTF show promise as the basis for large scale direct flux reactor designs. Extensive industrial experience in high-temperature radiantly heated solids reactors — rotary kilns, and in radiantly heated gas phase reactors — reformers, form the basis for selecting these two designs. Derivations of these conceptual and commercial designs can form the baselines for conceptual direct flux reactor design.

The most seriously limiting factor for direct flux reactor development is the limited availability of, and experience with, transparent material designs. More development and experience is required to demonstrate materials compatibility, erosion, and corrosion of these transparent materials. This indicates a high level of technical uncertainty in the design of commercial scale direct flux receiver/reactors.

REFERENCES

1. Chubb, T. A., Nemecek, J. J. and Simmons, D. E., "Design of a Small Thermochemical Receiver for Solar Thermal Power," _Solar Energy_, Vol. _23_, 217-221, 1979.

2. Li, C. H. et al., "Heat and Mass Transfer Analysis of a Chemical Converter/Heat Exchanger for the SO_2/SO_3 Distributed Solar Energy Collection System." Paper presented at the International Solar Energy Society Meeting, Atlanta, GA: May 28, 1979.

3. Pierre, J. F. and Summers, W. A., "Development of a Solar Chemical Receiver." Paper presented at AIChE Meeting, Orlando, FL.

4. McCrary, J. H. et al., "Experimental Study of SO_3 Dissociation as a Mechanism for Converting and Transporting Solar Energy," _Solar Energy_, Vol. _27_ No. 5, 433-440, 1981.

5. Chubb, T. A. et al., "Thermochemical Receiver and Chemical Furnace Tests." _Proc. Annu. Meet. — Am. Sect. Int. Sol. Energy Soc._, Philadelphia, PA: May 26, 1981, 166-169.

6. Wright, J. H. et al., "Solar Energy Collection Using the Reversible Ammonia Dissociation Reaction." Paper presented at the International Solar Energy Society Meeting, Atlanta, GA: May 28, 1979.

7. Williams, O. M., "Design and Cost Analysis for an Ammonia-Based Solar Thermochemical Cavity Absorber," _Solar Energy_, Vol. _24_ No. 3, 1980.

8. Gregg, D. W., "Solar Gasification of Coal, Activated Carbon Coke and Coal-Biomass Mixtures," _Solar Energy_, Vol. _25_ No. 4, 353-364, 1980.

9. Pangborn, J. P., "Experimental Work on a CdO-Based Solar Cycle for Water Splitting." Paper presented at the Users Association Solar Fuels Workshop, Albuquerque, NM: November 28, 1979.

10. Whaley, T. P., Yudow, B. D. and Schreiber, J. D., "Solar Production of Elemental Phosphorus." Final Report prepared by Institute of Gas Technology, Chicago: November 1981.

11. Gregg, D. W., "Apparatus for Solar Coal Gasification," Patent No.: U.S. Application 029,962.

12. Flamant, G. et al., "Experimental Aspects of the Thermochemical Conversion of Solar Energy; Decarbonization of $CaCO_3$," _Solar Energy_, Vol. _24_ No. 4, 385-395, 1980.

13. Krishnan, G. N., Bartlett, R. W. and Cubicciotti, D. D., "Design of an Experimental High Temperature Materials Processing System for the Solar Thermal Test Facility (at Sandia)." _Proceedings of Solar-Fuels Workshop_, SRI International, 189-197, Menlo Park, CA: 1979.

14. Shell, P. K. et al., "Zinc Sulfate Decomposition in a Solar Rotary Kiln." Annual Business Meeting Solar Thermal Test Facilities User's Association, Houston, TX: April 6, 1982.

15. Antal, Jr., M. J., Hofmann, L. and Moreira, J. R., "Radiant Flash Pyrolysis of Biomass: Basic and Applied Research at Princeton." Proceedings of Annual Meeting: Technical Sessions, User's Association Annual Meeting, 89-94, Las Cruces, NM: April 15, 1980.

16. Antal, M. J., et al., "Solar Flash Pyrolysis of Biomass," ISES Silver Jubilee 1979 International Congress, (1979) Atlanta.

17. Antal, Jr., M. J. et al., "Experimental Evaluation of a Solar Fired Flash Pyrolysis of Biomass Reactor." Proc. Annu. Meet. — Am. Sect. Int. Sol. Energy Soc., 189-192, Philadelphia, PA: May 26, 1981.

18. Antal, M. J., et al., "Design and Operation of a Solar Fired Biomass Flash Pyrolysis Reactor" Princeton University, Princeton, NJ: 1981.

19. Hunt, A. J., "New Solar Thermal Receiver Utilizing Small Particles." Paper presented at the International Solar Energy Society Meeting, Atlanta, GA: May 28, 1979.

20. Bachovchin, D. M., Archer, D. H., Keairns, D. L., "A Fluidized Bed Solar Receiver," ACTF Users Workshop, 15-29, February, 1981.

21. Bachovchin, D. M. et al., "Development and Testing of a Fluidized Bed Solar Thermal Receiver," in Glenn, B. H. and Franta, G. E., Eds., Proceedings of the 1981 Annual Meeting of the AS/ISES, Vol. 4.1, Newark, DE: American Section of the International Solar Energy Society, Inc., 1981.

FS-   1

10723
US DEPARTMENT OF ENERGY
ATTN S D ELLIOTT, DIR
SOLAR ONE PROJECT OFFICE
PO BOX 366
BARSTOW, CA   92327